THE FUNCTIONAL CONSEQUENCES OF IgA IMMUNE COMPLEX CAPTURE BY FcRL4+ B CELLS

by

KATE BARNEY

A thesis submitted to the University of Birmingham for the degree of

DOCTOR OF PHILOSOPHY

Institute of Inflammation and Ageing

College of Medical and Dental Sciences

The University of Birmingham

September 2024

Dedication

This thesis is dedicated to my grandad

Albert Royston Nash

He believed education was the greatest gift a person could receive and was the only family member who I wasn't able to celebrate my greatest educational milestone with.

My passion for learning wouldn't exist without you.

Abstract

RA is a systemic, chronic autoimmune disease that is generally first observed in the small joints. An invasive, inflammatory filtrate develops in the synovium. If left untreated, in the long term, this leads to joint damage and disability. The success of B cell-depleting therapies has indicated a role for B cells in the pathogenesis of rheumatoid arthritis but the presence of autoantibodies post-treatment indicates B cells have an antibody-independent function. A subset of RANKL-producing B cells in rheumatoid arthritis synovial fluid has been defined by its expression of Fc receptor like 4 (FcRL4) and FcRL4 captures IgA immune complexes on their surface. Here, we addressed the hypothesis that capture of IgA immune complexes by FcRL4 lead to its internalisation before processing and presentation on the cell surface. We also addressed whether IgA IC binding to FcRL4 impacted signalling pathways activated by the BCR in primary cells. In transduced priess cells, tonsil B cells and rheumatoid arthritis synovial fluid B cells, IgA immune complexes bound to FcRL4 was internalised to acidified intracellular compartments. High expression of co-stimulatory molecules CD80, CD86 and HLA-DR by FcRL4+ B cells suggest that they can act as antigen presenting cells and that the internalised IgA immune complex is potentially processed and presented on the surface. Crosslinking of IgA immune complex-bound FcRL4 with the BCR increases phosphorylation of the inhibitory signalling molecules Hck, Fgr and SHP-1 whilst simultaneously decreasing phosphorylation of activatory signalling ERK1/2, PLCγ2 and Syk in FcRL4+ transduced priess cells, tonsil B cells and rheumatoid arthritis synovial fluid B cells. Together, these results suggest that expression of FcRL4 on B cells acts as a molecular switch to downregulate BCR signalling and prioritise internalisation of IgA immune complexes.

Acknowledgements

This project would not have been possible without an army of individuals' supporting me over the past 4 years.

Firstly, I would like to thank my supervisors for their leadership throughout this project. To Professor Dagmar Scheel-Toellner for providing endless support through some challenging sets of experiments, constantly inspiring new ideas and expanding my immunological knowledge. To Dr Amy Anderson, for welcoming me into the team in Newcastle and for taking the time to nurture and develop my flow cytometry skills, instilling confidence in my experimental ability. To Professor Karim Raza and Professor John Isaacs, for watching over my project and providing feedback on my thesis.

A huge thank you to Rheumatology Research Group in Birmingham and the Immunology and Immunotherapy group in Newcastle as well as the members of the Scheel-Toellner team: Dr Yuxin Liu and Dr Dina Abdelmottaleb. An honorary mention to Kathryn Frost, Emily Powell & Maryam Imran, for always stepping in to look after my experiments when train strikes prevented me from travelling. To RACE and Versus Arthritis for funding the project. A special thank you to the patient research partners for their input into the project and to patients who have donated samples, this work would not be possible without your generosity.

Finally, to my parents for encouraging me to pursue my passions and never doubting my capabilities. To Sam, for being my biggest cheerleader, celebrating with me during my high's and pushing me on when I began to doubt myself. Your unwavering support was nothing short of amazing.

Table of Contents

Introduction.....31-77

1.1 Autoimmune Disease.....31-33

1.2 Rheumatoid Arthritis

1.2.1 Aetiology, Epidemiology, Risk Factors & Co-Morbidities.....33-35

1.2.2 Clinical Presentation.....36

1.2.3 Cellular Presentation.....36-37

1.3 B Cell Development

1.3.1 Formation of the pre-BCR (VDJ Ligation).....37-39

1.3.2 B Cell Migration.....40

1.3.3 B Cell Activation.....40-41

1.3.4 Affinity Maturation.....41-44

1.3.5 Class Switch Recombination.....45

1.4 B Cell Subsets

1.4.1 Pro, Pre & Immature B Cells.....46

1.4.2 Transitional & Naïve.....46-47

1.4.3 Marginal Zone.....47

1.4.4 Centroblasts & Centrocytes.....47-48

1.4.5 Extrafollicular Memory & Plasma Cells.....48

1.4.6 Memory B Cells……49

1.4.7 Long Lived Plasma Cells……49-50

1.4.8 Autoimmunity-Associated Memory B Cells……50-53

1.5 B Cell Function

1.5.1 B Cell Signalling……54-56

1.5.2 Autophagy……56-57

1.5.3 Antigen Presentation……57-59

1.5.4 Cytokine Production……60-61

1.6 B Cells in RA

1.6.1 B Cell Role in Immune Tolerance & Autoimmunity……61-63

1.6.2 Autoantibodies……63-64

1.6.3 IgA……64-66

1.6.4 Antigen Presentation……67

1.7 B Cell Targeting Therapeutics in RA

1.7.1 B Cell Depleting Therapies (BCDT)……68-69

1.7.2 Interfering with B Cell Interactions……69

1.8 FcRL4+ B Cells

1.8.1 FcR & FcRL……69-72

1.8.2 Characterisation of FcRL4+ B Cells……73-74

1.8.3 FcRL4+ B Cells in Chronic Infectious Diseases……74-75

1.8.4 FcRL4+ B Cells in Autoimmune Diseases……75-76

1.9 Hypothesis & Aims

1.9.1 Hypothesis……77

1.9.2 Aims……77

Materials & Methods……78-108

2.1 Patients and Patient's Materials……78

2.2 Sample Preparation

2.2.1 PBMC Isolation from a Leukocyte Reduction Filter (cone)……78-79

2.2.2 PBMC Isolation from Whole Blood……79

2.2.3 Plasma Isolation……79

2.2.4 Tonsil Dissociation & Mononuclear Cell Isolation……80

2.2.5 Synovial Fluid Mononuclear Cell (SFMC) Isolation……80-81

2.3 Cell Culture……81-82

2.4 IgA Immune Complex Preparation

2.4.1 Heat Aggregation of Colostrum IgA……82

2.4.2 Streptavidin Lightning Link of Colostrum IgA……82

2.4.3 Biotinylation of Colostrum IgA……83

2.4.4 Biotinylation of Citrullinated Enolase Peptide & Citrullinated Enolase Protein..83

2.4.5 Immune Complex: Biotinylated Enolase & Streptavidin……..84

2.4.6 Immune Complex: HA Biotinylated IgA & pHrodo Avidin™……..84

2.5 IgA Binding

2.5.1 Glycine Acid Wash – *Ex-Vivo* Primary Cells……..84

2.5.2 IgA Binding & Cell Staining – FcRL4+ Priess Cells & *Ex-Vivo* Primary Cells…..85-86

2.6 FcRL4-Tet-On Vector Production

2.6.1 FcRL4 Plasmid Isolation……..87

2.6.2 Plasmid Amplification……..88-89

2.6.3 Plasmid Clean-Up……90

2.6.4 Insert Phosphorylation and Ligation……..90

2.6.5 Bacterial Transformation……..91

2.6.6 Plasmid Isolation & Verification……92-93

2.6.7 Viral Concentration……93-94

2.6.8 Priess Cell Viral Transduction & Selection……..94

2.6.9 FcRL4 Induction……95

2.7 Cell Sorting……96

2.8 pHrodo Avidin™ Internalisation

2.8.1 Live Cell Imaging……97

2.8.2 Flow Cytometry……98

2.9 Antigen Presentation

2.9.1 Co-Culture……99

2.9.2 IL-2 ELISA……100

2.10 FcRL4+ B Cell Signalling: PhosFlow

2.10.1 Sample Preparation……100

2.10.2 Stimulation of PBMCs……101

2.10.3 Cell stimulation with anti-IgG + IgM f(ab')$_2$ fragment only……101

2.10.4 Cell stimulation with HA colostrum IgA IC only……101-102

2.10.5 Stimulation with anti-IgG + IgM f(ab')2 fragment and HA colostrum IgA IC: separate and together……102

2.10.6 Crosslinking the BCR and FcRL4……102-104

2.10.7 Labelling of anti-pFgr and anti-pHck by Lightning Link……105

2.10.8 Cell Staining……105-106

2.11 Buffers & Washes……107

2.12 Isotype Controls……108

Results……109-270

3 FcRL4-Expressing B Cell Model……109-144

3.1 Introduction……..109-114

3.2 Results

3.2.1 FcRL4 Expression in the Constitutively-Expressing B Cell Model……115-116

3.2.2 TLR7L, TLR9L and TGFβ Stimulated Cells

3.2.2.1 PBMCs……117-118

3.2.2.2 Untransduced Priess Cells……119-120

3.2.3 Tet-On Inducible B Cell Model

3.2.3.1 Viral Transduction Success Rate……..121-122

3.2.3.2 FcRL4 Expression in Tet-On Inducible Priess Cells ……..123-124

3.2.3.3 FcRL4 Expression Post-Puromycin Retreatment……125-126

3.2.3.4 FcRL4 Expression 2-48h……127-128

3.2.3.5 FcRL4 Expression 24-96h, One Treatment at 0h with 1µg/ml Doxycycline……129-130

3.2.3.6 FcRL4 Expression 24-96h, Treated at Regular 24h Intervals with 1µg/ml Doxycycline……131-132

3.2.3.7 Doxycycline Titration……133-134

3.2.3.8 Expression of CD80, CD86 and HLA-DR……135-138

3.2.3.9 HA Colostrum IgA IC Binding……..139-141

3.3 Discussion……142-144

4 Internalisation & Antigen Presentation of IgA ICs in FcRL4+ B Cells 145-193

4.1 Introduction.....145-147

4.2 Results

4.2.1 IgA IC pHrodo avidin™ validation

4.2.1.1 IgA IC & pHrodo avidin™ titration.....148-151

4.2.1.2 1% BSA test.....152-153

4.2.2 IgA IC Internalisation.....154-155

4.2.2.1 FcRL4+ Transduced Priess Cells.....156-161

4.2.2.2 FcRL4+ Tonsil B Cells.....162-168

4.2.2.3 FcRL4+ RA SF B Cells.....169-174

4.2.3 Presentation of Citrullinated Enolase Peptide.....175

4.2.3.1 Untransduced Priess Cells.....175-177

4.2.3.2 FcRL4+ Transduced Priess Cells.....178-179

4.2.3.3 FcRL4+ Tonsil.....180-184

4.2.4 IgA IC

4.2.4.1 Recombinant IgA & Citrullinated Enolase.....185-186

4.2.4.2 Streptavidin IgA + Citrullinated Enolase Peptide.....187-188

4.2.5 Transduced FcRL4+ Priess Cells.....189

4.3 Discussion.....190-193

5 Effects of FcRL4 on BCR Signalling……194-270

5.1 Introduction……194-195

5.2 Results

5.2.1 FcRL4 Staining Following Pemeabilisation with BD Perm III

5.2.1.1 anti-FcRL4 PE Biolegend Perm III Stability Test……196-197

5.2.1.2 CytoFix Epitope Stability Test……198-199

5.2.1.3 CytoFix Titration……200-201

5.2.2 FcRL4 Staining with 4% Formaldehyde

5.2.2.1 anti-FcRL4 & Rat anti-Mouse BV711 2° Antibody……202

5.2.2.2 anti-FcRL4 Lightning-Link® FITC & AF488……202-203

5.2.2.3 anti-FcRL4 Abcam Lightning-Link® FITC……203

5.2.2.4 anti-FcRL4 Biotechne AF350 & AF594……203-206

5.2.3 FcRL4 Staining with BD CytoFix and BD Perm III

5.2.3.1 anti-FcRL4 & Rat anti-Mouse BV711 2° Antibody……207

5.2.3.2 anti-FcRL4 Abcam Lightning-Link® FITC……207

5.2.3.3 anti-FcRL4 Lightning-Link® FITC & AF488……208-209

5.2.4 FcRL4 Biolegend PE & FITC Lightning-Link® Perm II Stability Test……210-211

5.2.5 Intracellular Antibody Validation

5.2.5.1 10µg/ml anti- IgG+ IgM f(ab')$_2$ fragment 0-60mins……212-215

5.2.5.2 10µg/ml anti-IgG + IgM f(ab')$_2$ fragment stimulation 0-20mins.216-220

5.2.5.3 50µg/ml HA Colostrum IgA stimulation 0-20mins……221-224

5.2.5.4 Antibody Titration BD Perm III……..225

5.2.5.5 Perm II Intracellular Antibody Staining……226-229

5.2.6 Signalling……230-231

5.2.6.1 pFgr……232-237

5.2.6.2 pHck……238-242

5.2.6.3 pSHP-1……243-247

5.2.6.4 pSyk……248-253

5.2.6.5 pPLCγ2……254-259

5.2.6.6 pERK1/2……260-265

5.3 Discussion……266-270

6 Discussion……271-276

6.1 Summary……271

6.2 Functional Consequences……271-273

6.3 Future Work and Limitations……274-276

6.4 Concluding Remarks……276

7 References……277-290

8 Appendix……………………………………………………………………………………..291-297

List of Figures

Figure 1.3.1 B cell development in the bone marrow……39

Figure 1.3.4 B cell development in a germinal centre……44

Figure 1.4 Markers expressed on B cells through development……53

Figure 1.6.3 IgA subclasses and isoforms……66

Figure 1.8.1 FcRL family……..72

Figure 2.5.2 Viability of induced transduced priess cells and *ex-vivo* tonsil cells……86

Figure 2.6.9 Viability of induced transduced priess cells……..95

Figure 2.9.1 E10P1 T cell hybridomas are most viable 48h post-media change……..99

Figure 2.10 PhosFlow stimulation conditions and plate plan detailing the signalling molecule staining panels being used……104

Figure 3.1I Lentiviral vector design for constitutive expression of FcRL4 in priess cells……..112

Figure 3.1II Lentiviral vector design for inducible expression of FcRL4 in priess cells……..113

Figure 3.1III Tet-On control of FcRL4 expression……114

Figure 3.2.1 FcRL4 expression in priess cells transduced with a constitutively active expression lentiviral vector……116

Figure 3.2.2.1 FcRL4 expression in stimulated PBMCs……118

Figure 3.2.2.2 FcRL4 expression in stimulated untransduced priess cells……120

Figure 3.2.3.1 Expression of mRuby2 fluorescent protein in transduced priess cells……122

Figure 3.2.3.2I FcRL4 expression increases in induced Tet-On lentiviral vector transduced priess cells compared to non-induced……..124

Figure 3.2.3.2II Anti-FcRL4 PE detects a greater percentage of FcRL4+ B cells than the GFP conjugated to FcRL4……..124

Figure 3.2.3.3 FcRL4 expression in transduced priess cells reselected with 4µg/ml puromycin……126

Figure 3.2.3.4 FcRL4 expression 2-48h post-induction with 1µg/ml doxycycline at 0h……128

Figure 3.2.3.5 FcRL4 expression 24-96h post-induction with 1µg/ml doxycycline at 0h…….130

Figure 3.2.3.6 FcRL4 expression at 24-96h when cells were treated with 1ug/ml doxycycline every 24h……..132

Figure 3.2.3.7 FcRL4 expression in transduced priess cells induced with different concentrations of doxycycline for 24h……..134

Figure 3.2.3.8I Expression of CD80, CD86 and HLA-DR in untransduced priess cells and transduced priess cells, unstimulated or stimulated with 1µg/ml doxycycline……137

Figure 3.2.3.8II Comparison of CD80, CD86 and HLA-DR expression between untransduced and transduced priess cells, unstimulated or stimulated with 1µg/ml doxycycline……138

Figure 3.2.3.9I IgA IC binding in FcRL4+ induced transduced priess cells……140

Figure 3.2.3.9II IgA IC binding in FcRL4+ *ex-vivo* tonsil B cells……140

Figure 3.2.3.9II Titration of IgA IC binding on FcRL4+ transduced priess cells……..141

Figure 4.2.1.1I pHrodo staining in cells incubated with 10µg/ml HA colostrum IgA……..150

Figure 4.2.1.1II pHrodo staining in cells incubated with 25µg/ml HA colostrum IgA……151

Figure 4.2.1.2 Addition of 1% BSA reduces IgA IC/pHrodo staining in FcRL4- and FcRL4+ induced transduced priess cells……153

Figure 4.2.2.1I., IgA IC/pHrodo internalisation by FcRL4- and FcRL4+ transduced priess cells raw flow cytometry data……157

Figure 4.2.2.1II IgA IC/pHrodo internalisation by FcRL4- and FcRL4+ transduced priess cells……158

Figure 4.2.2.1III Fluorescence for live cell imaging of FcRL4- induced transduced priess cells and pre-treated induced transduced priess and HA colostrum IgA IC/pHrodo……159

Figure 4.2.2.1IV Live cell fluorescent images of FcRL4+ transduced priess cells in 0.5% type II rat tail collagen gel……160

Figure 4.2.2.1V IgA IC/pHrodo staining colocalises with FcRL4+ transduced priess cells……161

Figure 4.2.2.2I IgA IC/pHrodo internalisation by FcRL4- and FcRL4+ *ex-vivo* tonsil cells raw flow cytometry data……164

Figure 4.2.2.2II IgA IC/pHrodo internalisation by FcRL4- and FcRL4+ *ex-vivo* tonsil cells……165

Figure 4.2.2.2III Fluorescence for live cell imaging of FcRL4- *ex-vivo* tonsil cells and pre-treated induced transduced priess and HA colostrum IgA IC/pHrodo……166

Figure 4.2.2.2IV Live cell fluorescent images of FcRL4+ *ex-vivo* tonsil cells in 0.5% type II rat tail collagen gel……167

Figure 4.2.2.2V IgA IC/pHrodo staining colocalises with FcRL4+ *ex-vivo* tonsil cells……168

Figure 4.2.2.3I IgA IC/pHrodo internalisation by FcRL4- and FcRL4+ *ex-vivo* RA SF cells raw flow cytometry data……..170

Figure 4.2.2.3II IgA IC/pHrodo internalisation by FcRL4- and FcRL4+ *ex-vivo* RA SF cells……171

Figure 4.2.2.3III Fluorescence for live cell imaging of FcRL4- *ex-vivo* RA SF cells and pre-treated induced transduced priess and HA colostrum IgA IC/pHrodo.……..172

Figure 4.2.2.3IV Live cell fluorescent images of FcRL4+ *ex-vivo* RA SF cells in 0.5% type II rat tail collagen gel……..173

Figure 4.2.2.3V IgA IC/pHrodo staining colocalises with FcRL4+ *ex-vivo* RA SF cells……..174

Figure 4.2.3.1 Presentation of a citrullinated enolase peptide by untransduced priess cells induces IL-2 production in citrullinated enolase recognising-T cell hybridomas……..177

Figure 4.2.3.2 Presentation of a citrullinated enolase peptide by FcRL4- and FcRL4+ transduced priess cells induces IL-2 production in citrullinated enolase recognising-T cell hybridomas……179

Figure 4.2.3.3I *Ex-vivo* FcRL4+ tonsil B cells maintain viability for 24h in culture……..182

Figure 4.2.3.3II *Ex-vivo* tonsil B cells express the highest percentage of FcRL4 when cultured with TLR9bL and TGFβ……..183

Figure 4.2.3.3III Presentation of a citrullinated enolase peptide by FcRL4- and FcRL4+ tonsil B cells induce IL-2 production in citrullinated enolase recognising-T cell hybridomas……..184

Figure 4.2.4.1 Binding of recombinant IgA + citrullinated enolase protein IC's to FcRL4+ transduced priess cells……..186

Figure 4.2.4.2 Binding of streptavidin IgA + biotinylated citrullinated enolase peptide IC's to FcRL4+ transduced priess cells……..188

Figure 5.2.1.1 Staining of FcRL4 is compromised in tonsil cells fixed with BD CytoFix and permeabilised with BD Perm III……197

Figure 5.2.1.2 BD CytoFix does not negatively impact FcRL4 staining……199

Figure 5.2.1.3 Reducing the concentration of BD CytoFix reduces the amount of pPLCγ2 fixed……..201

Figure 5.2.2I BV711 and FITC anti-FcRL4 staining in cells fixed with 4% formaldehyde……..205

Figure 5.2.2II AF488, AF594 and AF350 anti-FcRL4 staining in cells fixed with 4% formaldehyde……206

Figure 5.2.3 FcRL4 staining in cells fixed with BD CytoFix and permeabilised with BD Perm III……209

Figure 5.2.4 FcRL4 staining in cells fixed with BD CytoFix and permeabilised with BD Perm II……211

Figure 5.2.5.1I Change in phosphorylation of pBtk/Itk, pERK1/2, pFgr, pHck and pp65NF-κB in CD19+ PBMC cells stimulated with 10µg/ml anti-IgG + IgM $f(ab')_2$ fragment 0-60mins ……213

Figure 5.2.5.1II Change in phosphorylation of pPLCγ2, pSHP-1, pSHP-2 and pSyk in CD19+ PBMC cells stimulated with 10µg/ml anti-IgG + IgM $f(ab')_2$ fragment 0-60mins……214

Figure 5.2.5.1III Peak phosphorylation of pBtk/Itk, pERK1/2, pFgr, pHck, pp65NF-κB, pPLCγ2, pSHP-1, pSHP-2 and pSyk in CD19+ PBMC cells stimulated with 10µg/ml IgG + IgM f(ab')$_2$ fragment 0-60mins……215

Figure 5.2.5.2I Change in phosphorylation of pAkt, pBtk/Itk and pERK1/2 in CD19+ PBMC's stimulated with 10µg/ml IgG + IgM f(ab')$_2$ fragment 0-20mins……217

Figure 5.2.5.2II Change in phosphorylation of pp65NF-κB, pPLCγ2 and pSHP-1 in CD19+ PBMC's stimulated with 10µg/ml IgG + IgM f(ab')$_2$ fragment 0-20mins……218

Figure 5.2.5.2III Change in phosphorylation of pSHP-2 and pSyk in CD19+ PBMC's stimulated with 10µg/ml IgG + IgM f(ab')$_2$ fragment 0-20mins……219

Figure 5.2.5.2IV Peak phosphorylation of pAkt, pBtk/Itk, pERK1/2, pp65NF-κB, pPLCγ2, pSHP-1, pSHP-2 and pSyk in CD19+ PBMC cells stimulated with 10µg/ml IgG + IgM f(ab')$_2$ fragment 0-20mins……220

Figure 5.2.5.3I Change in phosphorylation of pFgr pHck and pSHP-1 in stimulated FcRL4+ PBMCs in response to 50µg/ml HA colostrum IgA IC 0-20mins……222

Figure 5.2.5.3II Change in phosphorylation of pSHP-2 in FcRL4+ stimulated FcRL4+ PBMCs in response to 50µg/ml HA colostrum IgA IC 0-20mins……223

Figure 5.2.5.3III Peak phosphorylation of pFgr, pHck, pSHP-1 and pSHP-2 in stimulated FcRL4+ PBMC stimulated with 50µg/ml HA colostrum IgA IC 0-20mins……224

Figure 5.2.5.5I Comparison of pAkt, pBtk/Itk, pERK1/2 and pFgr staining in *ex-vivo* CD19+ tonsil cells permeabilised with BD Perm III and Perm II……227

Figure 5.2.5.5II Comparison of pHck, pp65NF-κB, pPLCγ2 and pSHP-1 staining in *ex-vivo* CD19+ tonsil cells permeabilised with BD Perm III and Perm II……228

Figure 5.2.5.5III Comparison of pSHP-2 and pSyk staining in *ex-vivo* CD19+ tonsil cells permeabilised with BD Perm III and Perm II ……229

Figure 5.2.6.1I pFgr is higher in FcRL4+ transduced priess, *ex-vivo* tonsil and RA SF cells compared to FcRL4-……234

Figure 5.2.6.1II pFgr does not change in response to BCR stimulation alone and IgA stimulation alone compared to the unstimulated condition……235

Figure 5.2.6.1III pFgr is higher in FcRL4+ *ex-vivo* tonsil cells compared to FcRL4-……236

Figure 5.2.6.2IV pFgr increases in response to BCR and IgA crosslinking compared to BCR stimulation alone in transduced priess cells and *ex-vivo* RA SF……237

Figure 5.2.6.2I pHck significantly increases in response to IgA stimulation alone compared to the unstimulated condition in FcRL4+ *ex-vivo* tonsil cells……239

Figure 5.2.6.2II pHck increases in response to stimulation with HA colostrum IgA alone in FcRL4+ *ex-vivo* tonsil and RA SF cells……240

Figure 5.2.6.2III pHck is higher in FcRL4+ transduced priess, *ex-vivo* tonsil and RA SF cells when in the BCRIgA_c condition compared to FcRL4-……241

Figure 5.2.6.2IV pHck increases in response to BCR and IgA crosslinking compared to BCR stimulation alone in FcRL4+ and FcRL4- transduced priess, *ex-vivo* tonsil and RA SF cells….242

Figure 5.2.6.3I pSHP-1 significantly higher in the unstimulated, BCR and IgA conditions in FcRL4+ transduced priess compared to the FcRL4- transduced priess……244

Figure 5.2.6.3II pSHP-1 increases upon stimulation of the BCR in FcRL4+ and FcRL4- transduced priess, *ex-vivo* tonsil and RA SF cells……245

Figure 5.2.6.3III pSHP-1 significantly higher in the BCR, BCRIgA$_t$, BCRIgA$_s$ and BCRIgA$_c$ and IgA in FcRL4+ transduced priess compared to the FcRL4- transduced priess……246

Figure 5.2.6.3IV pSHP-1 doesn't change in the BCRIgA$_t$, BCRIgA$_s$ and BCRIgA$_c$ compared to the BCR condition in FcRl4+ and FcRL4- transduced priess, *ex-vivo* tonsil and RA SF cells...247

Figure 5.2.6.4I pSyk is significantly higher in the BCR condition in FcRL4+ *ex-vivo* tonsil cells compared to the FcRL4-……250

Figure 5.2.6.4II pSyk increases in response to BCR stimulation and does not change in response to IgA stimulation alone compared to the unstimulated condition in *ex-vivo* tonsil and RA SF cells……251

Figure 5.2.6.4III there is no difference in pSyk in the BCR, BCRIgA$_t$, BCRIgA$_s$ and BCRIgA$_c$ conditions in FcRL4+ and FcRL4- transduced priess, *ex-vivo* tonsil and RA SF cells……252

Figure 5.2.6.4IV pSyk decreases in response to BCR and IgA crosslinking compared to BCR stimulation alone in tonsil and RA SF cells……253

Figure 5.2.6.5I pPLCγ2 is significantly higher in the BCR condition in FcRL4- *ex-vivo* tonsil cells compared to the FcRL4+……256

Figure 5.2.6.5II pPLCγ2 increase in response to BCR stimulation alone and does not change in response to IgA stimulation alone compared to the unstimulated condition in *ex-vivo* tonsil and RA SF cells……257

Figure 5.2.6.5III there is no difference in pPLCγ2 in the BCR, BCRIgA$_t$, BCRIgA$_s$ and BCRIgA$_c$ conditions in FcRL4+ and FcRL4- transduced priess, *ex-vivo* tonsil and RA SF cells……..258

Figure 5.2.6.5IV pPLCγ2 decrease in response to BCR and IgA crosslinking compared to BCR stimulation alone in *ex-vivo* tonsil and RA SF cells……..259

Figure 5.2.6.6I pERK1/2 is higher in the BCR condition in FcRL4- transduced priess, *ex-vivo* tonsil and RA SF cells compared to the FcRL4+……...262

Figure 5.2.6.6II pERK1/2 significantly increases in response to BCR stimulation alone and does not change in response IgA stimulation alone compared to the unstimulated condition in FcRL4+ and FcRL4- *ex-vivo* tonsil cells……..263

Figure 5.2.6.6III there is no difference in pERK1/2 in the BCR, BCRIgA$_t$, BCRIgA$_s$ and BCRIgA$_c$ conditions in FcRL4+ and FcRL4- transduced priess, *ex-vivo* tonsil and RA SF cells……264

Figure 5.2.6.6IV pERK1/2 decreases in response to BCR and IgA crosslinking compared to BCR stimulation alone……..265

Figure 5.3 Schematic of the signalling molecules investigated downstream of FcRL4 and the BCR……..270

Figure 8.2 Gating strategy used for the induced transduced priess cells used in the HA colostrum IgA IC/pHrodo internalisation experiments……292

Figure 8.3 Gating strategy used for the *ex-vivo* tonsil cells used in the HA colostrum IgA IC/pHrodo internalisation experiments……293

Figure 8.4 Gating strategy used for the *ex-vivo* RA SF cells used in the HA colostrum IgA IC/pHrodo internalisation experiments……294

Figure 8.5 Gating strategy used for the induced transduced priess cells used in the PhosFlow experiments……295

Figure 8.6 Gating strategy used for the *ex-vivo* tonsil cells used in the PhosFlow experiments……296

Figure 8.7 Gating strategy used for the *ex-vivo* RA SF cells used in the PhosFlow experiments……297

List of Tables

Table 2.1 Ethics approval reference for the tissue sample collection……..78

Table 2.3 Medias used for cell culture……82

Table 2.4.4 Characteristics of citrullinated enolase-derived peptide……83

Table 2.5.2 Antibodies and washing conditions used to stain for IgA binding in both FcRL4+ transduced priess cells and ex-vivo FcRL4+ tonsil cells……..85

Table 2.6.2I Reagents used for amplification of FcRL4 gene……..88

Table 2.6.2II DNA sequence of primers used to amplify FcRL4 gene and Tet-On lentiviral vector……89

Table 2.6.2III PCR cycle details used for amplification of FcRL4 gene……89

Table 2.6.2IV Protocol used for 1% agarose gel……..89

Table 2.6.5 Protocol used for ampicillin-treated agar plates……91

Table 2.6.6 Protocol used for glycerol stock to freeze successfully transformed bacteria…….93

Table 2.6.7 Protocol used for viral concentration of FcRL4-expressing Tet-On lentiviral vector……94

Table 2.7.1 Antibodies used to stain FcRL4+ cells for separation using the FACS Aria Fusion cell sorter……96

Table 2.8.1 Protocol used for 0.5% collagen gel……97

Table 2.8.2 Antibody used to stain FcRL4+ cells for IgA internalisation experiment……98

Table 2.10.2 Stimulants and the final concentration used to upregulate FcRL4 expression.101

Table 2.10.8 Antibodies and their dilutions used for PhosFlow experiments……106

Table 2.11 Protocol used for buffers and washes……107

Table 2.12 Isotype controls used to check specificity of antibodies used……108

Table 5.2.2 Antibodies and fluorophores tested to stain FcRL4 in FcRL4+ transduced Raji cells and *ex-vivo* tonsil cells treated with BD CytoFix and BD Perm III…….204

Table 5.2.5.4 Antibody dilutions recommended by the company and those that were determined to be best for staining following titration……225

Table 8.1 HLA-typing data from tonsil samples……291

Abbreviations

ABC – autoimmunity-associated memory B cell

ACPA – anti-citrullinated protein antibody

ADE – antibody dependent enhancement

AID – activation-induced cytidine deaminase

APC – antigen presenting cell

APRIL – a proliferation-inducing ligand

BAFF – B cell activating factor

BCDT – B cell depleting therapies

BCR – B cell receptor

BCR-Ag – B cell receptor-antigen

BEV – bacterial extracellular vesicles

CD – cluster of differentiation

CDK – cyclin-dependent kinase

CDR – complement determining region

CMV – cytomegalovirus

CSR – class switch recombination

CVID – common variable immunodeficieny

DC – dendritic cell

DMARD – disease modifying anti-rheumatic drug

DN – double negative

EAE – experimental autoimmune encephalomyelitis

EBV – Epstein Barr virus

EC - extracellular

fDC – follicular dendritic cell

FcR – Fc receptor

FcRL – Fc receptor-like

GC – germinal centre

GWAS – genome wide analysis study

HA – heat aggregated

HIV – human immunodeficiency virus

HLA – human leukocyte antigen

IgA IC – IgA immune complex

IC - intracellular

IFN – interferon

IL – interleukin

ITAM – intracellular tyrosine activating motif

ITIM – intracellular tyrosine inhibitory motif

KO – knockout

mAb – monoclonal antibody

MALT – mucosal associated lymphoid tissue

MBC – memory B cell

MHC – major histocompatibility complex

MS – multiple sclerosis

NK – natural killer

PAD – peptidylarginine deiminase

PB – peripheral blood

PBC – primary biliary cholangitis

PBMC – peripheral blood mononuclear cells

PC – plasma cell

PCA – principal component analysis

PGI – proteoglycan-induced

pIgR – polymeric Ig receptor

PTPN22 – protein tyrosine phosphatase non-receptor type 22

RA – rheumatoid arthritis

RAG – recombination activating gene

RANKL – receptor activator of nuclear factor kappa-b ligand

RF – rheumatoid factor

SE – shared epitope

SF – synovial fluid

SFMC – synovial fluid mononuclear cells

SHM – somatic hypermutation

sIgA – secretory IgA

SjS – Sjögrens syndrome

SLE – systemic lupus erythematosus

T1D – type I diabetes

TCR – T cell receptor

Tfh – follicular helper T cells

Th – helper T cells

TGFβ – transforming growth factor β

TLR – toll-like receptor

TNF – tumour necrosis factor

UNG – uracil DNA glycosylase

1.1 Autoimmune Disease

Autoimmunity is caused by a breach in immune tolerance, which results in recognition of self-antigens and raises a response from the innate and adaptive immune systems. There is usually an induction, propagation and resolution phase although the resolution phase tends to be temporary [1]. Without resolution, there is persistent activation of the immune system against self-antigens, which eventually results in diseases that affects 3-5% of the world's population [2]. Autoimmune diseases can be classified as organ-specific, such as Type I Diabetes (T1D) and Multiple Sclerosis (MS) or systemic, such as Rheumatoid Arthritis (RA) & Systemic Lupus Erythematosus (SLE). Many of them are more frequent in women, for example the male : female ratio in SLE is 1:9, and in RA is about 1:2 [3,4]. The sex bias is not well understood but there is some evidence for a role of androgens and oestrogen in the regulation of the adaptive immune response. While some autoimmune diseases develop at a young age, for example T1D, others, for example RA, become more prevalent at middle age due to ageing of innate and adaptive immune systems [2,5,6]. Autoimmunity is different from autoinflammation, which is mainly caused by inappropriate activation of the innate immune system and often is monogenic [6,7].

Autoimmunity is considered to be caused by a combination of genetic and environmental factors. The biggest genetic contribution to autoimmunity can be found in the HLA alleles, for example HLA-DRB1 is a risk allele where variations in the amino acid sequence, particularly at position 11, 70, 71 and 74, confer a greater risk of developing RA [8]. Other genetic factors that can increase the risk of autoimmunity include polymorphisms in specific genes, such as PTPN-22, which result in defective regulation of immune cells and lowering of lymphocyte activation thresholds [1]. It can also be caused by failed removal of autoreactive B

and T cells, where somatic hypermutations (SHMs) can confer specificity to self-antigens and failure to clear autoreactive cells can occur [7]. There is also epitope spreading where suboptimal epitopes mimic a dominant epitope that expand and diversify and can lead to autoimmunity [2]. Skewing of autoimmune disease towards females has been attributed to expression of immunoregulatory genes on the X chromosome. For example, TLR-7 is an X-linked gene and its recognition of self-nucleic acids has been shown to induce a type I IFN response and its deletion in a lupus mouse model reduced autoantibody titres and overall disease phenotype [6]. Additionally, the presence of oestrogen appears to have an effect on B cell and T cell tolerance [9].

Although genetic factors can predispose individuals to autoimmune disease, environmental factors can activate self-reactive lymphocytes [1]. Usually, autoreactive B and T cells are quiescent due to their exclusion from immunologically privileged sites but can infiltrate upon barrier disruption caused by infection or injury to tissue [6]. The onset of some autoimmune diseases, such as systemic lupus erythematosus (SLE), Sjogren's syndrome (SjS) and multiple sclerosis (MS) has been linked to a bacterial or viral infection prior to induction of autoimmunity [5]. One cause could be molecular mimicry, which is when a pathogenic and self-antigen are similar in structure so that immune cells accidentally recognise the self-antigen on their surface. This has been observed in MS, where myelin epitopes have sequence homology to the opening reading frame in EBV and the myelin may be presented as the antigen instead [10]. Reduced exposure to microbes early in life has been correlated to increased incidences of autoimmunity, which suggest that exposure to a wider variety of pathogens trains the immune system better to recognise the difference between self and non-self[2]. Finally, dysbiosis has been linked to the initiation of autoimmune disease where there is a shift in the microbiota from beneficial to pathogenic subtypes, for example

expansion of *E.Coli* in the gut has been associated with an enhanced Th17 inflammatory response [6]. Additionally, a reduction in commensal bacterial species can alter the metabolites available and as a consequence the composition of the immune system. For example, supplementation of butyrate in an antigen-induced arthritic mouse model increased the suppressive effect of IL-10-producing Bregs and increased the ratio of Bregs to plasmablasts and GC B cells[11]. Overall, autoimmunity is associated with an imbalance between effector and regulatory cells with effector cells dominating immune responses in disease [1].

1.2 Rheumatoid Arthritis

1.2.1 Aetiology, Epidemiology, Risk Factors & Co-Morbidities

RA is a chronic, systemic autoimmune disease where inflammation initially begins in the small finger joints and affects larger joints and then spreads to the vasculature, lungs and skin. Approximately 0.5-1% UK population has RA, a male to female ratio 1:2 and generally affects those who are over 55 years old. Studies in monozygotic twins identified that the genetic risk of developing RA is 30-40% and that first degree relatives of someone who has been diagnosed with RA are at a 3-fold greater risk of developing RA compared to individuals without [12,13]. The chronic inflammation caused by synovitis eventually develops into systemic inflammation throughout the body and increases the risk of developing other co-morbidities. For example, the risk of developing cardiovascular disease is 50% higher and patients are twice as likely to have a myocardial infarction. Additionally, 20-30% of patients develop an inflammatory lung disease as early manifestation of the RA [14,15].

To identify specific genetic risk alleles that could predispose an individual to developing RA, GWAS was performed and >100 genetic loci that were identified as suspected RA-risk alleles [13,14]. Of those identified, the gene associated with most genetic risk is the HLA genes because specific HLA types express the SE, two amino acids at position 70 and 71 in the peptide binding groove that appear to confer stronger binding to citrullinated proteins [12,14]. The shared epitope (SE) has been shown to be most associated with seropositive RA and is expressed in HLA-DRB1 *0101, *0401 and *1001 [12,14,16]. Conversely, individuals that express the HLA-DRB1*1301 allele have a decreased risk of developing RA [14].

Another RA-risk gene is a single nucleotide polymorphism in the phosphatase PTPN22, as it lowers the activation threshold of T cells and increase responsiveness to potentially autoreactive B cells [16]. Additionally, PADI4 is also a risk-allele for RA as it is the enzyme responsible for deiminating arginine- to citrulline-side chains and therefore creating autoantigens [14]. Increased expression of risk alleles for IL-6, STAT4, CTLA-4 and NF-κB have also been implicated as genetic risk factors for RA due to their ability to affect multiple inflammatory pathway's.

There are also environmental risks associated with RA, with exposure to tobacco smoke having the strongest association [14]. Smoking was shown to increase the risk of developing periodontitis and lung disease, which could lead to breaches in mucosal tolerance caused by local inflammation of the mucosal tissue [12–14]. Additionally, exposure to cigarette smoke or coal dust could increase levels of citrullinated proteins, as PAD is upregulated in the lungs [12,13,17].

In the pre-clinical phase of RA, some patients were diagnosed with periodontitis [14]. Additionally, RA patients with periodontal disease were shown to have a higher abundance

of oral bacteria in their blood compared to those with no periodontal disease [18]. A potential breach in mucosal tolerance could be explained by the presence of *P.Gingivalis* in periodontitis. *P.Gingivalis* has been shown to express the bacterial form of PAD and this can citrullinate human as well as bacterial proteins, which could activate the immune system and cause local inflammation in the oral cavity [14]. Interestingly plasmablasts isolated from human RA patients produced autoantibodies directed against citrullinated antigens, which could cross react with citrullinated bacterial lysates *in vitro* but not native bacterial species [18].

Subsets of B cells present in the synovium are overrepresented with an IgA BCR, which suggests that inflammation has been caused by a break in mucosal tolerance, due to IgA-producing B cells being primarily located in the mucosae [17,19]. Additionally, ACPA+ RA was shown to develop more frequently in individuals with elevated levels of IgA+ plasmablasts, suggesting increased immune reactivity at mucosal sites [12,17]. Prior to the onset of RA, the variable region of ACPA-expressing B cells have an N-linked glycan attached, which may enhance its binding to bacterial lectins [18]. In the gut microbiome, there was also expansion of *Prevotella* and *Streptococcus* species, which have been associated with more severe RA [13,18]. One potential way that bacteria are able to transport some of their cellular components to the joint may be through bacterial extracellular vesicles (BEV). BEVs are nanosized EC vesicles with diameters ranging from 20 to 400nm. They are mainly shed by gram negative bacteria. Due to their small size, they are thought to travel freely through host tissues [20]. BEVs from *Kingella Kingae* have been associated with increased joint damage in RA, as their binding to osteoblasts and synovial cells increases production of GM-CSF and IL-6 [20].

1.2.2 Clinical Presentation

Joints are characterised by a cavity surrounded by synovial tissue that is encapsulated by an articular capsule and fibrous connective tissue that attaches to the periarticular bone [21]. This keeps the joint flexible and lubricated for free movement. However, due to an infiltration of inflammatory leukocytes into the synovium, the joints can become swollen and their movement is restricted by the inflammation, known as synovitis [22]. It usually presents symmetrically in multiple small synovial joints, such as the fingers, but progress to the larger joints such as the elbows and knees [23]. There may also be manifestation of rheumatoid nodules in the skin, vasculitis that decreases blood flow and pleural effusions with fluid collecting in the lung pleural cavity [21].

1.2.3 Cellular Presentation

The healthy synovium is a thin layer of connective tissue, with a lining layer approximately 1-3 cells thick, that covers the internal surface of the joint capsule, tendons and bursas. The synovial tissue is mostly acellular apart from the superficial intima that consists of mesenchymal fibroblast and macrophages that work synergistically to lubricate the joint and clear debris. There is also the subintima that contains blood vessels, nerves and lymph vessels [24]. However, inflammation of the synovium causes hyperplasia of the fibroblast-like synoviocytes, causing it to thicken to an 8-12 cell thick layer and increases the infiltration of immune cells that form an invasive synovial tissue called the pannus [12]. Cells in the pannus produce cytokines that perpetuate an inflammatory environment, prevent pro-inflammatory cells from entering apoptosis and cause development of ectopic lymphoid structures [24,25]. The type of inflammatory infiltrate in RA can be subcategorised into lympho-myeloid,

diffuse-myeloid and pauci-immune [26]. Recent PCA analysis of 49 RA samples and 27 normal controls indicated that there was a statistically significant increased CD8+ T cells, CD4+ activated T cells, Tfh cell and M1 macrophages in the synovial samples of RA patients compared to normal controls [27]. More recently, scRNA-seq of 73 RA samples defined 6 major cell types: T cells, B cells, plasma cells (PC), NK cells, myeloid, stromal and endothelial cells [28]. Another cell type important in regulating bone destruction is osteoclasts, which are bone resorbing cells. They differentiate in response to RANKL, which is produced by multiple cell types in the synovium including B cells [29].

1.3 B Cell Development

1.3.1 Formation of the Pre-BCR (VDJ Ligation)

Pro-B cells rearrange their heavy chains by ligating D elements, J elements and the Vh region to form a functional heavy chain, a process which is controlled by RAG (recombination activating gene) enzymes [30,31]. The rearranged heavy chain by VDJ associates with a κ light chain and the Igα/β heterodimer to form the pre-BCR on pre-B cell [31,32]. Early B cell development doesn't appear to depend on association with the Igα and Igβ subunits, as B cells with a truncated BCR were not prevented from maturing into transitional B cells [30]. Subsequently, the κ locus is deleted by the κ deleting element and induces gene rearrangement in the λ chain. The κ light chain undergoes further V-J rearrangement and forms a fully functional BCR, represented as IgM, on the cell surface of immature B cells. This process produces a wide range of BCRs with varying antigen-binding specificities and those that do not recognise self-antigens enter the blood. Self-reactive BCRs undergoing can

undergo a process of further receptor editing [33]. If continued receptor editing still results in a self-reactive BCR, the cell will undergo clonal anergy or deletion[32].

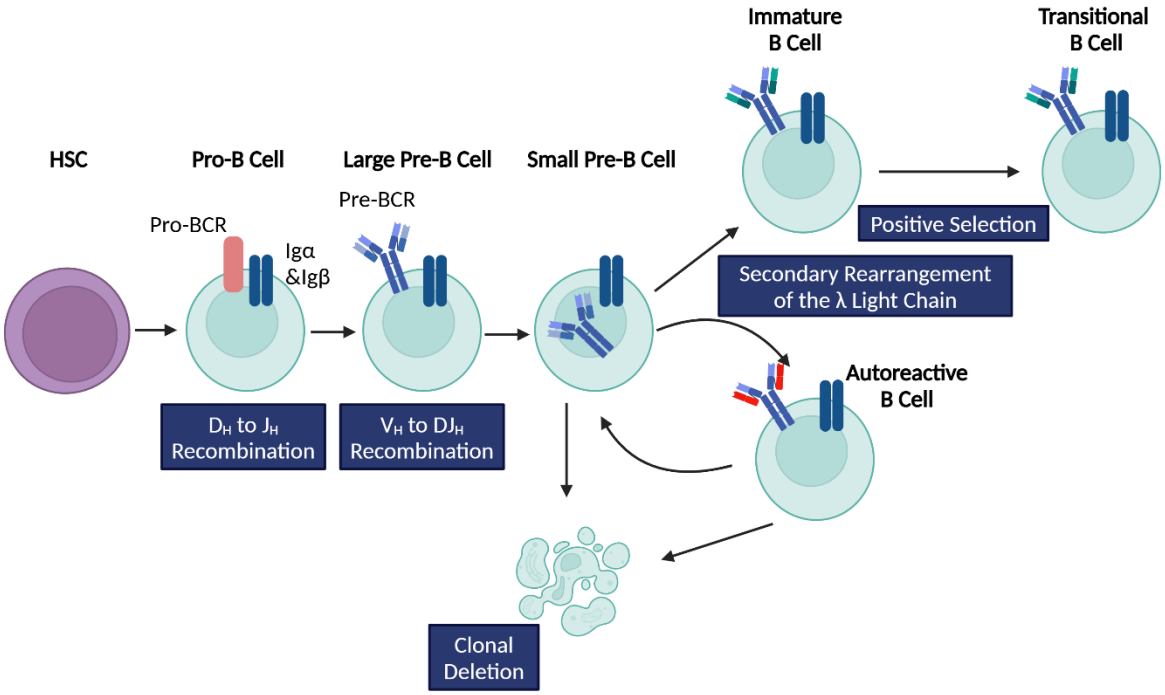

Figure 1.3.1., B cell development in the bone marrow. *B cells develop from the HSC progenitor cell. HSCs differentiate into a pro-B cell that expresses a non-functional pro-BCR and subunits Igα and Igβ. Pro-B cells rearrange their heavy chains under control of RAG enzymes to form a functional heavy chain. The rearranged heavy chain associates with a κ light chain and the Igα/β heterodimer to form the pre-BCR on pre-B cells. The κ locus is deleted and induces gene rearrangement in the λ chain, also controlled by RAG enzymes. The formation of the pre-BCR triggers tonic signalling in small pre-B cells. Non-autoreactive B cells receive a positive survival signal and enter the transitional B cell pool. Small pre-B cells that express an autoreactive or underactive BCR undergo secondary rearrangement of the λ light chain until either a non-autoreactive BCR is generated and positively selected or it is clonal deleted/rendered anergic. The functional BCR expressed on immature B cells is represented as an IgM.*

1.3.2 B Cell Migration

Immature B cells enter circulation and home to the spleen and lymph nodes from the bone marrow [34]. They only survive for 1-4 days as they are highly susceptible to apoptosis in response to BCR stimulation [30]. This is because approximately 40% of transitional B cells express a self-reactive BCR. Expression of a functional BCR is important as ablation experiments demonstrated a rapid loss in mature B cells when the BCR was ablated in the peripheral B cell population [30]. Immature B cells will either differentiate into T1 or T2 transitional B cells, with the latter entering the follicular niche, becoming a naïve B cell [30,32].

1.3.3 B Cell Activation

Naïve T cells circulate through the lymphatic system and migrate through the T cell zone until they encounter their specific antigen presented on dendritic cells (DCs). They are activated and upregulate CXCR5 so they can migrate towards the follicle in response to CXCL13 [32,35–37]. Naïve B cells concentrate in the interfollicular zone where they bind their antigen presented by a follicular dendritic cell (fDCs) or macrophages. Once activated, naïve B cells upregulate CCR7 and CXCR5 to bind CXCL13 and migrate to the region between the follicle and T cell zone [37]. B cells interact with their cognate T cells through antigen presentation and if successful, its survival is promoted through CD40/CD40L interactions [38]. Additional interaction with ICOS/ICOSL ensures terminal differentiation of the T cell into a Tfh cell by increasing expression of Bcl-6, PD-1 and GL7 [36].

The activated naïve B cell then re-enters the interfollicular region and begins to aggregate and begin to form a germinal centre (GC) [36]. Tfh cells entered the follicle after in larger

numbers but remain largely diffuse in the follicle whilst B cells aggregated into GC's [36]. Bcl-6+PD-1+GL-7+ cells enter the GC whilst the PD1-CXCR5- Tfh relocate back to the T cell zone [36].

Some B cells that engage with their cognate antigen transiently will differentiate into short-lived plasmablasts and produce low affinity antibodies that can begin to neutralise their pathogen. Additionally, marginal zone B cells can also differentiate into plasmablasts and produce low affinity antibodies directed at T-independent antigens [30,39,40]. Interestingly, one group has suggested that some naïve B cells that express a high affinity BCR favour plasmablast differentiation over becoming a GC B cells or memory B cells (MBC)[41].

1.3.4 Affinity Maturation

GCs are transient structures with a specialised microenvironment that form in secondary lymphoid tissue, such as the lymph node, spleen or Peyer's patches, where activated B cells undergo multiple rounds of receptor refinement to produce a BCR with the highest affinity for its antigen [34,42]. In some autoimmune disease, such as RA and SjS, tertiary lymphoid structures develop in at the site of inflammation and contain GCs. These more frequently generate autoreactive B cells due to the lacking checkpoints and producing a greater amount of survival factors [43].

The GC is polarised into 2 zones: the dark and light zone. Polarisation of the GC results in appropriate temporal intervals between SHM and removal of autoreactive clones, which prevents premature egression from the GC [42]. The dark zone is densely packed with centroblasts and is rich in CXCL12 that binds to CXCR4 on centroblast so they are retained

long enough to introduce SHMs. The light zone contains centrocytes, fDCs, macrophages and Tfh cells and is rich in CXCL13, which binds to CXCR5 on centrocytes and promotes their migration to the light zone [43].

In the dark zone, centroblasts rapidly proliferate and diversify their BCR by introducing SHMs into their Vh gene, creating a broad range of clones with varying specificity towards its antigen [42]. Experimentally, a significant increase in SHMs was observed 10 days post-immunisation in high affinity cell populations [44]. Centroblasts that have a low affinity BCR may enter apoptosis because higher affinity centroblasts are clonally expanding at a higher rate and therefore suppress lower affinity centroblasts [45]. Activation-induced cytidine deaminase (AID) is an enzyme that is critical for introducing SHMs as it deaminates cytosine to uracil in the Igκ and Igλ chain, creating a mismatch with guanine. The presence of uracil recruits uracil DNA glycosylase (UNG) to the damaged DNA, and converts it to an abasic site which initiates either base excision or the mismatch repair mechanism [46]. Extrafollicular plasmablasts are also capable of introducing a small proportion of SHMs into the Vh gene of their BCR, as they express AID but this happens more often when it is chronically challenged by its antigen [45].

Upon expansion, centroblasts differentiate into centrocytes and migrate to the light zone where the most specific clone is selected [42]. The centrocytes interact with FDCs who carry captured native antigen on their surface and those centrocytes that express highest affinity BCR will capture, process and present the antigen on its surface. It then interacts with its cognate Tfh cell and forms a connection via CD40/CD40L. The CD40/CD40L stabilise the B cell/T cell interaction and provides pro-survival signals to the centrocyte and positively selects it [32,39]. As an extra selection pressure, some centrocytes become PCs that produce

antibodies with increasing affinity to compete with centrocytes for antigen binding. This ensures that the centrocyte with the highest affinity BCR is positively selected [42]. Interaction of centrocyte and Tfh cell can also negatively select low affinity BCRs and those that are autoreactive. This is in part controlled by CD95 (Fas), which induces apoptosis in centrocytes that fail to interact with the Tfh cell and prevents accumulation of autoreactive B cells.

B cells that are positively selected will upregulate CXCR4 and migrate back to the dark zone in response to CXCL12 and will undergo multiple rounds to refine the affinity of the BCR. This is known as affinity maturation.

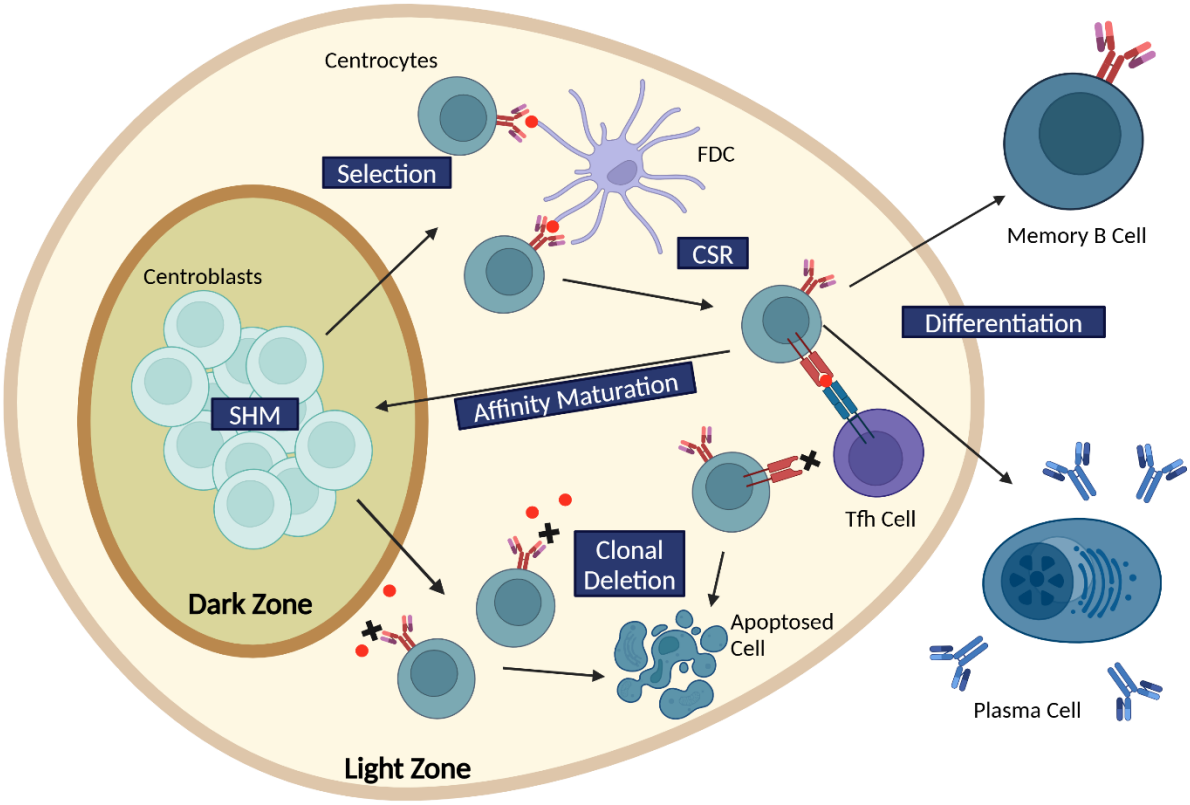

***Figure 1.3.4., B cell development in a germinal centre**. Once activated by their cognate T cells, B cells differentiate into centroblasts that are positioned in the dark zone of the GC. Centroblasts proliferate rapidly and introduce SHMs into their BCR via AID. The cells then differentiate into centrocytes and enter the light zone. Centrocytes interact with fDCs and Tfh cells and the clone expressing the highest affinity BCR is positively selected. Centrocytes expressing autoreactive or low affinity BCRs are clonally deleted. Centrocytes can either re-enter the dark zone to refine their BCR by affinity maturation or they can induce CSR, to isotype switch the immunoglobulin expressed. Positively selected centrocytes can then exit the germinal centre and differentiate into a memory B cell or a long-lived plasma cell Adapted from McHeizer & Williams.*

1.3.5 Class Switch Recombination

To allow antibodies to deliver a range of effector mechanism and access to sites such as mucosal surfaces, B cells undergo class switch recombination (CSR), changing their immunoglobulin from IgM to IgG, IgA or IgE. Immunoglobulins subclasses are defined based on what constant region is expressed in their heavy chain. CSR itself will not lead to a change in the antigen-binding region [47]. Like SHMs, CSR is controlled by AID and UNG, which is critical for CSR, as UNG-/- mice only class switched to IgG1 in 1-2% of their splenic B cells due to being incapable of removing uracil bases [46,48]. AID substitutes cytosine with uracil and initiates base excision repair or the mismatch repair pathway, which creates a double stranded DNA break between switch regions and allows them recombine upstream of the constant heavy chain exons [46,47]. The immunoglobulin class that the B cell decides to switch to is in part controlled by cytokine produced by Tfh cells. For example, IL-4 can direct switching from IgG1 to IgE via STAT6 whilst TGFβ can induce class switching to IgA via SMAD3, 4 and RUNX in the mucosae [47,48]. This process is irreversible, as excision of the switch region for IgM is permanently excised out of the DNA and another switch region takes its place. CSR can also happen independently of T cells, as B cells that recognise bacterial cell wall polysaccharides are switched to the IgG1 isotype. This is most likely via TLR signalling, as deletion of TLR's reduce serum IgG antibody levels. They can also enhance class switching to IgG3 or IgA when synergised with the BCR and co-stimulated with IL-4 or TGFβ respectively [47].

1.4 B Cell Subsets

1.4.1 Pro, Pre & Immature B Cells

B cells are derived from the haematopoietic stem cell lineage in the bone marrow and initially differentiate into pro-B cells. Commitment to the B cell lineage is controlled by E2A transcription factor family, which upregulate Pax5. Pax5 is an essential for B cell lineage commitment and therefore is expressed throughout B cell development [49]. Pro-B cells differentiate into pre-B cells once they express the pre-BCR and is reliant on subunit Igα for maturation, as truncation of its cytosolic tail prevented B cell development [50]. At this stage the subunit Igβ is redundant. Once the cells undergo VDJ rearrangement and the BCR is expressed as an IgM it becomes an immature B cell. These cells are CD24+CD10+.

1.4.2 Transitional & Naïve

As mentioned previously, transitional B cells can be categorised as T1, defined as IgM+IgD-CD23-CD21-CD35-, or T2, defined as IgM+IgD+CD23+CD21+CD35+. Both T1 and T2 transitional B cells also express CD14 and CD18 [40]. T2 transitional B cells either differentiate into a long-lived follicular B cell, which are responsible for development of the adaptive immune response through T cell activation or a marginal zone B cell, where they filter blood for foreign antigens. The latter were defined by expression of AA4, as it is marker for non-proliferative cells that defines marginal zone B cell precursors [30].

Naïve B cells maintain expression of CD10, CD21 and IgM but can be differentiated from CD27- B cells by their expression of the protein ATP-binding cassette B1 transporter [40]. If the

naïve B cell is autoreactive, they downregulate anti-apoptotic genes Bcl-Xl and A1 in response to negative selection from signals through their BCR.

1.4.3 Marginal Zone

Work done in mice found that marginal zone B cells diverge from naïve B cells at the transitional stage in the spleen and their development is maintained by Notch2 signalling [40]. Interestingly, their BCR also have a shorter CDR3 compared to naïve B cells, which may determine their reduced response to antigen and direct them to a marginal zone fate [40]. A human marginal zone B cell population has been described to be IgM+IgD+CD27+ [51]. They can be differentiated from mantle zone B cells by their higher expression of CD21 and CD1c. During development, marginal zone B cells downregulate expression of CD5, CD9, CD10 and CD23. Marginal zone B cells also appear to be a clonally expanded population although there are far less proliferation Ki67+ cells compared to adjacent GC B cells[40]. However, marginal zone B cells undergo clonal expansion, as an expanding IgM+IgD+CD27+ MBC pool has been observed, albeit at a two-fold lower mutational frequency than isotype-switched MBCs [40].

1.4.4 Centroblasts & Centrocytes

In the GC, both centroblasts and centrocytes have increased expression of Bcl-6 to aid their survival [42]. AID is highly expressed in both centroblasts and centrocytes due to its central role in SHMs and CSR. This is regulated canonical (p65) and non-canonical (p52) NF-κB signalling as well as Bcl-6, which positively regulates AID expression by repressing microRNAs that inhibit its function [48].

Centroblasts express CXCR4, CXCR5 and Ki67, which defines their highly proliferative capacity and their retention in the dark zone. They also downregulate surface proteins that are required for Tfh cell interaction, such as CD83, Ly5 and Slamf1 [52]. Upon entry to the light zone where the centroblasts become centrocytes, CXCR5 and Ki67 are downregulated whilst CD83, ICOSL, IL-21R, BAFFR and Slam1 are upregulated, to allow centrocytes to interact with Tfh cells [52]. ICOS is also important for the generation of high affinity MBCs [45].

Once centrocytes have matured and refined their BCRs, they downregulate expression of AID & Bcl-6 to prevent further DNA mutations and allow them to leave the GC whilst genes, such as cFLIP are unregulated so they are resistant to Fas-induced apoptosis [32,42,45,53]. PD-1 signalling in Tfh cells is important in the differentiation of centrocytes into long-lived PC generation via IL-21 [45,54].

1.4.5 Extrafollicular Memory & Plasma Cells

Extrafollicular MBCs express IgM, lack SHMs, and are not involved in long-term immunological memory whilst the PCs produce low-affinity antibodies that neutralise pathogens by binding to different epitopes [39,42,55]. PC are defined by surface expression of CD138 and CD44 [51]. Additionally, they express low levels of Bcl-6 due to developing independently of the GC and express high levels of CD95, which makes them susceptible to apoptosis [51,55,56].

1.4.6 Memory B Cells

MBCs are part of the reactive phase in humoral immunity, as they have a stem-like quality that allows them to maintain themselves for long periods of time and to differentiate rapidly into long-lived PCs upon secondary exposure to an antigen [39]. MBCs have a lower threshold for antigen stimulation compared to naïve B cells, which allows them to rapidly proliferate and differentiate in response to a second challenge [45]. They also tend to express IgA, IgG or IgE, which have longer cytosolic tails that increases their sensitivity to an antigen [57]. Rechallenged MBCs will modify their BCR and aggregate into a GC in order to refine the specificity of their BCR to the antigen [52].

Classically, CD27 is used to define MBCs and those that express CD27 exclusively express mutated immunoglobulins [51]. However, some IgG1+ and IgG3+ class switched MBCs do not express CD27. MBCs also express higher levels of CD80, CD86 and 95 than IgD+ naïve cells whilst they have lower expression of CD23 [51].

1.4.7 Long Lived Plasma Cells

Long lived PCs contribute to the constitutive phase in humoral immunity, as they produce high affinity antibodies that neutralise pathogens and are able to do so rapidly before symptoms of illness can occur upon secondary exposure [39]. Cells that differentiate into PCs express the highest affinity BCR, BLIMP1 and XBP1 in response to IL-21 [51,58]. This was confirmed in mice deficient for the IL-21R, as they had low numbers of PCs and increased number of MBCs [51]. Their selection also is driven by BAFF and APRIL whilst IL-6 and CXCL12 assist with the induction of PC differentiation as well as their ongoing maintenance [51]. Long-

lived PCs also express CD138, CD27, IRF4, as well as CD38, which confirms their relationship to the GC [26,39,49]. However, one group has proposed that PCs do not express CD38 until they have emigrated to the bone marrow, as tracking of a CD38- group found that they upregulated it once they differentiated in the bone marrow [51]. Differentiation of PCs reduces expression of CD20, which means they are not depleted by current BCDT's that target CD20.

Once they have migrated to the bone marrow for long term maintenance, PCs upregulate cell cycle arrest genes, such as CDK's and do not express Ki67, a marker of proliferation [51]. They also begin to alter their BCR, as the BCR complex subunits Igα and Igβ are downregulated meaning that it can no longer signal through the BCR [51].

1.4.8 Autoimmunity-Associated Memory B Cells

Autoimmunity-associated B cells (ABCs) are a MBC population expanded in chronic and autoimmune disease, which have a reduced ability to respond to antigenic stimulation, which impacts long-term immunity and generation of long-lived PCs [59]. They were originally referred to as age-associated B cells as they were expanded in older populations. However, there is no correlation between age and the frequency of ABCs, meaning that they are more often called autoimmunity-associated B cells due to their expansion in autoimmune disease [60]. Usually, ABCs make up 3-5% of the circulating peripheral B cell population but in cases of chronic and autoimmune disease this increases up to 50% [59,61]. Genome-wide expression profiling has identified that ABCs are transcriptionally different to naïve and MBCs but are similar in HIV, malaria and RA patients [59]. Additionally, single cell transcriptomics determined that ABCs were not enriched in the DN B cell population and were found to primarily be switched MBCs [17,26]. However, in some cases ABCs are defined as CD27- [60]. ABCs

characterised in peripheral blood (PB) taken from a murine lupus mouse model found that the IgM+ ABC population could be split into a CD80+PD-L2+ group and a CD73+CD80+ group, which is a phenotype associated with secondary PC generation. Additionally, ABCs characterised in early RA patients expressed higher levels of PC markers PRDM1, BLIMP1 and XBP1 than naïve B cells, suggesting that ABCs are capable of differentiating into PCs [60,62].

ABCs are characterised as CD21-, CD11c+ and T-bet+ as well as expressing FcγRIIα, FcγRIIβ, FcRL3, FcRL4 and FcRL5 [59,60,63]. In the case of FcRL's their expression appeared to be influenced by anatomical location, as FcRL3 and 5 were more highly expressed on ABCs in the PB whilst FcRL4 was more highly expressed in synovial fluid (SF) ABCs [60]. Interestingly, ABCs in SF expressed more IgG and IgA than ABCs in the peripheral blood. There is greater expression of CXCR3, CXCR4 and CXCR5, which indicates that ABCs have a migratory capacity towards sites of inflammation [60]. ABCs can be subcategorised into resting (CD86-MHC-II-) , and activated (CD86+MHC-II+Fas+) [61].

The reduced responsiveness of ABCs is reflected in their inability to produce high levels of cytokines. Compared to naïve and MBCs, ABCs produced lower levels of IL-6, IL-10 and TNFα. This was confirmed by a group that took ABCs from healthy donors and seropositive RA patients and stimulated with anti-BCR and CpG. They observed similar production of IL-10 and IL-6 after 24h and IL-10 and TNFα after 72h [64]. Clustering analysis identified an ABC population enriched in samples from malaria exposed patients and that crosslinking of the BCR with soluble anti-Ig saw an enrichment in genes associated with the IL-10 inflammatory pathway[65].

In HIV, ABCs in patients with high viraemic load are associated with a reduced ability to proliferate upon crosslinking of the BCR, which results in reduced production of cytokines

and antibodies [59]. However in RA and hepatitis C infection, expansion of the ABC compartment was associated with increased production of proinflammatory cytokines and autoreactive antibodies [59,61]. FcRL5+ ABCs in malarial patients were unable to secrete of antibodies in response to crosslinking with the BCR and CpG [59]. The lack of responsiveness in ABCs taken from murine lupus mice PB initially suggested that these could be a functionally anergic autoreactive B cell population. However, crosslinking of the BCR with an anti-IgM indicated hyperresponsiveness, as demonstrated by rapid Ca^{2+} flux, which suggested that ABCs may play an active role autoimmune disease [62].

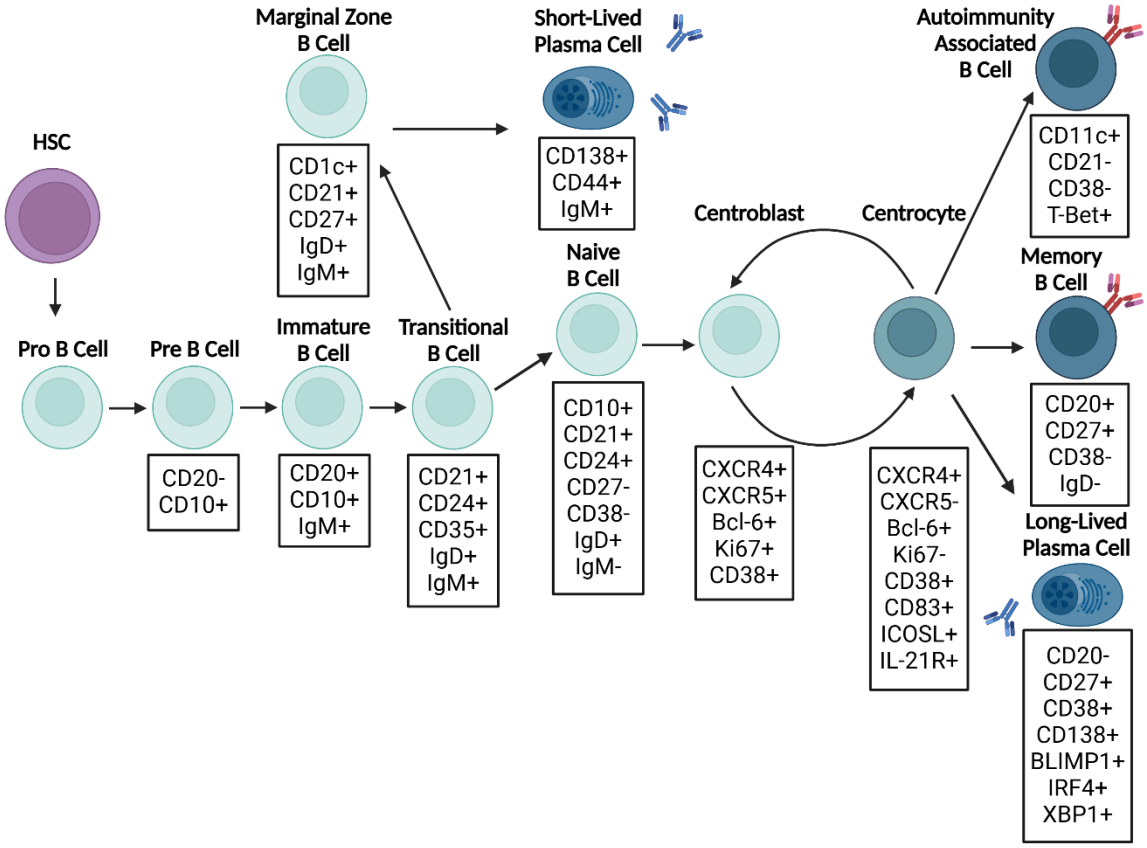

Figure 1.4., Markers expressed through B cell development. *B cell development begins in the bone marrow where HSCs differentiate into a pro-B cell and progress to transitional B cell stage upon positive selection of a functional BCR. Transitional B cells initially circulate until encountering their antigen where they migrate to secondary lymphoid organs and form germinal centres. B cells undergo multiple rounds of SHMs and positive selection by fDCs and Tfh cells until a high affinity BCR is generated. B cells then undergo CSR and either differentiate into a memory B cell and long-lived plasma cell. Naïve B cells can also differentiate into marginal zone B cells that contribute to the extrafollicular response by differentiating into short-lived plasma cells.*

1.5 B Cell Function

1.5.1 B Cell Signalling

B cell signalling is important for proliferation, differentiation and maturation of B cells. Generally, there are no significant differences in phosphorylation kinetics between naïve and MBCs but activation signals are increased in the GC MBCs, as they express more class switched immunoglobulins, which have longer cytoplasmic tails that enhance BCR signalling [66]. This enhanced signalling is characterised by increased calcium mobilisation in MBCs that express IgA or IgM compared to naïve B cells [66]. Usually when an antigen binds to the BCR, the BCR undergoes conformational change and forms a heterodimeric complex with the transmembrane proteins CD79a and CD79b, Ig-α and Ig-β respectively [50,67]. Igβ can act as an amplifier for Igα phosphorylation, as it can increase receptor sensitivity and lower its activation threshold [50]. However, Igβ may have a redundant function in the early B cell development stages, as its deletion in pre-B cells did not prevent them from maturing further. In contrast, intact Igα is required for pre-B cell maturation, as expression of an Igα with a truncated cytosolic tail could not mature [50].

The BCRs cytoplasmic domain contains intracellular tyrosine activating motifs (ITAMs) that recruit Lyn upon phosphorylation. This can recruit and phosphorylate tyrosine kinase Syk and Btk [68]. Syk can also recruit Btk, which acts as an adapter protein for kinases such as Akt, Vav, Nck, Grb2 and PLC-γ2. PLC-γ2 is important in maintenance of MBCs, as inducible deletion of PLC-γ2 significantly decreased the size of the IgG1+ MBC compartment [39]. Vav and Nck are involved in remodelling of the actin cytoskeleton whilst Grb2 activates the Ras pathway [50]. These signalling proteins activate downstream effector proteins NF-kB and MAPK, which translocate to the nucleus and effect the transcriptional profile of the cell. Akt

is also involved in the activation of NF-kB [66–68]. Using electron microscopy, phosphorylation of Lyn could be detected as early as 30 seconds [69]. Src kinases can also inhibit BCR signalling if they are activated by a co-receptor that has phosphorylated intracellular tyrosine inhibitory motifs (ITIMs)[68].

One of the roles BCR-antigen binding plays in the development of autoreactive B cells it that engagement of immature B cells with a self-antigen prevents them from downregulating CXCR4, which prevents them from moving out the bone marrow into the circulation [70]. Activation of ERK and calcineurin can also prevent immature B cells from progressing further as they induce anergy in autoreactive B cells [50]. Additionally, BCR signalling can induce apoptosis in self-reactive transitional B cells and reduce the population by 50% [70]. B cell signalling is also important in the survival of mature B cells, as conditional deletion of the BCR using IFNγ resulted in apoptosis of peripheral B cells [50]. Antigen binding is also important for regulating signalling in mature B cells, as engagement of the BCR increases phosphorylation of Syk, which initiates autophagy through Nrf2. If inhibited there is reduced autophagy and subsequent cell death, indicating an important role for Syk in cell survival [71].

BCR signalling is important in antigen internalisation and loading. It determines the antigen presenting capabilities of B cells, as B cells that are able to form more complete, high affinity interactions with their antigen will generate a more robust signal through their BCR [72]. Additionally, the signalling checkpoints spatially and temporally regulate the internalisation and subsequent trafficking of the BCR from the membrane to the endosomal compartments. Work done in mice showed that phosphorylation of Lyn and Syk coincide with the initial internalisation of the BCR-Ag complex [69]. This signal is sustained until the BCR-Ag has reached the early endosomal compartment, as pLyn and TfR, an early endosomal marker,

were colocalised. There is also upregulation of HLA-DO and MHC-II to prepare for antigen presentation [34]. pLyn and pSyk are downregulated upon entry to the early endosome whilst pJnk, pERK and pp38-MAPK were upregulated 5 minutes post-BCR stimulation and phosphorylation was sustained for up to 30minutes. The increase in pERK phosphorylation appears to influence the MHCII-rich compartment of the endosome, as it is localised around multivesicular bodies, where the antigen is loaded onto MHC-II[34,69,73]. As the BCR is trafficked through the early endosome, pJnk and pp38-MAPK begin to colocalise with LAMP1, a lysosomal marker [69]. However, when actin polymerisation or dynamin were inhibited, internalisation of the BCR was inhibited and signalling molecules hyperphosphorylated and colocalised with the cell membrane resulting in dysregulation of spatial phosphorylation [69].

1.5.2 Autophagy

Autophagy is a highly conserved mechanism that maintains cellular health by recycling and degrading dysfunctional components of the cytoplasm and plasma membrane. Autophagy is at its highest in the early stages of B cell development and declines as the cell matures[74]. It is initiated by vesicle nucleation at the plasma membrane.LC3-I is converted to LC3-II by ATG5 in the inner and outer leaflet of the autophagosome as the nucleated vesicle expands [75–77]. Other proteins such as ATG7, ATG12 and Beclin-1 are important for double membrane formation in the autophagosome and are vital for autophagic nucleation [71,77]. Next, the autophagosome is trafficked into the cell and fuses with endosomes and lysosomes to form the autophagolysosome, where cellular components are either degraded to be used as fuel by the cell or loaded onto MHC-II molecules to be presented on the surface [77]. Autophagy is

positively regulated by transcription factors, such as Nrf2, that upregulate expression of autophagic factors but is negatively regulated by anti-apoptotic proteins such as Bcl-2 and p62 that arrest autophagy and prevent autophagosome formation [71]. Additionally, autophagy can be regulated by cytokines such as TNFα, which increased the rate of autophagy and the number of autophagosomes in fibroblast-like synoviocytes through increased NF-κB signalling whilst BAFF inhibited autophagy by decreasing phosphorylation of ULK1, a complex protein involved in autophagosome formation [74–76].

If autophagy is impaired, B cells will develop normally but fewer MBCs are maintained over time and there is a reduced response to secondary antigenic stimulation. This is thought to be caused by a metabolic shift from oxidative phosphorylation to glycolysis, as a result of damaged mitochondria and this causes the cells to become less efficient at rapid proliferation and antibody production[74]. Binding of an antigen to the BCR appears to act as a molecular switch that causes the cell to favour receptor-mediated endocytosis rather than autophagy [74,78].

1.5.3 Antigen Presentation

Antigen presentation by B cells has primarily been attributed to their positive or negative selection in GCs to select cells capable of producing high affinity antibodies. Unlike DCs and macrophages that capture antigens by phagocytosis or fluid phase pinocytosis, B cells express a clonally restricted BCR on their surface, which allows them to bind a specific antigen and internalise it by receptor-mediated endocytosis [34,73,79–82]. This method of antigen capture is thought to be 100-10,000-fold more efficient than non-BCR mediated antigen capture and allows B cells to initiate an immune response at lower antigen

concentrations [80–82]. B cells are localised in draining lymph nodes, marginal zones and epithelia to detect pathogens whilst DCs and macrophages are involved in peripheral surveillance in tissues such as the skin and gut [81,83].

The chance of B cells encountering their cognate T cell is a $1x10^8$. This occurs at the boundary of B cell/T cell zone in secondary lymphoid structures, which is enhanced by expression of MDC, MIP1-α and MIP-1β by B cells and CXCR5 by T cells [84]. Once captured, the BCR-Ag complex is internalised and trafficked to an MHC-II rich compartment of the endoplasmic reticulum ER. MHC-II is associated with the invariant chain Ii, which is cleaved by cathepsin S and L to yield CLIP. CLIP occupies the MHC-II binding groove to prevent premature peptide. This is assisted by DO, a protein that inhibits DM from assisting peptide loading outside of acidic cellular compartments [34]. In the presence of the BCR-Ag, DO stops inhibiting DM, which allows the antigen to be loaded onto MHC-II molecules [34,73,79]. The antigen-loaded MHC-II is then trafficked to the cell surface. There is also upregulation of CD86, CD80 and CD40 to interact with CD28, CTLA-4 and CD40L on T cells [34,85].

Engagement of CD40 with CD40L stabilises the immunological synapse and induces rearrangement of their plasma membrane to favour antigen presentation[34,73]. It also matures the B cell into an antigen presenting cell (APC) and promotes its survival, as gene enrichment analysis of CD40L stimulated B cells showed downregulation of genes associated with apoptosis [86]. Interestingly, there is also downregulation of genes associated with antigen uptake and BCR signalling, as they are no longer a required once the antigen is recognised by its cognate T cell [86]. CD80 and CD86 are equally important for stabilising of the B cell/T cell interaction, as cells treated with anti-CD86 and anti-CD80 resulted in an 80% reduction in T cell proliferation 8 days post-immunisation [85].

Antigen presentation by B cells was initially observed when B10.A (B cell competent) and µMT (B cell deficient) mice were challenged with cytochrome c. T cell response was 75% less in µMT mice compared to B10.A mice indicating that T cell response was controlled by B cells. Additionally, when µMT were transfected with immunised CD86+ B cells, they increased T cell proliferation and response [85]. B cells may have a role in T cell priming, as adoptive transfer of antigen-specific B and T lymphocytes to a lymphocyte deficient mice was sufficient to prime T cells in the absence of macrophages and DCs [34]. Another study in mice observed decreased activation of T cells in B cell KOs, which could be restored upon adoptive transfer supporting their role in T cell priming and activation [87]. However, B cells are not required for T cell priming, as a separate B cell-deficient mouse model had primed T cells [34].

Studies exploring the role of B cells as professional APCs mainly focussed on viral infectious models [81]. To investigate their antigen presenting capabilities, WT and Myd88-/- mice were immunized with Qβ-Ova-VLP and then injected with naïve ovalbumin-recognising CD4 T cells. Ovalbumin-recognising CD4 T cells differentiated into Tfh cells in WT mice, whilst Myd88-/- mice had impaired T cell proliferation. To confirm if B cells were responsible, naïve OT-II CD4 T cells were transferred into a transgenic mouse, which lacked the antigen-specific BCR. Immunisation of these mice resulted in impaired differentiation of naïve CD4 T cells to Tfh, indicating that B cells presented the antigen to CD4 T cells to initiate proliferation [81]. This was repeated with a separate antigen and similar results were observed. Additionally, when mice deficient for DCs were immunised, there was no impairment of Tfh proliferation, indicating DCs were not acting as professional APCs [81].

1.5.4 Cytokine Production

In autoimmune diseases, B cells are able to produce cytokines such as IL-1, IL-6, IL-10, IL-12, GM-CSF, RANKL and TGFβ, which mediate T-cell, DC and osteoclast function, regulate wound healing and control lymphoid tissue development and organisation [76,88,89]. This was demonstrated in mice that had their B cells depleted, as they had impaired lymphoid tissue organogenesis, reduced thymocyte numbers and defects in their spleen and T-cell compartments as well as disrupted GC networks caused by a reduction in the number of fDCs [87,88,90]. Another study in mice found that mice which possess no IL-6 producing B cells had greater reduction in disease severity compared to WT mice after challenge with EAE [91]. In contrast, when CD86+ B cells from seropositive RA patients were stimulated *in vitro* with anti-IgM/IgG and CpG for 72h, they did not produce significantly higher levels of IL-6 or TNF-α compared to B cells from healthy control individuals suggesting that certain subsets of B cells are responsible for producing high levels of proinflammatory cytokines [64].

BAFF is another cytokine that is important for B cell survival and proliferation and its presence positively correlates with autoantibody levels and synovitis in early RA patients [38,92]. In contrast, it appears to determine which B cells survive, as autoreactive B cells are negatively selected due to their poor ability to capture of BAFF compared to their non-autoreactive counterparts [70].

Not all B cells that produce cytokines are thought to be pro-inflammatory, as IL-10 produced by Bregs is able to expand Tregs, which was confirmed by an adoptive transfer experiment of Bregs into an arthritic mouse model [54]. Additionally, the presence of IL-10 producing Bregs suppress inflammation in a murine inflammatory arthritis model [88]. Therapeutically, IL-10 has been shown to be important in restoring homeostasis as B cell depleting therapy

restored the IL-10-producing peripheral B cell population in patients with active MS and improved disease phenotype in SLE patients treated with an IL-10 mAb [54,88].

1.6 B Cell in RA

1.6.1 B Cell Role in Immune Tolerance & Autoimmunity

Approximately 50-75% of B cells generated in the bone marrow are autoreactive but are prevented from maturing at a number of checkpoints [93]. Central tolerance deletes autoreactive B lymphocytes in the bone marrow whilst peripheral tolerance involves a range of mechanisms. For example Tregs have been proposed to remove autoreactive B cells through immune surveillance [2,94]. Peripheral tolerance involves interaction of CD40 on B cells with CD40L on T cells, as CD40L deficient patients had a higher frequency of polyreactive mature naïve B cells compared to healthy patients, indicating CD40/CD40L is also important in the maintenance of Tregs, as they fail to develop in its absence [38]. MHC-II is also important in negative selection of autoreactive B cells[38]. Additionally, autoreactive B cells are identfied at the entrance into primary follicles, entrance to the GC, by fDCs and Th cells on the T/B cell border [32,33,95]. If they are detected, they either undergo anergy or receptor editing, which aims to rearrange the κ light chain genes until they no longer react to a self-antigen [32,33,93]. T cells are selected in the thymus where autoreactive T cells are negatively selected in the thymic medulla whilst the non-autoreactive are positively selected in the thymic cortex. If they evade negative selection in the thymus, they are either deleted or made anergic [2]. The initial loss of tolerance is caused by SHM, which introduces mutations into the BCR gene and can cause autoreactivity. BCR signalling is important in maintaining central tolerance, as mutations in downstream molecules such as Btk and AID were

negatively correlated with the maintenance of central tolerance [94,96]. Additionally, BCR signalling was abrogated by a mutation in the PTPN22 allele [94].

In RA, a loss of tolerance is characterised by the development of persistent synovitis that perpetuates systemic inflammation of the joints [33]. This development can be partially attributed to changes in the B cell compartment. RA patients have elevated levels of autoreactive transitional and naïve B cells, ectopic GCs that generate autoreactive B cells and an altered MBC compartment [26,94,95,97–99]. When MBCs from synovial tissue were compared between ACPA- and ACPA+ patients there was no significant difference in the total frequency of MBCs but a significantly higher proportion of switched, IgD-CD27+, and double negative (DN), IgD-CD27 MBCs were present in ACPA+ RA patients compared to ACPA- [26,98]. Single transcriptomic analysis of B cells from synovial tissue identified elevated levels of HLA-DRB1, CD40, CD80 and CD86 suggesting these B cells have the potential to interact with T cells in the synovium [26,58].

Autoreactive B cells also exacerbate inflammation by producing specific cytokines. mRNA cytokine profiling of immune cells identified B cells as a significant source of RANKL in the synovium, which promotes osteoclastogenesis and inhibits osteoblast differentiation [29,58,100]. To confirm this, switched MBCs, IgD-CD27+CD95+, were co-cultured with monocytes and resulted in increased differentiation of monocytes into osteoclasts [29]. Additionally, stimulation of switched MBCs by IFN-γ increased production of TNF-α and decreased osteoprotegerin, further exacerbating bone erosion [58,101]. IFNγ also promotes trafficking of switched MBCs to sites of inflammation in RA SF, as B cells upregulated CXCR3 and CD11c [58,63]. In RA, B cells have a survival advantage, as levels of BAFF and APRIL are elevated in the

SF of RA patients compared to healthy controls and promote B cell proliferation and survival [97].

1.6.2 Autoantibodies

RA is associated with autoantibodies that are used clinically for early detection of RA and can aid prognostication. In the context of RA, the first autoantibody described was RF, antibodies that target the Fc-portion of IgG, in the 1940s when elevated levels were associated with immune dysregulation [12]. Approximately, 60-80% patients are seropositive for RF and those that were RF IgA+ had a worse prognosis [99,102]. However, RF alone is not a good biomarker as it is elevated in healthy people (especially the healthy elderly) and in other diseases, such as SjS and hepatitis C infection [99].

An autoantibody class that is more specific to RA are anti-citrullinated protein antibodies (ACPAs), which are antibodies against citrullinated self-antigens and are produced by autoreactive B cells [7,12]. They are a more closely associated with RA than RF as they are present in 70-80% of RA patients, 1-3% healthy patients and at much lower levels in other autoimmune diseases [12,103]. However, a longitudinal study suggest that the presence of ACPAs in the general population had an 8% associated risk with developing RA after 3 years of monitoring [16]. RA patients often produce ACPAs many years before disease onset and their presence increases the risk of RA development four-fold. In addition, RA patients who were ACPA+ had a more erosive phenotype [98]. One study expanded dominant BCR clones from ACPA+ patients and upon re-expression 5 successfully cloned BCRs, 2 were found to be reactive to anti-CCP2 and 1 clone originated from 2 identical PCs indicating not only autoreactive populations in the synovium but expansion of these autoreactive PCs from a

single cell [26]. Additionally, if individuals express over >5 dominant BCR clones they are significantly more likely to develop RA [13,103,104].Interestingly the presence of ACPAs appears to be associated with some HLA risk alleles, as patients expressing the HLA-DRB1*0401 allele had significantly higher titres of autoantibodies directed towards citrullinated α-enolase [105]. Additionally, ACPA+ patients express higher levels of bone resorption markers CTX, TRAP5b and cathepsin [106]. However, in mice models, autoantibodies alone were only enough to cause transient, mild RA but required activation of autoreactive T cells for development of severe RA[82].

Recently, ACPAs have been included in a larger group of biomarkers termed anti-post-translationally modified protein antibodies, as they appear pre-RA and are strongly associated with development of RA. These include carbamylation (anti-CarP), acetylation (Kac) and glycosylation of IgG [13]. However, approximately 20-30% patients are seronegative and do not have a predictive biomarker for RA[98].

1.6.3 IgA

IgA is the second most common immunoglobulin in the immune system and approximately 3-5mg/ml is synthesised daily and mainly exists as a monomer in humans [107,108]. In serum IgA mainly exists as a monomer, which in serum produces a strong anti-inflammatory effect [108]. IgA also exist as a dimer, which is two IgA monomer joined by a J chain [109]. Additionally, there is secretory (sIgA), which is located in the mucus and originates from dimeric IgA that is translocated through epithelial cells upon binding to a pIgR. It is proteolytically cleaved and retains part of the pIgR as a secretory element [107,109]. It is particularly important in neutralising pathogenic bacteria in the mucosae [47]. Interestingly, one group tested the

binding capacity of different IgA conformations on IgA receptors FcRL3 and FcRL4 and presence of the secretory element appears to confer binding specificity of IgA to FcRL3, which specifically bound sIgA but not monomeric or dimeric IgA, whilst FcRL4 was unable to bind sIgA suggesting that the secretory element determined its ability to bind to different receptors [109].

IgA exists as 2 subclasses, IgA1, which is primarily located in serum, and IgA2, which is primarily associated with sIgA. The differences lie in the hinge region between C_H1 and C_H2, where the hinge region is 13 amino acids shorter in IgA2 compared to IgA1. This makes it less effective at antigen binding due to reduced flexibility in the Fab_2 fragment but it is more resistant to bacterial protease cleavage, as the secretory element protects it [107,108]. In RA, IgA can exist in immune complexes and these were enough to induce synovitis even if the antigen was not necessarily associated with RA [12].

IgA receptors include, but not exhaustive, FcαRI, CD71, ASPGR, SIGNR1, FcRL3 and FcRL4 [108].

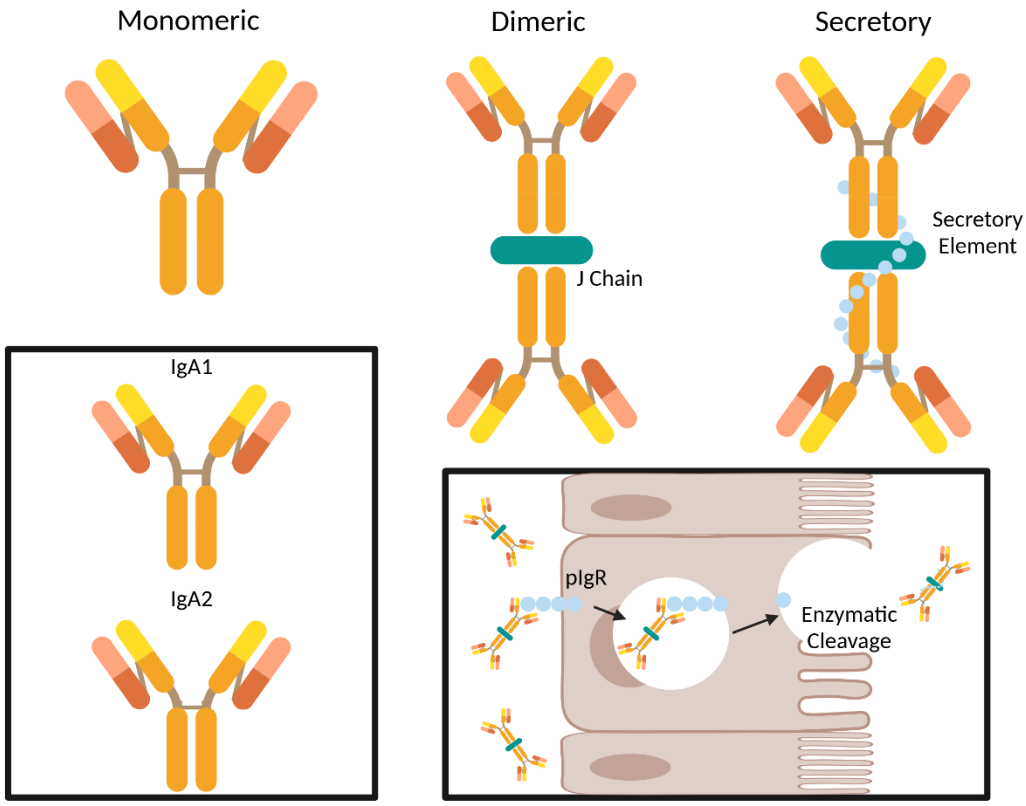

Figure 1.6.3., IgA subclasses & isoforms. *IgA exists either as monomeric, dimeric or secretory IgA. Dimeric IgA is two monomers connected by a J chain whilst secretory IgA is dimeric IgA tbat has an additional secretory element attached. Dimeric IgA binds to a pIgR on the basal side of an epithelial cell, which is subsequently internalised and transcytosed across to the lumen. Secretory IgA is released by the epithelial cell by enzymatic cleavage of the pIgR, with part of it remaining attached to the IgA as the secretory element. Monomeric IgA also exists as two subclasses: IgA1 and IgA2, with the hinge region being 13 amino acids shorter in IgA2, making it more inflexible and less susceptible to proteolytic cleavage.*

1.6.4 Antigen Presentation

The selection process in the GC reaction is a key example for the ability of B cells to present antigens to elicit help signals from Tfh cells. Centrocytes need to bind, internalise, process and present the antigens they have captured from fDCs to the Tfh cell.

B cells antigen-presenting capabilities are thought to have an important role in autoimmune disease. Patients treated with B cell-depleting therapies (BCDT) not only had decreased B cell numbers but there was a decrease in activated autoreactive T cells, indicating a potential role for B cells in antigen presentation[81]. Disruption of these interactions could be important, as inflammatory responses in IL-6 producing B cells appear to be controlled by T cells [91]. Analysis of the B cell composition in the SF of patients with RA found that antigen presenting B cells, defined as CD21+CD86+, made up most of the B cell compartment [60,86,110]. To investigate the relationship of B cells with T cells, CD4+ GC T cells were transferred to an SCID mouse model. It had reduced IFN-γ and IL-1β production compared to synovial tissue containing B cells and was dependent on MHC-II, as adoptive transfer of tissue-matched MHC-II cells was sufficient to activate CD4+ T cells compared to unmatched [111,112]. In a PGI arthritis model, only immunised WT mice developed arthritis whilst a B cell deficient mouse model did not [82]. This was found to be antigen-specific, as transfer of non-selected B cells to B cell deficient mice was not sufficient to induce arthritis whilst B cells challenged with proteoglycan conjugated to hapten-NP, an antigen that can be recognised by 2-4% BCRs, induced transient arthritis in 60% of the population.

Although these results indicated that antigen-presentation by B cells is important in activating CD4+ T cells in synovitis, antigen presentation alone was not enough to develop severe arthritis and that autoantibody production was also required.

1.7 B Cell Targeting Therapeutics in RA

1.7.1 B Cell Depleting Therapies

The aim of BCDTs is to reduce clinical symptoms and prevent further joint destruction. In RA, the amount of B cell depletion in synovial tissue correlates to clinical score, as those with greater B cell depletion experienced greater disease remittance [101]. Therapies aim to target antigen-independent pathways by either binding cell surface proteins or preventing cytokines production [97,101]. The first drug to directly target B cells in RA was rituximab, a mAb directed against CD20. This defines most B cells and increases in expression as the B cell matures. In one study, patients were treated with either a single course of rituximab, or rituximab in combination with conventional DMARDs and were compared with an untreated control group. The disease activity score (DAS28) improved in all treatment groups compared to controls and, specifically co-treatment of rituximab with a conventional DMARD demonstrated a significant decrease in ACR50 response in patients, which was maintained 48-weeks post-treatment [56,113,114]. Its success is partially due to its effects on cytokine production. Another, is that it is able to significantly reduce RANK+ osteoclasts as well as RANKL expression, which resulted in stabilisation of bone destruction preventing further bone loss [113]. Rituximab has its limitations as there is re-accumulation of CD27+ B cell population upon treatment withdrawal in both RA and SLE and it does not reduce levels of autoantibodies [115].

However, the limitations in efficacy of rituximab treatment have been elucidated in B cell lymphomas where response to treatment varies between different types of lymphomas. This was shown to be a result of greater internalisation of CD20 upon binding the mAb and this effect was in part governed by FcγRIIb [116]. It exists in 2 isoforms: IIb1 & IIb2 and the latter is

associated with increased internalisation of CD20. The IIb2 isoform is expressed on lymphocytic leukaemia whilst IIb1 was significantly higher in healthy patients suggesting that some B cell lymphomas have adapted to avoid anti-CD20 treatment by internalising the antibody removing its blocking capabilities [116].

1.7.2 Interfering with B Cell Interactions

There are treatments that impact the ability of B cells to interact with T cells. Abatacept is a fusion protein between Fc fragment of IgG1 and the extratcellular (EC) portion of CTLA-4, which prevents CD80/86 on B cells binding to CTLA-4 on T cells. In one study, a 6-month treatment regimen allowed over 70% of patients to achieve clinical remission, which was shown to be associated with a decrease in the CD19+ B cell population and an increase in the Breg and Treg populations. This collectively reduced T cell activation [101,117]. However, abatacept treatment alone was not enough to provide life-long remission in RA patients and treatment didn't correlate with reduce autoantibody levels indicating that B cells also have an antibody independent function in RA [91,101].

1.8 FcRL4+ B cells

1.8.1 FcR & FcRL

Fc receptor-like (FcRLs) are related by their chromosomal position, genomic organisation and structural similarity to the Fc receptors (FcRs)[118]. Their genes are mapped to the chromosomal position 1q21-22, spanning a 300kB region and encodes type I transmembrane glycoproteins that contain 3-9 EC Ig-like domains and an IC region consisting

of ITIMs or ITAMs [118,119]. FcRL6, A & B are also closely related but are positioned at a different gene locus and the latter 2 are considered IC proteins as they lack an EC domain and transmembrane region [119]. In addition to this, mice express FcRLs but there are variations in structure and distribution compared to humans, for example mice do not possess an analogue to FcRL4 and their FcRL5 is structurally similar to human FcRL2 & 3 [119]. Human FcRL expression is restricted to lymphocytes with preference to B cells; the only exception to this is FcRL6 that is preferentially expressed in cytotoxic CD8+ and CD4+ T cells. FcRL expression increases in B cells as they progress through development and different FcRLs appear to define different B cell subsets. FcRL3 and 4 define MBCs that suppress suppresses the plasma cell phenotype in response to TLR9-induced B cell activation [120]. FcRL5 is expressed on MBCs that are poised to become plasmablasts and has been detected on bone marrow-residing plasma cells in patients with multiple myeloma [109,119,120]. Additionally, FcRL4 specifically defines MBCs that reside in the mucosal associated lymphoid tissue (MALT) whilst FcRL1, 2, 3 and 5 can be detected on circulating MBCs [120].

FcR antigens are well characterised whilst not all FcRLs antigens have clearly identified ligands. As FcRs are defined by their ability to bind to the Fc portion of immunoglobulins it was considered whether FcRLs could do the same [121]. Currently, the ligands for FcRL1 and FcRL2 are still to be identified but incubation of other FcRLs with different immunoglobulin isotypes determined that FcRL3 and FcRL4 are IgA receptors whilst FcRL5 is an IgG receptor with various binding affinities dependent to IgG subclasses [122,123]. More specifically, FcRL3 has been defined as a receptor for sIgA whilst FcRL4 has been suggested to be a receptor for dimeric IgA [109]. Conversely, FcRL6 does not bind any immunoglobulins but has been defined as a receptor for HLA-DR [120].

The primary function of FcRs and FcRLs appears to be regulating BCR signalling by acting as a co-receptor. IC domains expresses either ITAMs, ITIMs, ITSMs. FcRs can be dichotomous in their expression of ITAMs or ITIMs whilst FcRLs can express ITAMs and ITIMs on their IC domain [120]. FcRs primarily support BCR-mediated activation with the exception of FcγRIIβ, whilst FcRLs primarily repress BCR-mediated activation, with the exception of FcRL1, which has 2 stimulatory ITAMs on its IC domain (Figure 1.8.1). The ability of FcRs and FcRLs to activate and repress BCR signalling suggest these receptors act bifunctionally on the BCR. Additionally, FcRs have a role in antigen presentation, for example FcγRIIα is important for capture of antigen by dendritic cells when levels of antigen are low [121].

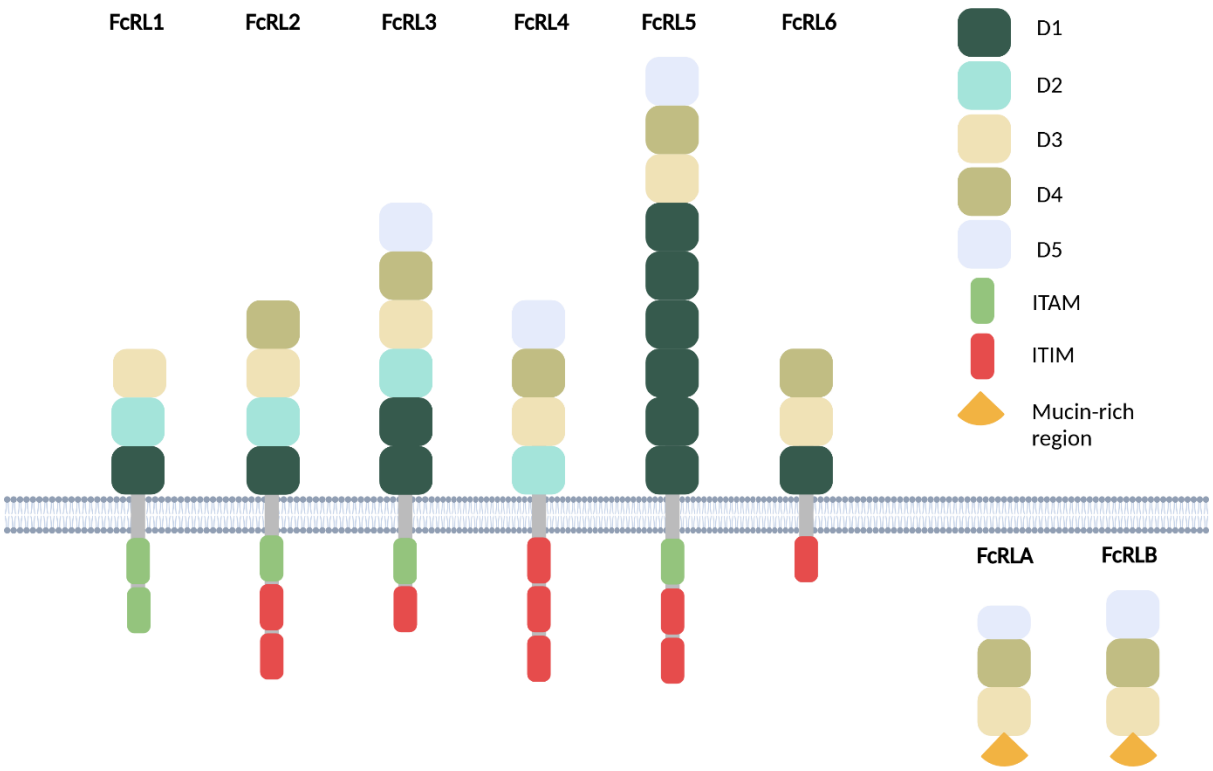

***Figure 1.8.1., FcRL family**., There are 8 members of the FcRL famiy: FcRL1-6 are type I transmembrane glycoproteins, and FcRLA and B are intracellular proteins. The EC domain consists of Ig-like domains, with their phylogenetic relationship indicated by the different colours. The IC domain expresses either ITAMs (green) or ITIMs (red) that regulate their signalling. FcRLA and B do not have any ITAMs or ITIMs but instead have a mucin rich domain.*

1.8.2 Characterisation of FcRL4+ B Cells

Out of all the FcRL receptors in the human genome, FcRL4 is the only one to be restricted to the B cell lineage, specifically a set of class switched MBCs[124]. They are usually located in MALT in the tonsils, gut or lungs and in much smaller populations in healthy peripheral blood and bone marrow [83,125,126]. When splenic and nodal marginal zone B cells were interrogated for FcRL4, its expression could not be detected [83]. FcRL4+ B cells are considered to be class switched MBCs as they express high levels of CD27 & CD20 and low levels of IgD [110,124–126]. However, there is a small population of FcRL4+ cells that are CD27- [51]. They also express high levels of CD95, CD11c, CXCR3, CCR1 and 5, CD80 and CD86, which promote their localisation to sites of inflammation, cell survival and potential ability to present antigen [19,125,127]. There is also a downregulation of cell cycle genes and upregulation of inhibitory receptor genes, which promotes the idea that FcRL4+ B cells have a non-proliferative phenotype[125]. Additionally, FcRL4+ B cells do not express any BLIMP1 or XBP1 and have a lot less rough endoplasmic reticulum than FcRL4- B cells indicating that the cells are not in process to differentiate into PCs [128,129]. However, when FcRL4+ B cells taken from tonsil were stimulated with CD40L, they were capable of proliferating and differentiating into antibody secreting cells [129].

Immunoglobulin gene analysis was performed on FcRL4+ and identified that the majority of cells expressed IgG compared to FcRL4- in SF. However, FcRL4+ cells expressed significantly more IgA and significantly less IgM than FcRL4- cells [19,126,128]. Since a higher proportion of cells express IgA on their surface it suggests that there is a link to mucosal immunity, as the highest number of IgA expressing cells are found in the MALT [19].

In chronic inflammation and autoimmune diseases, FcRL4 + B cells tend to migrate out of their usual residence and to sites of inflammation. Analysis of FcRL4+ B cells identified that it has a similar number of SHMs compared to FcRL4- B cells indicating that they have undergone antigen driven selection. Additionally, FcRL4 has an enrichment of VH1-69 segments, a gene associated with autoimmune disease[19].

FcRL4+ B cells have an overlapping phenotype with ABCs. FcRL4 expression has been detected on ABCs in RA, SLE, malaria and HIV. In RA, FcRL4 expression is higher in ABCs isolated from the synovium compared to the PB [60]. Additionally, there is heterogeneity between FcRL4+ B cells and ABCs in the surface markers, immunoglobulins and IC proteins they express. Heterogeneity between samples could possibly be caused by the tissue that ABCs have been characterised in or if ABCs have been characterised in human samples or those taken from murine mice models, as mice do not express an equivalent FcRL4 receptor and therefore would not be detected on ABCs isolated from mice [62,119].

1.8.3 FcRL4+ B Cells in Chronic Infectious Diseases

In the case of chronic infectious diseases, FcRL4+ B cells migrate out of the MALT and into the peripheral blood as a result of chronic immune activation and accumulate in response to repeated antigen exposure [63,109,125,130,131]. FcRL4+ B cells have been identified in the peripheral blood of CVID and HIV patients. FcRL4 was also upregulated alongside FcRL5 on CD19+ PB B cells from patients diagnosed with chronic hepatitis B that had been stimulated with the highly immunogenic HBV core protein [132]. However, FcRL4 was not expressed on PB B cells from patients infected with malaria, which preferentially express FcRL5 [129]. In HIV-infected individuals, FcRL4+ B cells are characterised by low proliferation caused by the

engagement of gp120 on HIV with α4β7 on B cells [133]. When B cells engaged Gp120, FcRL4 expression was upregulated and sustained for longer than 72hrs compared to cells stimulated with TLR-9L alone. TGFβ1 also has a similar effect on B cells proliferative capacity as gp120 and proliferation was restored when cells were neutralised with TGFβ1 [133]. As well, FcRL4+ B cells in HIV viraemic individuals do not produce antibodies, as chronic stimulation causes the cell to adopt an 'exhausted' phenotype [134]. This was confirmed when FcRL4+ B cells treated with anti-FcRL4 had restored B cell proliferation and antibody production.

In rare cases, breaks in chromosome 1 can form a fusion protein between FcRL4 and C-a which is expressed on B cells in multiple myeloma[135]. The FcRL4-C-a fusion protein no longer has an EC domain, which could promote proliferation and survival of tumours cells as FcRL4 is no longer able to exert its inhibitory effects[135].

1.8.4 FcRL4+ B cells in Autoimmune Diseases

FcRL4+ B cells have been identified in RA, SLE and SjS [110,127,130]. In RA patients, FcRL4+ B cells are found in the SF and immunohistochemistry identified that they are localised beneath the synovial lining and around blood vessels [110]. As previously mentioned, mRNA cytokine profiling identified that B cells were a primary source of RANKL and also produced high levels of TNF-α and IL-6 [89,91,128]. They also produced IL-12p40 and IL-12p35, which may dimerise to form functional IL-12 [89]. To determine what could be the antigenic drivers of these cells to produce RANKL, FcRL4+ B cells were cultured with heat aggregated immunoglobulins and binding analysed using flow cytometry. The results indicated that FcRL4 was unable to bind IgE or IgM but conferred specificity towards IgA; FcRL4 has demonstrated binding to serum IgA1 and IgA2 although the latter did not reach significance.

However, as the IgA1 isotype is more abundant in the serum than the IgA2 isotype it hasn't been investigated whether the preferential binding to IgA1 is because of its increased relative abundance [19,123,136]. FcRL4 was determined to define class-switched MBCs, as their BCR had high level of SHMs in the complement determining region (CDR), suggesting they had been selected in an antigen and T cell dependent manner [19]. However, further analysis of gene expression of these cells suggested that they are not yet differentiating into PCs, as they express a significantly lower amount of Ig genes. Although FcRL4+ B cells do not favour PC differentiation, under the influence of IL-2 these cells were able to produce antibodies that react towards citrullinated peptides. Additionally, 8 antibodies isolated and cloned from FcRL4+ B cells from known ACPA+ patients were found to have a binding affinity to citrullinated proteins. This relationship between IgA and reactivity towards RF and ACPA suggests that they may differentiate into IgA ACPA-producing PCs [19].

FcRL4+ B cells are also expanded in SjS patients and the increased number of positive cells is positively correlated with the number of epithelial lesions in the parotid gland [127]. Additionally, SjS patients with a higher number of MALT-lymphomas also had a higher % of FcRL4+ B cells suggesting that they may be a driver in lymphoma development [127,130]. In SLE, FcRL4 is expressed on CD21-/TBet+ B cells in the peripheral blood and the presence of FcRL4 correlates with SLEDAI score, a measure of disease activity in SLE, and autoantibody levels [129].

However, what we currently do not know is what happens to the cells once they interact with an IgA immune complex (IgA IC). Two potential functions of this interaction are changes in BCR signalling upon co-ligation with FcRL4/IgA IC and antigen presentation where FcRL4+ B cells can internalise, process and present the IgA IC on the cell surface.

1.9 Hypothesis & Aims

1.9.1 Hypothesis

- IgA IC binding to FcRL4 causes internalisation and presentation of antigen to CD4+ T cells and can regulate signalling downstream of the BCR

1.9.2 Aims

- To create an FcRL4-expressing B cell model to explore the function of IgA IC binding.
- To determine if FcRL4 is internalised with the IgA IC upon binding
- To investigate if FcRL4+ cells can process and present antigens to CD4+ T cells
- To assess the impact of FcRL4-IgA binding on BCR signalling in FcRL4+ B cells ex-vivo and transgenic cell lines.

2 Materials & Methods

2.1 Patients and Patient Materials

SF samples were collected through the rheumatology department at the Queen Elizabeth Hospital, Birmingham, tonsil samples through HBRC at the Queen Elizabeth Hospital, and PBMC samples were obtained from healthy donors at the Queen Elizabeth Hospital, Birmingham and the Royal Victoria Hospital, Newcastle Upon Tyne. Samples were obtained with patient consent and in accordance with their local research ethics committee approval, as detailed in Table 2.1.

Tissue Collected	Ethics Approval Reference
SF	LREC #07/H1203/57
Tonsil	LREC #HBRC 13-131
PBMC	Birmingham – LREC #ERN12-0079
	Newcastle Upon Tyne – LREC #1659/10369/2019

Table 2.1., Ethics approval reference for the tissue sample collection

2.2 Sample Preparation

2.2.1 PBMC Isolation from a Leukocyte Reduction Filter (Cone)

The cone was positioned over a 50ml Falcon tube using a clamp stand and the seal cut at the top and bottom of the cone to release the sample. Cone flushed with 20ml RPMI + 2mM EDTA using a syringe and needle. Volume was made up to 50ml with RPMI + 2mM EDTA and layered over ficoll at a 1:1 ratio in a separate 50ml Falcon tube. Sample centrifuged at 900G, 30mins, RT, brake and acceleration = 6. PBMC layer transferred to a 50ml Falcon tube.

Volume was made up to 50ml in cold RPMI + 1 % HIFCS and centrifuged at 600G, 8mins, 4°C. Supernatant was removed and the wash step repeated. 50ml cold RPMI +1% HIFCS was added to the cells and suspension was filtered using a 70µM cell strainer. Cells counted using a haemocytometer and centrifuged at 400G, 8mins, 4°C. Supernatant was removed and cells were frozen in HIFCS + 10% DMSO at a cell density of 1-2x10^7.

2.2.2 PBMC Isolation from Whole Blood

Whole blood was collected in citrate tubes. Sample was transferred to a 50ml Falcon tube and diluted 1:1 in sterile PBS. Sample layered onto ficoll at a 3:1 ratio and centrifuged at 300G, 30mins, RT, brake and acceleration at a minimum. PBMC layer transferred to a 50ml Falcon tube and made up to 10ml in cRPMI (Table 2.3) and centrifuged at 300G, 5mins, RT. The supernatant was discarded and cells resuspended in 10ml cRPMI and cells counted using a haemocytometer. Sample centrifuged at 300G, 5mins, RT and supernatant discarded. Sample was either used directly in an experiment or frozen in HIFCS + 10% DMSO at a cell density of 1-2x10^7.

2.2.3 Plasma Isolation

Whole blood collected in EDTA tubes. Samples centrifuged at 3000rpm, 10mins, RT. Plasma transferred to 5ml sterile Eppendorfs and frozen for long term storage.

2.2.4 Tonsil Dissociation & Mononuclear Cell Isolation

Tonsil tissue was washed in 4-5ml RPMI to remove peripheral blood. RPMI (R0883, Sigma) dispose and replaced with fresh RPMI. Tissue cut into 2mm pieces using sterile scalpels and transferred to a 50ml falcon tube. Centrifuged at 300G, 8mins, RT. The supernatant was removed and wash step repeated in 10ml PBS. The supernatant was removed, tissue resuspended in 10ml RPMI and transferred to a sterile stomacher bag. Air was squeezed out and bag sealed before being transferred to the Stomacher®80 circulator and ran on normal mode at 265rpm for 6mins. The contents of bag were filtered into a 50ml falcon tube using 70µm nylon cell strainer. The supernatant was centrifuged at 1200rpm, 8mins, RT. The supernatant was discarded and cells resuspended in 15ml RPMI and lay over ficoll at a 3:1 ratio. Cells were centrifuged at 300G, 30mins, RT, brake and acceleration at a minimum. The lymphocyte layer was transferred to a 50ml Falcon tube and topped up with 10ml RPMI. Cells were centrifuged at 300G, 8mins, RT and the supernatant discarded. Cells were resuspended in 10ml PBS for cell count using a haemocytometer. The cells were centrifuged at 300G, 8mins, RT. The supernatant was discarded and cells resuspended in 1ml HIFCS + 10% DMSO at a cell density of $1x10^8$ or $1x10^7$ and transferred into labelled cryovials.

2.2.5 Synovial Fluid Mononuclear Cell (SFMC) Isolation

10µl of 1000U/ml endotoxin-free hyaluronidase (PL 29831/0113, Wockhardt) was added per 1ml of SF and incubated at 37°C for 15 minutes. SF was layered on ficoll at a 3:1 ratio and centrifuged at 300G, 30mins, RT, brake and acceleration at a minimum. The lymphocyte layer transferred to a 50ml Falcon tube and centrifuged at 300G, 6mins, RT. The supernatant was discarded and cells resuspended in 10ml cRPMI (Table 2.3) for cell count using a

haemocytometer. The cells were centrifuged at 300G, 6mins, RT. The supernatant was discarded and either resuspended in 1ml HIFCS + 10% DMSO.

2.3 Cell Culture

Cryopreserved cells were thawed in a water bath at 37°C until the pellet had defrosted and transferred to a universal containing 20ml pre-warmed cRPMI (Table 2.3). The sample was centrifuged at 300G, 5mins, RT and supernatant discarded. Cells were resuspended in 5ml cRPMI and transferred to a $25cm^3$ culture flask. Whilst cells were maintained between experiments, 90% of the cells were discarded and the remaining 10% were cultured in 5ml new media. When cells were being grown for experiments, cells were split every 3-4 days and each time they were split 25-50% of cells were discarded whilst the remaining cells were cultured in new media. Cells that were frozen for stock maintenance, were washed in 10ml cRPMI, and frozen in HIFCS + 10% DMSO.

Cell Type	Media	Reagent	Company	Volume
ECCAC Priess & FcRL4+ Priess	cRPMI	RPMI 1640	Sigma, US	445ml
		FCS	LabTech, UK	50ml
		GPS	Sigma, US	5ml
E10P1 T cell Hybridoma	cRPMI + 1% NEAA	RPMI 1640	Sigma, US	440ml
		FCS	LabTech, UK	50ml
		GPS	Sigma, US	5ml
		NEAA	Sigma, US	5ml
HEK293T	cDMEM	DMEM	Sigma, US	445ml
		FCS	LabTech, UK	50ml
		GPS	Sigma, US	5ml

Table 2.3., Medias used for cell culture

2.4 IgA Immune Complex Preparation

2.4.1 Heat Aggregation of Colostrum IgA

100µg/ml colostrum IgA (I1010, Sigma) was heated at 63°C for 30 minutes on a thermoplate to aggregate IgA. The IgA was cooled at RT before use, kept at 4°C and used within 1 week of aggregation.

2.4.2 Streptavidin Lightning Link of Colostrum IgA

Colostrum IgA was lightning linked to streptavidin (ab102921, Abcam) according to the manufacturer's instructions and stored at +4°C for long term storage.

2.4.3 Biotinylation of Colostrum IgA

Colostrum IgA was biotinylated using the EZ-Link™ Sulfo-NHS-LC-Biotinylation Kit (21425, ThermoFisher) according to the manufacturer's instructions. To confirm elution of protein post-biotinylation, a BCA assay (A55860, ThermoFisher) was performed and the protein concentration measured using the NanoDrop One Spectrophotometer. Biotinylation of the protein was confirmed using a HABA assay (21425, ThermoFisher) and measured using the Biotek Synergy HT plate reader.

2.4.4 Biotinylation of Citrullinated Enolase Peptide & Citrullinated Enolase Protein

The citrullinated enolase peptide (SC1208, GenScript) (Table 2.4.4) and citrullinated enolase protein (21585, Cayman Chemical) were diluted to 2mg/ml stock concentration. They were biotinylated using the EZ-Link™ Micro Sulfo-NHS-LC-Biotinylation Kit (21295, ThermoFisher) according to the manufacturer's instructions. To confirm elution of protein post-biotinylation, a BCA assay was performed and the protein concentration measured using the NanoDrop One Spectrophotometer. A HABA assay could not be performed due to sample volume being too low.

Peptide	Amino Acid Sequence	Molecular Weight (g/mol)
Citrullinated Enolase (E2)	DLTVTNPK(Cit)IAKAVNEKSCNCLLLKVNQIG	3807.3

Table 2.4.4., Characteristics of citrullinated enolase-derived peptide

2.4.5 Immune Complex: Biotinylated Enolase & Streptavidin

200µg/ml of streptavidin-linked IgA and 200µg/ml biotinylated citrullinated enolase peptide or protein were incubated for 2 hours on shaker at 100rpm, RT prior to allow sufficient binding time.

2.4.6 Immune Complex: HA Biotinylated IgA & pHrodo Avidin™

10µl of 1mg/ml biotinylated IgA was aggregated at 63°C for 30mins on a heat block. The heat aggregated biotinylated IgA was diluted 1:40 and the pHrodo avidin™ (P35362, Invitrogen) diluted 1:750 in RPMI + 0.025% HEPES + 1% BSA and incubated for at least 30mins before use.

2.5 IgA binding

2.5.1 Glycine Acid Wash – *Ex-Vivo* Primary Cells

To remove receptor-attached IgA, cells were either incubated in 200µl pH3 0.75% glycine acid wash (Table 2.11) on ice for a 1min. 1ml cRPMI (Table 2.3) was added to the glycine acid washed cells and centrifuged at 300G, 5mins, RT. Supernatant was discarded and cells were resuspended in 100µl/well PBS and transferred to a 96-well flexiplate. Cells were centrifuged at 300G, 5mins, RT and supernatant discarded.

2.5.2 IgA Binding & Cell Staining – FcRL4+ Priess Cells & *Ex-Vivo* Primary Cells

100µl of HA IgA was added to glycine acid washed cells and 100µl PBS added to the unwashed cells. Cells were incubated for 30mins, RT. 50µl PBS was added to each well and centrifuged at 300G, 5mins, RT. The supernatant was discarded, cells resuspended in 50µl Fc Block (130-059-901, Miltenyi) diluted 1:10 in PBS and incubated for 10mins, on ice. 50µl PBS was added to each well and cells were centrifuged at 300G, 5mins, RT. The supernatant was discarded, cells resuspended in 50µl ZombieAqua (423102, Biolegend) diluted 1:200 in PBS and incubated for 20mins, on ice, in the dark. 50µl PBS was added to each well and the cells were centrifuged at 300G, 5mins, RT. The supernatant was discarded, cells resuspended in 100µl antibody master mix diluted in FACS buffer (Table 2.5.2) and incubated for 30mins, on ice, in the dark. Compensation beads (552843, BD) were also prepared for corresponding fluorophores. 50µl PBS was added to each well and cells were centrifuged at 300G, 5mins, RT. The supernatant was discarded and cells fixed in 100µl fixative medium A (GAS001S100, Invitrogen). Cells were incubated for 10mins, RT, in the dark. Cells were transferred to labelled FACS tubes containing 200µl PBS and samples were acquired using the BD Fortessa-X20.

Phenotyping	Protein	Fluorophore	Species	Isotype	Clone	Company	Titration Used
IgA Binding	CD19	BV421	Mouse	IgG1	HIB19	Biolegend, US	1:100
	FcRL4	PE	Mouse	IgG2b	413D12	Biolegend, US	1:100
	IgA	APC	Mouse	IgG1	IS11-8E10	Miltenyi, Germany	1:100

Table 2.5.2., Antibodies and washing conditions used to stain for IgA binding in both FcRL4+ transduced priess cells and ex-vivo FcRL4+ tonsil cells

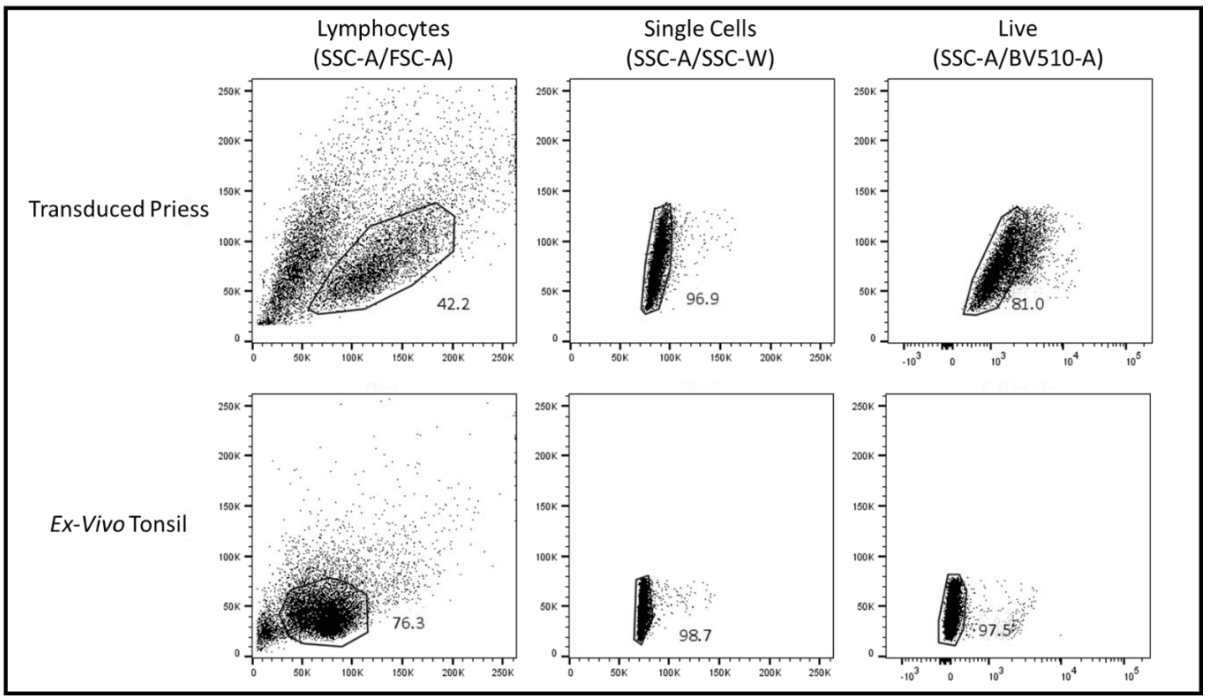

Figure 2.5.2., Viability of induced transduced priess cells and ex-vivo tonsil cells*. Representative FACS plots of induced transduced priess cells (n = 1) and ex-vivo tonsil cells (n=1) were stained with Zombie Aqua to determine the percentage of viable cells when investigating HA colostrum IgA IC binding. Cells were initially gated on the lymphocyte population and then the singlet population before gating on the live population, defined as BV510-/lo. The number next to the gate represents the percentage of viable cells for each population.*

2.6 FcRL4-Tet-On Vector Production

2.6.1 FcRL4 Plasmid Isolation

Frozen bacterial glycerol stock was scraped and transferred into 50ml of lysogeny broth containing 50µg/ml ampicillin in a conical flask and incubated at 37°C, 5%CO_2 on a shaker at 250rpm overnight. Bacteria culture was transferred to a 50ml falcon, centrifuged 4000G, 10mins, 4°C and supernatant discarded. Using the GeneJET miniprep kit (K0502, ThermoFisher Scientific, US), the pellet was resuspended in 1.5ml 100µg/ml RNase in resuspension buffer. To retrieve the plasmid, 1.5ml lysis buffer (K0502, ThermoFisher Scientific) was added, mixed thoroughly by inversion and incubated for 3mins, RT. 2ml of neutralisation buffer (K0502, ThermoFisher Scientific) was added and the sample inverted to mix. The lysate was distributed into 1.5ml Eppendorfs and centrifuged at 13,200G, 10mins, RT. The supernatant was collected, transferred to a 15ml falcon and mixed with 5ml 1X, 96% ethanol for 5 secs. 700µl aliquots were layered onto 5 GeneJET spin-columns (K0502, ThermoFisher Scientific) and centrifuged at 13,200G, 30secs, RT. The flow through was discarded and step repeated 3 times with the same spin-columns until all the sample was run. 500µl of wash buffer (K0502, ThermoFisher Scientific) was added to each column and centrifuged at 13,200G, 30secs, RT. Flow through was discarded and the wash step repeated. The spin columns were transferred to clean collection tubes. To elute the plasmids, 35µl nuclease-free H_2O was added and columns incubated for 2mins, RT. Columns were centrifuged at 13,200G, 2mins, RT and the eluted DNA was collected into one tube. The DNA concentration was measured using the NanoDrop One Spectrophotometer and noted. For long-term storage, the sample was stored at -20°C.

2.6.2 Plasmid Amplification

3ng FcRL4 template DNA was mixed with Q5 high-fidelity 2X master mix (M0492S, NEB) (Table 2.6.2I & 2.6.2II) and inserts were amplified for 33 cycles using a thermocycler (Table 2.6.2III). Restriction digests were performed on 1µg PCR product and 1µg LV_TetOne vector using 5 units of DpnI (R0176S, NEB) and 10 units BstZ171-HF (R3594S, NEB) respectively. These were mixed with 5µl 10X restriction buffer (B6004S, NEB) according to the manufacturer's instructions and made up to 50µl with nuclease free water. 250u/ml Quick CIP (M0525S, NEB) was added and the sample incubated at 37°C, 30mins. Quick CIP dephosphorylates the 3' & 5'ends of the DNA to prevent re-ligation. Digest and amplification efficacy were tested by loading 15µl of sample and 5µl DNA (N3232S, NEB) were loaded onto 1-2% agarose gel (Table 2.6.2IV) and ran in 1X TAE buffer at 150V for 60-90mins. The gel was visualised using a ChemiDoc.

	Reagent	Company	Concentration	Volume
PCR Master Mix	Q5 high-fidelity master mix	NEB, UK	2X	37.5µl
	Forward Primer	Merck, US	100µM	3.75µl
	Reverse Primer	Merck, US	100µM	3.75µl
	Template DNA	OriGene, US	5.2088µg/µl	5.76µl
	Nuclease-Free Water	NEB, UK		up to 75µl

Table 2.6.2I., Reagents used for amplification of FcRL4 gene

		Sequence
Primers	FcRL4 forward	aattcccgtaatgGCGATCGCCATGCTGCTG
	FcRL4 reverse	caccggtgtactaTTCTTCACCGGCATCTGCATC
	TetOne forward	tgaagaatagTACACCGGTGCCGGCGGA
	TetOne reverse	cgatcgccatTACGGGAATTCTTTACGAGGGTAGGAAGTGG

Table 2.6.2II., DNA sequence of primers used to amplify FcRL4 gene and Tet-On lentiviral vector

	Step	Temp	Time
Cycling Conditions	Initial denaturation	98°C	30s
	33 Cycles	98°C	10s
		50-72°C	30s
		72°C	30s/kb
	Final Extension	72°C	2mins
	Storage	4°C	

Table 2.6.2III., PCR cycle details used for amplification of FcRL4 gene

	Reagent	Company	Concentration	Volume
Agarose Gel	Agarose	Sigma, US	100X	2.5g
	SybrSafe	ThermoFisher, US	10,000X	25µl
	TAE	Fisher, UK	1X	250ml

Table 2.6.2IV., Protocol used for 1% agarose gel

2.6.3 Plasmid Clean-Up

70µl of 3ng/µl PCR amplified inserts were mixed with an equal amount of membrane binding solution (A9281, Promega) and layered onto a Wizard® SV mini-column (A9281, Promega). Samples were incubated for 1min and centrifuged at 13,200G, 1min, RT. Flow through was discarded and 700µl of membrane wash solution (A9281, Promega) was added to the column. Samples were centrifuged at 13,200G, 1min, RT. Flow through was discarded and wash step repeated with 500µl membrane wash solution and centrifuged at 13,200G, 5mins, RT. Flow through was discarded and column centrifuged for a final minute to remove residual wash buffer. Mini column was transferred to a clean 1.5ml Eppendorf and 30µl nuclease-free water (P1193, Promega) was transferred to the column. Column was incubated for 5mins, RT and centrifuged at 13,200G, 1min, RT. The mini-column was discarded and DNA contents of sample was measured using the NanoDrop One Spectrophotometer. For long term storage, sample was stored at -20°C.

2.6.4 Insert Phosphorylation and Ligation

To calculate the volume of T4 PNK required to phosphorylate 22µl 100ng/µl DNA, the NEB biocalculator dsDNA was used to calculate the moles of DNA 5' ends in the sample. 0.5µl 400u/ml T4 PNK (M0201S, NEB) was added to the sample on ice before it was incubated for 30mins, 37°C. To stop the reaction, T4 PNK was heat inactivated at 65°C, 20mins. 1.93µl 100ng/µl FcRL4 DNA was mixed on ice with 1.57µl 362ng/µl LV_TetOne backbone and 0.5µl 20,000u/ml T4 DNA ligase (M020S, NEB). This was made up to 10µl using 1µl T4 ligase buffer (NEB) and 5µl nuclease-free H_2O and incubated for 2h, RT. To stop the reaction, T4 PNL was heat inactivated at 65°C, 10mins. Sample was chilled on ice prior to transformation.

2.6.5 Bacterial Transformation

The newly constructed plasmid was diluted to 0.5ng/ml and 2µl was added to 50µl of NEB 5 alpha competent *E.Coli* (C2987I, NEB) and incubated in 950µl NEB® 10-beta/stable outgrowth medium (B9035S, NEB) on ice for 30mins. Transformed bacteria were heat shocked at 42°C for 30secs and transferred to ice for a further 5mins. The sample was gently mixed with 950µl of SOC medium (B9020S, NEB) and incubated at 37°C, 1h on a shaker at 250rpm. 100µl of sample was pipetted onto and Amp-treated LB agar plates (Table 2.6.5) and streaked using a sterile inoculation loop to isolate single colonies. Plates were incubated overnight at 37°C, 5% CO_2.

	Reagent	Company	Concentration	Volume
Agar Plates	LB Agar	Sigma, US	35g/L	7g
	Milli-q H2O	Sigma, US	1X	192.8ml
	Ampicillin	Sigma, US	50mg/ml	200µl

Table 2.6.5., Protocol used for ampicillin-treated agar plates

2.6.6 Plasmid Isolation & Verification

Plasmid DNA was isolated from bacterial colonies using the GeneJet Plasmid Miniprep Kit, according to the manufacturer's instructions (K0502, ThermoFisher). 8-10 colonies were randomly selected, and each colony was transferred to 5.5ml bacteria liquid culture containing 100µg/ml ampicillin and incubated for 15h at 250rpm, 37°C, 5% CO_2 in a shaking incubator. 5ml of bacterial culture was centrifuged at 6,800G, 2mins, RT whilst the remaining cultures were stored at 4°C for upscaling after identification of the respective construct. The supernatant was discarded and the bacterial suspension was resuspended in 250µl resuspension buffer containing 100µg/ml RNase. The bacterial suspension was transferred to a 1.5ml microcentrifuge tube, mixed with 250µl lysis buffer and incubated for 4mins at RT. 250µl neutralisation buffer was added and the sample centrifuged at 6,800G, 5mins, RT to pellet cell debris and chromosomal DNA. The supernatant was layered onto a GeneJet spin column and centrifuged at 13,200G, 1min, RT. The flow through was discarded and the column was washed using 500µl washing solution before centrifuging at 13,200G, 30secs, RT. The flow through was discarded and the wash step repeated one more time. To elute the plasmid DNA, 35µl nuclease free water was added to the column membrane and incubated for 2mins before centrifuging at 13,200G, 2mins, RT. DNA concentration and quality was measured using the Nanodrop 2000 spectrophotometer.

To verify the gene insert had been ligated into the LV_TetOne vector in the correction orientation, 15µl of sample and 5µl DNA ladder (N3232S, NEB) were loaded onto 1-2% agarose gel (Table 2.6.2.4) and ran in 1X TAE buffer at 150V for 60-90mins. The gel was visualised using a ChemiDoc.

The remaining bacterial cultures were centrifuged at 5,000G, 5mins, RT and the supernatant discarded. The pellets were resuspended in 1ml glycerol stock (Table 2.6.6) and frozen at -80°C in 1.5ml microcentrifuge tubes for long-term storage.

	Reagent	Company	Concentration	Volume
Glycerol Stock	LB medium	Sigma, US	1X	800µl
	Glycerol	Fisher, US	1X	200µl

Table 2.6.6., Protocol used for glycerol stock to freeze successfully transformed bacteria

2.6.7 Viral Concentration

HEK-293T cells were cultured in cDMEM without geneticins (Table 2.3) until 90% confluent. HEK293T cells were transfected with a lentiviral system containing the LV_TetOne (631849, Takara) encoding FcRL4, a VSV-G envelope expressing plasmid pMD2.G (12259, Addgene) and a 2nd generation lentiviral packaging plasmid psPAX2 (12260, Addgene). Transfection solution 1 and 2 (Table 2.6.7) were prepared and mixed well. Solutions were mixed together and incubated for 20mins, RT. Media was removed from the HEK-293T cells and replaced with 6ml of cDMEM (Table 2.3) The transfection media was added indirectly to the culture flask and mixed gently. Cells were incubated for 6 hours at 37°C, 5% CO_2. Transfection media was removed and replaced with 12ml HEK-293T culture media. 48h & 96h post-transfection, supernatant was collected and transferred to a 50ml Falcon tube and stored at 4°C. Supernatant was replaced with 12ml of fresh cDMEM at 48h. Supernatant centrifuged at 3,200G, 15mins, 4°C. Supernatant filtered through a 0.45µM pore syringe filter and resuspended with 5X PEG (ab102538, Abcam) at a 1:4 ratio of PEG:viral supernatant,

according to the manufacturer's instructions, and incubated overnight at 4°C. Supernatant centrifuged at 3,200G, 50mins, 4°C. The supernatant was removed and the pellet resuspended in 100µl virus re-suspension solution. The viral resuspension was split into 20µl aliquots and frozen at -80°C for long term storage.

	Reagent	Company	Concentration	Volume
Solution 1	Optimem	ThermoFisher, US	1X	1.5ml
	P3000	ThermoFisher, US	1X	35µl
	PSPAX2	Addgene, US	3.1996µg/µl	2.6µl
	pMD2.G	Addgene, US	1.625µg/µl	1.62µl
	Lenti-Vector	In house	1µg/µl	14.4µl
Solution 2	Optimem	ThermoFisher, US	1X	1.5ml
	Lipofectamin	ThermoFisher, US	1X	41µl

Table 2.6.7., Recipe for viral concentration of FcRL4-expressing Tet-On lentiviral vector

2.6.8 Priess Cell Viral Transduction & Selection

$1x10^6$ priess cells (86052111, ECACC) were plated in 2ml cRPMI (Table 2.3) in a 6-well plate and transduced with 20µl lentivirus. Transduced cells were cultured at 37°C, 5% CO_2 for 3 days. Cells were centrifuged at 300G, 5mins, RT and washed in 1ml cRPMI. Cells were centrifuged at 300G, 5mins, RT and then cultured in 4µg/ml puromycin (A1113803, ThermoFisher) in cRPMI in a 6-well plate alongside an untransduced control. Selection media was changed every 24h until the untransduced controls were inviable.

2.6.9 FcRL4 Induction

Transduced priess cells were grown in cRPMI (Table 2.3) for long term maintenance. For FcRL4 induction, a 90% of transduced cells were transferred to a new T25cm^3 culture flask and cultured in 1µg/ml doxycycline (D9891, Sigma) in cRPMI for 24h at 37°C, 5% CO_2.

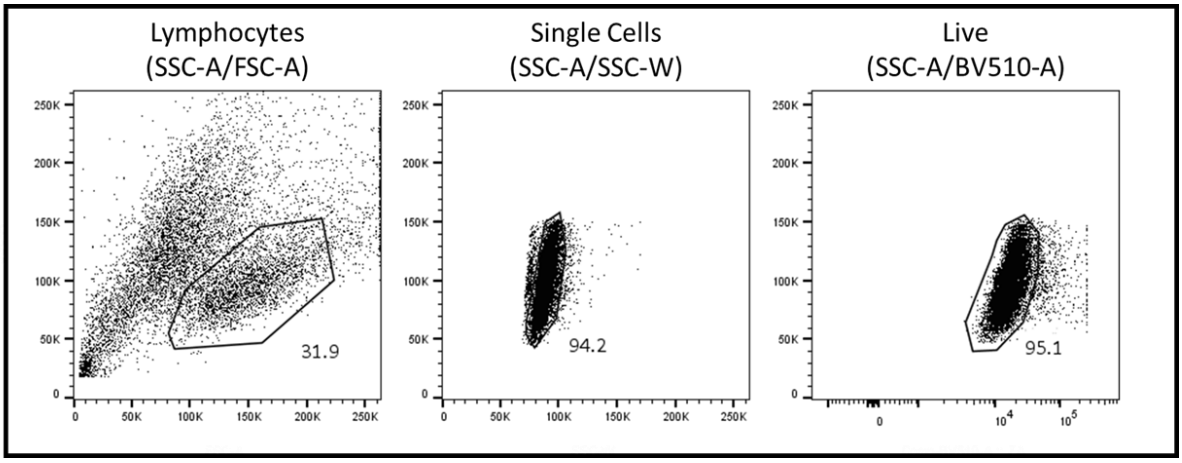

***Figure 2.6.9., Viability of induced transduced priess cells**. Representative FACS plots of induced transduced priess cells (n = 1) were stained with Zombie Aqua to determine the percentage of viable cells when investigating HA colostrum IgA IC binding. Cells were initially gated on the lymphocyte population and then the singlet population before gating on the live population, defined as BV510-/lo. The number next to the gate on the SSC-A/BV510-A plot represents the percentage of viable cells for each population.*

2.7 Cell Sorting

1-5x10^7 defrosted or induced cells were resuspended in 1ml PBS and 100µl of suspension transferred to a separate FCS-coated falcon tube for the isotype control. Both tubes were topped up to 10ml with PBS and centrifuged at 300G, 5mins, RT. The supernatant was discarded and cells resuspended in Zombie Aqua (423102, Biolegend) diluted 1:200 in PBS for 20 minutes on ice. 10ml PBS was added to each tube and centrifuged at 300G, 5mins, RT. The supernatant was discarded and 1-5x10^7 cells resuspended in 500µl stain master mix (Table 2.7.1) for 30minutes on ice. Compensation beads (552843, BD) were also prepared for each fluorophore and two 15ml falcon tubes were coated with FCS and filled with 2ml cRPMI for collection. 10ml PBS was added to each stained tube and centrifuged at 300G, 5mins, RT, supernatant discarded and cells resuspended in PBS + 1% FCS; 400µl was added to the isotype control whilst the cells to be sorted were resuspended at a cell density of 5x10^7/ml. Samples were filtered using a 70µM filter into sterile, labelled FACS tubes ready for acquisition. Cells were sorted using the FACS Aria Fusion Cell Sorter.

Cells	Protein	Fluorphore	Species	Isotype	Clone	Company	Titration Used
FcRL4+ Priess	FcRL4	PE	Mouse	IgG2b	413D12	Biolegend, US	1:100
Tonsil & SFMC (Antigen Presentation)	CD19	BV421	Mouse	IgG1	HIB19	Biolegend, US	1:100
	FcRL4	PE	Mouse	IgG2b	413D12	Biolegend, US	1:100
Tonsil & SFMC (Internalisation)	FcRL4	APC	Mouse	IgG2b	413D12	Biolegend, US	1:100

Table 2.7.1., Antibodies used to stain FcRL4+ cells for separation using the FACS Aria Fusion cell sorter

2.8 pHrodo Avidin™ Internalisation

2.8.1 Imaging

$1x10^6$ transduced priess cells were stimulated with 1µg/ml doxycycline and incubated overnight at 37°C, 5% CO_2. Cells were transferred to a universal, washed with 10ml PBS and centrifuged at 300G, 5mins, RT. The supernatant was discarded, and cells resuspended at a cell density of $5x10^6$/ml. As a positive control, a proportion of induced cells were incubated with 100µl 25µg/ml IgA/pHrodo avidin™ ICs for 2 hours at 37°C, 5% CO_2. An acellular and cellular 0.5% type II rat tail collagen gel was made up (Table 2.8.1). 15µl acellular gel was loaded into each well of a 6-well µ perfusion slide (80376, Ibidi) and then 15µl of each condition were added on top in separate wells. The slide was incubated on ice for 45-60mins before the coverslip was placed on top. The slide was loaded onto the microscope stage for imaging. Non induced and induced priess cells were perfused with 100µl 25µg/ml IgA/pHrodo avidin™ IC's and reservoirs topped up with RPMI + 0.025% HEPES. Cells were imaged using the Zeiss LSM880 Airyscanner.

	Reagent	Volume (µl)
0.5% Collagen Gel	cRPMI + 10% FCS	10
	1M NaOH	1.1
	dH2O	67
	NaHCO3	3
	cRPMI + 1% FCS	25
	1M HEPES	3.8
	5mg/ml collagen	15
	Cell suspension/RPMI	25

Table 2.8.1., Protocol used for 0.5% collagen gel

2.8.2 Flow Cytometry

5-10x10^6 transduced priess cells were stimulated with 1µg/ml doxycycline and incubated overnight at 37°C, 5%CO_2. Cells were transferred to a universal, was with 10ml PBS and centrifuged at 300G, 5mins, RT. The supernatant was discarded and cells resuspended in 500µl cRPMI. 50µl/well was transferred into a 96-well plate and 50µl of 25µg/ml biotinylated IgA/pHrodo avidin™ ICs were added to each well. Cells were fixed with BD CytoFix (554655, BD) at time points and incubated for 12mins, 37°C, 5% CO_2. Fixed cells were transferred to labelled FACS tubes containing 500µl PBS and kept on ice until the time course was complete. Cells were centrifuged at 300G, 5mins, RT and supernatant discarded. Cells were resuspended in 50µl ZombieAqua (423102, Biolegend) diluted 1:200 in PBS and incubated for 20mins, on ice, in the dark. 500µl PBS was added to each tube and the cells were centrifuged at 300G, 5mins, RT. The supernatant was discarded, cells resuspended in 100µl antibody master mix diluted in FACS buffer (Table 2.8.2) and incubated for 30mins, on ice, in the dark. Compensation beads (552843, BD) were prepared for corresponding fluorophores. 500µl PBS was added to each tube and cells were centrifuged at 300G, 5mins, RT. The supernatant was discarded and cells resuspended in 300µl PBS for acquisition using the BD Fortessa-X20.

Phenotyping	Protein	Fluorphore	Species	Isotype	Clone	Company	Titration Used
Tonsil & SFMC IgA Internalisation	FcRL4	APC	Mouse	IgG2b	413D12	Biolegend, US	1:100

Table 2.8.2., Antibody used to stain FcRL4+ cells for IgA internalisation experiment

2.9 Antigen Presentation

2.9.1 Co-Culture – 96-well plate

The antigen was diluted at a 2X concentration in cRPMI (Table 2.3) and a 1:10 serial dilution made. 50µl of B cells at $2x10^5$, 50µl of T cell hybridoma at $1x10^5$ and 100µl of antigen was added to each well in a 96-well round bottom plate. Cells incubated overnight at 37°C, 5%CO_2. 100µl supernatant collected from each condition and frozen at -80°C until used.

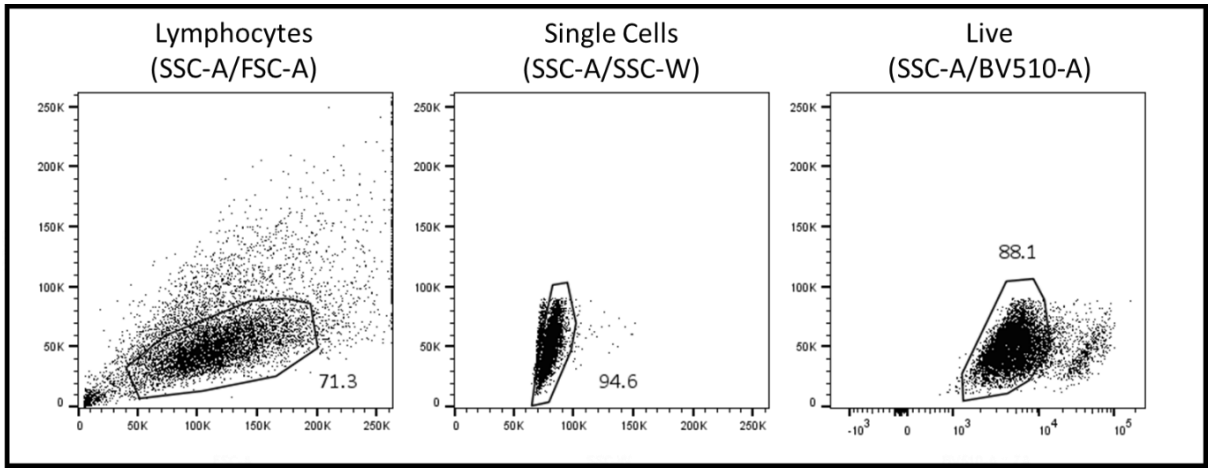

Figure 2.9.1., E10P1 T cell hybridomas are most viable 48h post-media change. *Representative FACS plots showing gating for viable E10P1 T cell hybridoma population. To determine the timepoint at which E10P1 T cell hybridoma cells were most viable, $5x10^6$ cells were removed from culture 24h, 48h, 72h and 96h post-media change and incubated with a 1:200 dilution of Zombie Aqua for 20mins. Cells were acquired on the BD FortessaX-20 and cells gated on the lymphocyte and singlet population before gating on the live population. 88.1% of E10P1 T cell hybridomas were viable in the sample taken at 48h post-media change. For all subsequent co-culture experiments, the culture media was changed 48h prior to the E10P1 T cell hybridomas being used for co-cultures.*

2.9.2 IL-2 ELISA

A plate coated with 100µl of capture antibody (503702, Biolegend) at a 1:1000 dilution in 1X coating buffer (421701, Biolegend) at 4°C overnight. The plate was washed 3x and blocked for 1h in 100µl 1% BSA (Table 2.11) at RT. The supernatants were diluted 1:5-1:20 in 1% BSA. The plate was washed 3x and incubated with 100µl diluted supernatant and reconstituted standard (575409, Biolegend) at 250pg/ml for the top standard for 2 hours at RT. The plate was washed 3x and incubated in 100µl IL-2 biotin detection antibody (503804, Biolegend) at 1:2000 dilution in 1% BSA for 1 hour at RT. The plate was washed 3x and incubated in 100µl HRP-avidin (405103, Biolegend) at 1:1000 dilution in 1% BSA for 30mins in the dark at RT. The plate was washed 3x and developed in 100µl TMB (N301, ThermoFisher) for 5mins. The reaction was stopped with 100µl H_2SO_4 (10734571, Fisher Scientific) The plate was read using the Biotek Synergy HT plate reader.

2.10 FcRL4+ B Cell Signalling: PhosFlow

2.10.1 Sample Preparation

Frozen cells were defrosted and transferred to 10ml cRPMI (Table 2.3) dropwise using a pasteur pipette. The sample was centrifuged at 400G, 8mins, RT. Supernatant was discarded and the wash step was repeated. Sample was resuspended in X-VIVO15 (02-060Q, Lonza) at a cell density of $1x10^7$/ml and 100µl was transferred to each stimulation condition in a 96 deep well V bottomed plate. Cells were rested for 2h at 37°C, 5% CO_2.

2.10.2 Stimulation of PBMCs

Cells were diluted to 1-2x10^7/ml in cRPMI (Table 2.3) and 1ml volumes transferred to a 24-well plate. 1ml of stimulation cocktail (Table 2.10.2) was added at 2X concentration to each of the wells and incubated overnight at 37°C, 5% CO_2.

	Reagent	Company	Concentration
Stimulation Cocktail	TLR-7L	Invivogen, CA, USA	10µg/ml
	TLR-9bL	Invivogen, CA, USA	5µM
	TGFβ	R&D Systems, MN, USA	10ng/ml

Table 2.10.2., Stimulants and the final concentration used to upregulate FcRL4 expression

2.10.3 Cell stimulation with anti-IgG + IgM f(ab')$_2$ fragment only

Anti-IgG + IgM f(ab')$_2$ fragment (16-5099-85, ThermoFisher) was diluted in X-VIVO15 (02-060Q, Lonza) to a concentration of 30µg/ml (Figure 2.10.6). 50µl of stimulant was added to wells containing 1-2x10^7/ml cells so that the total cell suspension volume was 150µl and the anti-IgG + IgM f(ab')$_2$ fragment was at a final concentration of 10µg/ml. Cells were incubated at 37°C, 5% CO_2 for a specific amount of time as indicated in Figure 2.10.6.

2.10.4 Cell stimulation with HA colostrum IgA IC only

HA colostrum IgA IC was diluted in X-VIVO15 to a concentration of 150µg/ml (Figure 2.10.6). 50µl of stimulant was added to wells containing 100µl 1-2x10^7/ml cells so that the total cell suspension volume was 150µl and the HA colostrum IgA IC was at a final concentration of

50µg/ml. Cells were incubated at 37°C, 5% CO_2 for a specific amount of time as indicated in Figure 2.10.6.

2.10.5 Stimulation with anti-IgG + IgM f(ab')$_2$ fragment and HA colostrum IgA IC: separate and together

To stimulate separately, 25µl of 150µg/ml HA colostrum IgA IC was added to wells containing 100µl 1-2x10^7/ml cells and incubated for 30mins at 37°C, 5% CO_2. At the designated stimulation time, as indicated in Figure 2.10.6, 25µl of 30µg/ml anti-IgG + IgM f(ab')$_2$ fragment was added so that the total volume of cell suspension was 150µl and the final concentration of anti-IgG + IgM -f(ab')$_2$ fragment 10µg/ml and the HA colostrum IgA IC was at a final concentration of 50µg/ml. Cells were incubated at 37°C, 5% CO_2.

To stimulate together, 25µl of 150µg/ml HA colostrum IgA IC and 25µl 30µg/ml anti-IgG + IgM f(ab')$_2$ fragment of was added to the wells containing 100µl 1-2x10^7/ml cells so that the total volume of cell suspension was 150µl and the final concentration of anti-IgG + IgM f(ab')$_2$ fragment 10µg/ml and the HA colostrum IgA IC was at a final concentration of 50µg/ml. Cells were incubated at 37°C, 5% CO_2 for a specific amount of time as indicated in Figure 2.10.6.

2.10.6 Crosslinking the BCR and FcRL4

Biotinylated anti-IgG + IgM f(ab')$_2$ fragment was diluted to 30µg/ml and HA biotinylated colostrum IgA IC was diluted to 150µg/ml in 200µl in X-VIVO 15 (Figure 2.10.6). 1mg/ml of streptavidin (405150, Biolegend) was added to the stimulants at a 1:1000 dilution and

incubated for at least 30mins before use. 50µl of stimulation cocktail was added to the wells containing 100µl 1-2x10^7/ml cells so that the total volume of cell suspension was 150µl and the final concentration of anti-IgG + IgM f(ab')$_2$ fragment 10µg/ml and the HA colostrum IgA IC was at a final concentration of 50µg/ml. Cells were incubated at 37°C, 5% CO_2 for a specific amount of time as indicated in Figure 2.10.6.

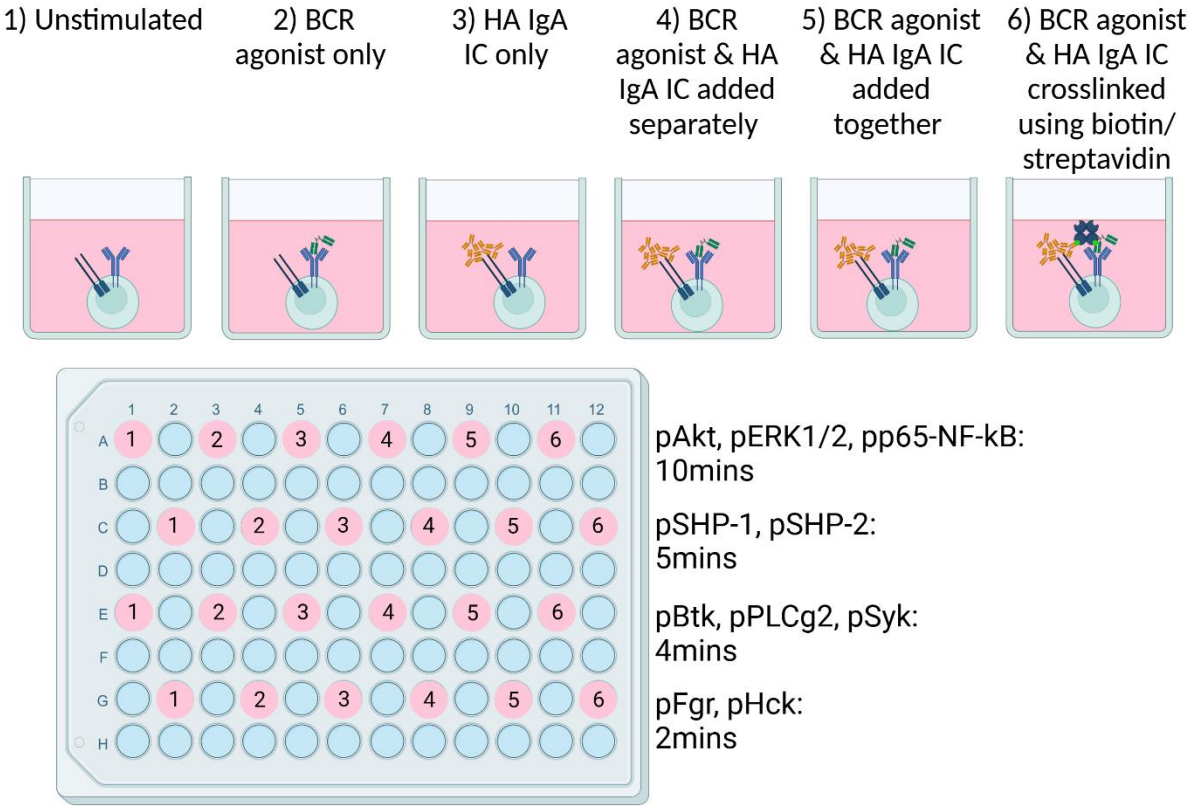

Figure 2.10.6, PhosFlow stimulation conditions and plate plan detailing the signalling molecule staining panels being used*. 6 stimulation conditions were used to explore the effects of IgA IC binding to FcRL4 on BCR signalling: 1) unstimulated (negative control), 2) BCR agonist only (anti IgG + IgM f(ab')$_2$ fragment), 3) FcRL4 agonist only (HA colostrum IgA IC), 4) BCR agonist and FcRL4 agonist added separately, 5) BCR agonist and FcRL4 agonist added together and 6) biotinylated BCR agonist and biotinylated HA colostrum IgA IC added together and crosslinked with streptavidin. The time that the BCR and FcRL4 agonist were added to the cells for each panel is detailed in the plate schematic; the length of time cells were stimulated for was determined by the point at which each signalling molecule phosphorylation peaked within a 20 minutes when stimulated with either the BCR agonist (pAkt, pERK1/2, pp65-NF-κB, pBtk, pPLCγ2 & pSyk) or the FcRL4 agonist (pSHP-1, pSHP-2, pFgr & pHck).*

2.10.7 Labelling of anti-pFgr and anti-pHck by Lightning Link

Anti-pFgr was labelled with PE and FITC (ab102918 & ab102884, Abcam) and pHck was labelled with APC (201807, Abcam) by “Lightning Link” technique according to the manufacturer’s instructions.

2.10.8 Cell Staining

Post-stimulation, cells were fixed in an equal volume of CytoFix (554655, BD) and incubated for 12 minutes at 37°C, 5% CO_2. Samples were centrifuged at 600G, 8mins, RT and the supernatant discarded. Cells were gently vortexed and 500µl of PhosFlow buffer (Table 2.11) was added to each well. Samples were centrifuged at 600G, 8mins, RT and the supernatant discarded. Cells were gently vortexed and resuspended in 50µl master mix containing antibodies (Table 2.10.8) and 2% human serum diluted in PhosFlow buffer. Samples were incubated for 15mins, RT in the dark. Cells were washed in 500µl of PhosFlow buffer and centrifuged at 600G, 8mins, RT. The supernatant was discarded and 150µl Perm II (558052, BD) added to the samples on ice. Samples were incubated overnight at -20°C. Cells were transferred to labelled FACS tubes on ice and washed with 3ml of chilled PhosFlow buffer. Cells were centrifuged at 600G, 8mins, 4°C and supernatant discarded. Samples were washed a further two times at RT. Cells were blocked in 50µl 4% mouse (M5905, Sigma) or rabbit serum (R9133, Sigma), dependent on host species of antibody, and incubated for 15mins, RT, in the dark. IC antibody master mix (Table 2.10.8) was added to the wells and cells incubated for an hour, RT, in the dark. Cells were washed in 500µl PhosFlow buffer and centrifuged at 600G, 8mins, RT. Supernatant discarded and cells resuspended in 300µl PhosFlow buffer and acquired straight away on the BD Fortessa X-20.

PhosFlow	Protein	Fluorophore	Species	Isotype	Clone	Company	Titration Used
IC protein	pAkt	BV421	Mouse	IgG1	M89-61	BD Biosciences, US	1:20
	pBtk/Itk	BV421	Mouse	IgG1	N35-86	BD Biosciences, US	1:50
	pERK1/2	AF488	Mouse	IgG1	MILAN8R	ThermoFisher, US	1:50
		PE					
	pFgr	FITC	Rabbit	IgG	Polyclonal	ThermoFisher, US	1:100
		PE					
	pHck	APC	Rabbit	IgG	Polyclonal	Abcam, UK	1:100
	pp65-NF-κB	PE-CF594	Mouse	IgG2b	K10-895.12.50	BD Biosciences, US	1:20
	pPLC-γ2	AF647	Mouse	IgG1	K86-689.37	BD Biosciences, US	1:20
	pSHP-1	FITC	Rabbit	IgG1	Shp1Y536-2A7	ThermoFisher, US	1:20
		PE					
	pSHP-2	AF647	Mouse	IgG2a	L99-921	BD Biosciences, US	1:10
	pSyk	AF488	Mouse	IgG1	I120-722	BD Biosciences, US	1:10
		PE					
Surface Protein	CD19	BUV395	Mouse	IgG1	SJ25C1	BD Biosciences, US	1:100
	CD3	AF700	Mouse	IgG2a	UCHT1	BD Biosciences, US	1:100
	FcRL4	PE	Mouse	IgG2b	413D12	Biolegend, US	1:50

Table 2.10.8., Antibodies and their dilutions used for PhosFlow experiments

2.11 Buffers & Washes

Buffer	Reagent	Company	Volume
Glycine Acid Wash	Glycine	Fisher, US	0.7507g
	NaCl	Fisher, US	0.5844g
	dH_2O		up to 100ml
	HCl	Fisher, US	to pH3
FACS Buffer	EDTA	Sigma, US	1.6ml @ 0.5Mμ
	BSA	Sigma, US	2g
	PBS	ThermoFisher, US	97.4ml
PhosFlow Wash Buffer	Sodium Azide	Sigma, US	4.5ml @ 10%
	BSA	Sigma, US	1g
	PBS w/ Mg^{2+} & Ca^{2+}	ThermoFisher, US	500ml
TGFβ Reconstitution Buffer	BSA	Sigma, US	160μl @ 7.5%
	HCl	ThermoFisher, US	40μl @ 4mM
	UltraPure H_2O	Sigma, US	11.8ml
Cell Sort Buffer	FCS	LabTech, UK	150μl
	PBS	ThermoFisher, US	14.85ml
Cell Sort Staining Buffer	RPMI 1640	Sigma, US	490ml
	GPS	Sigma, US	5ml
	FCS	LabTech, UK	5ml
ELISA Wash Buffer	Tween-20	ThermoFisher, US	500μl
	PBS	ThermoFisher, US	1L
ELISA Blocking Buffer (1% BSA)	BSA	Sigma, US	1g
	PBS	ThermoFisher, US	99ml

Table 2.11., Protocols used for buffers and washes

2.12 Isotype Control

Fluorophore	Isotype	Species	Clone	Company	Concentration (μg/ml)
APC/AF647	IgG1	Mouse	MOPC-21	Biolegend, CA, USA	200
	IgG2a	Mouse	MOPC-173	Biolegend, CA, USA	200
	IgG2b	Mouse	MPC-11	Biolegend, CA, USA	100
AF700	IgG1	Mouse	11711	R&D Systems, MN, USA	20
APC-Cy7	IgG2a	Mouse	MOPC-173	Biolegend, CA, USA	200
PE	IgG1	Mouse	MOPC-21	Biolegend, CA, USA	200
	IgG2b	Mouse	27-35	Biolegend, CA, USA	200
PE-CF594	IgG2a	Mouse	G155-178	BD Biosciences, CA, USA	200
BV421	IgG1	Mouse	MOPC-21	Biolegend, CA, USA	100
BV711	IgG2b	Mouse	MPC-11	Biolegend, CA, USA	100
FITC/AF488	IgG1	Mouse	P3.6.2.8.1	ThermoFisher, MA, USA	500
BUV395	IgG1	Mouse	X40	BD Biosciences, CA, USA	200

Table 2.12., Isotype controls used to check specificity of antibodies used

Results

3 FcRL4-Expressing B Cell Model

3.1 Introduction

In healthy individuals, FcRL4 defines memory B cells that mainly reside in the MALT, such as the tonsils and Peyer's patches [83,125,126]. However, in the case of autoimmunity they have been located in immune filtrates, for example in the synovial fluid of RA patients and in the parotid glands of SiS patients [110,127,130]. FcRL4 has also been detected on peripheral blood B cells in patients diagnosed with HIV, SLE or CVID [125,131,133]. FcRL4 is expressed primarily on switched MBCs, defined as CD27+IgD-, but has been found on the surface of a subset of DN MBCs, defined as CD27-IgD-, in the tonsil [51,110,124–126]. They are not poised to become PCs as FcRL4+ B cells don't express BLIMP1 and XBP1 but they express high levels of cell cycle genes and Ki67, indicating they are an activated proliferative population [125,128,129]. They may, however, be at a stage of differentiation that allows them to rapidly differentiate towards plasmablasts. They do express high levels of CD80 and CD86, which suggest that FcRL4+ B cells could be capable of presenting antigen [19,125,127]. Morphologically, FcRL4+ B cells have previously been described as monocytoid, which is a morphology associated with macrophages and dendritic cells, immune cells known for their role as professional APCs [124].

In the MALT, specifically the tonsils, FcRL4 has been found to define 6-8% of the total B cell population. In RA SF, FcRL4 can define up to 32% of the CD19+ population, as determined by flow cytometry of RA SF B cells whilst FcRL4 defines up to 2% of the total lymphocyte population in the primary SjS patients, defined by relative immunohistochemical surface staining of FcRL4 in parotid gland tissue sections [110,130]. Although FcRL4 expression is

enriched in B cells of RA and SjS patients, the total number of B cells is relatively low. To explore our hypothesis and validate subsequent experiments, the number of B cells expressing FcRL4 needs to be much higher. One method that could increase the number of FcRL4+ B cells would be transducing a B cell line with the FcRL4 gene.

Priess cells (RRID: CVCL_E813) are an immortalised EBV-transformed lymphoblastoid B cell line. It was selected as a B cell model to investigate antigen presentation, as the Wraith group had developed an antigen presentation assay that co-cultured priess cells with a citrullinated enolase peptide and mouse T cell hybridomas expressing a human TCR that recognised citrullinated enolase. This particular assay was of interest, as the antigen used was a citrullinated protein and ACPAs, antibodies that recognise citrullinated proteins, are used as a marker of seropositive RA. Additionally, priess cells express HLA-DRB1*0401, an HLA risk allele associated with seropositive RA, due to its expression of the SE [12,14,16]. Additionally, HLA-DRB1*0401 allele has been associated with significantly higher titres of autoantibodies directed towards citrullinated α-enolase [105]. Together, these suggest that priess cells would be suitable to explore the functional consequences of IgA IC binding to FcRL4 in the context of RA. The citrullinated protein specific T cell line we used as a readout for the antigen presentation has been selected for recognition of citrullinated enolase derived peptides when presented on the matching human HLADR4 allele. The mouse strain was transgenic for human HLADR4 allele HLADRB1*0401.

Cells can be transduced with an FcRL4-expressing lentiviral vector that either constitutively expresses FcRL4 or can induce its expression in the presence of doxycycline. The constitutively expressing vector uses a CMV promoter that strongly drives expression of the gene downstream, meaning that cloning the FcRL4 gene into this system would result in its

continuous expression. This may not be beneficial for proliferation and expansion of an FcRL4+ B cell population, as the mean number of cell divisions was 2-fold less in FcRL4+ B cells compared to FcRL4- B cells and FcRL4+ B cells express lower levels of cell cycle genes [125]. In confirmation, we found that stably FcRL4-expressing cell lines would be outcompeted in mixed cultures. Therefore, as an alternative, an inducible lentiviral vector was considered. We designed a Tet-On system with a lentiviral vector that expresses the Tet-On 3G gene and FcRL4 gene in a single vector. The Tet-On 3G protein is constitutively expressed and will conformationally change shape in the presence of doxycycline. This means that the Tet-On 3G protein can bind specifically to the promoter upstream of FcRL4 and induce its expression. This would allow initial expansion of the priess cells before inducing FcRL4 expression, creating a large FcRL4+ B cell population. We hypothesised that expression of FcRL4 using an inducible lentiviral vector system would generate a more viable FcRL4+ B cell model and this model would be suitable to explore subsequent functions of IgA IC binding to FcRL4.

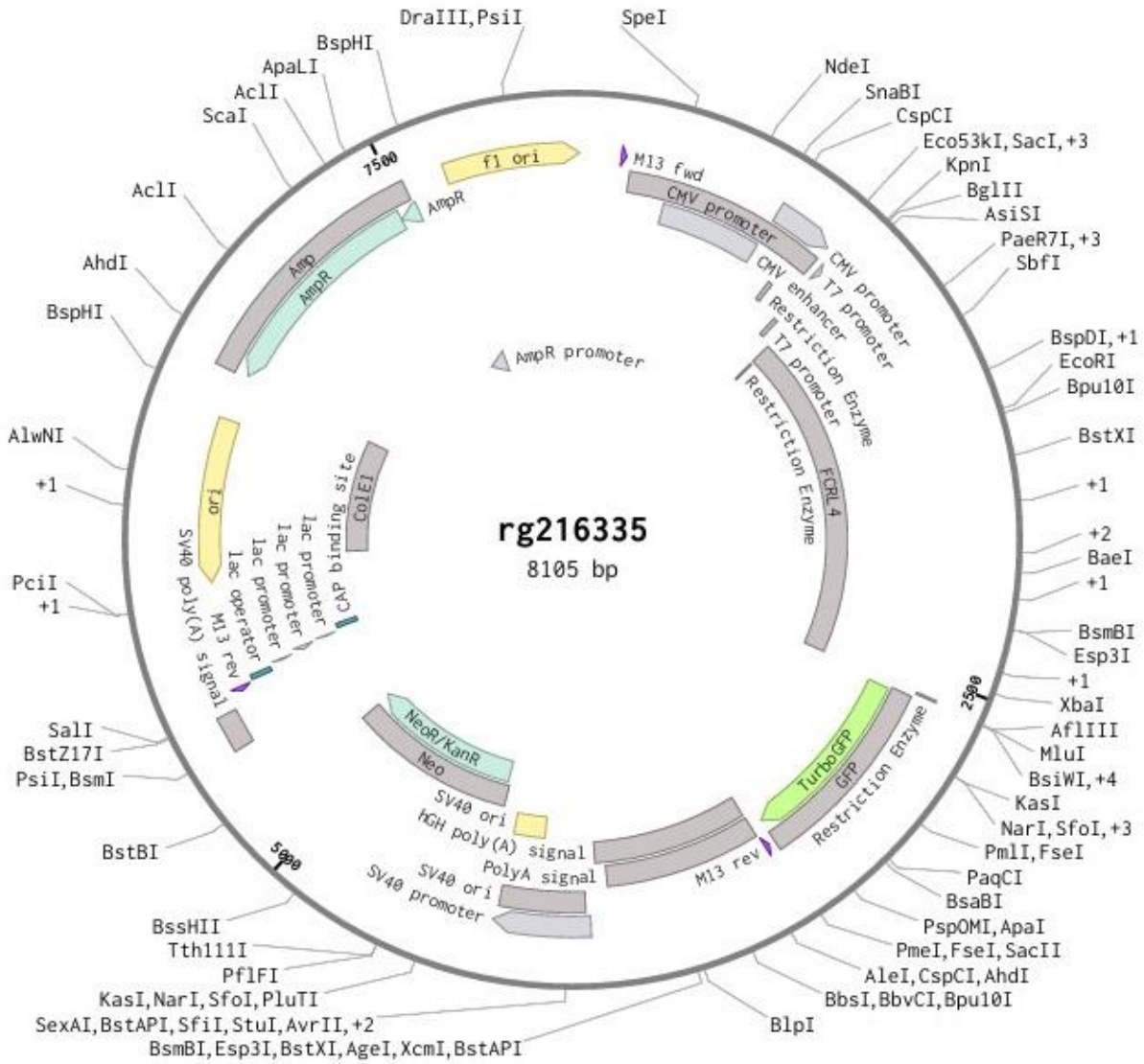

Figure 3.1I – Lentirviral vector design for constitutive expression of FcRL4 in priess cells*. The FcRL4 gene is tagged to GFP at its carboxy terminus so that it can been detected. The FcRL4 gene has been cloned into the vector using the Sbf1 and MIuI sites. It contains a puromycin selection marker for selection in mammalian cells as well as a chloramphenicol selection marker for use in E.Coli. Expression is induced by a CMV promoter.*

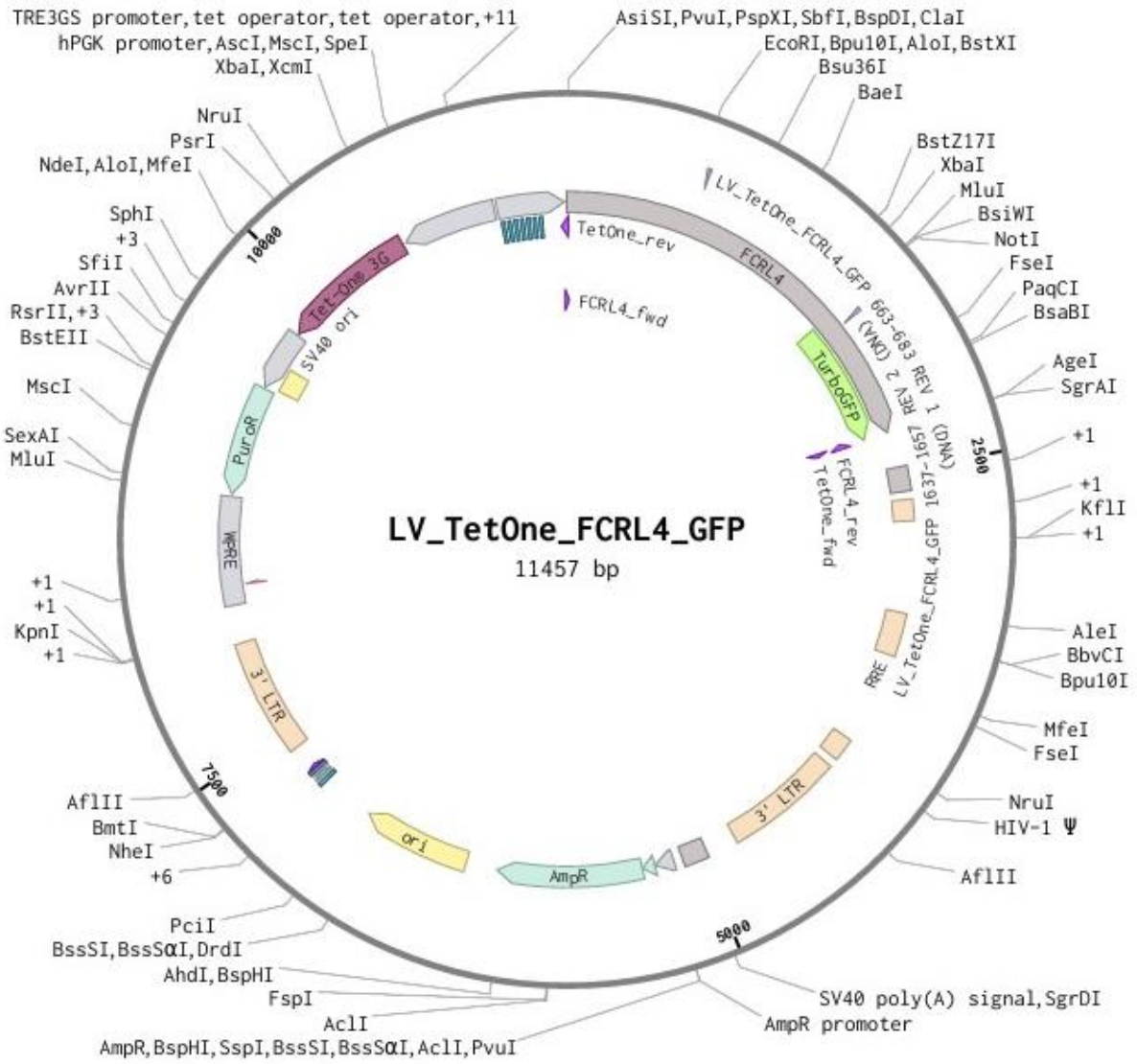

Figure 3.1II., Lentiviral vector design for inducible expression of FcRL4 in priess cells. FcRL4-GFP fusion protein was cloned into the vector using the EcoRI and BstZ17I sites. Tet-One 3G gene is cloned into the same vector and is constitutively expressed in transduced cells. It contains a puromycin selection marker for selection in mammalian cells and an ampicillin selection marker for use in E. Coli. The FcRL4 gene is downstream of the TRE3GS promoter that induces expression upon binding to conformationally changed Tet-One 3G protein.

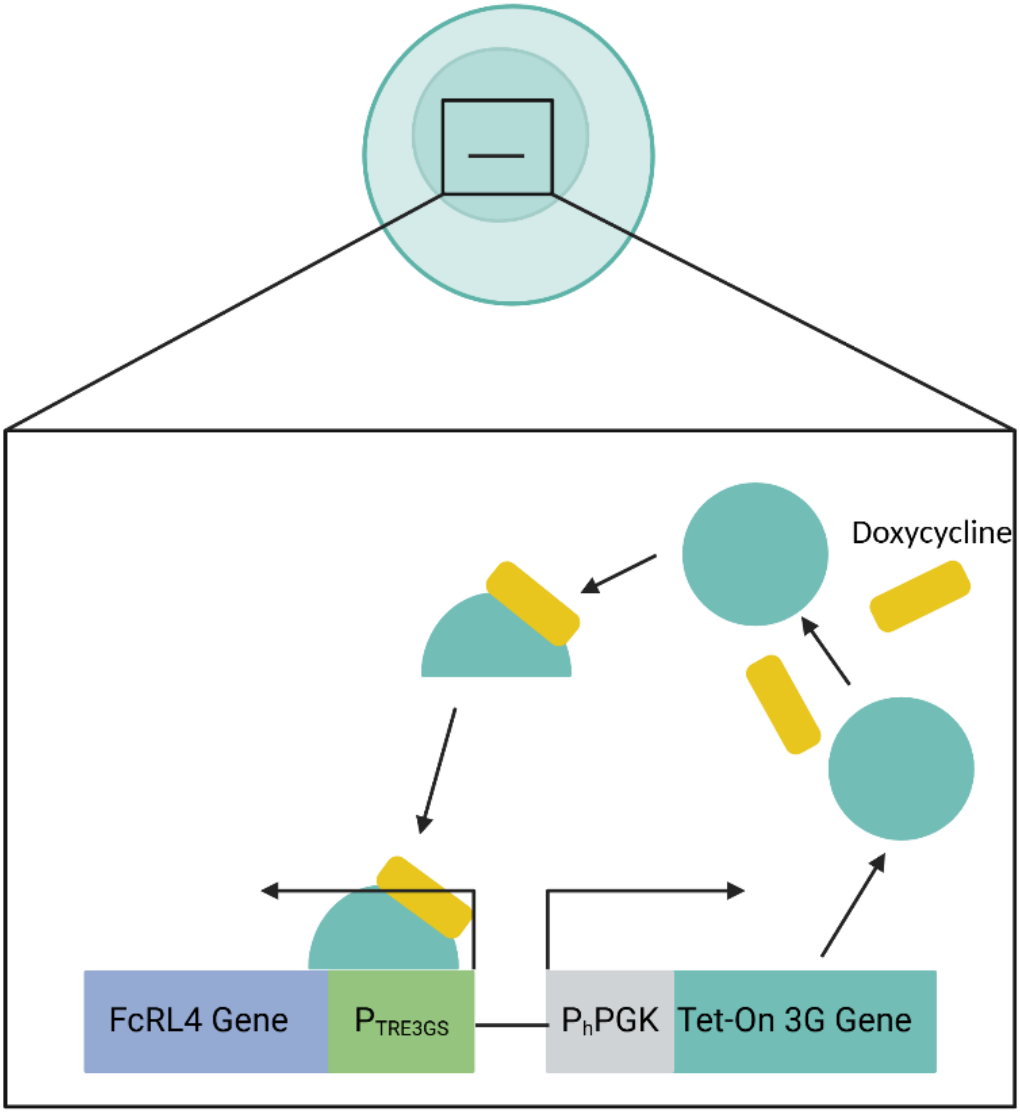

Figure 3.4., Tet-On control of FcRL4 expression. *The P_hPGK promoter constitutively expresses the transactivator protein Tet-On 3G, which is unable to bind P_{TRE3GS} controlling FcRL4 expression in the absence of doxycycline. When doxycycline is added it binds the Tet-On 3G gene protein, conformationally changing its structure so that it can bind specifically to the P_{TRE3GS} and activate expression of FcRL4. Once the doxycycline is used up the conformationally changed Tet-On 3G protein is degraded and new Tet-On 3G protein cannot bind P_{TRE3GS}, ceasing the expression of new FcRL4. Schematic adapted from the Takara Bio website: [Tet-One technology overview (takarabio.com)]*

3.2 Results

3.2.1 FcRL4 Expression in the Constitutively-Expressing B Cell Model

Priess cells are an immortalised EBV-transformed lymphoblastoid B cell line that express HLA-DR4. Previously, priess cells had been transduced with a lentiviral vector that expressed FcRL4 constitutively. These cells were brought up in culture and stained with anti-FcRL4 and ZombieAqua™ BV510 to distinguish viable FcRL4+ cells. In the sample, 6.15% of transduced priess cells were viable and of those 2.41% expressed FcRL4 (n = 1) (Figure 3.2.1.). This suggested that continuous expression of FcRL4 did not support a viable transduced population.

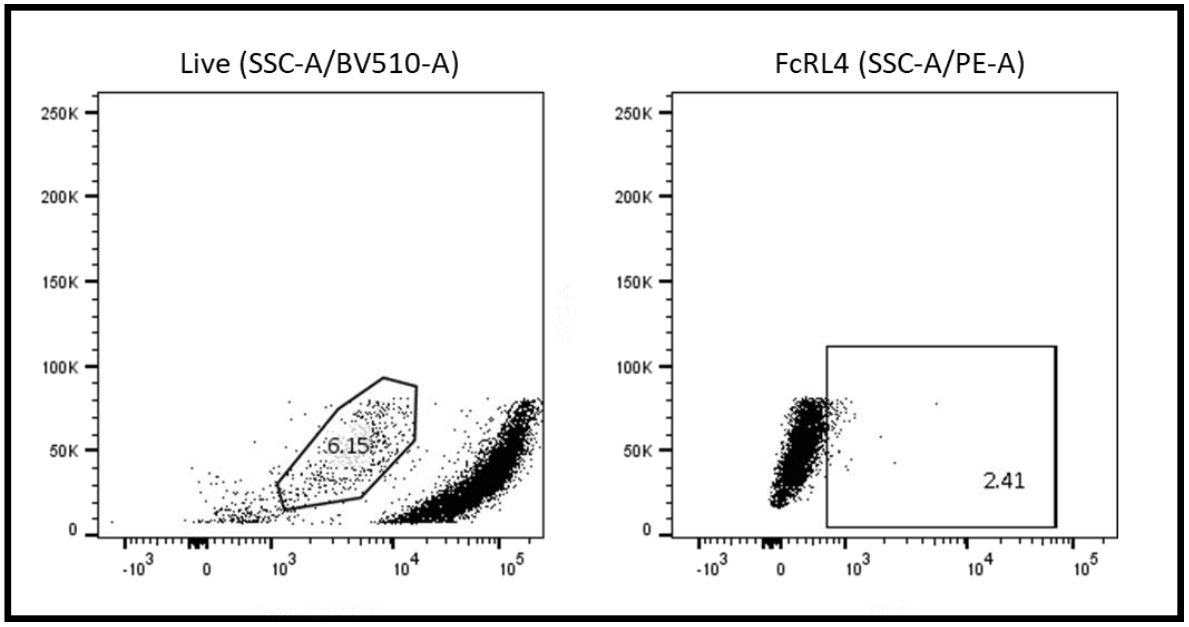

Figure 3.5.1., FcRL4 expression in priess cells transduced with a constitutively active expression lentiviral vector*. (n = 1) Representative FACS plot of FcRL4 expression in viable cells. The number in the gate indicates the percentage of viable cells (left hand FACS plots) and percentage of FcRL4+ cells (right hand FACS plot).*

3.2.2 TLR7L, TLR9L and TGFβ Stimulated Cells

3.2.2.1 PBMCs

FcRL4 has been shown to be upregulated in sorted tonsil B cells stimulated TLR-9bL and TGFβ. To observe if this applied to B cells in the peripheral blood, PBMCs were cultured overnight with TLR-9bL and TGF-β as well as TLR-7L. They were then stained for CD19 and FcRL4 expression. Compared to unstimulated PBMCs, there was an increase in FcRL4 expression on B cells from 3.02% to 55.0% indicating that stimulating B cells in peripheral blood could upregulate FcRL4 expression and that the stimulation cocktail could be applied to different tissues (n = 1) (Figure 3.2.2.1). However, these cells were not selected for the HLADR4/DRB1*0401 type, which would not be recognised by the citrullinated enolase specific T cell hybridoma.

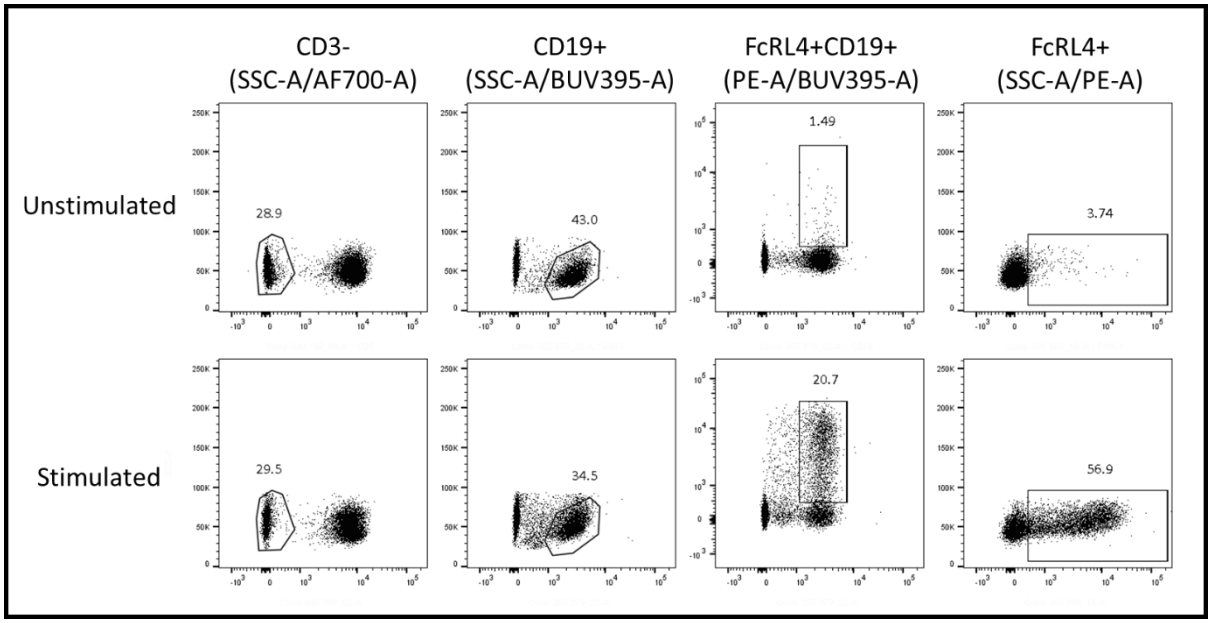

Figure 6.2.2.1, FcRL4 expression in stimulated PBMCs. *(n = 1) Representative FACS plots demonstrating the difference in FcRL4 expression between unstimulated and stimulated CD19+ B cells. Cells were gated on the singlet and lymphocyte population before the FcRL4+ population was defined as CD3-CD19+. The number in the gate represents the percentage of FcRL4+ CD19+ B cells.*

3.2.2.2 Untransduced Priess Cells

Next, the same stimulation protocol was applied to untransduced priess cells to investigate if they could upregulate FcRL4 in response to stimulation. The cells were cultured overnight with TLR-7L, TLR-9bL and TGFβ and stained for FcRL4. Unlike the PBMCs, there was no difference in the FcRL4+ priess cell populations between the unstimulated and stimulated samples (n = 1) (Figure 3.2.2.2). The percentage of FcRL4+ cells decreased from 2.17% to 0.98%, indicating that stimulation was not suitable for upregulating FcRL4 in priess cells.

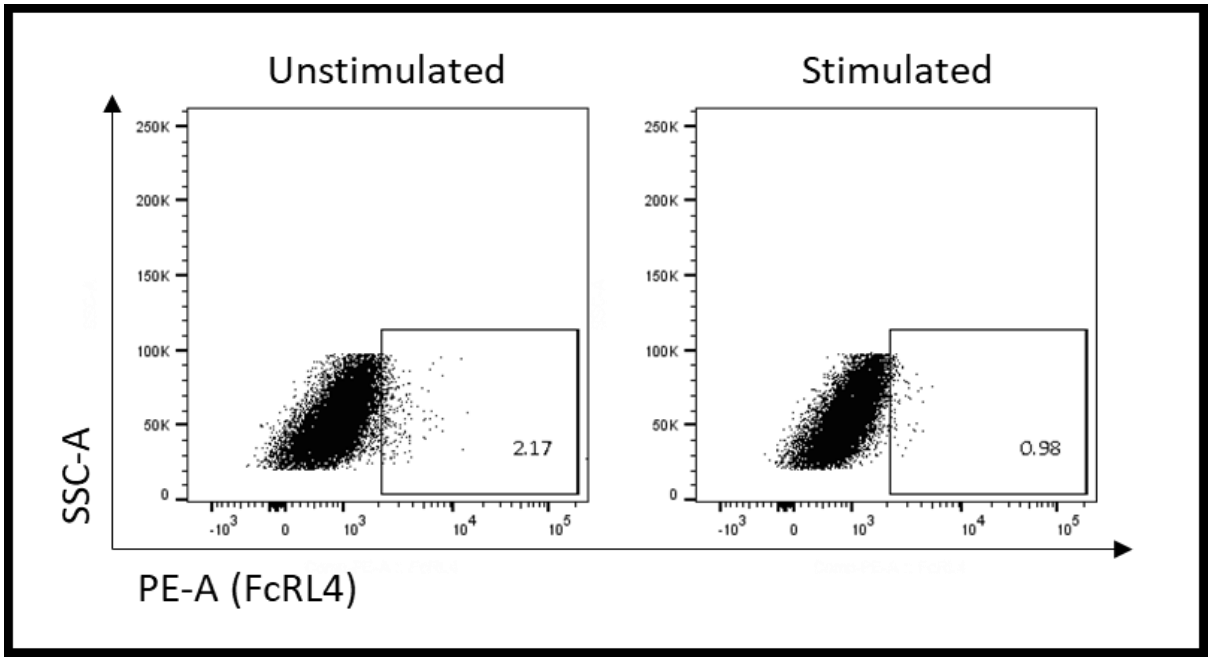

Figure 3.2.2.2., FcRL4 expression in stimulated untransduced priess cells*. (n = 1) Representative FACS plots demonstrating the difference in FcRL4 expression between unstimulated and stimulated untransduced priess cells. The number in the gate represents the percentage of FcRL4+ B cells.*

3.2.3 Tet-On Inducible B Cell Model

3.2.3.1 Viral Transduction Success Rate

As demonstrated previously, priess cells that were transduced with a constitutively expressing lentiviral vector not only expressed very little FcRL4 but the majority of cells were inviable. Before designing and creating a FcRL4-expressing inducible lentiviral vector, priess cells were transduced with a doxycycline-inducible WPI_mRuby2_14-3-3b-expressing lentiviral vector to check that transduction with a lentiviral vector wasn't causing the cells to become inviable (n = 1). Cells were cultured with the lentiviral vector for 3 days and then cultured with 1µg/ml doxycycline for 24h to induce expression of the fluorescent protein. Transduced priess cells were corrected for autofluorescence using untransduced priess cells cultured with doxycycline (Figure 3.2.3.1). mRuby2 expression was detected in transduced priess cells and visually these cells appeared to be viable suggesting that lentiviral transduction is suitable for priess cells (Figure 3.2.3.1).

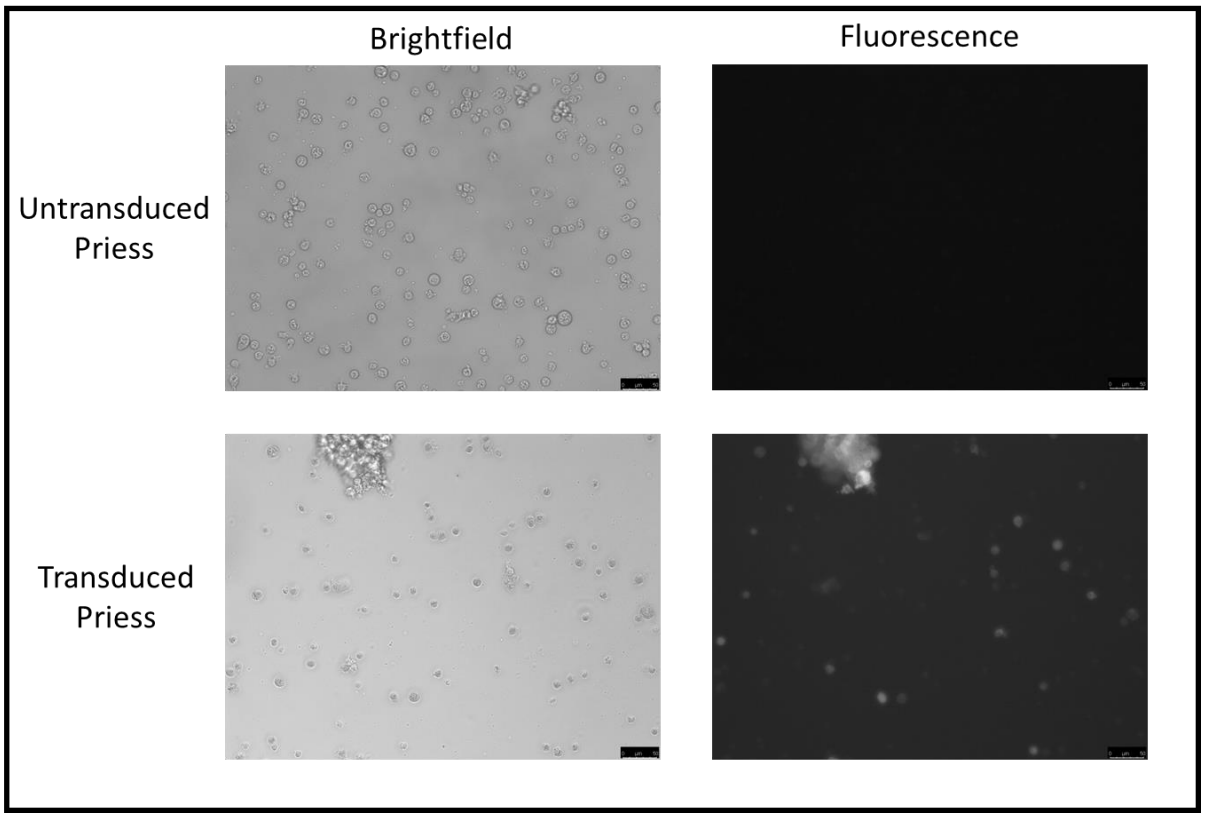

Figure 3.2.3.1., Expression of mRuby2 fluorescent protein in transduced priess cells*. (n = 1) Untransduced and transduced priess cells were imaged on brightfield to visually inspect their viability. Untransduced priess cells were imaged fluorescence image used to correct autofluorescence. Brightfield and fluorescence images indicate mRuby2 expression in WPI_mRuby2_14-3-3b-expressing in transduced priess cells.*

3.2.3.2 FcRL4 Expression in Tet-On Inducible Priess Cells

Subsequent to a successful trial run of transduction with a lentiviral vector, a FcRL4-expressing Tet-On lentiviral vector was designed and transduced into priess cells. The Tet-On system only allows expression of FcRL4 when cells are cultured with doxycycline. Transduced priess cells were induced with 1µg/ml doxycycline for 24h and stained for FcRL4. Compared to 0.57% FcRL4+ in non-induced, 28% of induced cells were FcRL4+ (n = 5) (Figure 3.2.3.2I). When induction was repeated, the proportion of FcRL4+ cells was significantly higher in the induced group compared to the non-induced group (p=0.0141) (Figure 3.2.3.2I). The FcRL4 gene that was ligated into the Tet-On vector was directly connected to a GFP reporter, meaning that if FcRL4 is expressed GFP should also be present. Interestingly when induced transduced priess cells were either stained with anti-FcRL4 PE or not, the percentage of FcRL4+ cells were significantly higher than cells that relied on GFP only to detect FcRL4 (p = 0.0042) (n = 5) (Figure3.2.3.2II).

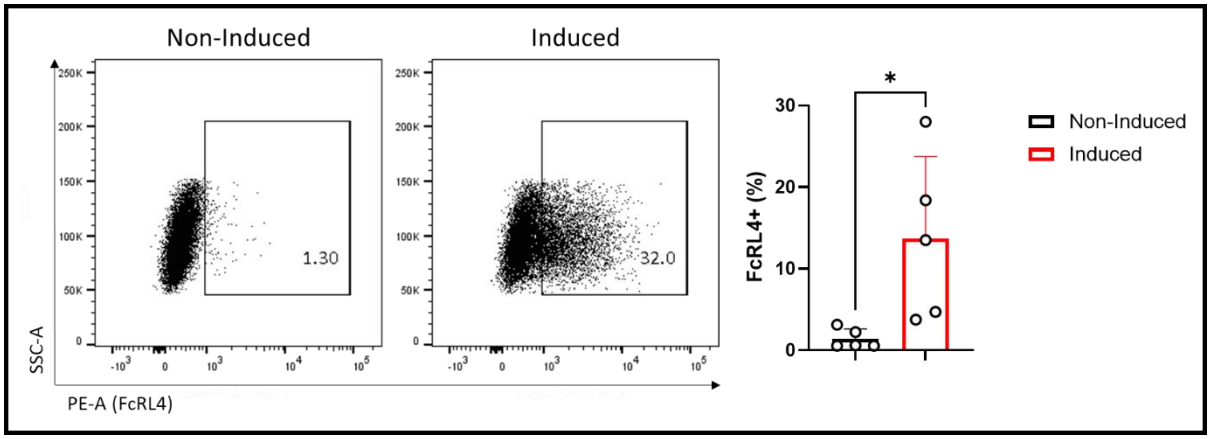

Figure 3.2.3.2I., FcRL4 expression increases in induced Tet-On lentiviral vector transduced priess cells compared to non-induced*. Representative FACS plots demonstrate the difference in the percentage of FcRL4+ cells between the non-induced and induced transduced priess cells. Number in gate represents the percentage of FcRL4+ cells (n=1). Bar chart details the significant difference in the percentages of FcRL4+ cells between non-induced and induced (n = 5) statistical test - paired T test. Replicates were taken from the same transduced priess cell line and FcRL4 expression was induced in cells between passage 1-10.*

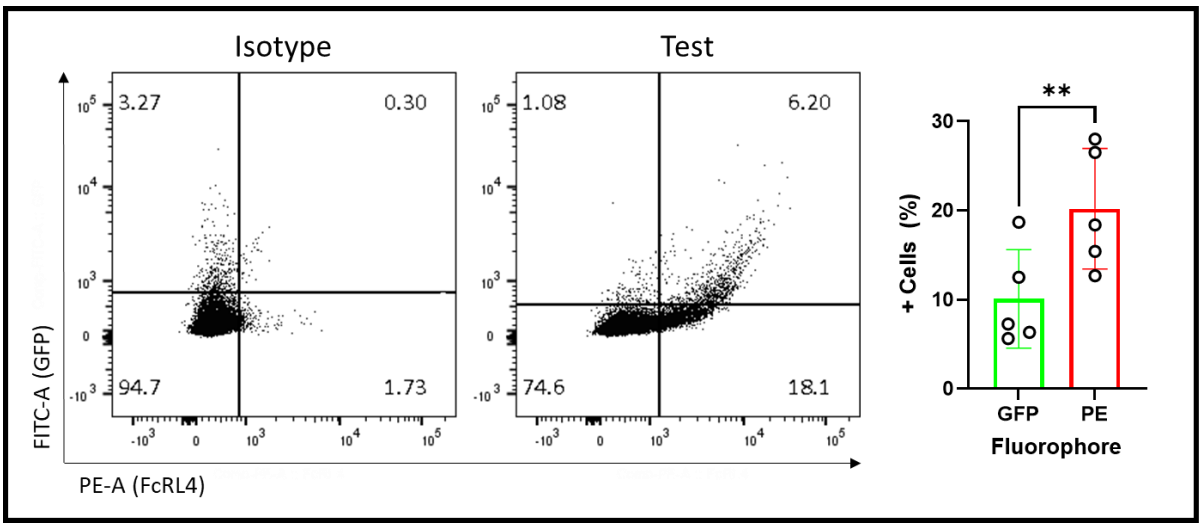

Figure 3.2.3.2II., Anti-FcRL4 PE detects a greater percentage of FcRL4+ B cells than the GFP conjugated to FcRL4. *Representative FACS plots demonstrate the differences co-staining of FITC-A/PE-A in induced transduced priess cells when FcRL4 was detected using anti-FcRL4 PE using an isotype control (n=1). Bar chart details the significant difference in the percentage of FcRL4+ cells when identified by GFP alone or when stained with Biolegend anti-FcRL4 PE (n = 5), statistical test - paired T test. Replicates were taken from the same transduced priess cell line and FcRL4 expression was induced in cells between passage 1-10.*

3.2.3.3 FcRL4 Expression Post-Puromycin Retreatment

When transduced priess cells were maintained in culture for 2-3 weeks, the percentage of FcRL4+ cells decreased post-induction. Therefore, it was questioned whether the proportion of FcRL4+ cells could be increased if they were reselected; puromycin was used as the selection antibiotic, which removes cells from culture that have not been successfully transduced with the FcRL4 Tet-On lentiviral vector. To explore this, transduced cells selected with 4µg/ml puromycin for 24h. The cells were stained for FcRL4 and compared to transduced cells were that had not been reselected. 8.64% of cell were FcRL4+ in the reselected group compared to 4.67% in the non-reselected group (n = 1) (Figure 3.2.3.3). However, compared to the percentage of FcRL4+ cells that have the potential to be induced, as seen in Figure 3.2.3.2I, reselection with puromycin is not sufficient to restore the original population of FcRL4+ cells and therefore was not included as part of the regular cell treatment protocol.

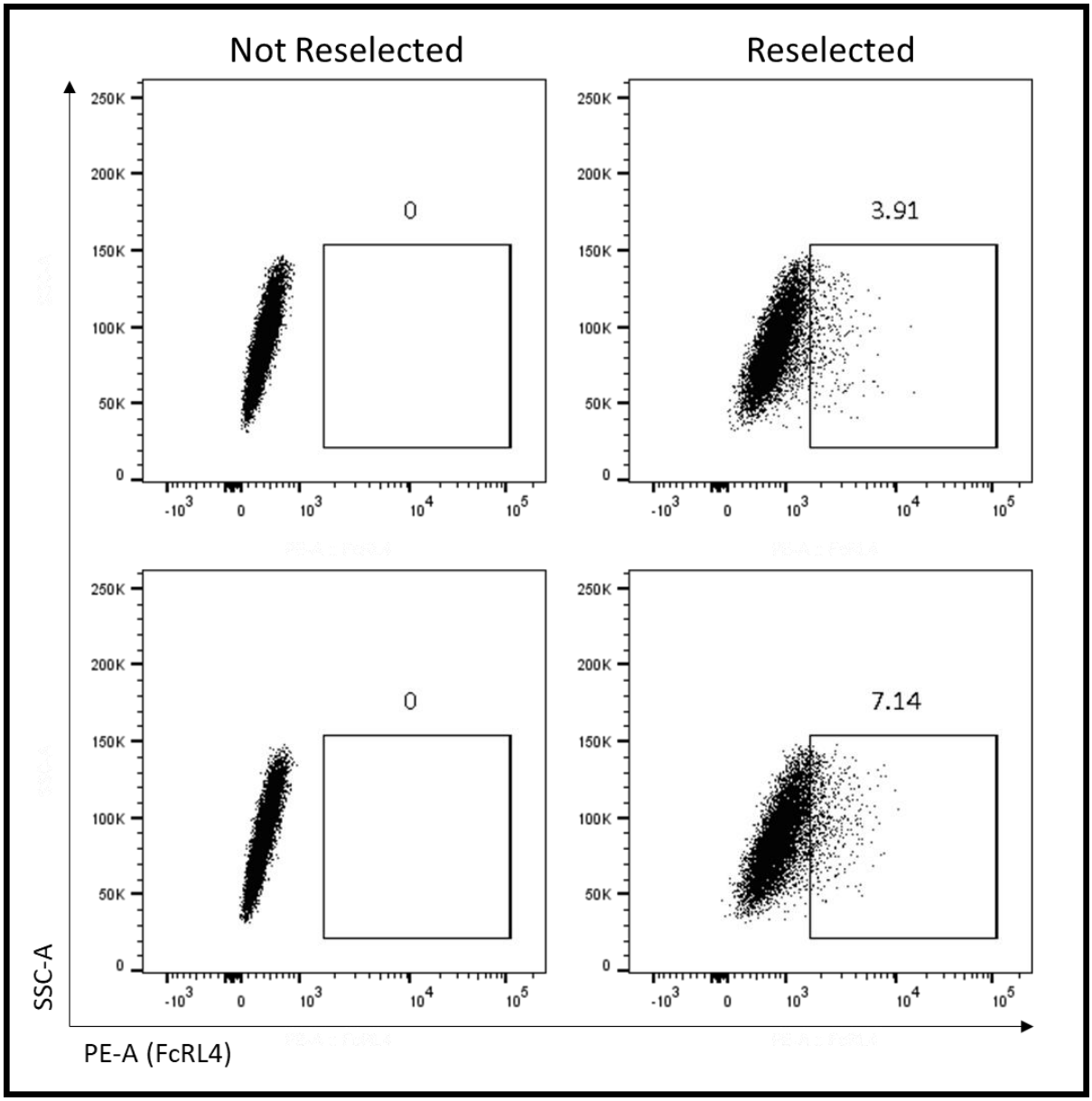

Figure 3.2.3.3., FcRL4 expression in transduced priess cells reselected with 4µg/ml puromycin. *(n =1) Representative FACS plots demonstrating the differences in the percentage of FcRL4+ cells between the non-reselected and reselected group. Induced transduced priess cells gated on lymphocyte, singlet and live population before using an FMO to define the FcRL4+ population. The number in the gate represents the percentage of FcRL4+ cells.*

3.2.3.4 FcRL4 Expression (2-48h Post-Induction)

To identify at which timepoint the peak FcRL4 expression was induced, transduced priess cells received a single treatment of 1µg/ml doxycycline for FcRL4 induction and were fixed at 2h, 4h, 8h, 24h and 48h. They were then stained for FcRL4. As time passed, the percentage of FcRL4+ cells increased from 1.61% at 2h to 29% at 48h and increased sequentially for each time point (n = 1) (Figure 3.2.3.4). Additionally, viability of these cells remained constant throughout the time course (data not shown). However, as seen in Figure 3.2.3.4, once the 48h time point was reached the percentage of FcRL4+ cells did not plateau suggesting that the peak induction of FcRL4 potentially hadn't been reached yet.

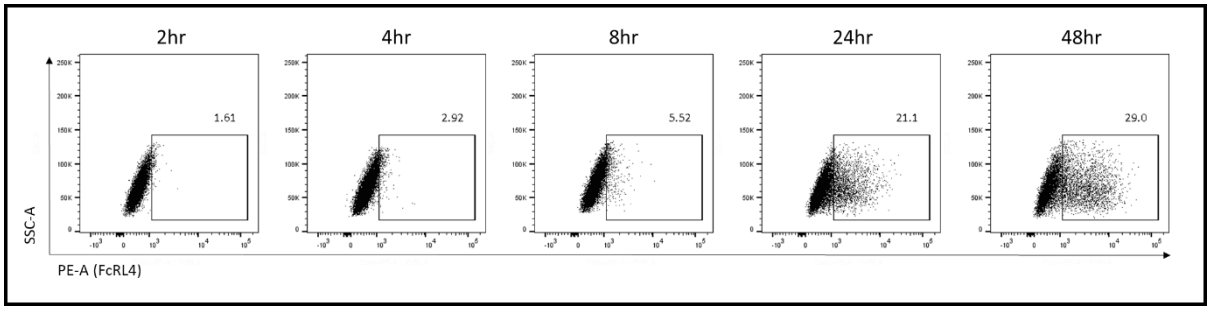

Figure 3.2.3.4., FcRL4 expression 2-48h post-induction with 1µg/ml doxycycline at 0h*. (n = 1) Representative FACS plots demonstrating the percentage of FcRL4+ cells at 2h, 4h, 8h, 24h and 48h. Induced transduced priess cells gated on lymphocyte, singlet and live population before using an FMO at each timepoint to define the FcRL4+ population. The number in the gate represents the percentage of FcRL4+ cells.*

3.2.3.5 FcRL4 Expression 24-96h, One Treatment at 0h with 1µg/ml Doxycycline

To see if the percentage of FcRL4+ cells peak was past 48h transduced priess cells received a single treatment of 1µg/ml doxycycline and were fixed at 24h, 48h, 72h and 96h. Similar to Figure 3.2.3.4, FcRL4 expression was highest at the 24h and 48h time points, 22.1% and 19.5% respectively (n = 1) (Figure 3.2.3.5). However, once past the 48h time point the % FcRL4+ cells decreased to 2.81% and 0.12% for the 72h and 96h time points respectively (Figure 3.2.3.5). Therefore, peak expression of FcRL4 was determined to be between 24-48h when transduced priess cells were cultured once with 1µg/ml doxycycline.

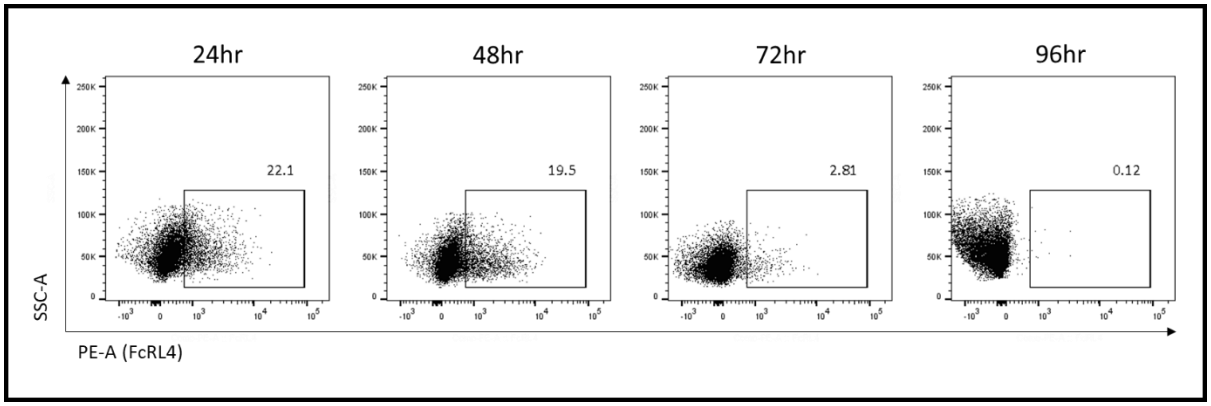

Figure 3.2.3.5., FcRL4 expression 24-96h post-induction with 1µg/ml doxycycline at 0h*. (n = 1) Representative FACS plots demonstrating the percentage of FcRL4+ cells at 24h, 48h, 72h and 96h. Induced transduced priess cells gated on lymphocyte, singlet and live population before using an FMO at each timepoint to define the FcRL4+ population. The number in the gate represents the percentage of FcRL4+ cells.*

3.2.3.6 FcRL4 Expression 24-96h, Treated at Regular 24h Intervals with 1µg/ml Doxycycline

In comparison to one treatment of 1µg/ml doxycycline at 0h, transduced priess cells were cultured with 1µg/ml doxycycline every 24h to see whether a higher level of FcRL4 expression could be induced with repeated inductions. Cells were still fixed at 24h, 48h, 72h and 96h and stained for FcRL4. Compared to the time matched samples in Figures 3.2.3.5, there was very little difference in the proportion of FcRL4+ cells at 24h, as these had both been stimulated once and therefore do not differ in their stimulation kinetics. The percentage of FcRL4+ cells increased at 48h from 19.5% to 24.8%, at 72h from 2.81% to 9.45% and at 96h from 0.12% to 4.10% when cultured every 24h with 1µg/ml doxycycline compared to one treatment at 0h (n = 1) (Figure 3.2.3.6).

Overall, it was decided that transduced priess cells would be stimulated for 24h to induce FcRL4 expression, as % FcRL4+ cells were comparable to 48h and cells were the most viable. This also meant that cells would only be treated once with 1µg/ml doxycycline due to the time point selected. Additionally, subsequent experiments to explore antigen presentation required cells to express FcRL4 for at least 48h, so stimulating cells for 24h would maintain FcRL4 expression whilst they were in a co-culture.

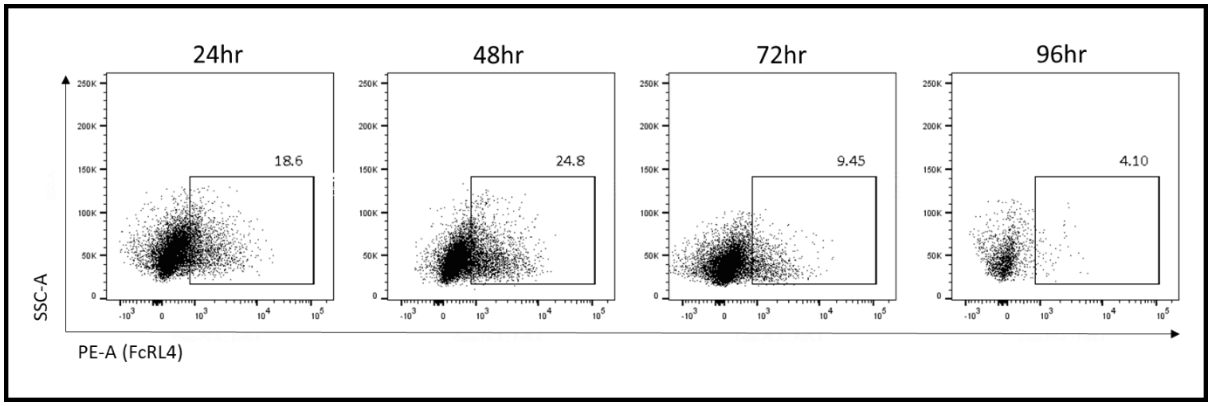

Figure 3.2.3.6., FcRL4 expression at 24- 96h when cells were treated with 1ug/ml doxycycline every 24h. *(n = 1) Representative FACS plots to demonstrate the percentage of FcRL4+ population at 24h, 48h, 72h and 96h. Induced transduced priess cells gated on lymphocyte, singlet and live population before using an FMO at each timepoint to define the FcRL4+ population. The number in the gate represents the percentage of FcRL4+ cells.*

3.2.3.7 Doxycycline Titration

To induce FcRL4 expression, doxycycline was being used at 1µg/ml, which equated to a 1:1000 dilution of a 1mg/ml stock solution. To investigate whether a higher concentration of doxycycline could induce more FcRL4 expression but simultaneously not impact cell viability, doxycycline was titrated to a 1:500 (2µg/ml), 1:250 (4µg/ml) and 1:100 (10µg/ml) and compared to 1:1000 (1µg/ml). Transduced priess cells induced at a 1:500 dilution and a 1:250 dilution induced 34.1% and 32.2% FcRL4+ cells respectively compared to the 29.9% induced at a 1:1000 dilution (n = 1) (Figure 3.2.3.7). However, when doxycycline was titrated to 1:100 the percentage of FcRL4+ cells decreased to 12.5% suggesting that the concentration of doxycycline was cytotoxic to the transduced priess cells and affected their ability to express FcRL4 (Figure 3.2.3.7). Due to inducing an optimal percentage of FcRL4+ cells whilst maintaining good cell viability, the original 1:1000 dilution was used for subsequent experiments.

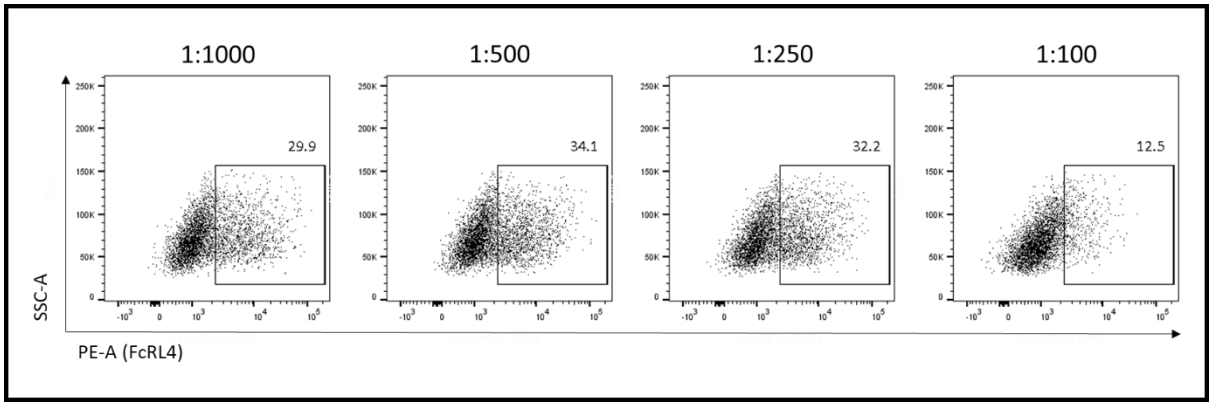

Figure 3.2.3.7., FcRL4 expression in transduced priess cells induced with different concentrations of doxycycline for 24h. *(n= 1) Representative FACS plots demonstrating the percentage of FcRL4+ cells induced with 1ug/ml, 2ug/ml, 4ug/ml and 10ug/ml doxycycline. Transduced priess cells gated on lymphocyte, singlet and live population before using an FMO to define the FcRL4+ population. The number in the gate represents the percentage of FcRL4+ cells.*

3.2.3.8 Expression of CD80, CD86 & HLA-DR

The transduced priess cells were intended to be used in subsequent experiments to explore FcRL4's role in antigen presentation so the expression of co-stimulatory molecules CD80, CD86 and HLA-DR was measured. Transduced priess cells were compared to untransduced priess cells and they were either unstimulated or stimulated for 24h with 1µg/ml doxycycline to determine whether doxycycline impacted expression of CD80, CD86 or HLA-DR. CD80, CD86 and HLA-DR expression was comparable in the untransduced priess cells regardless of whether they were cultured or not with doxycycline (CD80 – 81.40% vs. 82.00%, CD86 – 83.77% vs. 84.63%, HLA-DR – 80.10% vs. 82.27%, untreated compared to treated respectively) (n = 3) (Figure 3.2.3.8I). There was no significant difference between the unstimulated and stimulated untransduced priess cells (CD80 p=0.5209, CD86 p=0.7227, HLA-DR p=0.6291) (Figure 3.2.3.8II). This indicated that culturing priess cells with 1µg/ml doxycycline does not impact the expression of CD80, CD86 or HLA-DR.

When stained for CD80, CD86 and HLA-DR, transduced, unstimulated priess cells had decreased expression of all three co-stimulatory molecules compared to the untransduced priess cells and a negative population appears for all three co-stimulatory molecules (CD80 – 58.97%, CD86 – 67.43%, HLA-DR – 58.07%) (Figure 3.2.3.8I). In comparison, stimulated, transduced priess cells expressed similar levels of each co-stimulatory molecule to the untransduced priess cells but there is still a small negative population for each co-stimulatory molecule that isn't present in the untransduced priess cells (CD80 –79.20%, CD86 – 88.07%, HLA-DR – 78.50%) (Figure 3.2.3.8I). There was no significant difference between the stimulated transduced priess cells compared to the unstimulated,

untransduced priess cells (CD80 p=0.9932, CD86 p=0.9811, HLA-DR p=0.9968) (Figure 3.2.3.8II).

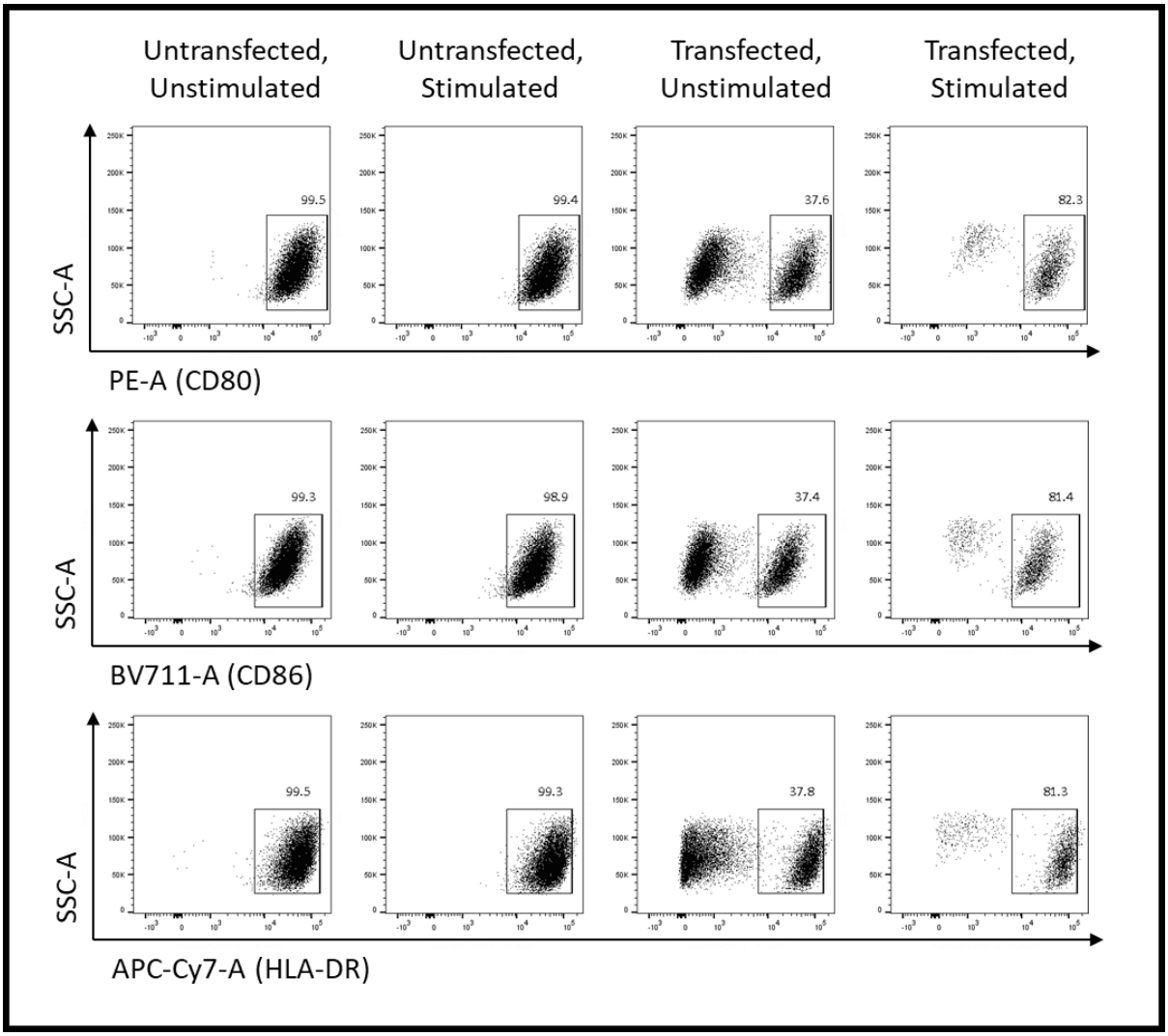

Figure 3.2.3.8I., Expression of CD80, CD86 and HLA-DR in untransduced priess cells and transduced priess cells, unstimulated or stimulated with 1µg/ml doxycycline*. (n = 1) (From left- right) Representative FACS plots of untransduced, unstimulated priess cells, untransduced, stimulated priess cells, transduced unstimulated priess cells and transduced, stimulated priess cells. (From top to bottom) %CD80+, %CD86+ and %HLA-DR+. The number in the gate represents the percentage of + cells.*

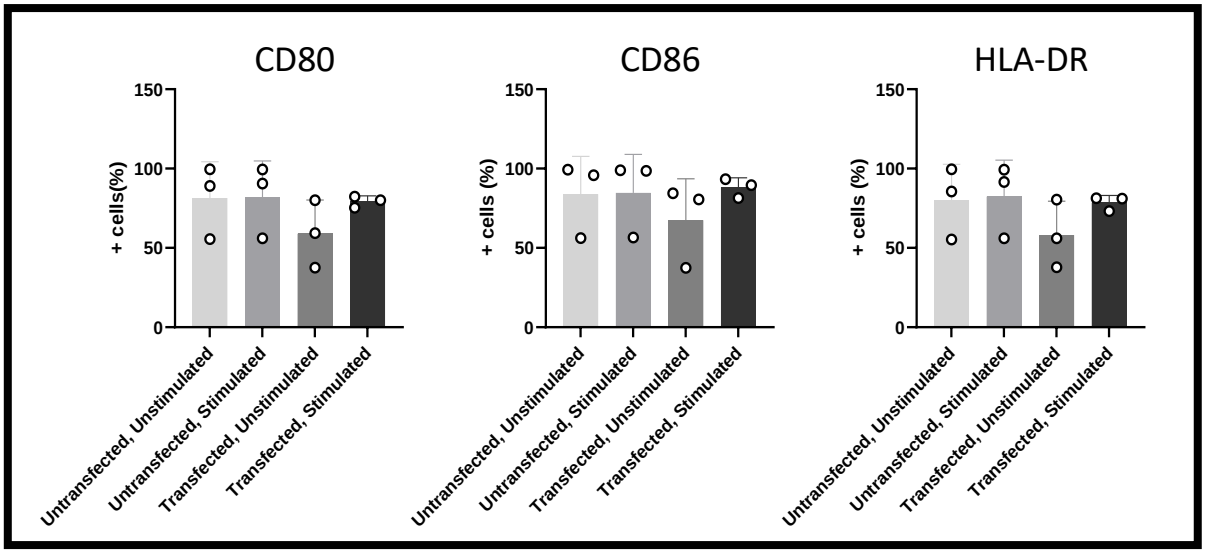

Figure 3.2.3.8II., Comparison of CD80, CD86 and HLA-DR expression between untransduced and transduced priess cells, unstimulated or stimulated with 1µg/ml doxycycline *(n = 3). CD80, CD86 and HLA-DR expression in the unstimulated untransduced priess cells was compared to the stimulated untransduced priess cells, unstimulated and stimulated transduced priess cells. Statistical test – Tukey's corrected one-way ANOVA.*

3.2.3.9 HA Colostrum IgA IC Binding

Finally, FcRL4+ transduced priess cells were tested for their ability to bind heat aggregated (HA) IgA, as this was required for investigating its functional consequences on FcRL4+ B cells. Firstly, FcRL4+ priess cells were incubated with 1mg/ml HA colostrum IgA for 30mins and then cells were stained for FcRL4 and IgA; the percentage value for FcRL4+IgA+ gate represents the percentage of FcRL4+ B cells whilst the movement of population up the y axis defines the FcRL4+IgA+ population. These were compared to FcRL4+ tonsil B cells that had been acid washed and incubated with 1mg/ml HA IgA. There was an increase in the FcRL4+IgA+ population in FcRL4+ transduced priess cells incubated with 1mg/ml HA colostrum IgA compared to FcRL4+ transduced priess cells incubated with 0mg/ml HA colostrum IgA (n = 1) (Figure 3.2.3.9I). The pattern of IgA binding observed in FcRL4+ transduced priess cells was similar to that in FcRL4+ tonsils (n = 1) (Figure 3.2.3.9II). Next, the concentration of HA colostrum IgA was titrated to determine the lowest concentration of IgA IC that could be used for subsequent experiments but still had detectable IgA binding using flow cytometry. IgA binding could be detected at 10µg/ml but was more obvious at 25µg/ml HA colostrum IgA (n = 1) (Figure 3.2.3.9III).

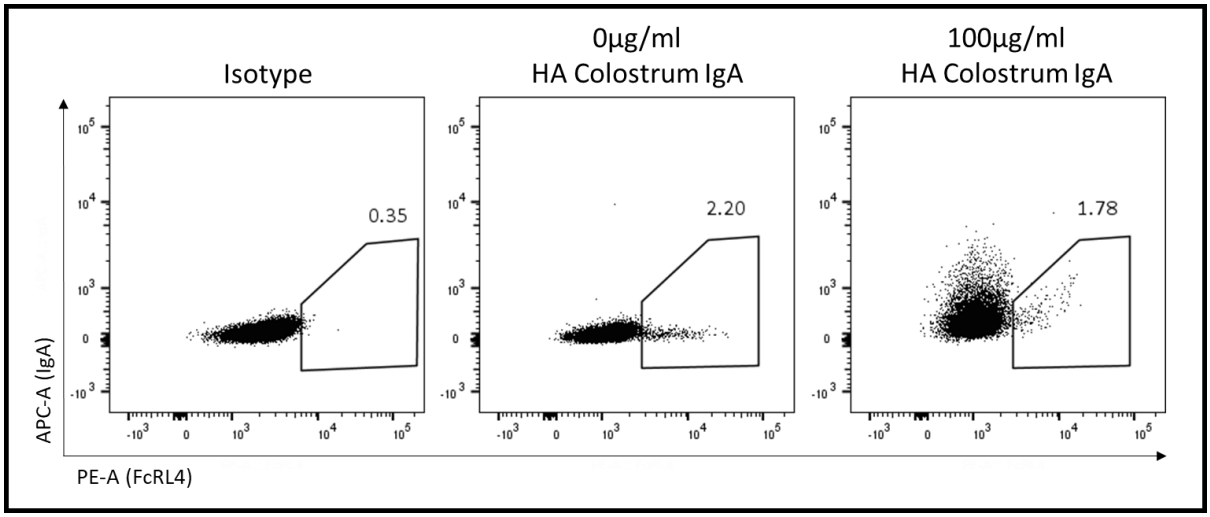

Figure 3.2.3.9I., IgA IC binding in FcRL4+ induced transduced priess cells. *(n = 1) Representative FACS plots demonstrate the differences in FcRL4+IgA+ populations when cells were incubated with or without 1mg/ml HA colostrum IgA. An isotype control was used to determine the FcRL4+ cells and the number above the gate represents the percentage of FcRL4+ cells in each sample. FcRL4+IgA+ population is located in the upper right quadrant of the FAC plot.*

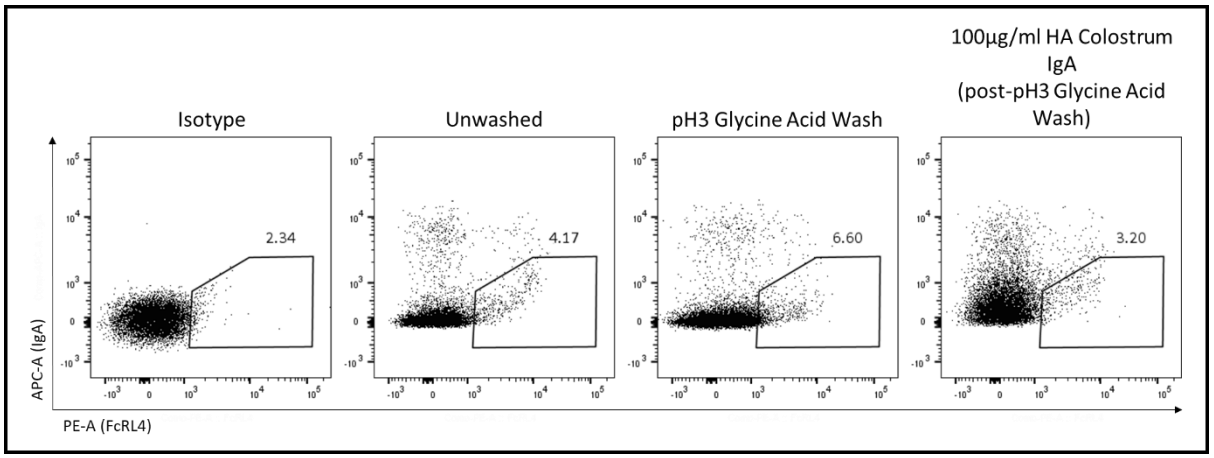

Figure 3.2.3.9II., IgA IC binding in FcRL4+ ex-vivo tonsil B cells. *(n = 1) Representative FACS plots demonstrate the differences in FcRL4+IgA+ populations when cells were incubated with or without 1mg/ml HA colostrum IgA. An isotype control was used to determine the FcRL4+ cells and cells were washed with pH3 glycine acid wash to determine the difference between surface bound and IgA BCR's. The number above the gate represents the percentage of FcRL4+ cells in each sample. FcRL4+IgA+ population is located in the upper right quadrant of the FAC plot.*

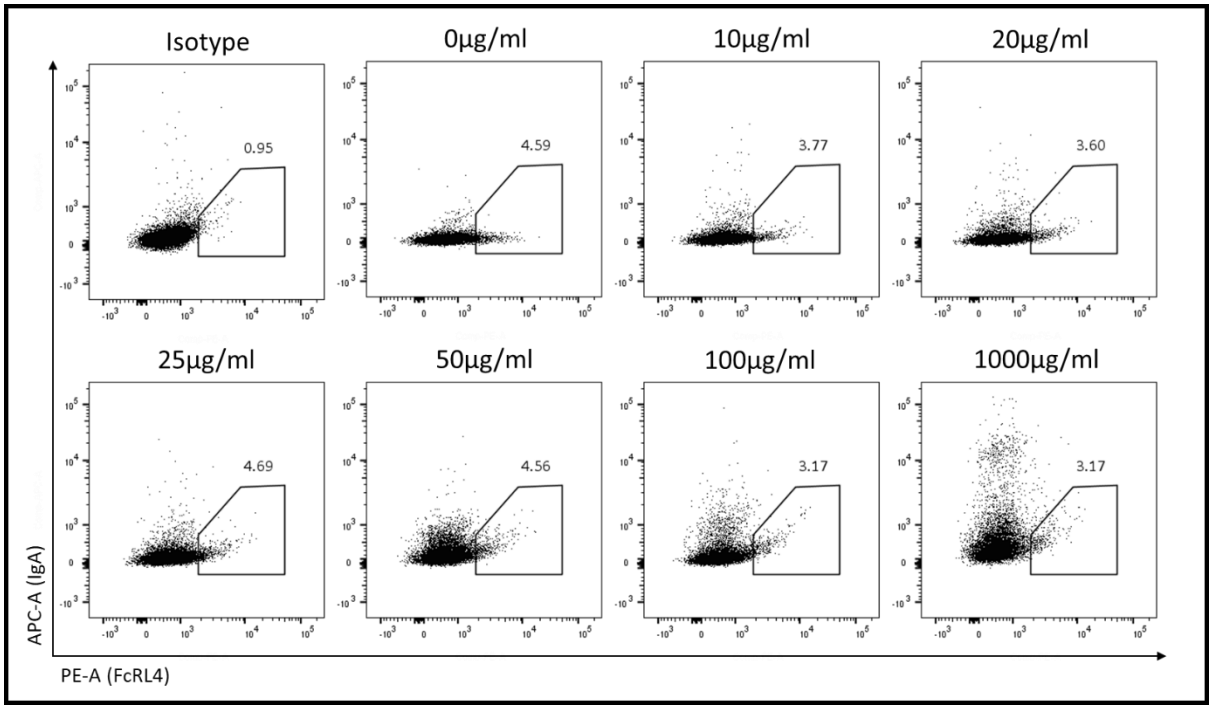

Figure 3.2.3.9III., Titration of IgA IC binding on FcRL4+ transduced priess cells. *(n = 1) Representative FACS plots demonstrating changes in the FcRL4+IgA+ population when IgA IC concentration increases. The FcRL4+IgA+ population is defined as a movement towards the upper right quadrant.*

3.3 Discussion

To explore the functional consequences of IgA IC binding to FcRL4+ B cells, an FcRL4-expressing B cell model needed to be created because total FcRL4+ B cell no. is relatively low in tonsils and in RA SF, which could make it challenging to explore functional consequences of IgA binding such as antigen presentation and BCR signalling [89,130]. The aim of the FcRL4-expressing model was to generate a high number of cells expressing FcRL4 but also to ensure these cells were viable long enough to explore their function. Our original priess B cell model constitutively expressed FcRL4 and resulted in a rapid loss of viable cells and low expression of FcRL4 suggesting that their needed to be tighter regulation on when FcRL4 was expressed to maintain cell viability and in turn FcRL4 expression. The Tet-On system was explored because ligation of the FcRL4 gene into the Tet-On expression vector meant that FcRL4 could not be expressed unless doxycycline was present. This produced a B cell model that could stably express FcRL4 for up to 48h before the cells began to undergo apoptosis and no longer be studied functionally. The transduced population was heterogenous, meaning some cells did not express FcRL4 on their surface although non transduced cells had been selected out previously using puromycin. This meant that for subsequent experiments, such as exploring internalisation and antigen presentation, the cells would need to be sorted prior to using to be confident that FcRL4- and FcRL4+ cells had been segregated.

The cloned FcRL4 gene was also conjugated to GFP, meaning that GFP-expressing cells were FcRL4+. This is important in the context of the PhosFlow experiments exploring effects on BCR signalling, as many of the IC staining antibodies were conjugated to PE or FITC/AF488, meaning that if these cells had to be stained for FcRL4 a lot of signalling molecules could not have been investigated in the transduced priess cells. However, it was determined that the

GFP defined population was significantly smaller than the anti-FcRL4 PE-stained population indicating that staining for FcRL4 with an antibody was a more reliable method for FcRL4 detection.

Once FcRL4 expression had been confirmed, the transduced priess cells needed to be interrogated further to determine whether they could be used in experiments to investigate consequences of IgA binding. FcRL4 was described to be a receptor for aggregated IgA but not monomeric IgA, so FcRL4+ transduced priess cells were incubated with 1mg/ml HA colostrum IgA and compared to tonsils as a positive control to see whether they could bind IgA IC's [19,123,136]. The FcRL4+ transduced priess cells bound to HA IgA in a similar manner to FcRL4+ tonsil B cells suggesting that these cells were capable of interacting with IgA so its function could be explored. There was also an FcRL4- population in the transduced priess cells that appear to bind HA IgA. IgA receptor expression has not been fully described in priess cells so the FcRL4-IgA+ population needs to be investigated to determine if the staining is a background signal or whether there is another IgA receptor expressed that can bind HA IgA.

Finally, to check if these cells were suitable to investigate antigen presentation, FcRL4+ transduced priess cells were stained for CD80, CD86 and HLA-DR. CD80 and CD86 are required to interact with CD28 whilst the antigen loaded HLA-DR interacts with the TCR on CD4+ T cells. Interaction of HLA-DR with the matching TCR activates the T cell whilst binding of co-stimulatory molecules CD80 and CD86 to CD28 and CTLA-4 stabilises the synapse and creates a more robust interaction between the B cell and T cell. If these are not present then the B cell is less likely to form an effective connection with its cognate T cell and initiate a response to the antigen [80]. When transduced priess cells had not been induced with

doxycycline there was a decrease in the expression of CD80, CD86 and HLA-DR compared to untransduced priess cells. In comparison, induction of FcRL4 expression, increased expression of CD80, CD86 and HLA-DR, similar to the untransduced priess cells. This indicated that induction of FcRL4 in transduced priess cells doesn't affect expression of CD80, CD86 and HLA-DR and may have rescued the minor loss of expression caused by transducing the cells with a lentiviral vector. As these cells express the necessary proteins to interact with T cells during antigen presentation it suggested that these would be a suitable FcRL4+ B cell model to explore their role in antigen presentation of IgA IC's.

Overall, using the Tet-On expression system has created a B cell model that stably expresses FcRL4 for 48h and is suitable to explore the functional consequences of IgA IC binding on BCR signalling as well as internalisation and antigen presentation. Therefore, these cells were taken forward to initially validate functional assays and then be used for comparison to *ex-vivo* FcRL4+ B cells from tonsil and RA SF.

4 Internalisation and Antigen Presentation of IgA IC by FcRL4+ B Cells

4.1 Introduction

Fc receptors, specifically FcγRs, are able to internalise antigens by binding to opsonised viruses or infected cells and internalise by antibody-dependent phagocytosis [72]. FcγR have also been shown to enhance antigen presentation in DCs by enhancing endosomal maturation and lysosomal fusion to facilitate antigen processing [72]. Unlike FcRL4, FcγRs capture IgG immune complexes and depending which isoform it binds can determine whether the antigen is internalised or not. Crosslinking of FcγRs, for example FcγRIIa, with an IgG immune complex initiates phosphorylation of the IC ITAMs, which promotes phagocytosis of the IgG immune complexes and receptor internalisation. However, when FcγRIIb is crosslinked with an IgG IC, internalisation of the receptor is inhibited, as the phosphorylation of its intracellular (IC) ITIMs recruits and phosphorylates phosphatases such as SHP-1 and SHP-2, which downregulate activating signals that promote receptor internalisation [72]. This was confirmed when conditional deletion of FcγRIIb resulted in enhanced antigen presentation, determined by increased T cell activation and upregulation of MHC-II [72]. Sometimes pathogens take advantage of this by a phenomenon known as antibody dependent enhancement (ADE) where pre-existing antibodies facilitate viral entry into host cells, increasing their virulence. FcγRs are key mediators of ADE of IgG-bound viruses and can only interact with them in an IC conformation. To investigate IgA IC internalisation by FcRL4, an IgA IC was created by biotinylating HA IgA and conjugating it to a pHrodo avidin™ dye. pHrodo dyes are pH sensitive meaning that they will only fluoresce in acidic environments, such as endosomes and lysosomes. Therefore, if the IgA IC was internalised, FcRL4+ cells would become fluorescent.

B cells are able to recognise antigens presented by macrophages or DC's forming an immunological synapse. The synapse between a B cell and either a DC or macrophage requires actin filaments to spread and contract around the B cell membrane to allow it to extract the antigen from the surface [73,78]. Additionally, the bond strength determines the extraction of high affinity antigens [78]. Previous bulk-RNA seq identified that FcRL4+ B cells expressed higher levels of CD80 and CD86 compared to FcRL4- B cells. This suggests that the expression of FcRL4 may be part of a programme that leads to a switch to an antigen presenting phenotype in B cells.

Targeting Antigen Presentation

Currently, there isn't many therapeutics available that target antigen presentation in RA. However, antigen-targeting therapies have demonstrated to have a level of efficacy in other autoimmune diseases. For example, glatrimer acetate (GA), a synthetic random basic copolymer, was trialled in patients with multiple sclerosis. Patients that received GA had decreased CD19+ B cells and CD4+ T cells, which was translated in mice models to be caused by increased B cell antigen-presenting capacity to Tregs. This reduced overall inflammation caused by proinflammatory T cells[137].

If antigen presentation could be inhibited, then this would reduce the number of CD4+ autoreactive T cells that are activated in the synovium and reduce their contribution in the inflammatory environment. Specifically, in regards to FcRL4+ B cells, this would be particularly important because they have already been identified as a cytokine-producing population. If they were identified as antigen-presenting as well, this would support the argument to therapeutically target of this cell population, as it would allow for a more specific B cell depleting therapy rather than the conventional blanket B cell depleting

therapies, such as Rituximab. This would reduce the immunosuppressive side effects in patients and give them a better quality of life.

4.2 Results

4.2.1 IgA IC pHrodo Avidin™ Validation

4.2.1.1 IgA IC & pHrodo Avidin™ Titration

pHrodo avidin™ is a pH sensitive fluorogenic dye that increases in fluorescence when it is in an acidic environment. Previous work done with the IgA IC & pHrodo avidin™ conjugation had used 5µg/ml biotinylated IgA IC and a 1:500 dilution of the pHrodo avidin™. However, upon repeating this work a signal could not be detected using the Zeiss LSM880 Airyscanner. Therefore, the concentration of IgA IC and dilution of pHrodo avidin™ needed to be titrated to determine the optimal ratio required for detection but also limited background detection. The IgA IC was titrated to 10µg/ml and 25µg/ml and the pHrodo avidin™ was titrated 4µg/ml(1:250), 2µg/ml (1:500), 1.33µg/ml (1:750) and 1µg/ml (1:1000). The IgA IC and pHrodo avidin™ were incubated together for at least 30 minutes to allow enough time for them to bind to each other before being added to induced, transduced priess cells for two hours. FcRL4- and FcRL4+ cells were gated based on their expression of GFP, as FcRL4 is conjugated to it in the transduced cells and pHrodo avidin™ is detected in the PE channel, the same as anti-FcRL4 PE from Biolegend.

Cells that were treated with 10µg/ml IgA IC produced a signal in both the FcRL4- and FcRL4+ populations and for each dilution of pHrodo avidin™ the percentage of IgA+ cells were higher in the FcRL4- population compared to the FcRL4+ population (n = 1) (Figure 4.2.1.1I). This suggested that there was a higher background signal when cells were treated with 10µg/ml IgA IC and could potentially be caused by there not being enough binding sites on the biotinylated IgA for the pHrodo avidin to bind to and therefore there was free pHrodo avidin™ in culture that has attached to the cells non-specifically. However, when the

concentration of IgA IC was increased to 25µg/ml the background signal of the pHrodo avidin™ in FcRL4- showed a dramatic decrease. Additionally, when pHrodo avidin™ was diluted to 2µg/ml the percentage IgA IC/pHrodo+ cells were greater in the FcRL4+ population compared to the FcRL4- population (n = 1) (Figure 4.2.1.1II). When pHrodo avidin™ was diluted more the signal was too weak to detect suggesting that the optimal ratio was 25µg/ml IgA IC and 2µg/ml pHrodo avidin™.

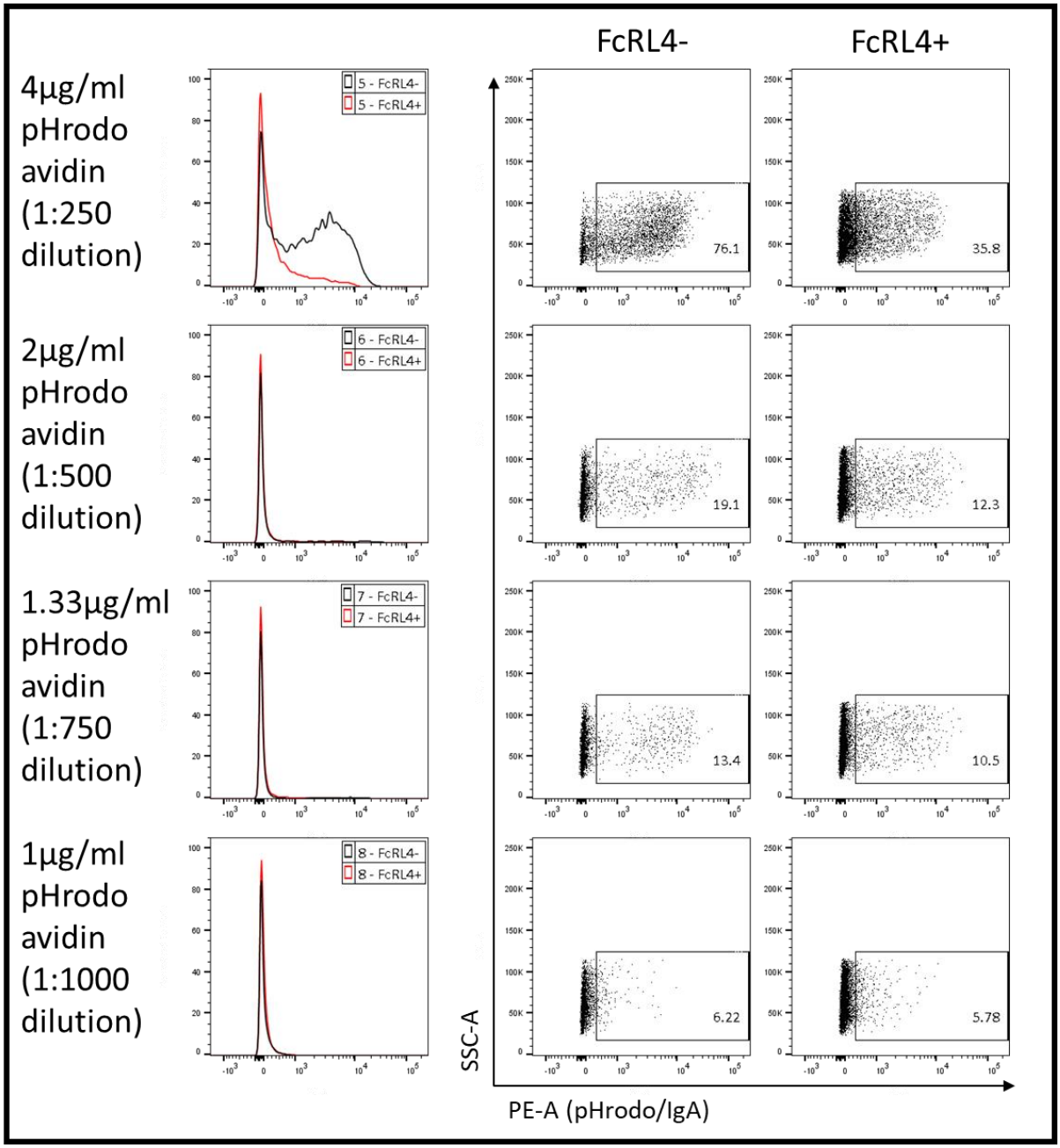

Figure 4.2.1.1I., pHrodo staining in cells incubated with 10µg/ml HA colostrum IgA. *(n = 1) 10µg/ml HA colostrum IgA was incubated with pHrodo avidin for 30mins at 1:250 (4µg/ml), 1:500 (2µg/ml), 1:750 (1.33µg/ml) and 1:1000 (1µg/ml) dilutions. The 10µg/ml HA colostrum IgA/pHrodo was then incubated for 2 hours with induced transduced priess before visualisation on the BD FortessaX-20. The histograms represent the difference in IgA/pHrodo staining between the FcRL4- and FcRL4+ cells: black line - FcRL4-, red line - FcRL4+. Representative FACS plots show the differences between the FcRL4- and FcRL4+ population The number in the gate represents the percentage of IgA/pHrodo+ cells.*

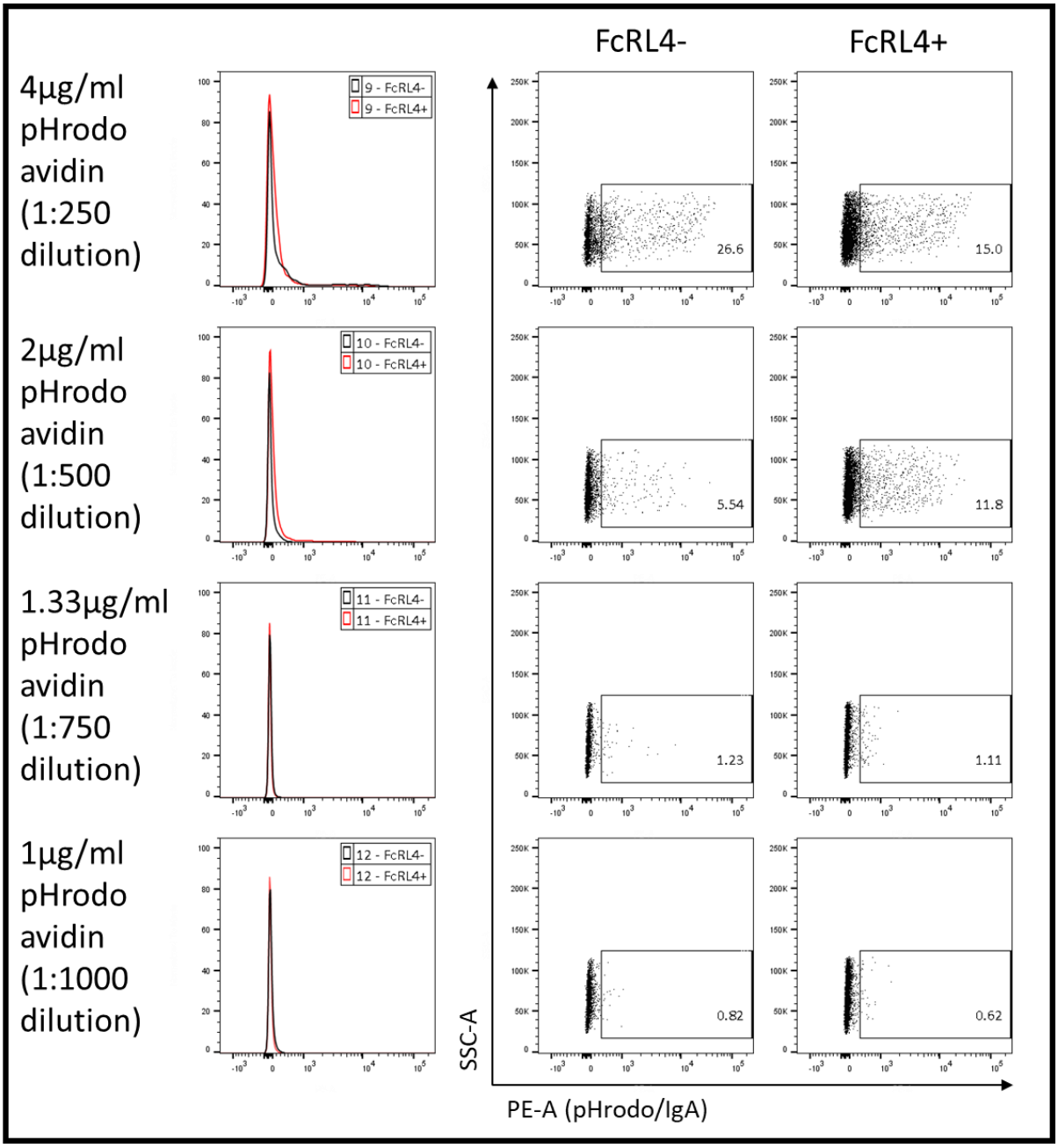

Figure 4.2.1.1II., pHrodo staining in cells incubated with 25µg/ml HA colostrum IgA. *(n = 1) 25µg/ml HA colostrum IgA was incubated with pHrodo avidin for 30mins at 1:250 (4µg/ml), 1:500 (2µg/ml), 1:750 (1.33µg/ml) and 1:1000 (1µg/ml) dilutions. The 25µg/ml HA colostrum IgA/pHrodo was then incubated for 2 hours with induced transduced priess before visualisation on the BD FortessaX-20. The histograms represent the difference in IgA/pHrodo staining between the FcRL4- and FcRL4+ cells: black line - FcRL4-, red line - FcRL4+. Representative FACS plots show the differences between the FcRL4- and FcRL4+ population The number in the gate represents the percentage of IgA/pHrodo+ cells.*

4.2.1.2 1% BSA Test

To reduce the background signal present in the FcRL4- population, the HA colostrum IgA IC and pHrodo avidin™ were incubated together in RPMI only or in RPMI + 1% BSA. 25µg/ml HA colostrum IgA IC and 2µg/ml pHrodo avidin™ were used, as determined by the titration experiment in Figure 4.2.1.2II. Similar to the previous experiment the percentage of IgA IC/pHrodo+ cells were higher in the FcRL4+ population compared to the percentage of FcRL4- population (90% vs. 67.6% respectively) (n = 1) (Figure 4.2.1.2). The addition of 1% BSA to RPMI reduced the IgA IC/pHrodo+ staining in both the FcRL4- and FcRL4+ population (38.5% vs. 68.5% respectively) indicating that addition of BSA to RPMI was sufficient at reducing non-specific binding in FcRL4- and FcRL4+ cells. As BSA supplementation to RPMI was sufficient to reduce the background signal created by pHrodo it was taken forward for subsequent experiments (Figure 4.2.1.2).

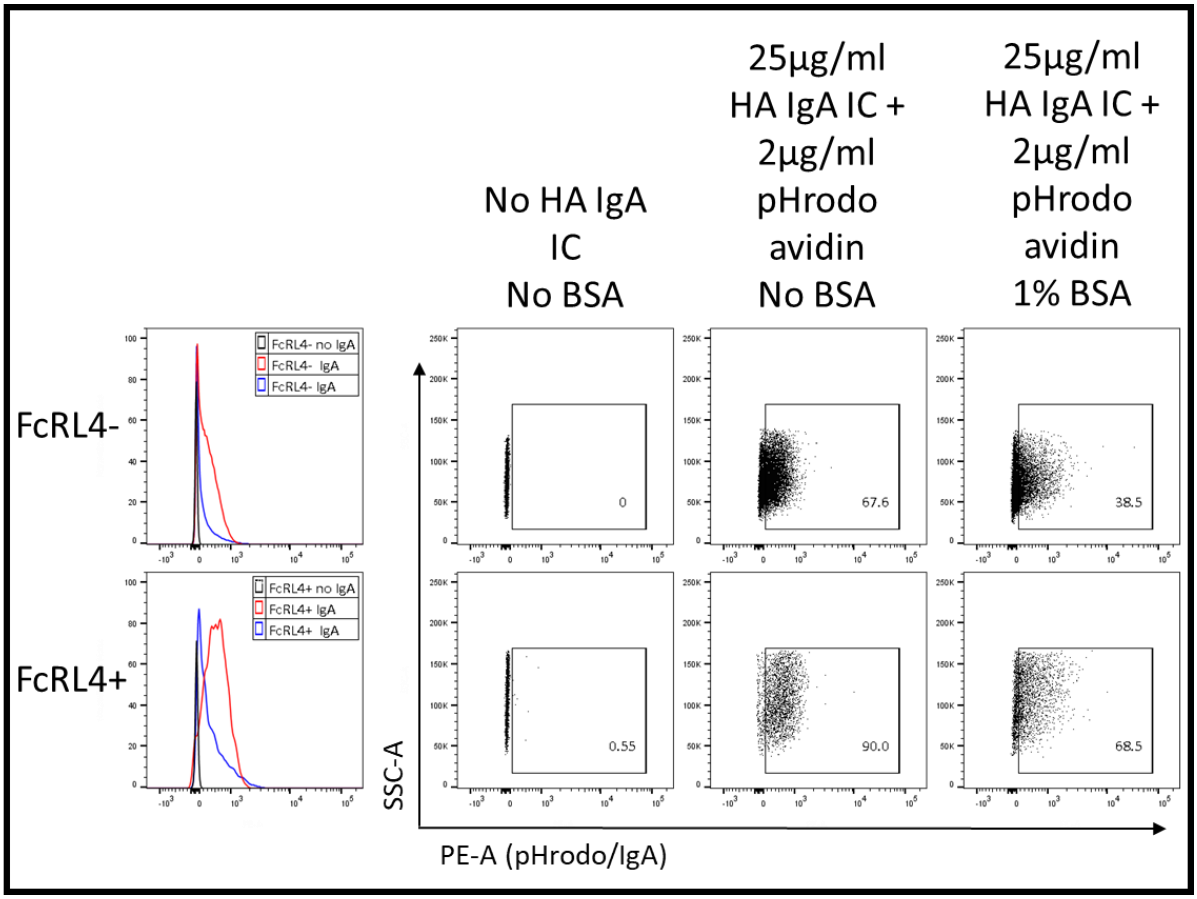

Figure 4.2.1.2., Addition of 1% BSA reduces IgA IC/pHrodo staining in FcRL4- and FcRL4+ induced transduced priess cells*. (n = 1) 25µg/ml HA colostrum IgA & 2µg/ml pHrodo avidin were incubated together for 30mins in either RPMI only or RPMI supplemented with 1%BSA. These were then added to induced transduced priess cells and incubated for 2 hours. Histograms demonstrating the differences in staining between FcRL4- and FcRL4+ with and without 1% BSA: black line - no HA IgA/pHrodo, red line - HA IgA/pHrodo, no BSA, blue line - HA IgA/pHrodo 1% BSA. The number in the gate on representative FACS plots indicates the percentage of HA IgA/pHrodo+ cells*

4.2.2 IgA IC Internalisation

To initially investigate internalisation of HA colostrum IgA IC, FcRL4- and FcRL4+ cells sorted from induced transduced priess, *ex-vivo* tonsil, and *ex-vivo* RA SF samples were suspended in 0.5% collagen gel and left to set on ice for at least an hour prior to imaging at 37°C. The FcRL4- cells were used as the negative control whilst FcRL4+ transduced priess cells that had been pre-treated with HA colostrum IgA IC/pHrodo avidin™ for two hours was used as a positive control, as previous titration experiments had observed IgA internalisation after 2 hours. The gain and laser intensity were initially set on the FcRL4- cells to reduce the background signal and then these same conditions were applied to the pre-treated FcRL4+ transduced priess cells to ensure that the FcRL4 and pHrodo signal could be detected. Images of the FcRL4- cells were only taken at the 0min and 120mins timepoint, as the FcRL4- cells were only imaged to check that none or little internalisation was observed, whilst the frame being imaged for the FcRL4+ cells needed to be consistent for each timepoint as to observe consistent changes in IgA internalisation. Using Zen software, the subsequent images were normalised to the same fluorescent intensity and then edited using Image J to enhance the contrast between FcRL4 in the FITC (transduced priess cells) and APC (tonsil and RA SF) channel with the IgA/pHrodo in the PE channel. ZombieAqua was not used to identify viable cells for imaging to reduce the number of colours being imaged and the chance of spillover between channels. Instead, a visual check of the cells using brightfield was done at the start and end of the imaging to ensure the cells still looked viable.

To support the fluorescent imaging data, cells from induced transduced priess cells cultures, tonsils and RA SF were plated and incubated with the HA colostrum IgA IC/pHrodo avidin™. To achieve a balance between allowing enough time for internalisation of IgA ICs but to not

compromise the viability of the cells in culture, cells were cultured for up to 2 hours and were fixed with BD CytoFix at 0, 10, 20, 30, 40, 50, 60, 90 and 120mins timepoints. Some cells were untreated and fixed at 0mins as a negative control for the pHrodo signal. These cells then stained for FcRL4 to allow for gating on the FcRL4- and FcRL4+ populations. The percentage of IgA IC/pHrodo+ cells was determined by gating on the 0mins group and the same gate applied to subsequent timepoints. The FcRL4- and FcRL4+ were then plotted against each other to determine the difference in percentage of IgA IC/pHrodo+ cells for each timepoint. A viability dye, such as ZombieAqua, was not included to maintain continuity in the cell populations being observed in the flow cytometry and fluorescent imaging data. Instead, the gating strategy in Figure 2.5.2 was used to define a viable population, as it defined 81.0% in induced transduced priess cells and 97.5% in *ex-vivo* tonsil cells when using ZombieAqua.

4.2.2.1 FcRL4+ Transduced Priess Cells

After gating the induced transduced cells (Figure 8.2), the percentage of IgA IC/pHrodo+ cells were investigated in the FcRL4- and FcRL4+ populations (n = 2). When compared to each other, both the FcRL4- and FcRL4+ show a steep increase in the percentage of IgA IC/pHrodo+ cells from 0-50mins, which then plateaus and maintained until 120mins. Although they demonstrate similar kinetics in internalisation of IgA, the percentage of IgA IC/pHrodo+ cells were higher for all timepoints in the FcRL4+ cells (30.79%) compared to the FcRL4- (24.15%) although at n=2 significance was not observed between any of the timepoints (Figure 4.2.2.1I & II). When interrogated separately, all timepoints proceeding 0mins in the FcRL4+ population were significantly different compared to 0mins (Figure 4.2.2.1II). A similar pattern was observed in the FcRL4- population, with only the 10mins timepoint not being significantly different to 0mins (Figure 4.2.2.1II).

To see if this increase in IgA internalisation could be detected using fluorescent imaging, untransduced priess cells were used to correct for autofluorescence and then pre-treated transduced priess cells were used to confirm the intensity at which the pHrodo signal could be detected to show IgA internalisation (Figure 4.2.2.1III). Similar to the flow cytometry data, pHrodo (red) could be detected as early as 10mins. The pHrodo fluorescence then began to appear in more cells whilst simultaneously becoming brighter in cells that had already internalised IgA (Figure4.2.2.1IV). To determine if this signal was specific to FcRL4+ cells, the FcRL4 stain and pHrodo IgA stain were split to determine where the staining was localised. The IgA staining, defined in red, colocalised entirely with FcRL4+ cells defined in green, suggesting that the IgA internalisation was specific to the FcRL4+ cells (4.2.2.1V).

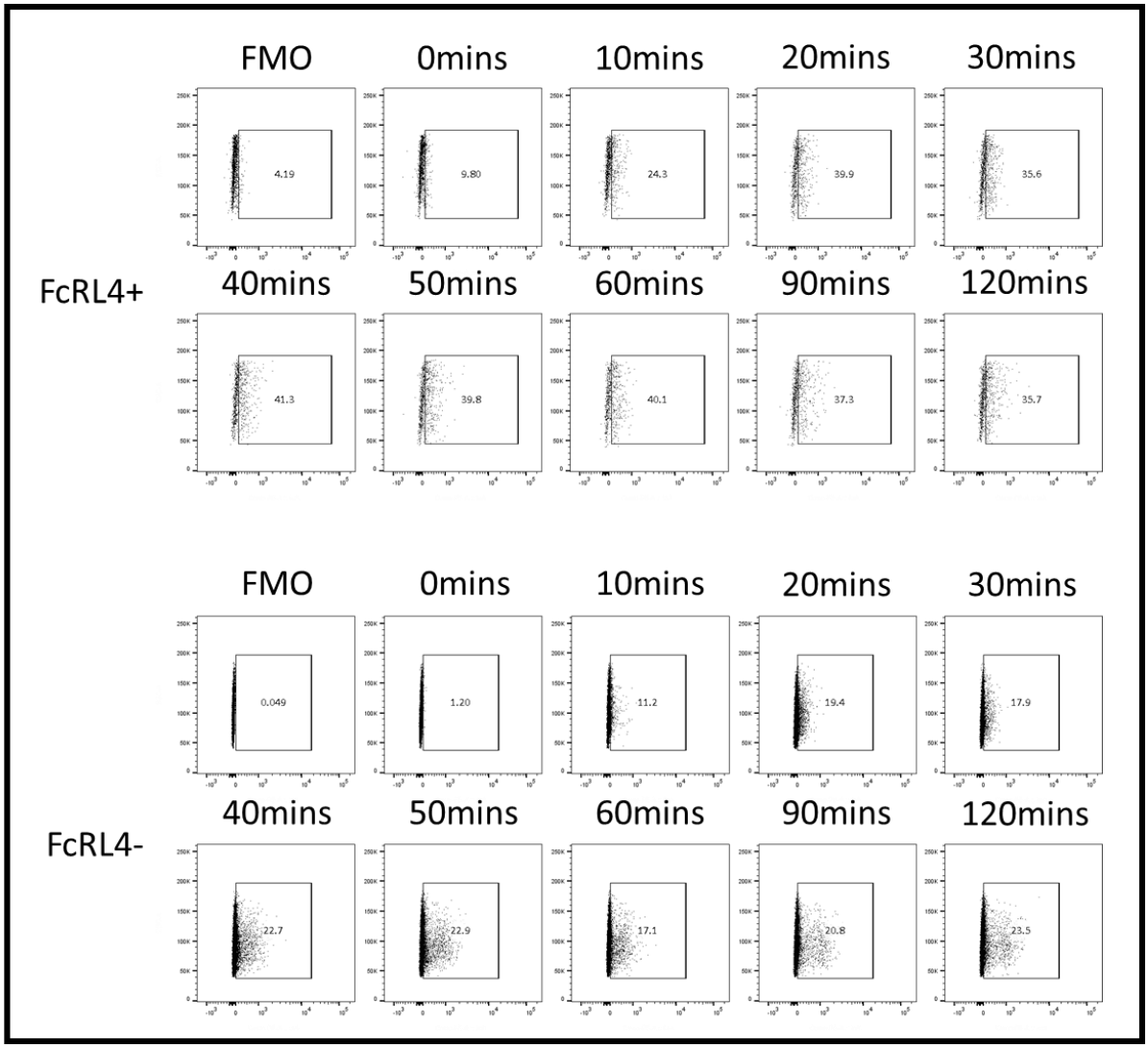

Figure 4.2.2.1I., IgA IC/pHrodo internalisation by FcRL4- and FcRL4+ transduced priess cells raw flow cytometry data. *(n = 1), representative FACS plots demonstrating the internalisation of 25µg/ml HA colostrum IgA IC/2µg/ml pHrodo by FcRL4- and FcRL4+ transduced priess cells. FcRL4- and FcRL4+ transduced priess were identified by gating on the lymphocyte population, as defined by FSC-A/SSC-A before distinguishing the FcRL4- population as SSC-A/FITC-A- and the FcRL4+ population as SSC-A/FITC-A+. To determine the cells that were internalising HA colostrum IgA IC/pHrodo the FcRL4- and FcRL4+ cells were gated on an FMO where the cells had not been incubated with the HA colostrum IgA IC/pHrodo, defined as SSC-A/PE-A+. The number in the gate defines the percentage of cells that have internalised the HA colostrum IgA IC/pHrodo.*

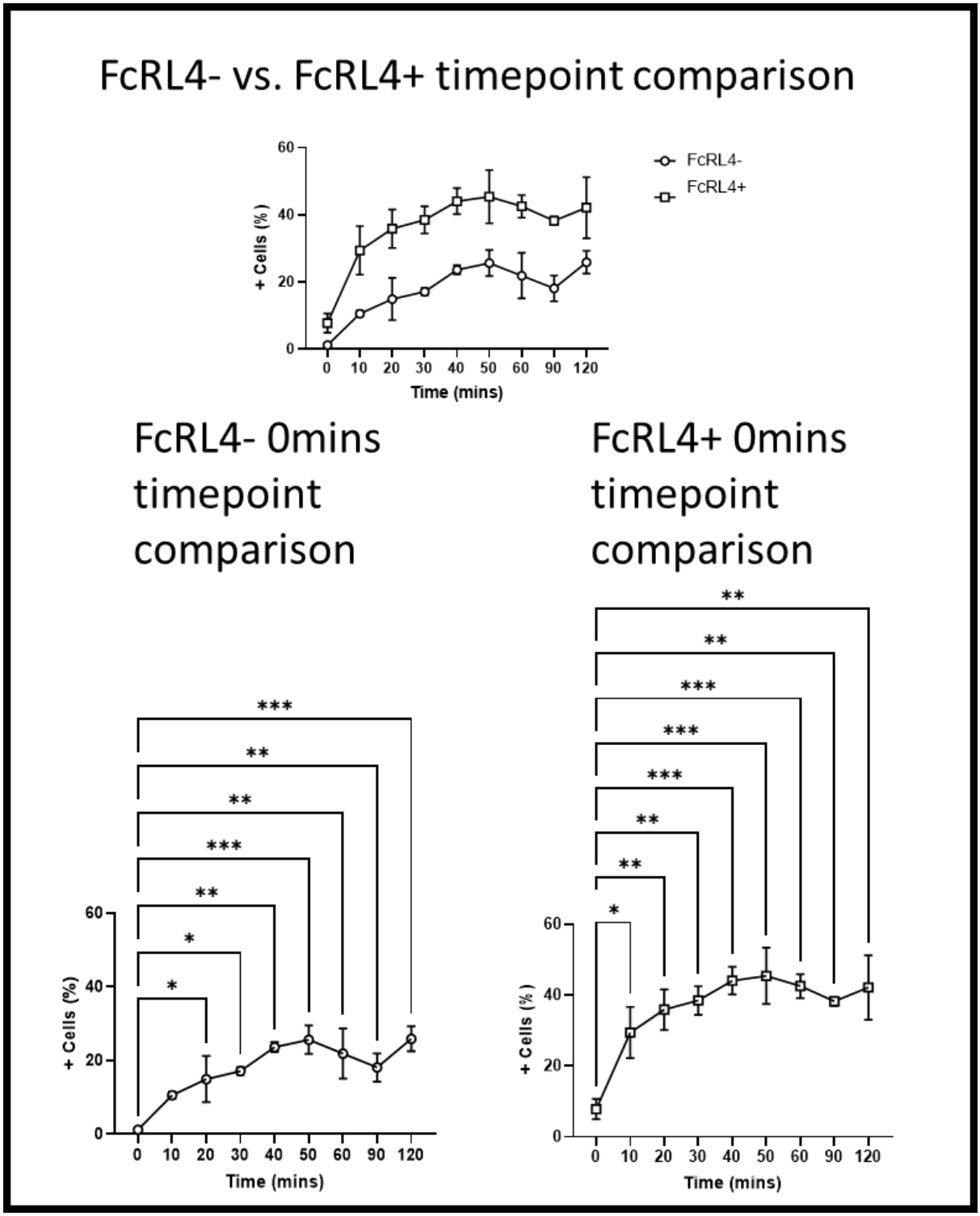

Figure 4.2.2.1II., IgA IC/pHrodo internalisation by FcRL4- and FcRL4+ transduced priess cells. *(n = 2) The percentage of HA colostrum IgA IC/pHrodo+ cells was taken at each timepoint for the FcRL4- and FcRL4+ transduced priess cells and the mean percentage of HA colostrum IgA IC/pHrodo+ cells was calculated. (Top graph) The mean change in the percentage of IgA IC/pHrodo+ cells in the FcRL4- and FcRL4+ population were compared to each other at every timepoint. Statistical test – Šidák's multiple comparison corrected two-way ANOVA. (Bottom graphs) The mean change in the percentage of IgA IC/pHrodo+ at each time point was compared to the 0mins timepoint for both the FcRL4- cells and FcRL4+ cells. Statistical test – Dunnett's multiple comparison corrected one-way ANOVA.*

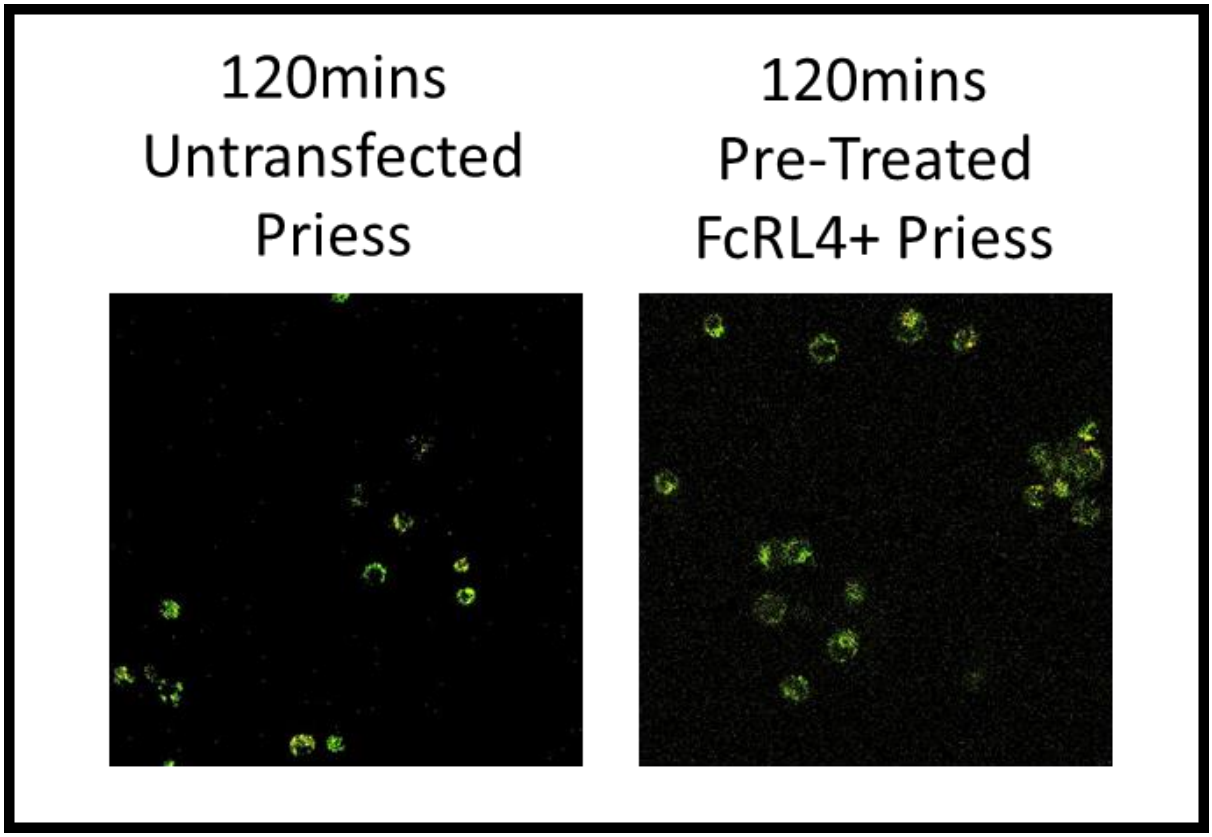

Figure 4.2.2.1III., Fluorescence for live cell imaging of FcRL4- induced transduced priess and pre-treated induced transduced priess and HA colostrum IgA IC/pHrodo*. (n = 1) FcRL4- induced transduced priess were kept after sorting from FcRL4+ induced transduced priess and imaged at 0mins to set the laser intensity and gain for GFP. 1x10^6 FcRL4+ induced transduced priess were incubated with 25µg/ml HA colostrum IgA IC/2µg/ml pHrodo 2 hours prior to imaging. The laser intensity and gain were increased when imaging until red could be visualised in the pre-treated FcRL4+ transduced priess. FcRL4- The settings were checked back against the FcRL4- transduced priess to check a red signal could not be detected in these cells.FcRL4- induced transduced priess were incubated with 25µg/ml HA colostrum IgA IC/2µg/ml pHrodo and imaged again at 120mins to visualise pHrodo staining (red).*

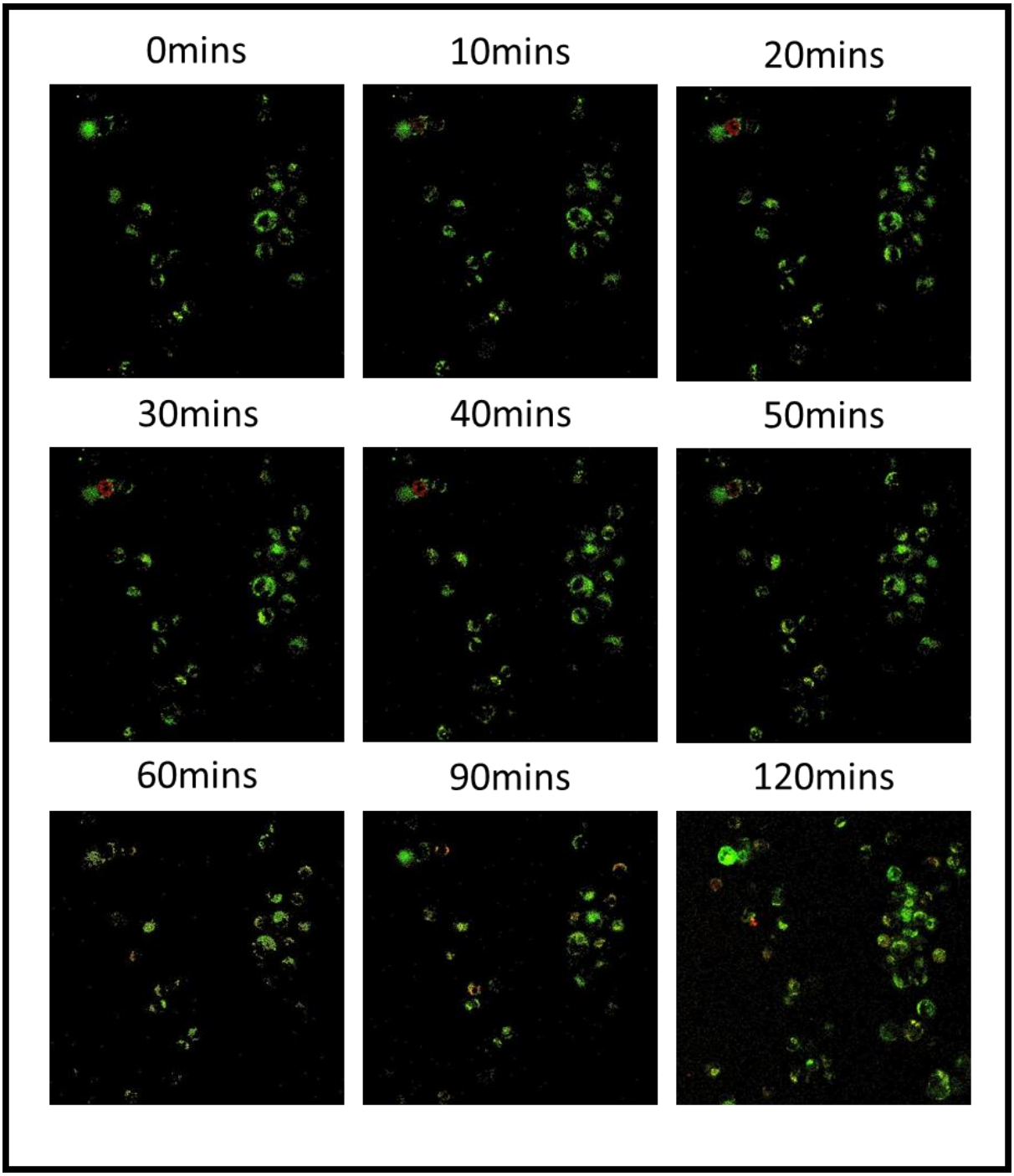

Figure 4.2.2.1IV., Live cell fluorescent images of FcRL4+ transduced priess cells in 0.5% type II rat tail collagen gel. *(n = 1) Transduced priess were induced with 1µg/ml doxycycline for 24h and then sorted on FITC to separate the FcRL4- and FcRL4+ priess cells. FcRL4- and FcRL4+ transduced priess cells were suspended in 0.5% type II rat tail collagen gel and plated in µ perfusion slides alongside pre-treated transduced priess cells that had been incubated with 25µg/ml HA colostrum IgA IC/2µg/ml pHrodo 2 hours prior to imaging, as a positive control. FcRL4- transduced priess cells were used to correct for autofluorescence in the FITC channel. FcRL4+ transduced priess were perfused with 25µg/ml HA colostrum IgA IC/2µg/ml pHrodo and imaged at 0mins, 10mins, 20mins, 30mins, 40mins, 50mins, 60mins, 90mins, 120mins. Green - FcRL4, Red - HA IgA/pHrodo.*

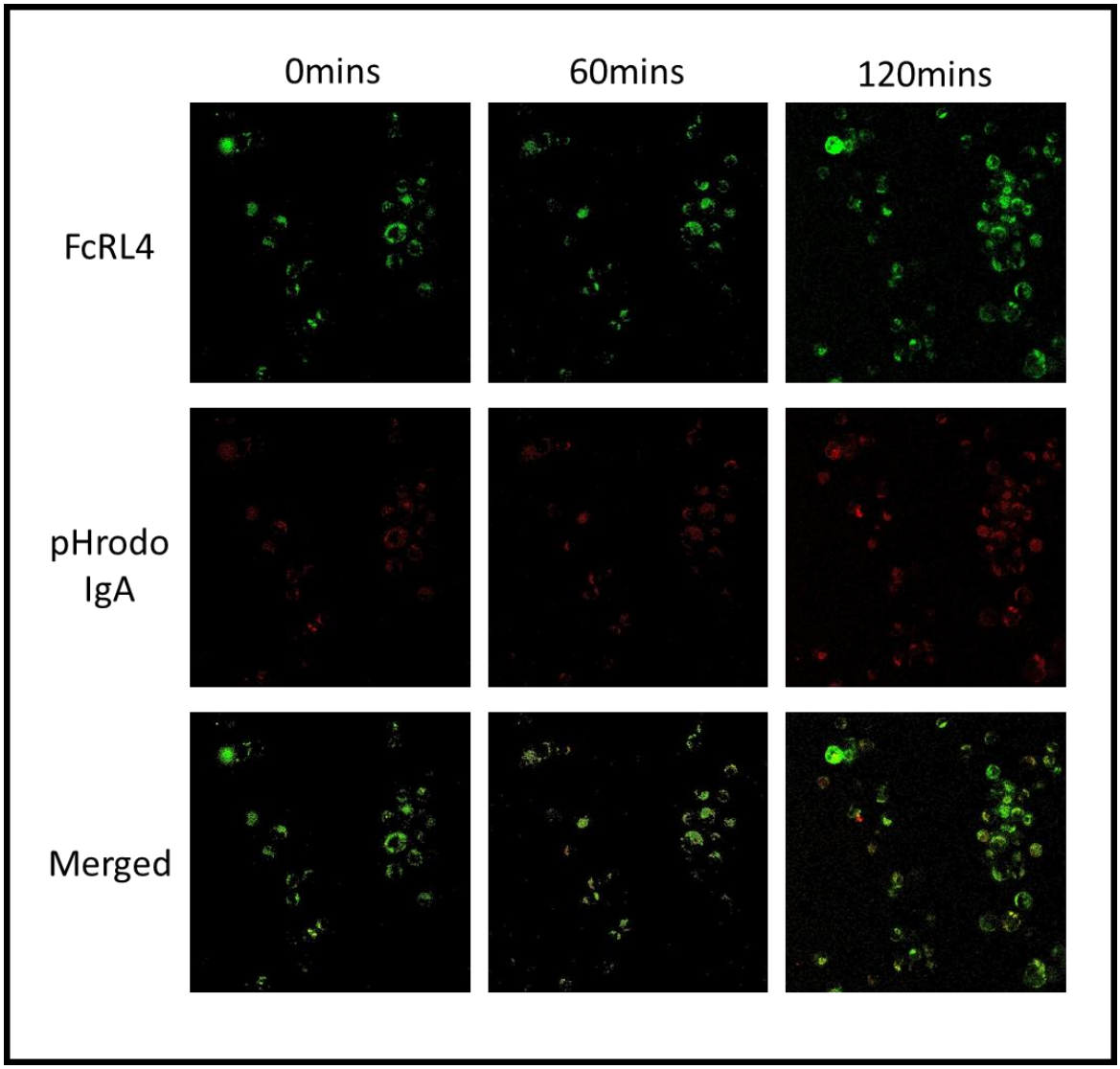

Figure 4.2.2.V., IgA IC/pHrodo staining colocalises with FcRL4+ transduced priess cells. *(n = 1) Live cell fluorescent images taken of FcRL4+ transduced priess cells suspended in 0.5% type II rat tail collagen gels. The same images in Figure 4.2.2.1III at timepoints 0mins, 60mins and 120mins were separated into FcRL4+ image layer (green) and HA colostrum IgA IC/pHrodo image layer (red) other to identify if the fluorescence generated by internalised pHrodo was co-localised with FcRL4+ transduced priess. From top to bottom: FcRL4 staining only (green) at 0mins, 60mins and 120mins, HA colostrum IgA IC/pHrodo staining only (red) at 0mins, 60mins, 120mins and FcRL4 and HA IgA/pHrodo staining together (merged) at 0mins, 60mins and 120mins.*

4.2.2.2 FcRL4+ Tonsil B Cells

Next, to see if the results obtained in the FcRL4+ transduced priess B cell model could be replicated in patient samples, ex-vivo tonsil samples were first tested due to them being a consistent source of FcRL4+ B cells (n = 3). FcRL4+ and FcRL4- cells were gated to exclude non-viable cells and defined as CD3- and CD19+ (Figure 8.3). Although the difference in the percentage of IgA IC/pHrodo+ cells between the FcRL4- and FcRL4+ B cells was less prominent in the tonsils compared to the transduced FcRL4+ priess cells, it was still higher for all timepoints in the FcRL4+ cells (Figure 4.2.2.2I & II). This difference was significant between the 30mins (p= 0.014), 60mins (p=0.0046) and 90mins (p = 0.04) timepoints and percentage of IgA IC/pHrodo+ cells peaked at 30mins (52%). When analysed separately, all the timepoints except 20mins was significantly different to 0mins in the FcRL4+ cells whilst only the 40mins (p = 0.0128) and 120mins (p = 0.0482) timepoints were significantly different to 0mins in the FcRL4- cells and percentage of IgA IC/pHrodo+ cells peaked at 40mins (35.07%) (Figure 4.2.2.2I & II).

For the tonsils, FcRL4- and FcRL4+ B cells had to be isolated from the rest of the B cell population by cell sorting to concentrate the number of FcRL4+ cells. To reduce the number of fluorophores that would be detected during imaging, FcRL4+ cells were only stained for FcRL4, as it only defines memory B cells and therefore there was a low risk of including other cell types within the sample. Unlike the FcRL4+ transduced priess cells, pHrodo did not start to fluoresce until 40mins and continued to intensify until 120mins (Figure 4.2.2.2IV). Similarly to FcRL4+ transduced priess cells, when the FcRL4 and IgA staining were separated to determine colocalization all the cells that were IgA+ cells were FcRL4+, strengthening the

idea that IgA/pHrodo internalisation was occurring at a higher level on FcRL4+ compared to FcRL4- B cells (Figure 4.2.2.2V).

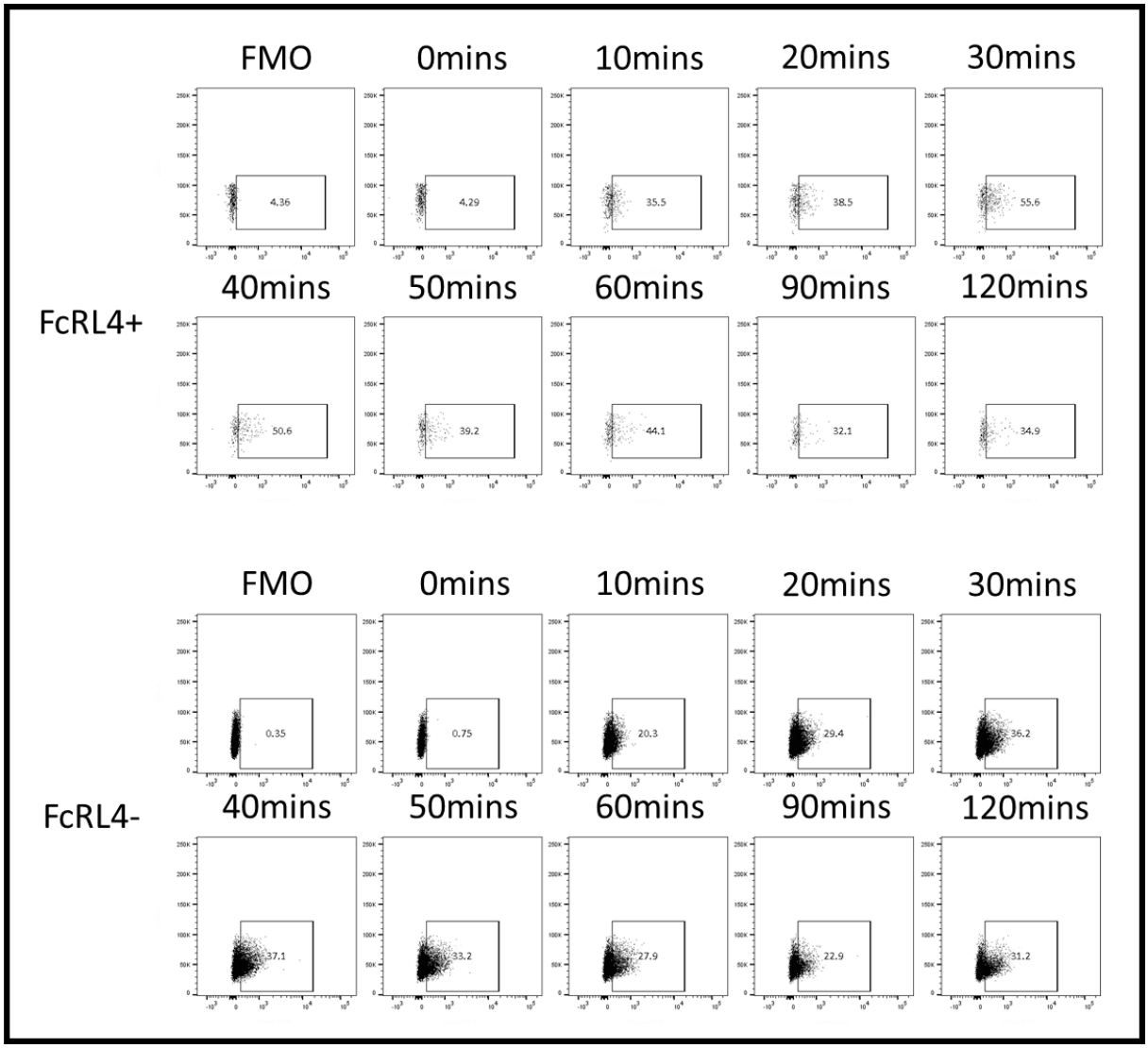

Figure 4.2.2.2I., IgA IC/pHrodo internalisation by FcRL4- and FcRL4+ ex-vivo tonsil cells raw flow cytometry data. *(n = 1), representative FACS plots demonstrating the internalisation of 25µg/ml HA colostrum IgA IC/2µg/ml pHrodo by FcRL4- and FcRL4+ ex-vivo tonsil cells. FcRL4- and FcRL4+ ex-vivo tonsil cells were identified by gating on the lymphocyte population, as defined by FSC-A/SSC-A before distinguishing the FcRL4- population as SSC-A/APC-A- and the FcRL4+ population as SSC-A/APC-A+. To determine the cells that were internalising HA colostrum IgA IC/pHrodo the FcRL4- and FcRL4+ cells were gated on an FMO where the cells had not been incubated with the HA colostrum IgA IC/pHrodo, defined as SSC-A/PE-A+. The number in the gate defines the percentage of cells that have internalised the HA colostrum IgA IC/pHrodo.*

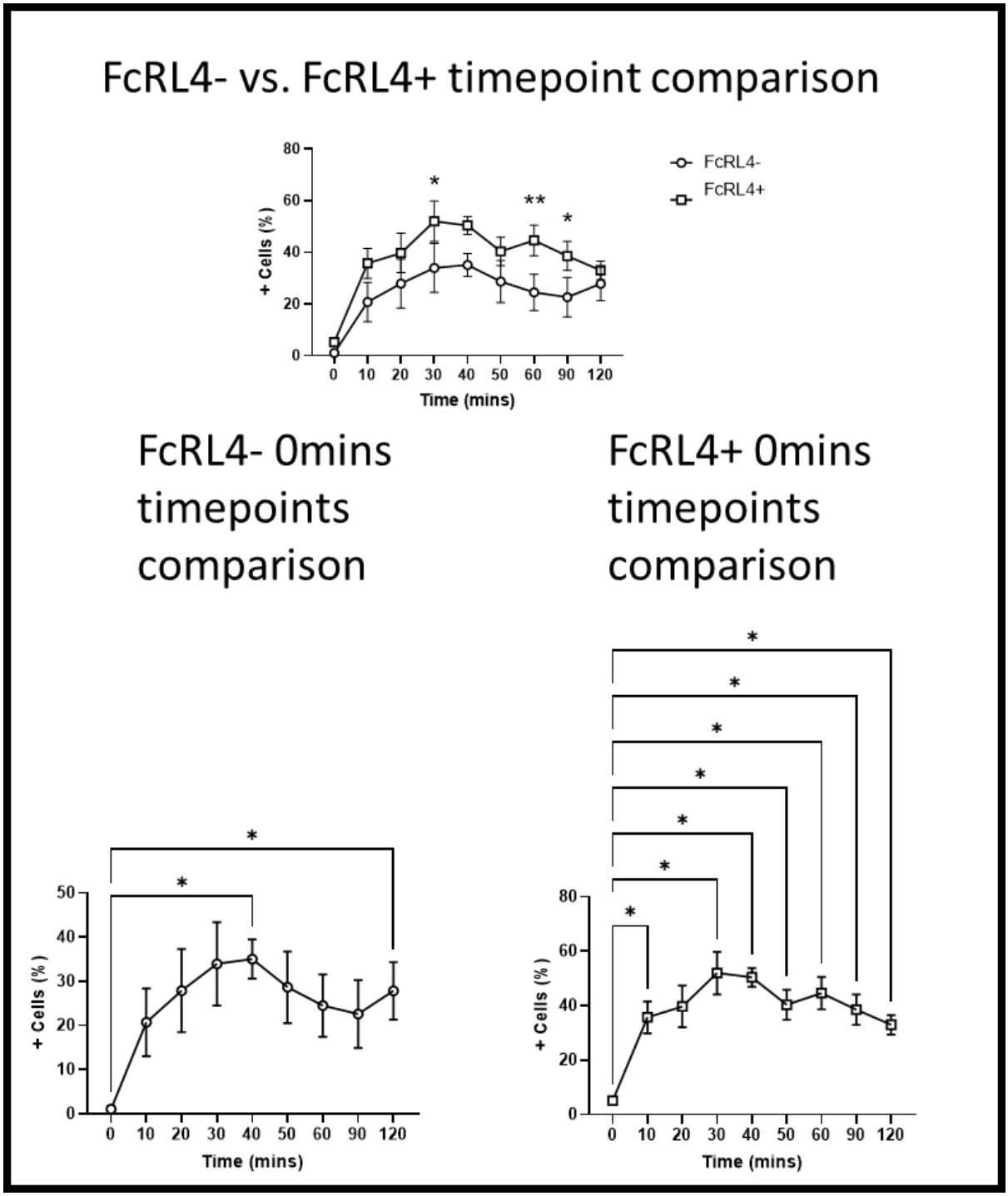

Figure 4.2.2.2II IgA IC/pHrodo internalisation by FcRL4- and FcRL4+ ex-vivo tonsil cells. *(n = 3) The percentage of HA colostrum IgA IC/pHrodo+ cells was taken at each timepoint for the FcRL4- and FcRL4+ ex-vivo tonsil cells and the mean percentage of HA colostrum IgA IC/pHrodo+ cells was calculated. (Top graph) The mean change in the percentage of IgA IC/pHrodo+ cells in the FcRL4- and FcRL4+ population were compared to each other at every timepoint. Statistical test – Šidák's multiple comparison corrected two-way ANOVA. (Bottom graphs) The mean change in the percentage of IgA IC/pHrodo+ at each time point was compared to the 0mins timepoint for both the FcRL4- cells and FcRL4+ cells. Statistical test – Dunnett's multiple comparison corrected one-way ANOVA.*

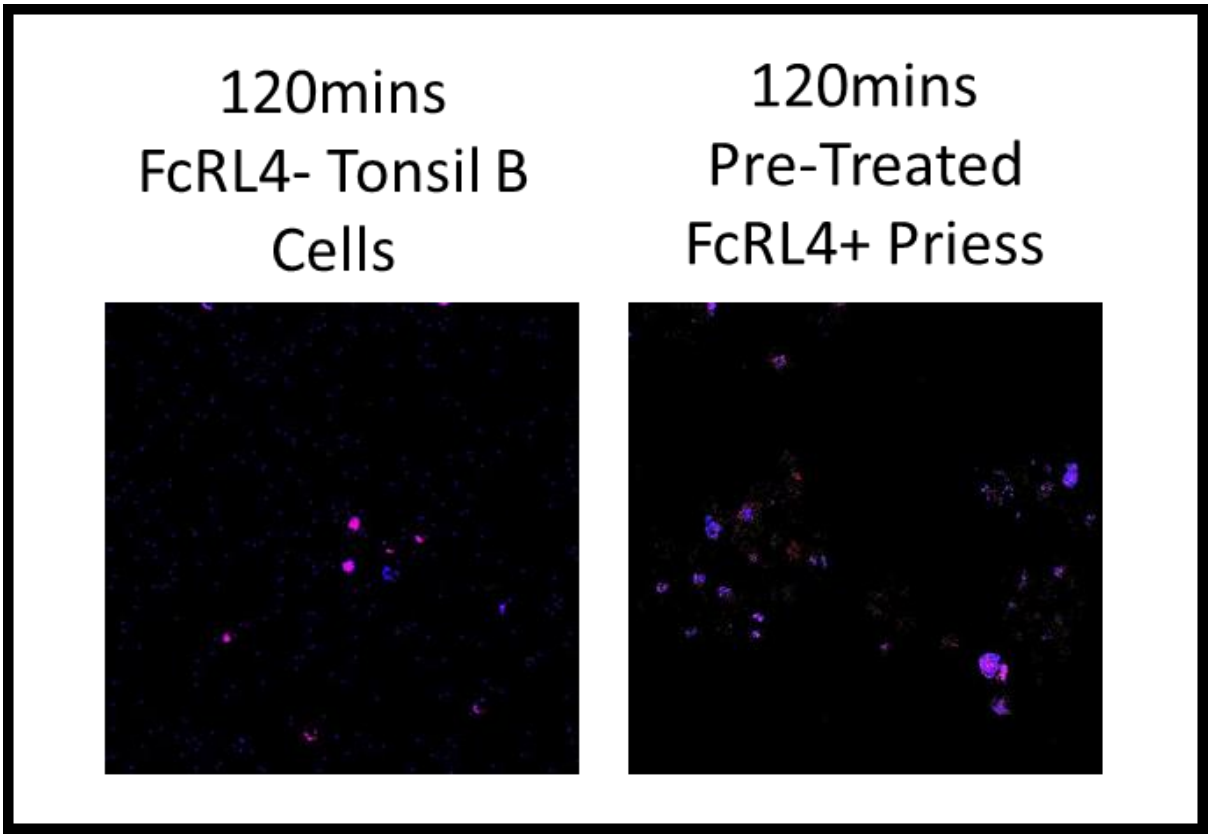

Figure 4.2.2.2III., Fluorescence for live cell imaging of FcRL4- ex-vivo tonsil cells and pre-treated induced transduced priess and HA colostrum IgA IC/pHrodo*. (n = 1) FcRL4- ex-vivo tonsil cells were kept after sorting from FcRL4+ ex-vivo tonsil cells and imaged at 0mins to set the laser intensity and gain for APC (blue). 1x10^{6} FcRL4+ induced transduced priess were incubated with 25µg/ml HA colostrum IgA IC/2µg/ml pHrodo 2 hours prior to imaging. The laser intensity and gain were increased when imaging until red could be visualised in the pre-treated FcRL4+ transduced priess. FcRL4- The settings were checked back against the FcRL4- transduced priess to check a red signal could not be detected in these cells.FcRL4- induced transduced priess were incubated with 25µg/ml HA colostrum IgA IC/2µg/ml pHrodo and imaged again at 120mins to visualise pHrodo staining (red).*

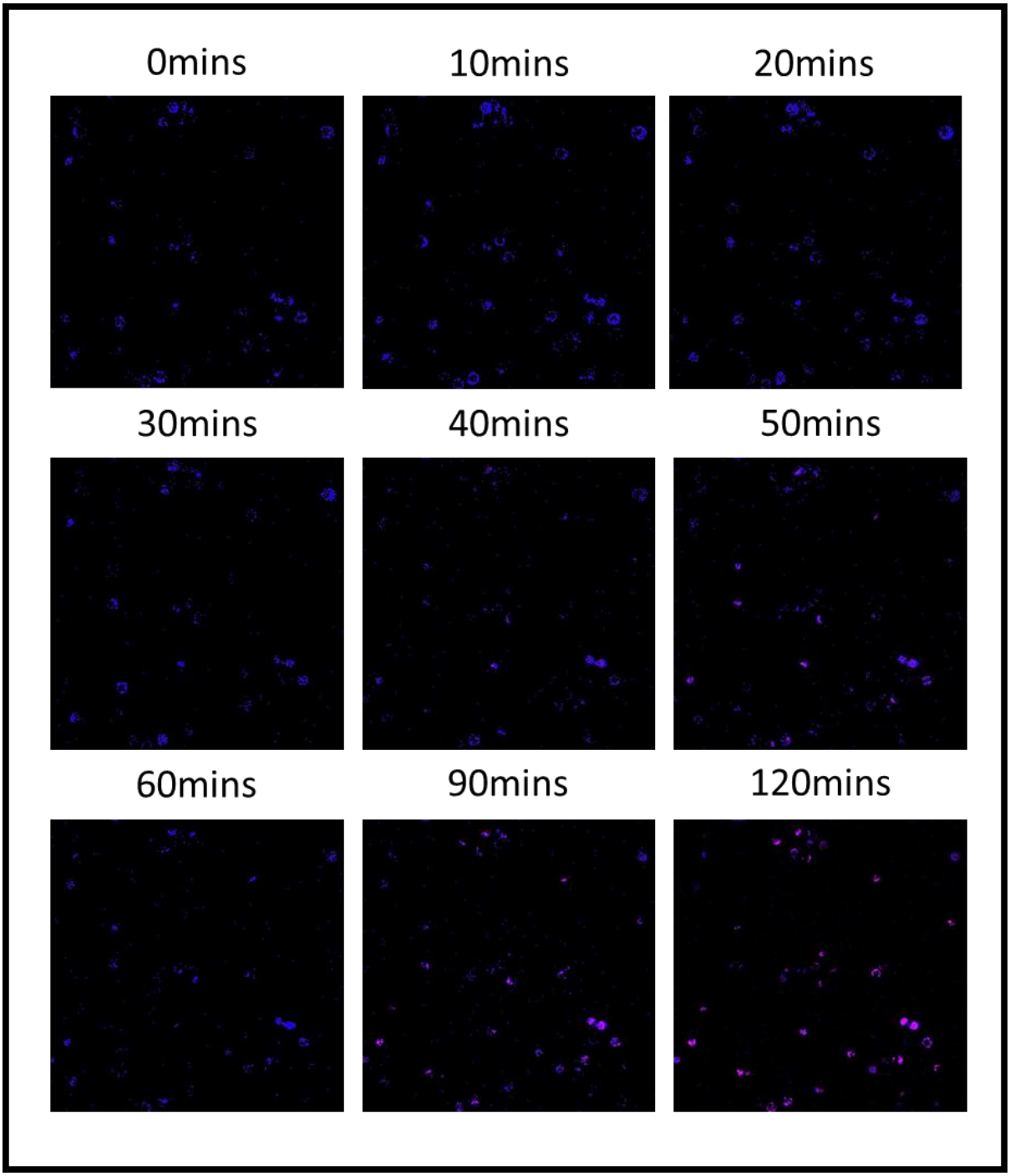

Figure 4.2.2.2IV., Live cell fluorescent images of FcRL4+ ex-vivo tonsil cells in 0.5% type II rat tail collagen gel. *(n = 1) Ex-vivo tonsil cells were stained for FcRL4 and sorted on APC to separate the FcRL4- and FcRL4+ ex-vivo tonsil cells. FcRL4- and FcRL4+ ex-vivo tonsil cells were suspended in 0.5% type II rat tail collagen gel and plated in µ perfusion slides alongside pre-treated transduced priess cells that had been incubated with 25µg/ml HA colostrum IgA IC/2µg/ml pHrodo 2 hours prior to imaging, as a positive control. FcRL4- ex-vivo tonsil cells were used to correct for autofluorescence in the APC channel. FcRL4+ ex-vivo tonsil cells were perfused with 25µg/ml HA colostrum IgA IC/2µg/ml pHrodo and imaged at 0mins, 10mins, 20mins, 30mins, 40mins, 50mins, 60mins, 90mins, 120mins. Blue - FcRL4, Red - HA IgA/pHrodo.*

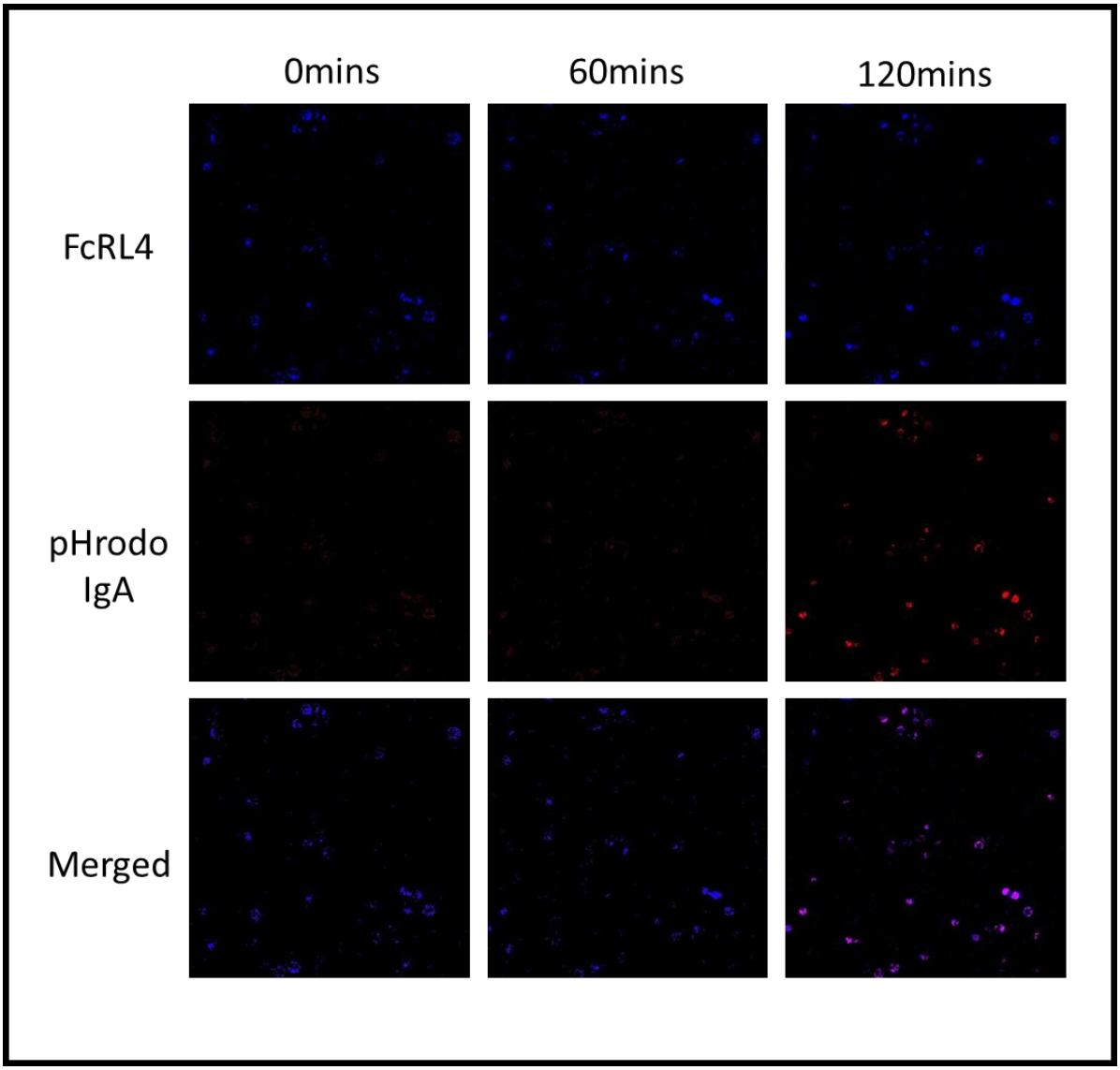

Figure 4.2.2.2V., IgA IC/pHrodo staining colocalises with FcRL4+ ex-vivo tonsil cells. *(n = 1) Live cell fluorescent images taken of FcRL4+ ex-vivo tonsil cells suspended in 0.5% type II rat tail collagen gels. The same images in Figure 4.2.2.1III at timepoints 0mins, 60mins and 120mins were separated into FcRL4+ image layer (blue) and HA colostrum IgA IC/pHrodo image layer (red) other to identify if the fluorescence generated by internalised pHrodo was co-localised with FcRL4+ ex-vivo tonsil cells. From top to bottom: FcRL4 staining only (blue) at 0mins, 60mins and 120mins, HA colostrum IgA IC/pHrodo staining only (red) at 0mins, 60mins, 120mins and FcRL4 and HA IgA/pHrodo staining together (merged) at 0mins, 60mins and 120mins.*

4.2.2.3 FcRL4+ RA SF B Cells

Finally, *ex-vivo* RA SF cells from RA patients were incubated with HA colostrum IgA IC/pHrodo avidin™ to investigate whether disease-relevant FcRL4+ B cells could internalise IgA ICs (n = 2). FcRL4+ and FcRL4- cells were gated to exclude non-viable cells and defined as CD3- and CD19+ (Figure 8.4). Similar to the tonsil samples, there was less difference in the percentage of IgA IC/pHrodo+ cells between the FcRL4- and FcRL4+ cells but the percentage of IgA IC/pHrodo+ cells were higher in the FcRL4+ population compared to the FcRL4- for each timepoint (Figure 4.2.2.3I & II). This difference was significant at 60mins ($p = 0.0393$). When analysed individually, 10mins ($p = 0.0403$), 20mins ($p = 0.0346$), 30mins ($p = 0.0466$) and 60mins ($p = 0.0278$) were all significantly different to 0mins in the FcRL4+ population and the percentage of IgA IC/pHrodo+ cells peaked at 60mins (27.35%) (Figure 4.2.2.3I & II). In the FcRL4- population, only the 30mins ($p = 0.0203$) and 60mins ($p = 0.0481$) timepoints were significantly different to the 0mins timepoint and the percentage of IgA IC/pHrodo+ cells also peaked at 60mins (21.1%) (Figure 4.2.2.3I & II).

Similar to the tonsil cells, FcRL4- and FcRL4+ cells were isolated from SFMCs using cell sorting and were only stained for FcRL4. Internalisation of IgA could be detected from 40mins (4.2.2.3IV) and the signal increased until the 120mins timepoint (Figure 4.2.2.3IV). When the FcRL4 and IgA staining were separated to determine colocalization, all the cells that were IgA IC/pHrodo+ were FcRL4+, which reflected the pattern seen in FcRL4+ transduced priess cells and FcRL4+ tonsil cells, suggesting that IgA internalisation was higher in FcRL4+ B cells (Figure 4.2.2.3V).

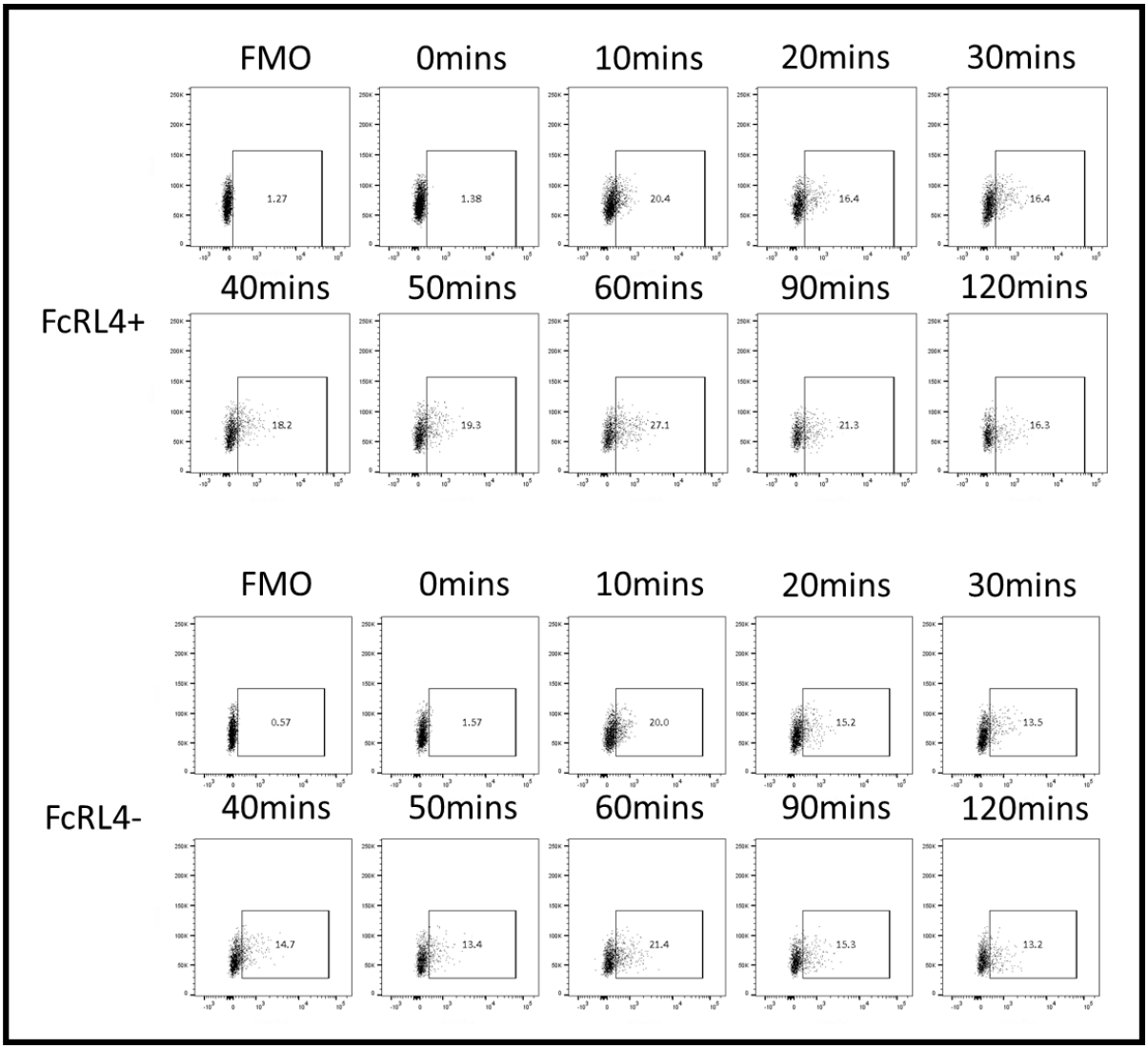

Figure 4.2.2.3I., IgA IC/pHrodo internalisation by FcRL4- and FcRL4+ ex-vivo RA SF cells raw flow cytometry data. *(n = 1), representative FACS plots demonstrating the internalisation of 25µg/ml HA colostrum IgA IC/2µg/ml pHrodo by FcRL4- and FcRL4+ ex-vivo RA SF cells. FcRL4- and FcRL4+ ex-vivo RA SF cells were identified by gating on the lymphocyte population, as defined by FSC-A/SSC-A before distinguishing the FcRL4- population as SSC-A/APC-A- and the FcRL4+ population as SSC-A/APC-A+. To determine the cells that were internalising HA colostrum IgA IC/pHrodo the FcRL4- and FcRL4+ cells were gated on an FMO where the cells had not been incubated with the HA colostrum IgA IC/pHrodo, defined as SSC-A/PE-A+. The number in the gate defines the percentage of cells that have internalised the HA colostrum IgA IC/pHrodo.*

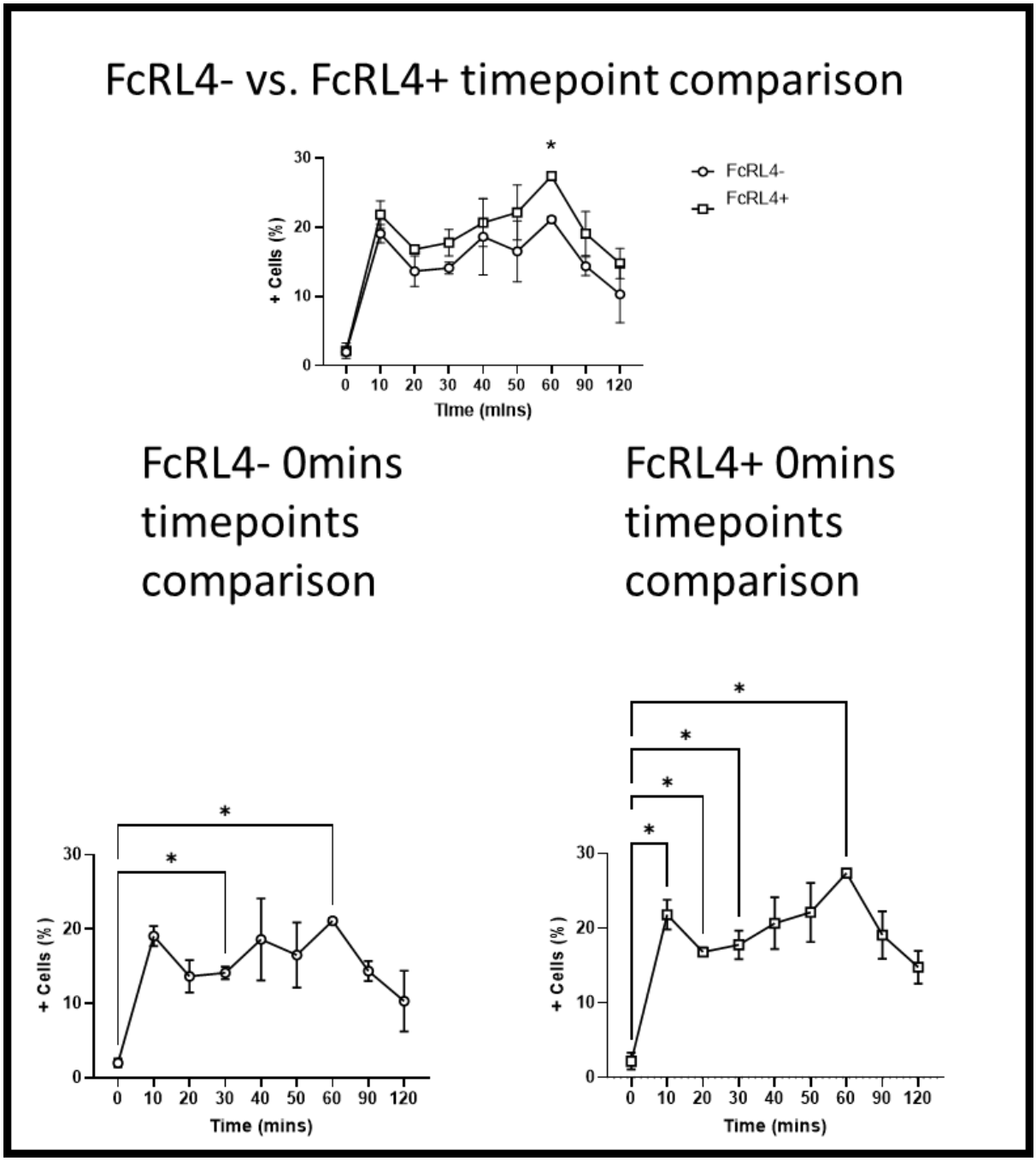

Figure 4.2.2.3II IgA IC/pHrodo internalisation by FcRL4- and FcRL4+ ex-vivo RA SF cells. *(n = 2) The percentage of HA colostrum IgA IC/pHrodo+ cells was taken at each timepoint for the FcRL4- and FcRL4+ ex-vivo RA SF cells and the mean percentage of HA colostrum IgA IC/pHrodo+ cells was calculated. (Top graph) The mean change in the percentage of IgA IC/pHrodo+ cells in the FcRL4- and FcRL4+ population were compared to each other at every timepoint. Statistical test – Šidák's multiple comparison corrected two-way ANOVA. (Bottom graphs) The mean change in the percentage of IgA IC/pHrodo+ at each time point was compared to the 0mins timepoint for both the FcRL4- cells and FcRL4+ cells. Statistical test – Dunnett's multiple comparison corrected one-way ANOVA.*

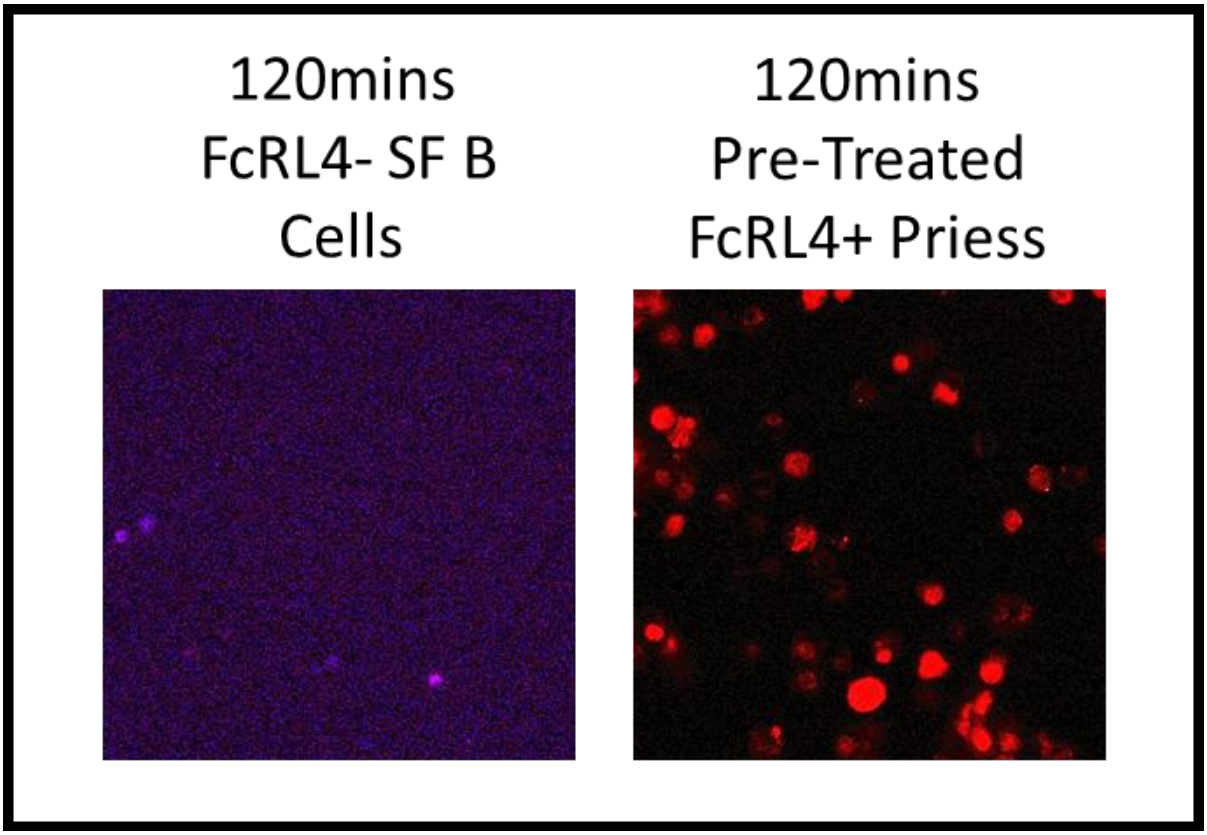

Figure 4.2.2.3III., Fluorescence for live cell imaging of FcRL4- ex-vivo RA SF cells and pre-treated induced transduced priess and HA colostrum IgA IC/pHrodo*. (n = 1) FcRL4- ex-vivo RA SF cells were kept after sorting from FcRL4+ ex-vivo RA SF cells and imaged at 0mins to set the laser intensity and gain for APC (blue). 1x10^6 FcRL4+ induced transduced priess were incubated with 25µg/ml HA colostrum IgA IC/2µg/ml pHrodo 2 hours prior to imaging. The laser intensity and gain were increased when imaging until red could be visualised in the pre-treated FcRL4+ transduced priess. FcRL4- The settings were checked back against the FcRL4- transduced priess to check a red signal could not be detected in these cells.FcRL4- induced transduced priess were incubated with 25µg/ml HA colostrum IgA IC/2µg/ml pHrodo and imaged again at 120mins to visualise pHrodo staining (red).*

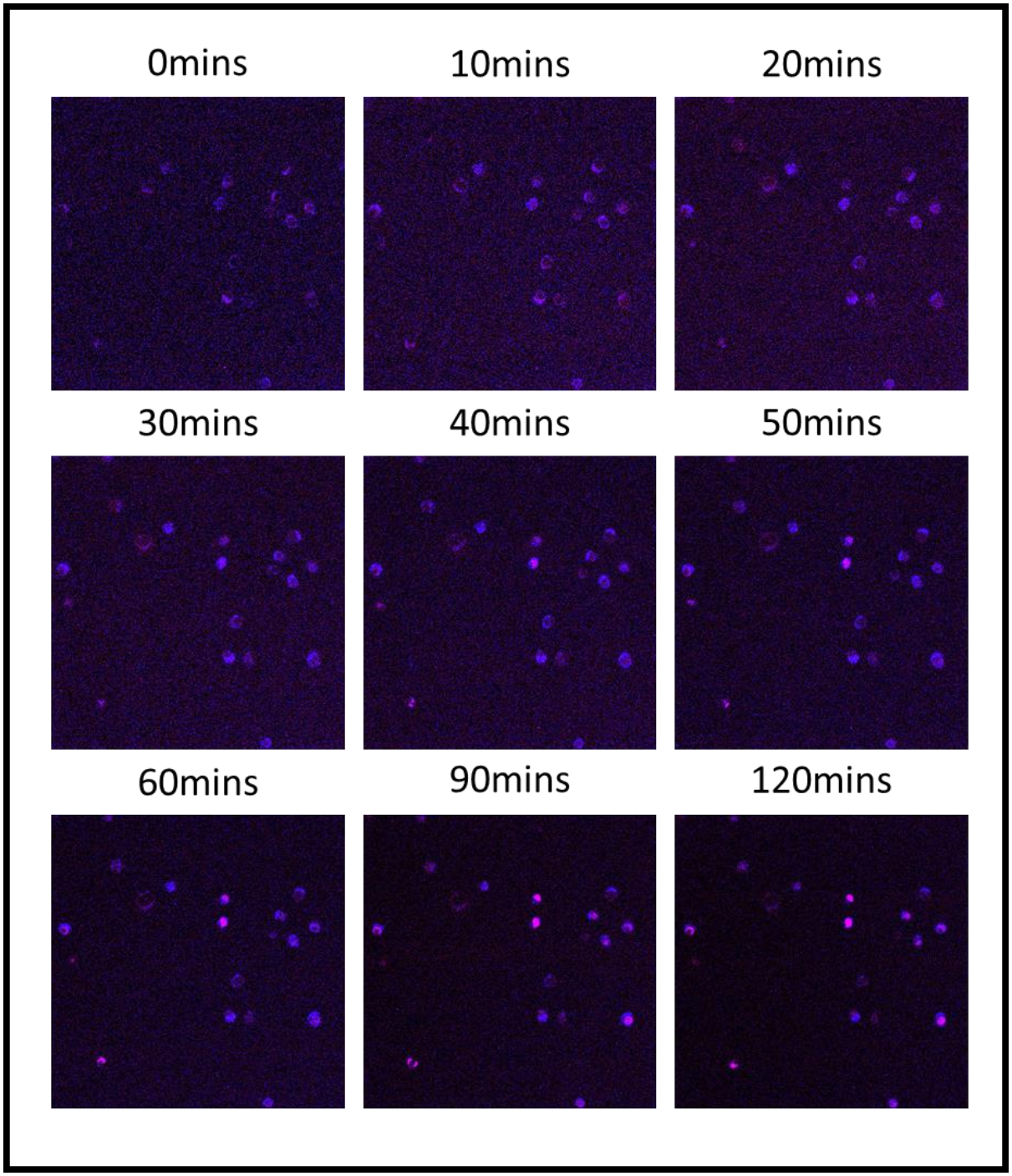

Figure 4.2.2.3IV., Live cell fluorescent images of FcRL4+ ex-vivo RA SF cells in 0.5% type II rat tail collagen gel. *(n = 1) Ex-vivo RA SF cells were stained for FcRL4 and sorted on APC to separate the FcRL4- and FcRL4+ ex-vivo to RA SF cells. FcRL4- and FcRL4+ ex-vivo RA SF cells were suspended in 0.5% type II rat tail collagen gel and plated in µ perfusion slides alongside pre-treated transduced priess cells that had been incubated with 25µg/ml HA colostrum IgA IC/2µg/ml pHrodo 2 hours prior to imaging, as a positive control. FcRL4- ex-vivo RA SF cells were used to correct for autofluorescence in the APC channel. FcRL4+ ex-vivo RA SF cells were perfused with 25µg/ml HA colostrum IgA IC/2µg/ml pHrodo and imaged at 0mins, 10mins, 20mins, 30mins, 40mins, 50mins, 60mins, 90mins, 120mins. Blue - FcRL4, Red - HA IgA/pHrodo.*

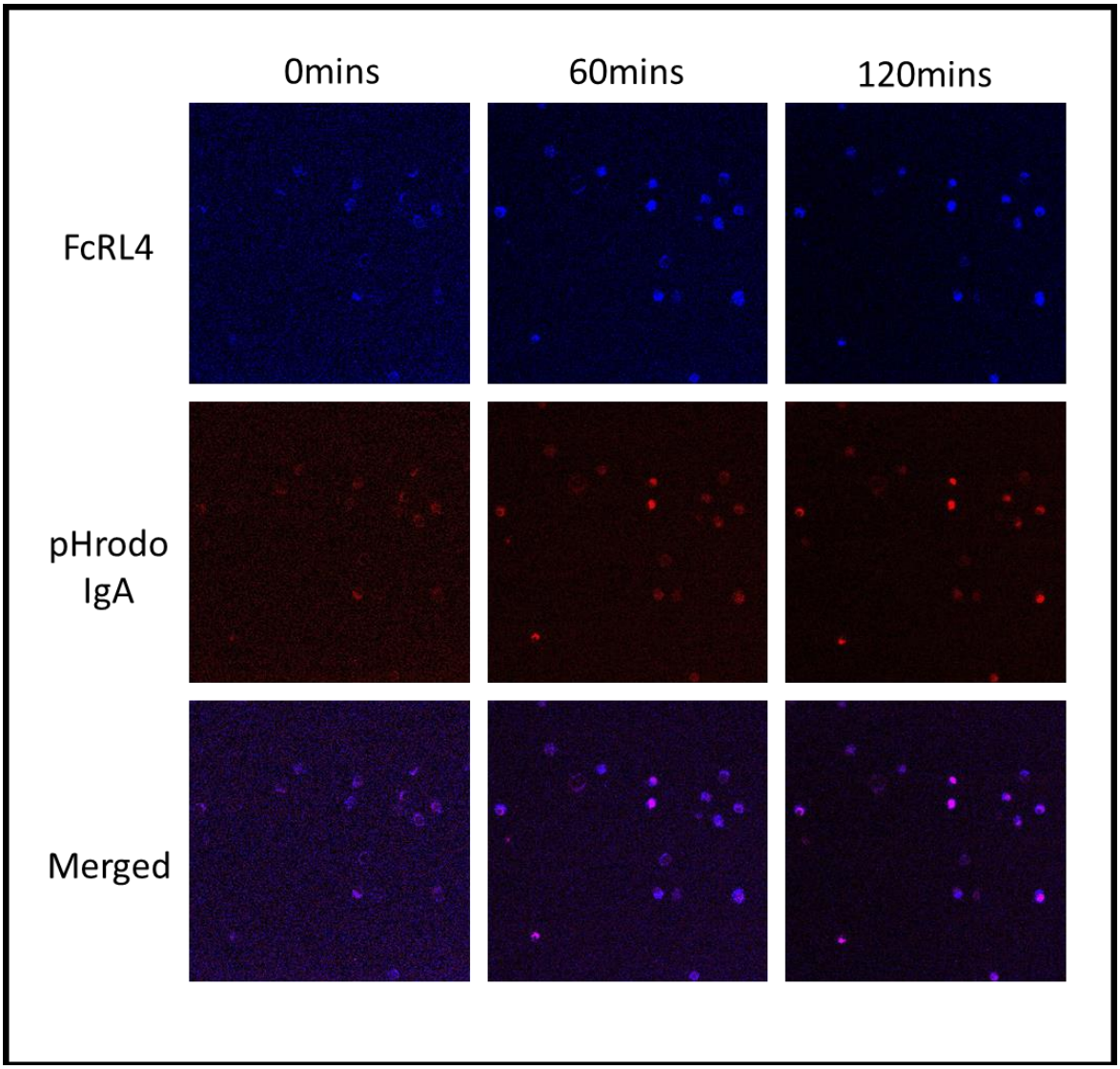

Figure 4.2.2.3V., IgA IC/pHrodo staining colocalises with FcRL4+ ex-vivo RA SF cells. *(n = 1) Live cell fluorescent images taken of FcRL4+ ex-vivo RA SF cells suspended in 0.5% type II rat tail collagen gels. The same images in Figure 4.2.2.1III at timepoints 0mins, 60mins and 120mins were separated into FcRL4+ image layer (blue) and HA colostrum IgA IC/pHrodo image layer (red) other to identify if the fluorescence generated by internalised pHrodo was co-localised with FcRL4+ ex-vivo RA SF cells. From top to bottom: FcRL4 staining only (blue) at 0mins, 60mins and 120mins, HA colostrum IgA IC/pHrodo staining only (red) at 0mins, 60mins, 120mins and FcRL4 and HA IgA/pHrodo staining together (merged) at 0mins, 60mins and 120mins.*

4.2.3 Presentation of Citrullinated Enolase Peptide

Once establishing that FcRL4+ B cells from a transduced priess cell line, tonsils and RA SF could internalise IgA IC's, the next step was to investigate whether the antigen was presented on the B cell surface to activate CD4+ T cells. David Wraith's group had a generated a mouse T cell hybridoma line expressing a human TCR that recognised citrullinated enolase presented by HLADRB1*0401-expressing cells. They had a demonstrated that presentation of a citrullinated enolase peptide could bind to surface HLA-DR and interact with the T cell hybridoma, activating them and producing IL-2 in response. However, this model does not necessarily depend on antigen internalisation as it is possible that the citrullinated enolase peptide can bind directly to the MHC-II. Still, it was relevant to assess whether this model allows antigen presentation.

4.2.3.1 Untransduced Priess Cells

Priess cells were chosen as a B cell model because they express HLADRB1*0401 and this was the HLA-type that the T cell hybridoma recognised. To confirm the results produced by the Wraith lab, untransduced priess cells were co-cultured with the T cell hybridoma at a 2:1 ratio and a citrullinated enolase peptide. This was added at 100µg/ml, 10µg/ml, 1µg/ml and 0µg/ml to see whether the T cell response was reduced upon addition of less antigen. The 0µg/ml condition was cRPMI and was included as a negative control. Measuring IL-2 from co-culture supernatants showed that the amount of IL-2 produced by T cell hybridomas increased in a dose-dependent manner in response to increasing concentrations of citrullinated enolase peptide (n = 1) (Figure 4.2.3.1). This demonstrated that the

experiments could be replicated and this co-culture format was taken forward as a positive control for subsequent experiments.

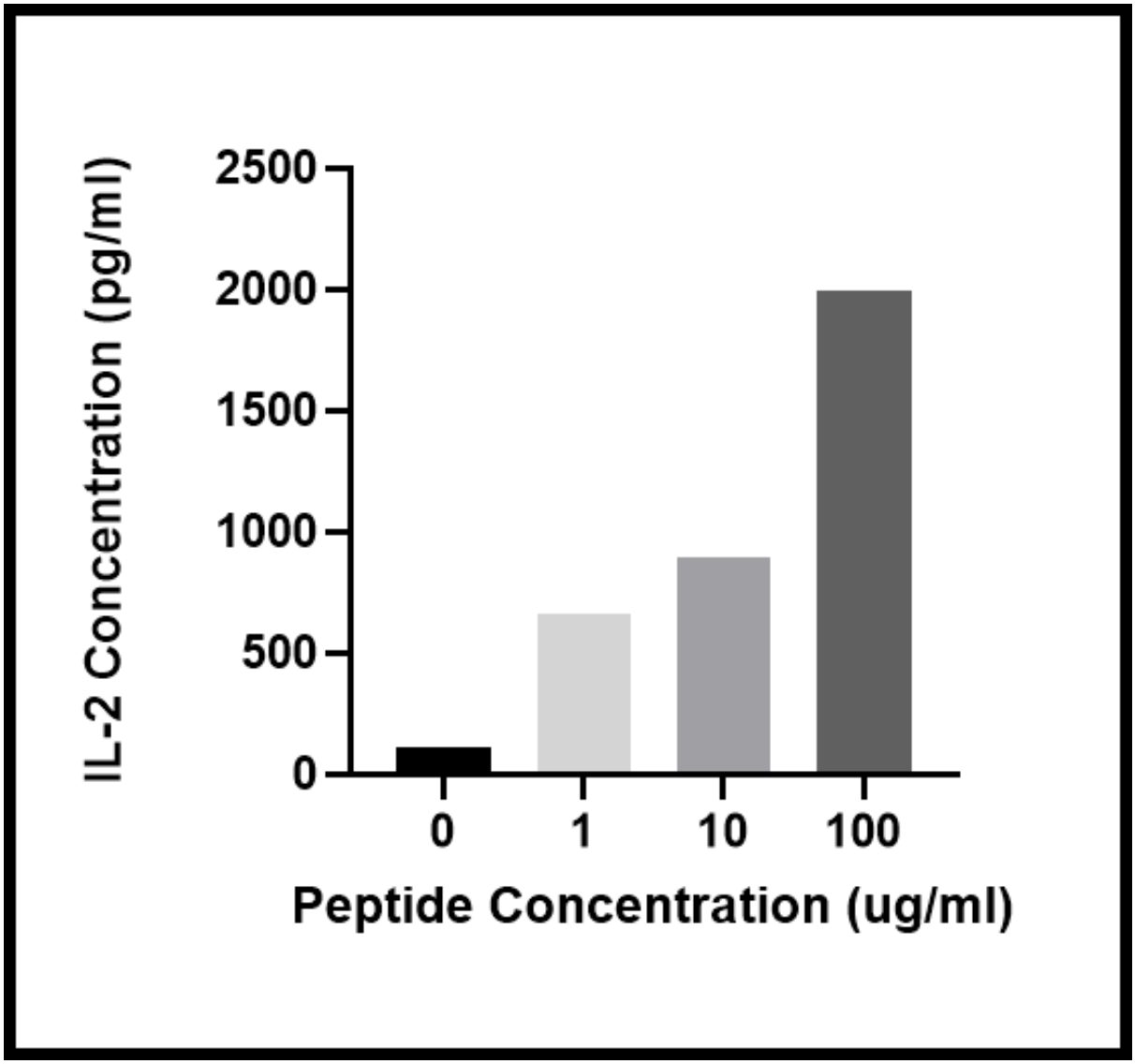

Figure 4.2.3.1., Presentation of a citrullinated enolase peptide by untransduced priess cells induces IL-2 production in citrullinated enolase recognising-T cell hybridomas. *(n = 1) Untransduced priess cells were co cultured with a citrullinated enolase peptide and citrullinated-enolase recognising T cell hybridoma. The concentration of IL-2 (pg/ml) was measured as a readout of T cell activation using an ELISA. Untransduced priess cells were co-cultured with citrullinated enolase peptide at different concentrations.*

4.2.3.2 FcRL4+ Transduced Priess Cells

Next, the same experiment was repeated in transduced FcRL4+ priess cells. Induced, transduced priess cells were sorted on GFP to isolate the FcRL4+ transduced priess cells from the FcRL4- transduced priess cells. The FcRL4- transduced priess cells were also co-cultured with the T cell hybridomas to observe whether the sorting process exerted any effects on the cells that would compromise their ability to capture the antigen on their surface and present it to the T cell. Following the same citrullinated enolase peptide titration in 4.2.3.1, both the FcRL4- and FcRL4+ transduced priess cells were able to induce IL-2 production in T cell in a concentration dependent manner (n = 3) (Figure 4.3.2.2). Both the FcRL4- and FcRL4+ cells were able to induce slightly higher IL-2 production in T cells compared to the untransduced priess cells but this difference was not significantly different. However, when IL-2 production was compared to the 0µg/ml negative control within the samples, the difference compared to the 100µg/ml in FcRL4+ transduced priess cells was significantly different ($p = 0.0168$). These results suggested that the FcRL4+ transduced priess cells were capable of inducing IL-2 production in T cell hybridomas upon interaction with a citrullinated enolase peptide.

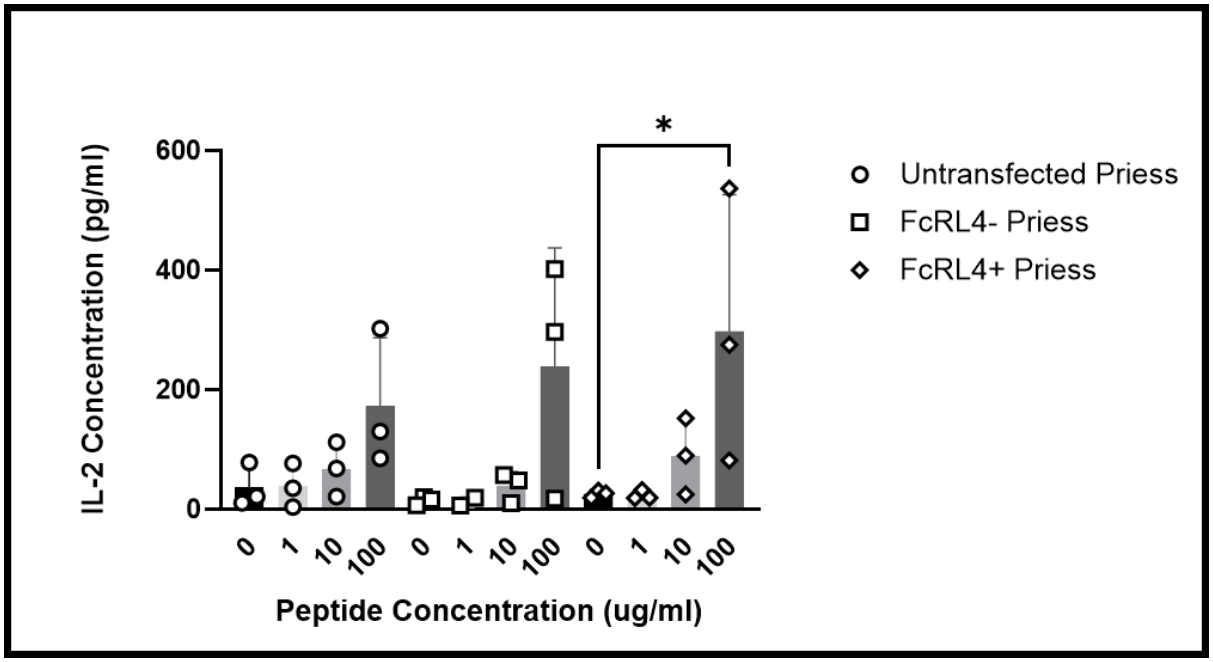

Figure 4.2.3.2., Presentation of a citrullinated enolase peptide by FcRL4- and FcRL4+ transduced priess cells induces IL-2 production in citrullinated enolase recognising-T cell hybridomas. *(n = 3) FcRL4- and FcRL4+ transduced priess cells were separated by cell sorting and co cultured with a citrullinated enolase peptide and citrullinated-enolase recognising T cell hybridoma. Untransduced priess cells were co-cultured under the same conditions as a positive control. The concentration of IL-2 (pg/ml) was measured as a readout of T cell activation using an ELISA. Cells were co-cultured with citrullinated enolase peptide at different concentrations. Statistical Test - –Šidák's multiple comparison corrected one-way ANOVA -*

4.2.3.3 FcRL4+ Tonsil

FcRL4+ tonsils were also tested in this co-culture system as an ex-vivo model, as this format required at least $4x10^5$ cells and SF from RA patients often do not have this high of a number of FcRL4+ cells and would require a more sensitive assay such as an ELISPOT. Similar to the FcRL4+ transduced priess cells, FcRL4- and FcRL4+ cells were separated using cell sorting and then co-cultured with the T cell hybridoma and citrullinated enolase peptide. However, these did not induce IL-2 production in T cells (data not shown) suggesting that something was preventing the B cells from effectively presenting the peptide to the T cells to induce a response.

Firstly, it was postulated that the FcRL4- and FcRL4+ tonsil B cells did not express the matching HLA-type for the T cells and that was preventing the cells from interacting. Subsequently, 9 tonsil samples were sent for typing on the HLADRB1 locus and 2 were identified as expressing HLA-DRB1*0401 (n = 9) (Table 8.1) and these were taken forward. Again, when the sorted FcRL4- and FcRL4+ HLA-typed tonsil B cells were co-cultured with the T cell hybridomas and citrullinated enolase peptide they did not induce IL-2 production (data not shown).

Having ruled out a mismatch in the HLA-type, the viability of these cells was tested. This had been done previously with the FcRL4+ transduced cells and they had good viability until 48h before they began to lose FcRL4 expression and then die. It had also been demonstrated by other members in the lab that culture of sorted ex-vivo cells resulted in a loss of viability after 1 day. Therefore, based on stimulation assays completed by a previous PhD student, tonsil cells were co-cultured for 24h individually or with a combination of TLR-7L, TLR9L, TGFβ and BAFF to see if the viability and maintenance of FcRL4 expression could be

improved. Due to the relatively low number of FcRL4+ cells that are sorted from tonsils, these experiments were done on unsorted cells so that a good number of events could be acquired on the Fortessa X-20. Pre-stimulation, 94.35% of cells were determined to be viable based on the absence of ZombieAqua staining. After 24h, 86.85% of unstimulated cells were still viable whilst the cell viability of stimulated ranged from 75.35-88.10% suggesting that the majority of tonsil cells were still viable when in culture for 24h (n = 2) (Figure 4.2.3.2I). Next, the percentage of FcRL4+ B cells in tonsils were evaluated pre- and post-stimulation. Pre-stimulation 9.47% of B cells were FcRL4+ and this declined to 1.28% in B cells that were unstimulated indicating that tonsil B cells lose expression of FcRL4 once in culture. Post-stimulation, the % FcRL4+ B cells ranged from 1.245-6.495% with the highest proportion being maintained in culture with TLR-9L and TGFβ Figure (n = 2) (4.2.3.2II). Therefore, for the next co-culture FcRL4+ were cultured in a media enriched with TLR-9L and TGFβ to try retain expression of FcRL4 as well as their viability.

Co-culture of the FcRL4+ in enriched media with the T cell hybridomas and citrullinated enolase peptide resulted in low amounts of IL-2 production by the T cell hybridoma (n = 1) (Figure 4.2.3.2III). However, there was almost a 10-fold difference in the amount of IL-2 produced by T cell hybridomas when co-cultured with FcRL4+ tonsil cells compared to FcRL4+ transduced priess cells (100µg/ml citrullinated enolase peptide: FcRL4+ transduced priess cells – 297.9pg/ml, FcRL4+ tonsil B cells – 29.92pg/ml). Together, these results suggested that, in this particular antigen presentation assay, that *ex-vivo* tonsils activated the T cell hybridoma too weakly to fully elucidate whether they could present antigens.

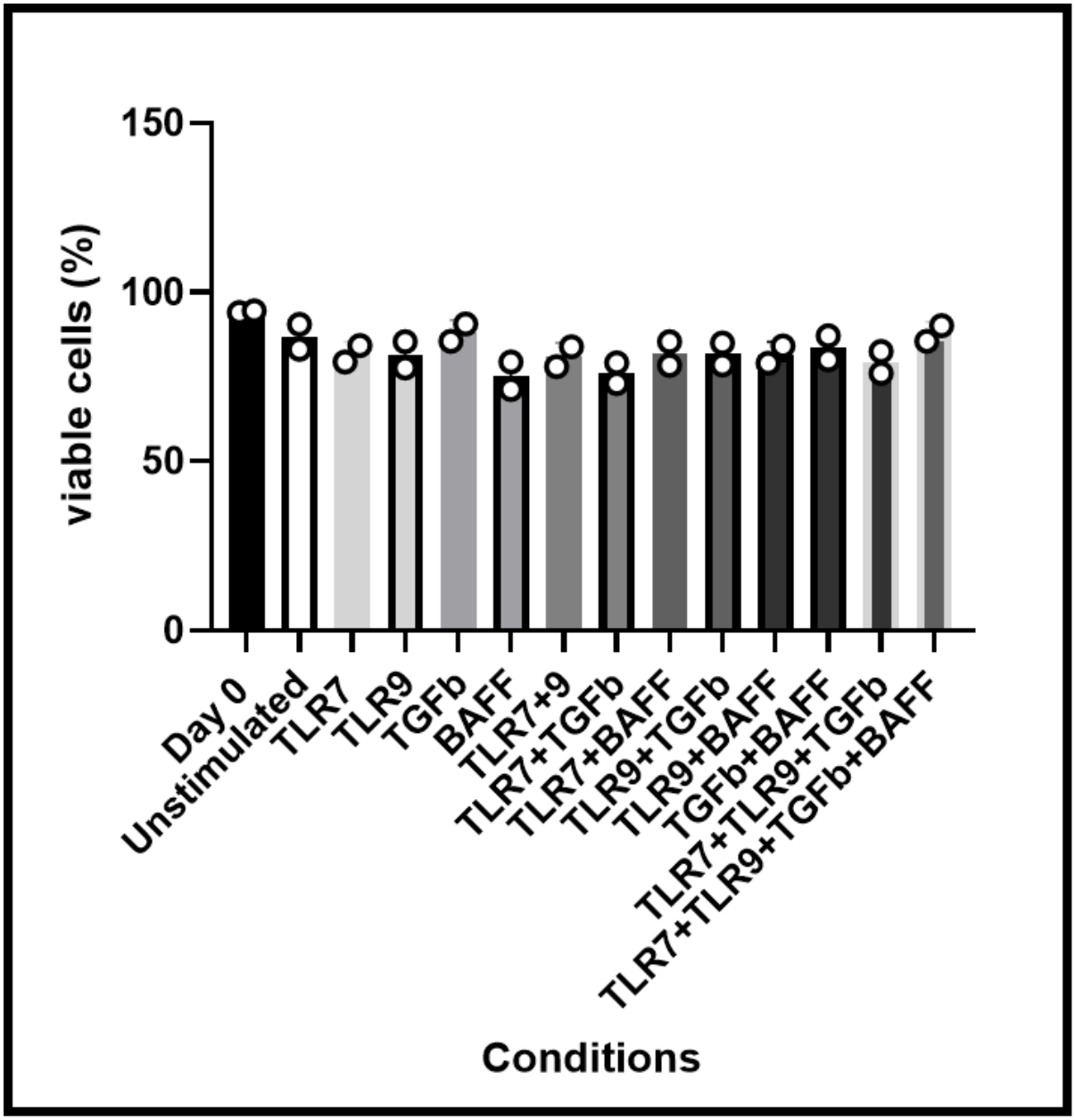

Figure 4.2.3.3l., Ex-vivo FcRL4+ tonsil B cells maintain viability for 24h in culture. *(n = 2) Ex-vivo tonsil cells were either unstimulated or stimulated with TLR7L, TLR9bL, TGFβ, BAFF or in tandem. Cells were stained with ZombieAqua™ to assess the viability of ex-vivo tonsil after 24h in culture either stimulated or unstimulated.*

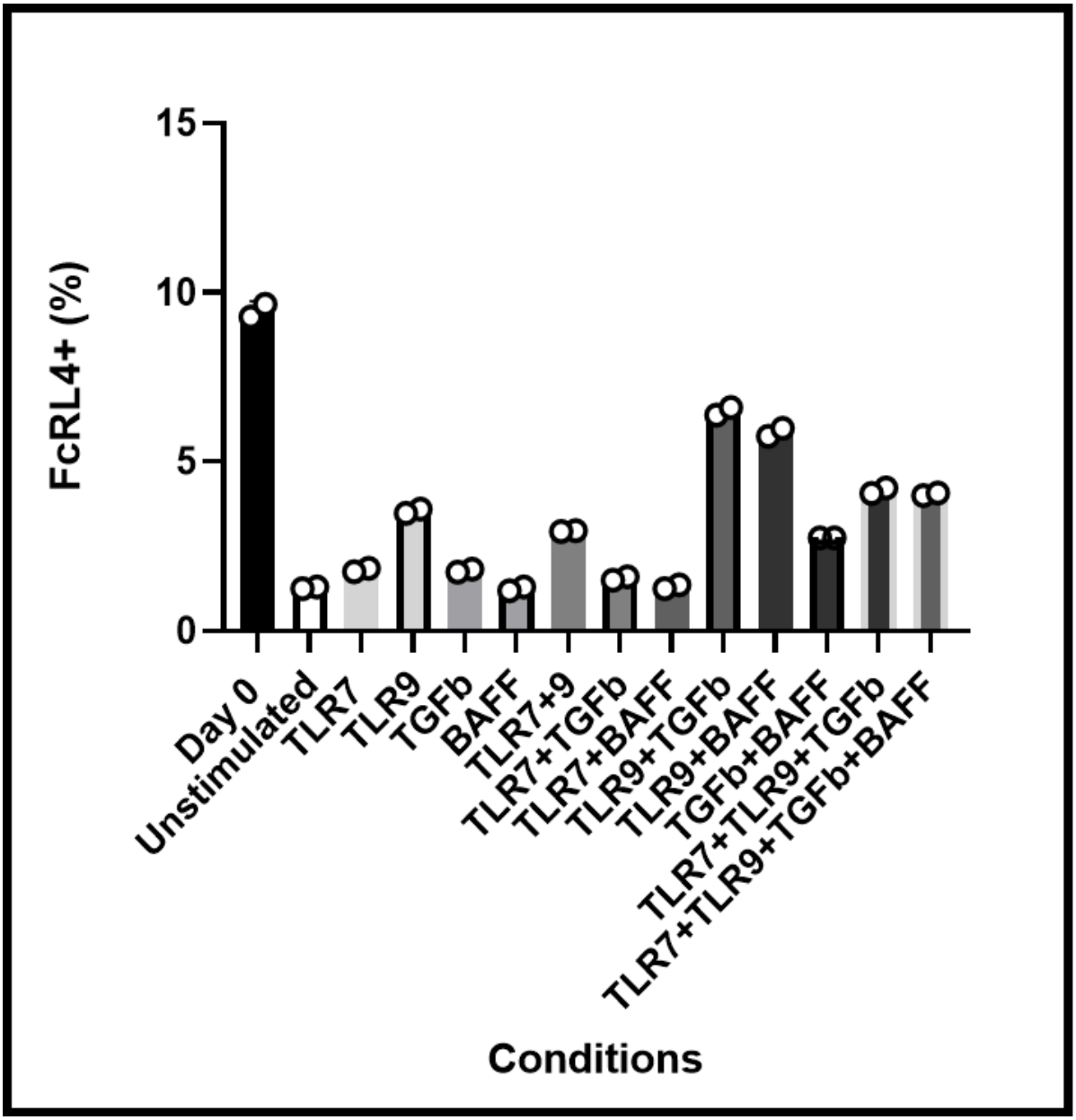

Figure 4.2.3.3II Ex-vivo tonsil B cells express the highest percentage of FcRL4 when cultured with TLR9bL and TGFβ. *(n = 2) Ex-vivo tonsil cells were either unstimulated or stimulated with TLR7L, TLR9bL, TGFβ, BAFF or in tandem. Cells were stained for FcRL4 using an anti-FcRL4 PE antibody and gated on the lymphocytes, singlets and live cells (determined as BV510-). The percentage of FcRL4+ ex-vivo tonsil cells was recorded in cells 24h cultures either stimulated or unstimulated.*

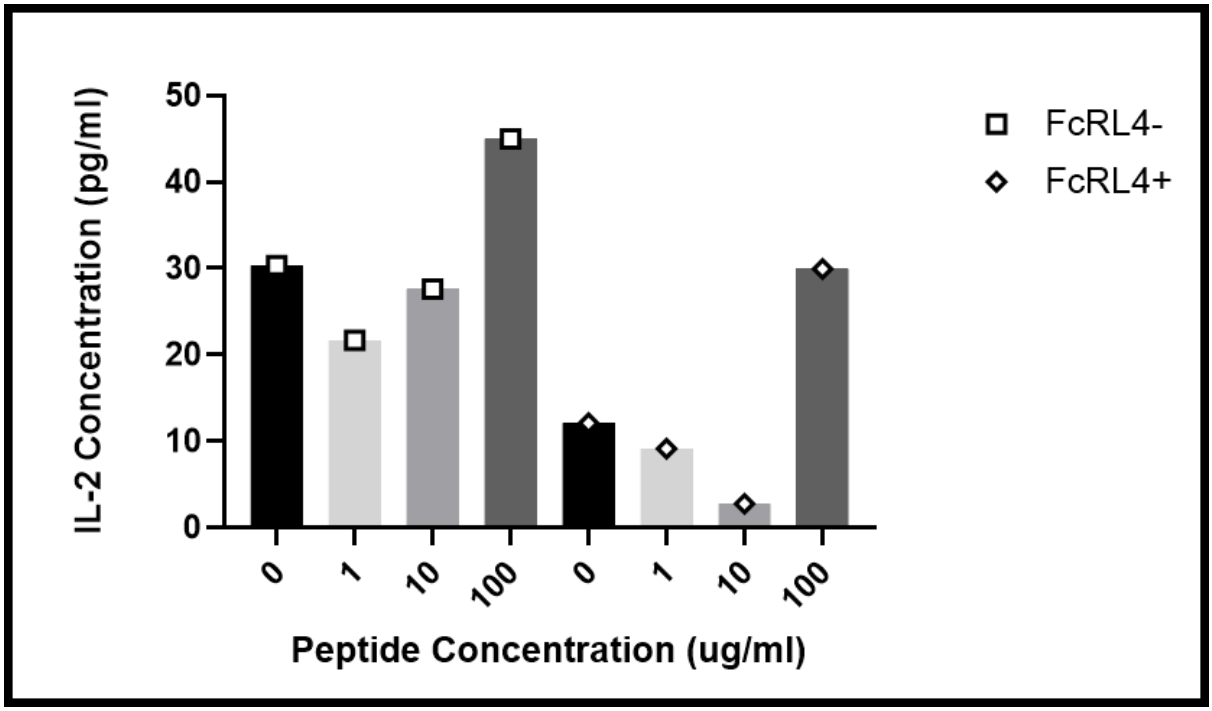

Figure 4.2.3.3II., Presentation of a citrullinated enolase peptide by FcRL4- and FcRL4+ tonsil B cells induce IL-2 production in citrullinated enolase recognising-T cell hybridomas. *(n = 1) CD19+ FcRL4- and FcRL4+ tonsil B cells were separated by cell sorting and co cultured with a citrullinated enolase peptide and citrullinated-enolase recognising T cell hybridoma. The concentration of IL-2 (pg/ml) was measured as a readout of T cell activation using an ELISA.*

4.2.4 IgA IC

4.2.4.1 Recombinant IgA & Citrullinated Enolase

Presentation of the a citrullinated enolase peptide doesn't require internalisation and processing by the cell in order for it to be presented, as it is short enough to bind HLA-DR molecules expressed on the cell surface. This means that the peptide can be presented independently of whether the cell expresses FcRL4 or not, as demonstrated by IL-2 production in cultures that contained untransduced priess cells and FcRL4- transduced priess cells. Therefore, the next step was to define an FcRL4-specific antigen. This needed to be aggregated as an IgA IC in order to bind to FcRL4 for internalisation but the IgA needed to be aggregated around citrullinated enolase, as this is the antigen that the TCR on the T cell hybridomas recognised.

The first IgA IC created consisted of a recombinant IgA clone that had previously been shown to weakly recognised citrullinated enolase derived peptides and a full length citrullinated enolase protein. These mixed for 2 hours at RT at a 100µg/ml concentration to allow sufficient time for the IgA and protein to aggregate. Induced transduced priess cells were incubated with the ICs for 30mins to allow sufficient time for binding before being stained for FcRL4 and IgA. IC binding was compared to 100µg/ml HA colostrum IgA and 100µg/ml HA recombinant IgA only. As demonstrated previously in FcRL4+ transduced priess cells, HA colostrum IgA was able to bind to FcRL4 (n = 1) (Figure 3.2.3.9I). However, no binding was observed in cells treated with 100µg/ml recombinant IgA and binding of 100µg/ml IgA IC was not specific to the FcRL4+ transduced priess cells suggesting that this was not a viable option for creating an IgA IC.

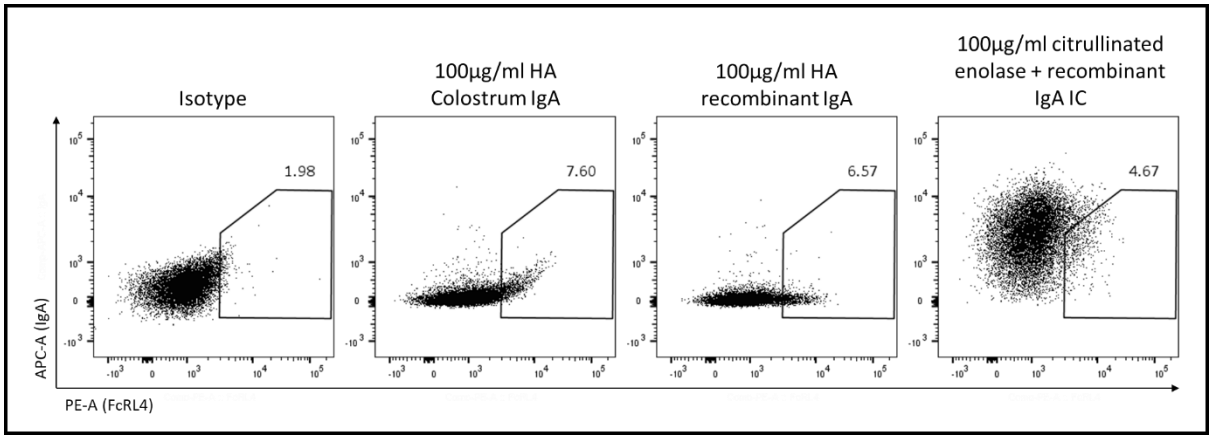

Figure 4.2.4.1., Binding of recombinant IgA + citrullinated enolase protein IC's to FcRL4+ transduced priess cells. *(n = 1) 100µg/ml colostrum IgA and recombinant IgA were heat aggregated for 30mins at 63°C whilst 100µg/ml recombinant IgA was mixed with 100µg/ml of citrullinated enolase protein at RT for 2 hours. FcRL4+ transduced priess cells were then incubated with the IgA IC's for 30mins and then stained for FcRL4 and IgA. An isotype control was used to determine the FcRL4+ population.*

4.2.4.2 Streptavidin IgA + Citrullinated Enolase Peptide

To overcome the non-specific binding of the recombinant IgA, the next IgA IC was made using the colostrum IgA, as it reliably bound to FcRL4. Therefore, the biotin/streptavidin system was employed to create an artificial IC where IgA was conjugated to streptavidin using a Lightning-Link kit and the citrullinated enolase peptide was biotinylated. 100µg/ml of each was mixed for 2 hours to allow sufficient time for binding and ICs were incubated with induced transduced priess cells for 30mins. These were compared to 100µg/ml HA colostrum IgA and 100µg/ml HA streptavidin-linked colostrum IgA to ensure that addition of IgA did not impair IgA binding to FcRL4. Compared to HA colostrum IgA, the HA streptavidin colostrum IgA was able to bind with similar efficacy suggesting that the streptavidin does not impact IgA binding (n = 1) (Figure 4.2.4.2). When it was in a complex with the citrullinated enolase peptide, there was a reduced amount of binding with the IC but there was a slight uptick in the FcRL4+IgA+ population indicating that the IC could bind in some capacity to FcRL4. Therefore, this was used as the IC for subsequent antigen presentation assays with FcRL4+ transduced priess cells.

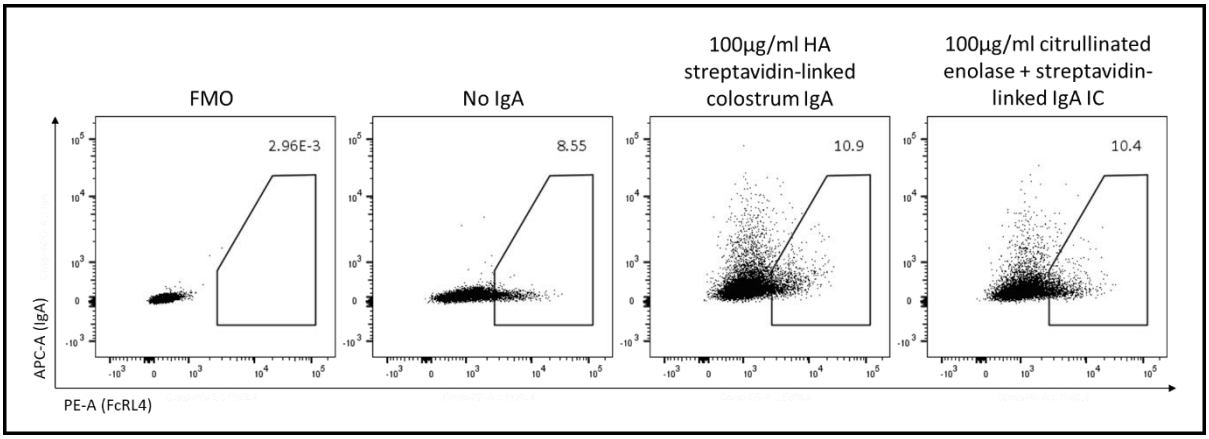

Figure 4.2.4.2., Binding of streptavidin IgA + biotinylated citrullinated enolase peptide IC's to FcRL4+ transduced priess cells. *(n = 1) 100µg/ml colostrum IgA and streptavidin IgA were heat aggregated for 30mins at 63°C whilst 100µg/ml streptavidin IgA was mixed with 100µg/ml of biotinylated citrullinated enolase peptide at RT for 2 hours. FcRL4+ transduced priess cells were then incubated with the IgA IC's for 30mins and then stained for FcRL4 and IgA. An FMO for FcRl4 was used to determine the FcRL4+ population.*

4.2.5 Transduced FcRL4+ Priess Cells

To investigate whether the streptavidin IgA/biotinylated citrullinated enolase peptide IC could be process and presented by FcRL4+ B cells, FcRL4- and FcRL4+ cells were sorted from induced transduced priess cells and were co-cultured with the citrullinated enolase-recognising T cell hybridomas. In separate wells, FcRL4- and FcRL4+ priess cells were also co-cultured with the citrullinated enolase peptide only. In response to the IgA IC, there appeared to be a massive induction in IL-2 production by T cells in both the FcRL4- and FcRL4+ wells when compared to when cells were co-cultured with the citrullinated enolase peptide alone. To determine if this was a consequence of the B cells, the T cells were cultured with the IgA IC alone. IL-2 production from the T cell only culture was similar to co-cultures containing the FcRL4- and FcRL4+ B cells indicating that the IC was able to interact with the T cells independently of the B cells (data not shown).

To prevent this off-target effect, sorted FcRL4- and FcRL4+ transduced priess cells were incubated with the IgA IC for at least an hour to allow for binding and internalisation before the cells were washed and co-cultured with the citrullinated enolase-recognising T cells for 24h. IL-2 production could not be detected using the IL-2 ELISA suggesting that this antigen might not be suitable to investigate antigen presentation by FcRL4+ B cells (data not shown). We have now received recombinant citrullinated enolase-specific IgA from Prof Toes' team in Leiden. It will be tested in this assay after the submission of this thesis.

4.3 Discussion

We hypothesised that FcRL4+ B cells are antigen presenting and that binding of IgA IC to FcRL4 would result in its internalisation, processing and loading onto MHC-II so that it can be presented to T cells. As mentioned, in order for an antigen to be presented by a B cell it first needs to be internalised with the receptor it is bound to. To investigate internalisation the IgA IC was biotinylated and conjugated to pHrodo avidin™ and fluorescent of pHrodo in acidified compartments was determined as internalisation of IgA IC. In our experiments, pHrodo staining was detected as early as 10mins in FcRL4+ transduced priess cells and 40mins in FcRL4+ tonsil and RA SF B cells, suggesting that binding of the IgA IC's to FcRL4 results in its internalisation to intracellular compartments. However, pHrodo staining was also detected in FcRL4- transduced priess, tonsil and RA SF cells albeit in a lower percentage of cells, which suggests that FcRL4- B cells also have the ability to internalise IgA ICs. One possibility for the similarities seen between FcRL4- and FcRL4+ B cells could be the expression of another IgA receptor is by FcRL4- B cells. FcRL3 is another member of the FcRL family that is expressed on B cells as well as T and NK cells and it has demonstrated binding to heat aggregated colostrum sIgA [28,136]. To investigate this further, FcRL4+ B cells could be co-stained for FcRL3 and then isolate an FcRL3+ and FcRL4+ B cell populations when they are sorted. The internalisation experiments using the HA colostrum IgA IC/pHrodo avidin could be repeated with the FcRL3+ cells to determine if they internalise HA colostrum IgA IC/pHrodo avidin similarly to FcRL4+ cells. Additionally, to investigate the specificity of IgA IC internalisation by FcRL4+ B cells, FcRL4 could be blocked prior to incubating with the HA colostrum IgA IC/pHrodo avidin

The process by which IgA IC-bound FcRL4 is internalised into the cell is not yet clearly identified. Receptor-mediated endocytosis is the invagination and budding off of the plasma membrane in response to a receptor binding its ligand and is most likely how IgA IC-bound FcRL4 was internalised. One experiment explored impairment of phagocytosis in macrophages from endometriosis patients and found that decreased phagocytosis was caused by reduced Hck signalling. In contrast, autophagy-related markers, such as ATG-5 and Beclin-1, were upregulated in THP-1 cells that expressed low levels of Hck [138]. Additionally, chimeric FcRL4 demonstrated robust phosphorylation of Hck upon ligand engagement, indicating that increased phosphorylation of Hck by FcRL4 supports initial receptor-mediated endocytosis [139].

Once IgA IC-bound FcRL4 has been internalised how it is processed is unknown. Autophagy, is the recycling of dying or degraded IC cellular components to maintain cellular health [74]. One study that supported a role for autophagy in IgA IC-FcRL4 internalisation was done in hepatocellular carcinoma cells that expressed high levels of STAT3, which induced expression of anti-apoptotic genes, Bcl-2 and Bcl-xL. Treatment of hepatocellular carcinoma cells *in vitro* with EPBS, a STAT3 inhibitor, or a BH3 mimetic, Bcl-2 family member inhibitor, increased phosphorylation of SHP-1 and SHP-2, which increased the expression of autophagy markers LC3II, ATG7 and Beclin by downregulating STAT3 induction. This also corresponded with decreased expression of Bcl-2 and Bcl-xL, suggesting that the induction of SHP-1 signalling induced autophagy in cells [77,140].

Phosphorylation of ITIMs on the IC domain of FcRL4 recruit Hck, which subsequently phosphorylates and recruits SHP-1, which have been shown to reduce whole cell tyrosine phosphorylation and Ca^{2+} mobilisation [134,139]. Conversely, inhibition of BCR internalisation

using Dynasore or Lat-A, inhibitors of dynamin and actin polymerisation respectively, hyperphosphorylated signalling molecules such as Jnk and ERK1/2 but they colocalised at the plasma membrane rather than at lysosomes indicating a dysregulation of spatial phosphorylation [69,141]. Together these results implicate that disruption of BCR signalling can impact BCR internalisation and IgA IC binding to FcRL4 could prevent BCR internalisation through Hck & SHP-1. This could instead prioritise FcRL4 internalisation. However, this still needs to be tested.

Next, antigen presentation was explored as a consequence of IgA IC internalisation. FcRL4+ B cells were found to express significantly higher levels of CD80 and CD86 compared to FcRL4- B cells in RA SF B cells indicating that they may be able to present antigens efficiently [110]. Initial, experiments demonstrated FcRL4+ transduced priess cells and to some extent FcRL4+ tonsils could activate citrullinated enolase-recognising T cell hybridomas by presentation of a citrullinated enolase peptide. However, the citrullinated enolase peptide is thirty amino acids long and can bind surface expressed MHC-II, meaning that activation of T cells wasn't specific to FcRL4+ B cells. Therefore, an IgA IC consisting of IgA and citrullinated enolase was constructed to mimic an antigen that FcRL4 could bind but needed to be internalised and processed before it could be presented on MHC-II. However, the results were inconclusive as IL-2 could not be detected in the supernatants taken from co-cultures of FcRL4+ transduced priess cells, citrullinated enolase-recognising T cell hybridomas and an IC made up of streptavidin IgA and biotinylated citrullinated enolase peptide. One possible explanation is that reduced binding was observed in FcRL4+ transduced priess cells that were cultured with these IC's compared to those cultured with HA streptavidin IgA. The reduced binding may have impacted how much was internalised, processed and presented. To continue

investigating antigen presentation in FcRL4+ B cells, a different IC model needs to be designed so that it has a similar binding affinity to FcRL4 compared to HA colostrum IgA.

5 Effects of FcRL4 on BCR Signalling

5.1 Introduction

Regulation of signalling in B cells is critical for maintaining their homeostasis and its dysregulation can lead to B cell pathogenesis and autoimmunity[142]. FcRL4 is an immunoregulatory receptor that includes ITIMs on its cytoplasmic domain and contains 3 tyrosine residues, which when phosphorylated can inhibit BCR signalling with and without co-ligation of the BCR[134]. Inhibition of BCR signalling by FcRL4 is associated with B cell exhaustion in Hepatitis C & HIV-infected individuals and knocking down or inhibiting of FcRL4 with an siRNA can restore B cell proliferation in HIV-infected cells [125,143].

To investigate the signalling pathways downregulated by FcRL4, the IC domain of FcRL4 was ligated to the transmembrane and EC domain of FcγRIIb and co-ligated that to the BCR. When the co-ligated BCR was stimulated with anti-IgG, there was a reduction in whole cell tyrosine phosphorylation and specifically reduced phosphorylation of Akt, ERK, PLCγ2 and Vav, similar to wildtype FcγRIIb, an inhibitory FcR [134,142]. Additionally, when mutations were introduced into the tyrosine residues of FcRL4, whole cell tyrosine phosphorylation was restored, which demonstrated FcRL4's inhibitory potential on signalling molecules downstream of the BCR [134,142].

Gene expression profiling was done on FcRL4- and FcRL4+ B cells to determine what regulated inhibition. In FcRL4+ B cells Fgr, Hck, SHP-1 and DUSP4 were upregulated and these signalling molecules are associated with reduced BCR signalling [19,125,139]. The upregulation of Fgr and Hck was confirmed by western blot. Further co-precipitation assays identified that SHP-1 and SHP-2 were associated with Fgr and Hck recruitment as the unmutated chimera was bound to both whilst mutated ITIMs were unable to interact with

either [119,142]. SHP-1 and SHP-2 are phosphatases that regulate signalling pathways downstream of the BCR. When SHP-1 was deleted in mice it was sufficient to cause autoimmune disease and autoreactive B cells to accumulate [32].

Stimulation of FcRL4 can also enhance TLR signalling, specifically TLR9. FcRL4+ and FcRL4- cells were incubated with CpG and CD23 expression measured as an indirect marker of TLR activation. CD23 expression increased in FcRL4+ cells and the amount expressed positively correlated with the amount of FcRL4 expressed[134]. The TLR response also modulated Hck, as FcRL4+ cells express more Hck and this results in TLR stimulation whilst cells expressing the mutant FcRL4 that cannot associate with FcRL4 have reduced TLR stimulation [131,134]. These experiments suggested that FcRL4 could have a dual function on cell signalling depending which pathways were being stimulated.

These studies were mainly performed in transduced cell lines or in the context of chronic infectious diseases. It would be useful to elucidate the inhibitory function of FcRL4 in the context of RA and observe if the effects seen in cell lines could be translated in *ex vivo* cells.

5.2 Results

5.2.1 FcRL4 Staining with BD Perm III

5.2.1.1 anti-FcRL4 PE Biolegend Perm III Stability Test

The 413D12 clone Biolegend was the most commonly used antibody for FcRL4 detection. Therefore, cells were stained with the anti-FcRL4 PE, as BD had confirmed successful staining of other surface markers using PE-conjugated antibodies when cells had been treated with BD CytoFix and BD Perm III. FcRL4+ tonsil B cells were stained with anti-FcRL4 PE were fixed BD CytoFix and permeabilised with BD Perm III and compared to cells fixed with 4% formaldehyde. 6.83% FcRL4+ cells were detected in the sample fixed with 4% formaldehyde whilst the sample treated with BD CytoFix and BD Perm III recognised 19.50% FcRL4+ cells (n = 1) (Figure 5.2.1.1). Usually, FcRL4 defines approximately 6-8% of tonsil B cells, suggesting that either the BD CytoFix or BD perm III were negatively impacting recognition of FcRL4 with the Biolegend anti-FcRL4 PE antibody.

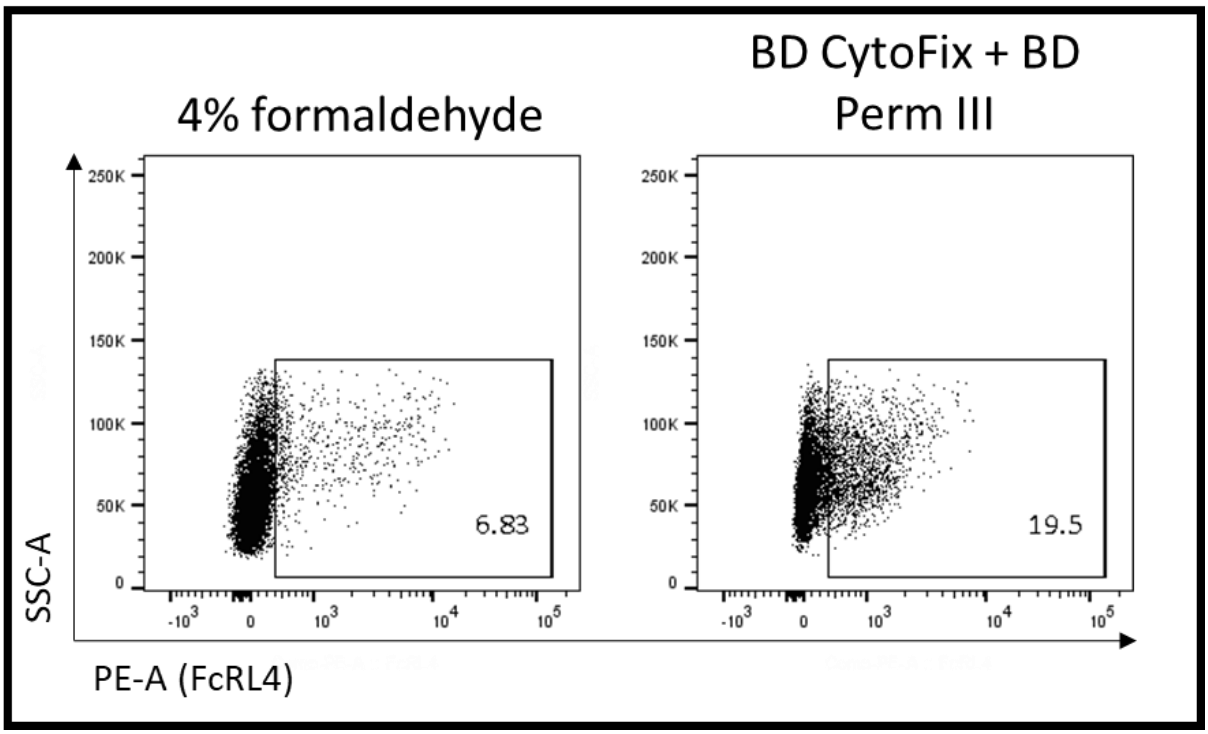

Figure 5.2.1.1., Staining of FcRL4 is compromised in tonsil cells fixed with BD CytoFix and permeabilised with BD Perm III. *(n = 1) Representative FACS plots of percentage of FcRL4+ tonsil B cells in sample fixed with 4% formaldehyde or fixed and permeabilised with BD CytoFix + BD Perm III. Cells were gated on the lymphocyte, singlet, CD3- and CD19+ populations before gating on the FcRL4+ population. The number in the gate represents the percentage of FcRL4+ cells.*

5.2.1.2 BD CytoFix Epitope Stability Test

BD CytoFix can affect the recognition of surface proteins by masking the epitope that staining antibodies recognise therefore preventing their binding. To check that the FcRL4 epitope was still recognisable, cells were fixed either with 4% formaldehyde or BD CytoFix and then stained for FcRL4. The FcRL4+ population recognised when fixed with either 4% formaldehyde or BD CytoFix was similar, 4.52% vs. 6.56% respectively (n = 1) (Figure 5.2.1.2). The FcRL4 stain in cells fixed with BD CytoFix appeared to less bright than those fixed with 4% formaldehyde suggesting that BD CytoFix had an effect on staining but did not negatively impact the percentage of FcRL4+ cells stained.

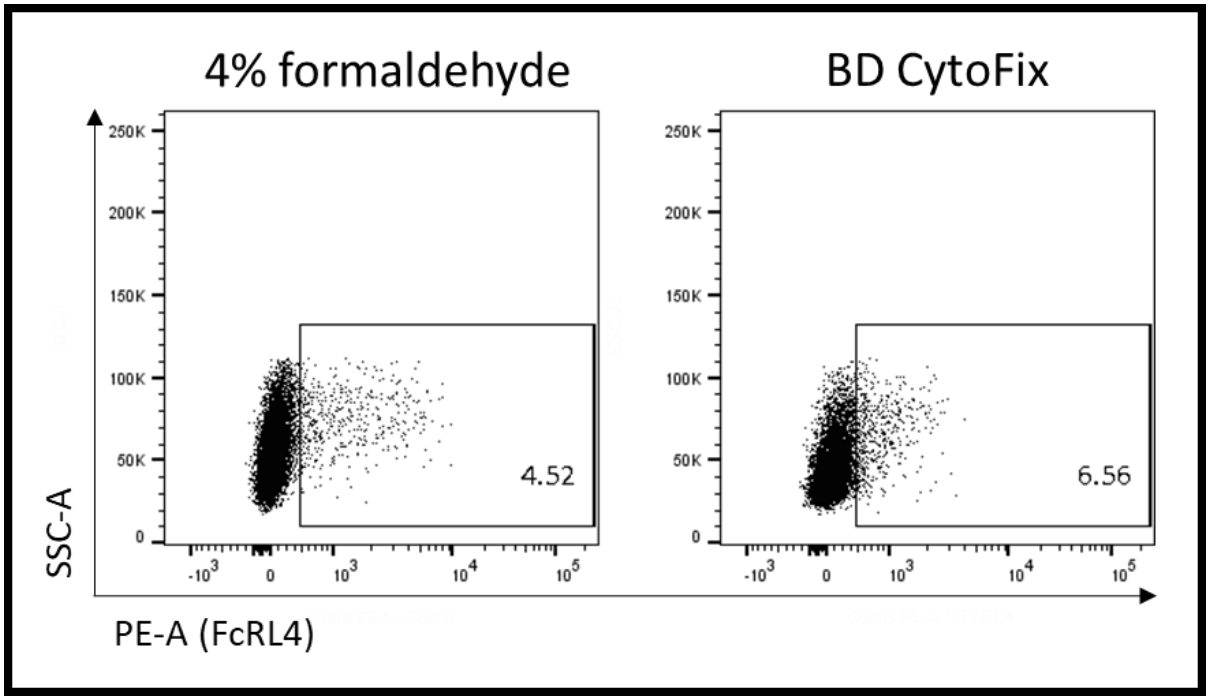

Figure 5.2.1.2., BD CytoFix does not negatively impact FcRL4 staining. *(n = 1) Representative FACS plots of cells fixed with 4% formaldehyde or BD CytoFix. Ex-vivo tonsil cells were stained for CD3, CD19 and FcRL4 and were gated on the lymphocyte, singlet, CD3- and CD19+ populations before gating on the FcRL4+ population. The number in the gate represents the percentage of FcRL4+ cells.*

5.2.1.3 CytoFix Titration

The concentration of BD CytoFix was also investigated to determine if it effected FcRL4 recognition. Prior to testing different concentrations on FcRL4 staining, cells were fixed at 4%, 3.6%, 3% and 2.5% BD CytoFix and stained for pPLC-γ2 to see if lowering the concentration would affect fixation of the phosphorylated proteins. When the concentration was decreased, there was loss of fixation of pPLC-γ2 (4.0% - 6.14%, 3.6% - 2.77%, 3.0% - 1.46%, 2.5% - 1.38%) (n = 1) (Figure 5.2.1.3). This suggested that 4% was the optimal concentration for fixation of phosphorylated signalling molecules and was not taken forward to test on FcRL4 staining.

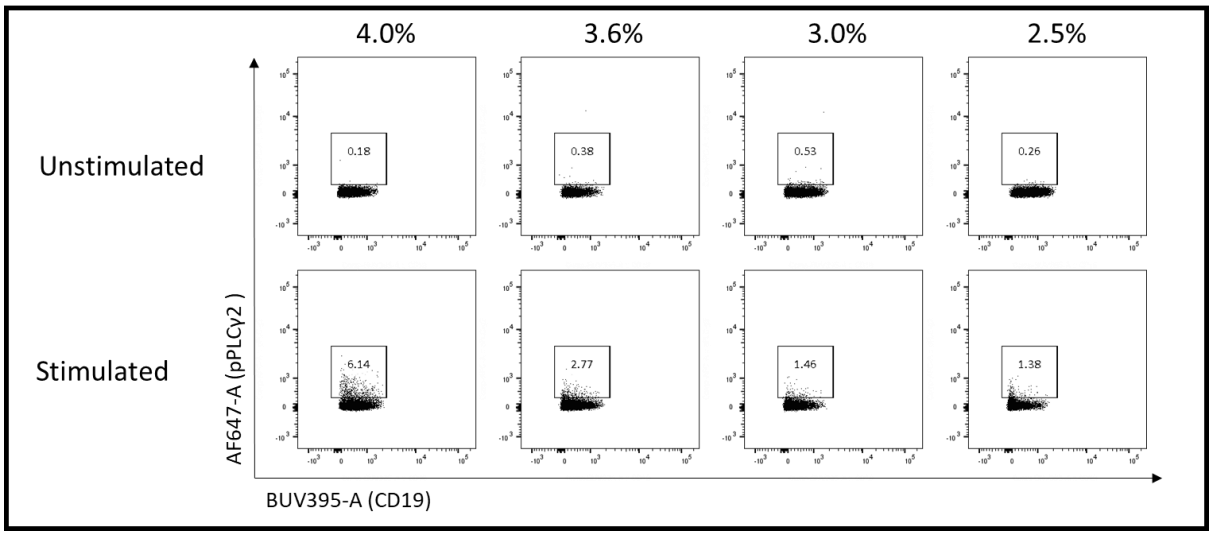

Figure 5,2.1.3., Reducing the concentrations of BD CytoFix reduces the amount of pPLCγ2 fixed*. (n = 1) Representative FACS plots of ex-vivo CD19+ tonsil cells that were unstimulated or stimulated with 10µg/ml IgG + IgM f(ab')$_2$ fragment for 5mins. These cells were then fixed in either 2.5%, 3%, 3.6% or 4% BD CytoFix for 12mins. Cells were stained for CD3 and CD19, permeabilised and stained for pPLCγ2. Ex-vivo tonsil cells were gated on the lymphocyte, singlet, CD3- and CD19+ populations. The number in the gate represents the percentage of pPLCγ2+ CD19+ cells.*

5.2.2 – FcRL4 Staining with 4% Formaldehyde

5.2.2.1 – anti-FcRL4 & Rat anti-Mouse BV711 2° Antibody

Generally, protein-based fluorophores such as APC and PE may not be compatible with Perm III so the available conjugated anti-FcRL4 from Biolegend was not suitable for PhosFlow staining and an alternative antibody needed to be validated. Firstly, to check that different antibodies could recognise FcRL4, cells were stained for 15 minutes, fixed in 4% formaldehyde and compared to anti-FcRL4 PE (Biolegend). An indirect staining method was tested using the unconjugated anti-FcRL4 (Biolegend) and a rat anti-mouse BV711 2° antibody (BD). BV711 was selected as it had been previously tested against BD Cytofix and Perm III and was found to be stable (data not shown). 62.1% of transduced Raji cells were FcRL4+ after staining with anti -FcRL4 PE whilst the indirect staining method detected 40.6% as FcRL4+ (n = 1) (Figure 5.2.2I). As it recognised a large enough population of FcRL4+ cells this method was taken forward to determine its stability in cells treated with BD CytoFix and BD Perm III.

5.2.2.2 anti-FcRL4 Lightning-Link® FITC & AF488

Next, as an alternative to using a secondary antibody to detect FcRL4, anti-FcRL4 (Biolegend) was directly conjugated to a fluorophore using a Lightning-Link® kit (Abcam). FITC and AF488 were selected for direct conjugation, as they're relatively bright fluorophores, AF488 more so than FITC, and they are also stable in BD CytoFix and BD Perm III. Compared to 12.4% FcRL4+ stained by anti-FcRL4 PE, 7.07% of cells were stained by anti-FcRL4 FITC (n = 1) (Figure 5.2.2I) whilst anti-FcRL4 AF488 only recognised 3.71% of FcRL4+ cells compared to

8.34% that was stained by anti-FcRL4 PE (n = 1) (Figure 5.2.2II). As a population of FcRL4+ cells were recognised, it indicated that the lightning-link had worked and was able to stain FcRL4 sufficiently and therefore was taken forward to test against BD CytoFix and BD Perm III.

5.2.2.3 anti-FcRL4 Abcam Lightning-Link® FITC

The three staining methods described each used anti-FcRL4 clone from Biolegend (Table 5.2.2) and when compared to anti-FcRL4 PE there was a reduction in the population of FcRL4+ cells recognised. Therefore, different clones were considered to determine if they could recognise FcRL4 better than the Biolegend clone. anti-FcRL4 from Abcam and was conjugated to FITC using a Lightning-Link® kit. It detected 2.89% FcRL4+ cells compared to 11.4% detected by the anti-FcRL4 PE (n = 1) (Figure 5.2.2I).

5.2.2.4 anti-FcRL4 BioTechne AF350 & AF594

Another option was an anti-FcRL4 from BioTechne that was already conjugated. The AF350 and AF594 conjugations were tested, as they are bright fluorophores and have good photostability according to the manufacturer. The anti-FcRL4 AF350 was not able to detect FcRL4 at the same degree of sensitivity compared to the anti-FcRL4 PE (n = 1) (Figure 5.2.2II). The experiment was repeated using the anti-FcRL4 AF594, as it's a brighter fluorophore than AF350. Again, the clone was not able to detect FcRL4 in 4% formaldehyde fixed cells (n = 1) (Figure 5.2.2II). Together, these results demonstrated that the anti-FcRL4 antibody from Biolegend recognised the FcRL4 epitope most effectively in cells fixed with 4% formaldehyde.

Due to their inability to recognise FcRL4 when cells were fixed with 4% formaldehyde the antibodies from BioTechne were not tested on cells fixed and permeabilised with BD CytoFix and BD Perm III.

Company	Clone	Species & Isotype	Fluorophores Tested
Biolegend	413D12	Mouse, IgG2b	PE
			BV711 (2° antibody)
			FITC
			AF488
Abcam	EPR21961	Rabbit, IgG	FITC
Biotechne	580810	Mouse, IgG1	AF350
			AF594

Table 5.2.2., Antibodies and fluorophores tested to stain FcRL4 in FcRL4+ transduced Raji cells and ex-vivo tonsil cells treated with BD CytoFix and BD Perm III

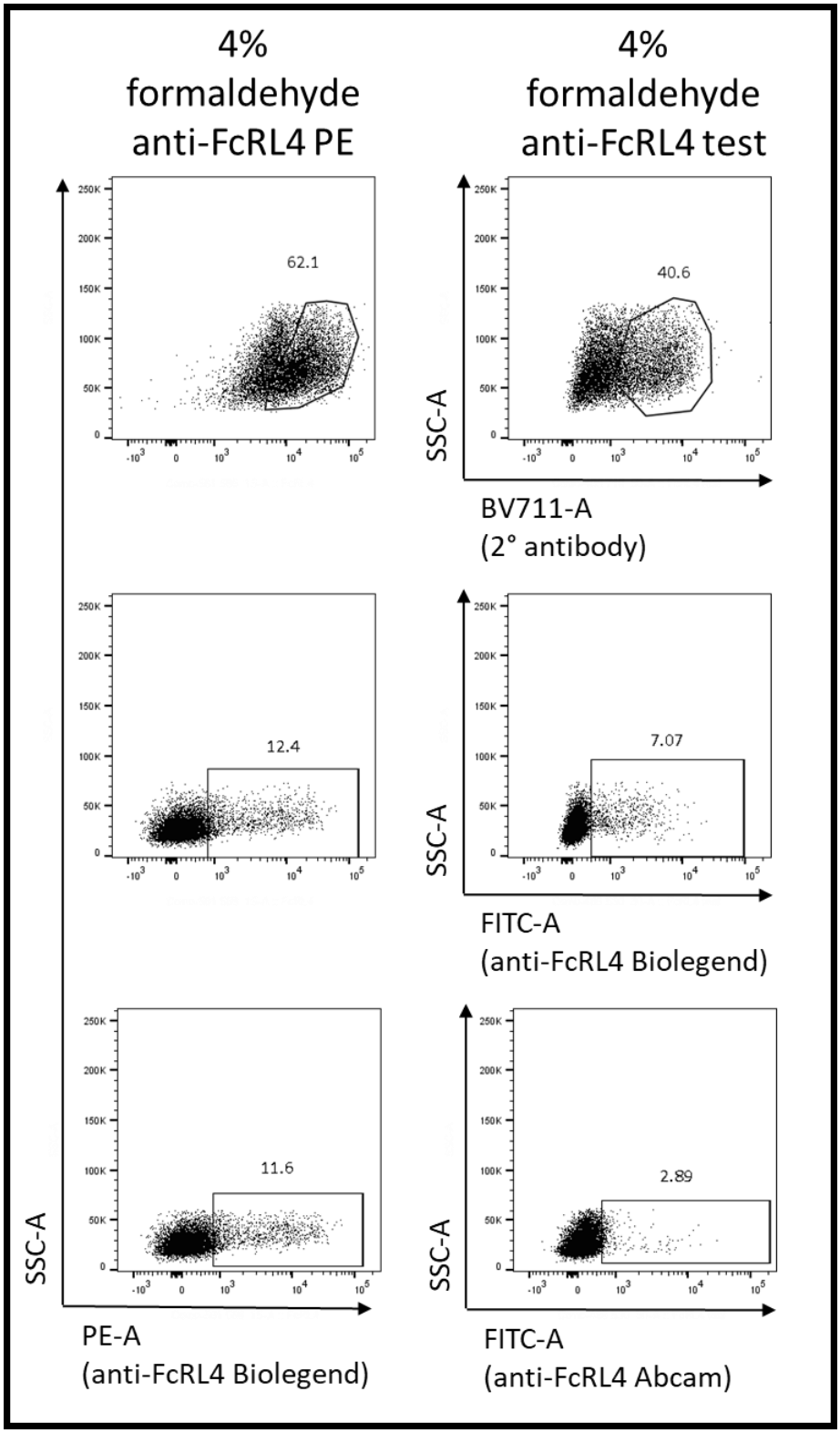

Figure 5.2.2I., BV711 and FITC anti-FcRL4 staining in cells fixed with 4% formaldehyde*. (n = 1) Representative FACS plots of the percentage of FcRL4+ cells. Anti-FcRL4 PE Biolegend was used at a 1:100 dilution as a positive control to determine the percentage of cells that were FcRL4+* ***(Top)*** *FcRL4 transduced Raji cells were stained with an unconjugated anti-FcRL4 Biolegend at a 1:100 dilution and a rat anti-mouse BV711 2° antibody Biolegend at a 1:50 dilution. Cells were gated on the lymphocyte and singlet population before gating on the FcRL4+ population.* ***(Middle)*** *ex-vivo tonsil cells were stained with a FITC lightning linked anti-FcRL4 Biolegend at a 1:100 dilution. Cells were gated on the lymphocyte, singlet, CD3- and CD19+ populations before gating on the FcRL4+ population.* ***(Bottom)*** *ex-vivo tonsil cells were stained with a FITC lightning linked anti-FcRL4 Abcam at a 1:100 dilution. Cells were gated on the lymphocyte, singlet, CD3- and CD19+ populations before gating on the FcRL4+ population. The number above the gate represents the percentage of FcRL4+ cells.*

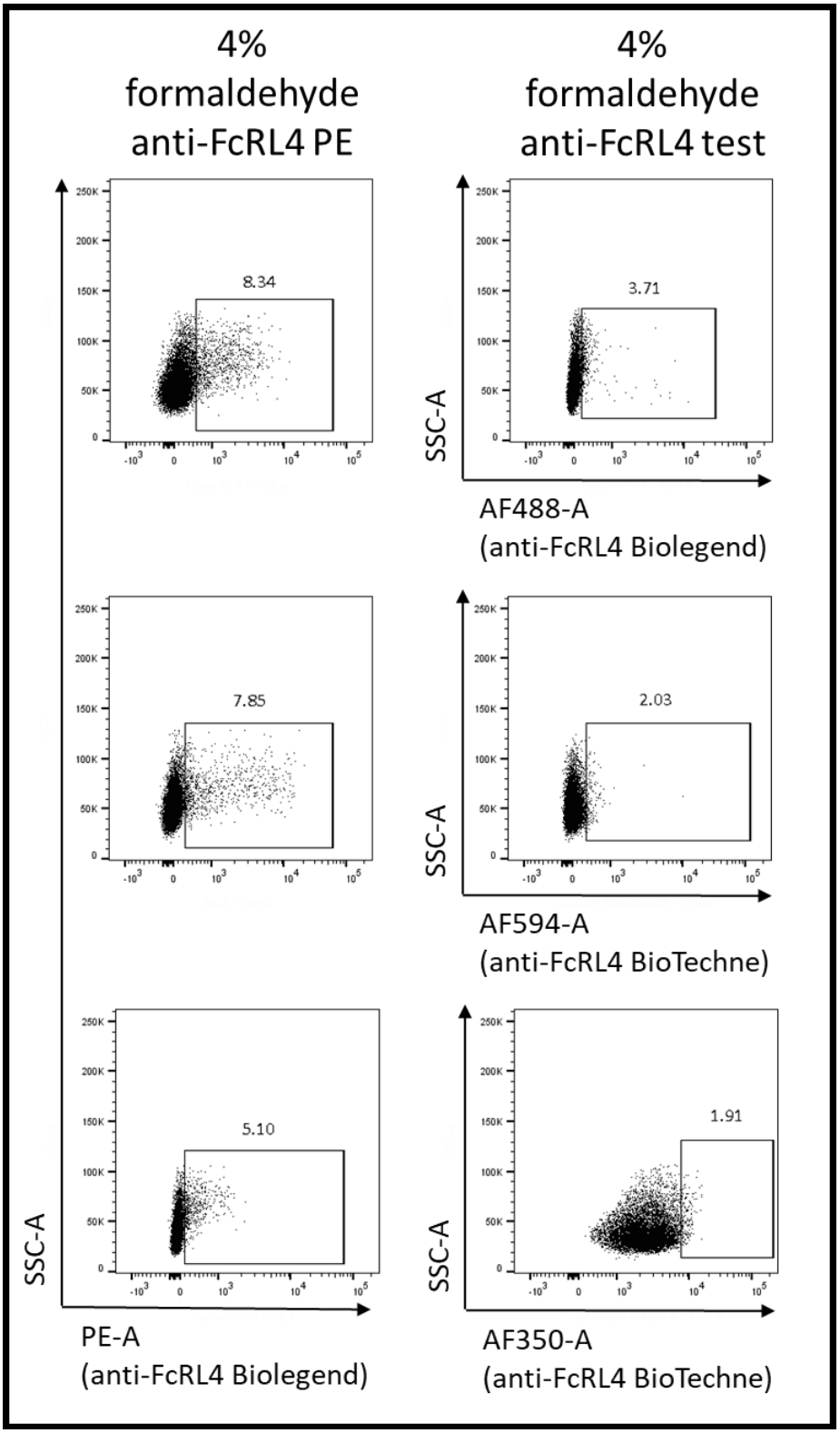

Figure 5.2.2II., AF488, AF594 and AF350 anti-FcRL4 staining in cells fixed with 4% formaldehyde*. (n = 1) Representative FACS plots of the percentage of FcRL4+ cells fixed with 4% formaldehyde. Anti-FcRL4 PE Biolegend was used at a 1:100 dilution as a positive control to determine the percentage of cells that were FcRL4+.* ***(Top)*** *ex-vivo tonsil cells were stained with a AF488 lightning linked anti-FcRL4 Biolegend at a 1:100 dilution. Cells were gated on the lymphocyte, singlet, CD3- and CD19+ populations before gating on the FcRL4+ population.* ***(Middle)*** *ex-vivo tonsil cells were stained with an AF594 anti-FcRL4 BioTechne at a 1:10 dilution. Cells were gated on the lymphocyte, singlet, CD3- and CD19+ populations before gating on the FcRL4+ population.* ***(Bottom)*** *ex-vivo tonsil cells were stained with an AF350 anti-FcRL4 BioTechne at a 1:10 dilution. Cells were gated on the lymphocyte, singlet, CD3- and CD19+ populations before gating on the FcRL4+ population. The number above the gate represents the percentage of FcRL4+ cells.*

5.2.3 FcRL4 Staining with BD CytoFix and BD Perm III

5.2.3.1 anti-FcRL4 & Rat anti-Mouse BV711 2° Antibody

Next, to test if the antibody staining method was compatible for PhosFlow, cells were fixed with BD CytoFix, stained for 15mins and then permeabilised overnight. These cells were compared to corresponding staining in 4% formaldehyde (Figure 5.2.2) and to cells that had been fixed in BD CytoFix only (Figure 5.2.3) to determine whether it was the fixation or permeabilization that would affect subsequent staining. First, cells stained using the indirect staining method showed a reduction in FcRL4+ cell population from 40.6% to 22.3% in cells fixed with BD CytoFix only and the signal was completely lost in cells treated with BD CytoFix and BD Perm III (n = 1) (Figure 5.2.3). To determine if the permeabilization was interfering with the binding of the 2° antibody to anti-FcRL4, it was added to the cells post-permeabilization. There was no change in the FcRL4+ population compared to those stained with the 2° antibody pre-permeabilization (data not shown), suggesting that using an indirect method to detect FcRL4 was not suitable.

5.2.3.2 anti-FcRL4 Abcam Lightning-Link® FITC

Next, the anti-FcRL4 FITC from Abcam was tested and detected 2.69% FcRL4+ cells fixed with CytoFix only compared to 2.89% FcRL4+ cells fixed with 4% formaldehyde. This then increased to 6.17% when cells were also permeabilised (n = 1) (Figure 5.2.3). However, this was a notable decrease from the 11.6% detected using the anti-FcRL4 PE from Biolegend (Figure 5.2.2) and confirmed that the Biolegend clone was a more suitable antibody.

5.2.3.3 anti-FcRL4 Lightning-Link® FITC & AF488

Finally, cells were stained with anti-FcRL4 AF488 and recognised only 0.64% when fixed and reduced further to 0.12% when fixed and permeabilised (n = 1) (Figure 5.2.3). However, cells stained with the anti-FcRL4 FITC detected 5.86% FcRL4+ cells fixed the BD CytoFix only. This then increased to 11.4% when cells were also permeabilised, a similar percentage to anti-FcRL4 PE fixed with 4% formaldehyde (Figure5.2.3). This suggested that the AF488 was a less suitable fluorophore than FITC for staining.

However, subsequent experiments that used the anti-FcRL4 FITC detected a lower proportion FcRL4+ cells than previously shown. Re-titration of the antibody did not improve staining (data not shown). This indicated that direct conjugation using a Lightning-Link® kit was not suitable for PhosFlow. As shown in Figure 5.2.1.2, BD CytoFix did not affect FcRL4 detection, which suggested that BD Perm III could be affecting the antibody or its fluorophore.

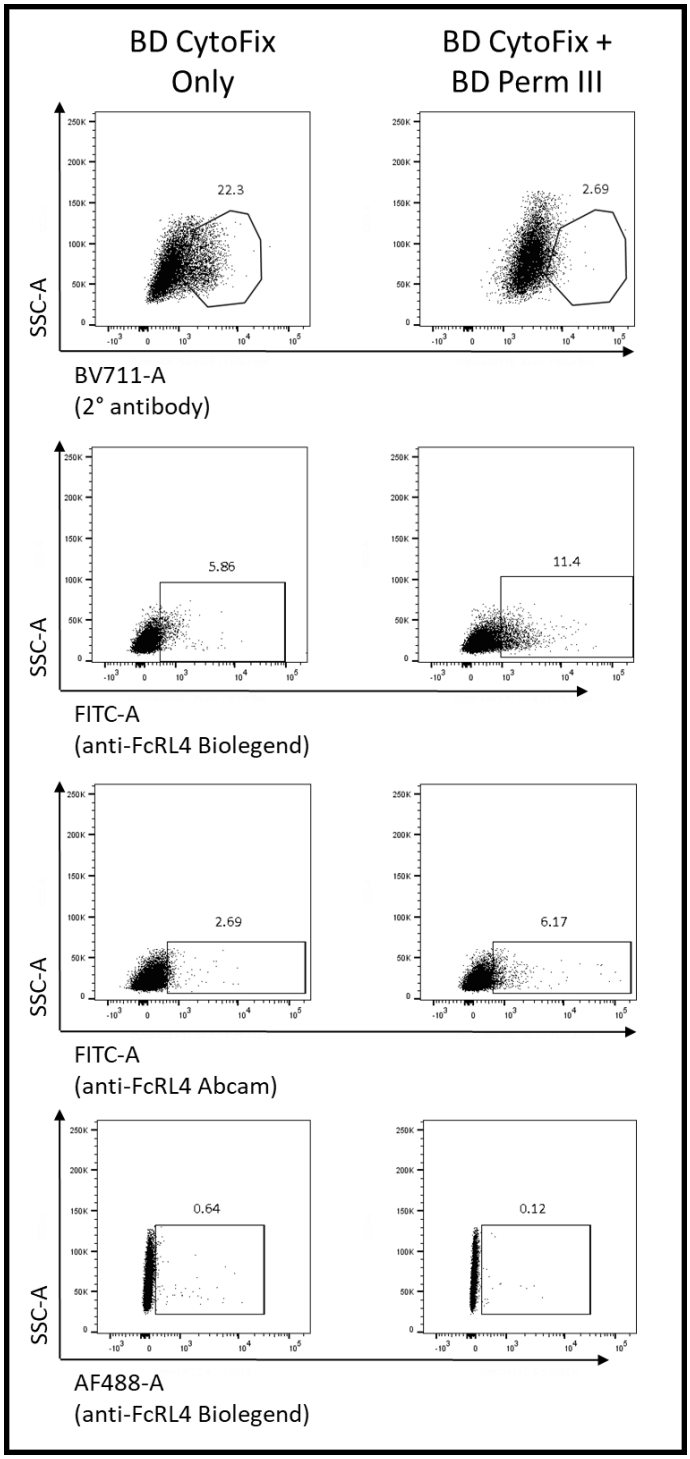

Figure 5.2.3., FcRL4 staining in cells fixed with BD CytoFix and permeabilised with BD Perm III. *(n = 1) Representative FACS plots of the percentage of FcRL4+ cells either fixed in BD CytoFix only or fixed in BD CytoFix and permeabilised with BD Perm III. The cells stained with anti-FcRL4 PE Biolegend at a 1:100 dilution and fixed with 4% formaldehyde in Figure 5.2.2I and II were used as a positive control to determine the percentage of cells that were FcRL4+* ***(Top)*** *FcRL4 transduced Raji cells were stained with an unconjugated anti-FcRL4 Biolegend at a 1:100 dilution and a rat anti-mouse BV711 2° antibody Biolegend at a 1:50 dilution. Cells were gated on the lymphocyte and singlet population before gating on the FcRL4+ population.* ***(Top Middle)*** *ex-vivo tonsil cells were stained with a FITC lightning linked anti-FcRL4 Biolegend at a 1:100 dilution. Cells were gated on the lymphocyte, singlet, CD3- and CD19+ populations before gating on the FcRL4+ population.* ***(Bottom Middle)*** *ex-vivo tonsil cells were stained with a FITC lightning linked anti-FcRL4 Abcam at a 1:100 dilution. Cells were gated on the lymphocyte, singlet, CD3- and CD19+ populations before gating on the FcRL4+ population.* ***(Bottom)*** *ex-vivo tonsil cells were stained with a AF488 lightning linked anti-FcRL4 Biolegend at a 1:100 dilution. Cells were gated on the lymphocyte, singlet, CD3- and CD19+ populations before gating on the FcRL4+ population. The number above the gate represents the percentage of FcRL4+ cells.*

5.2.4 FcRL4 Biolegend PE & FITC Lightning-Link® Perm II Stability Test

To determine whether BD Perm III was the primary contributor to low FcRL4 detection, BD Perm II was tested for cell permeabilisation, as its methanol content is 64.86% compared to 87.68% in BD Perm III. Both the FITC lightning-linked and PE-conjugated anti-FcRL4 (Biolegend) were tested in Perm II-treated cells, as these had demonstrated the best detection of FcRL4 in previous experiments (Figure 5.2.1.2 and 5.2.3). FcRL4+ cells detected using the anti-FcRL4 FITC improved in Perm II treated cells compared to Perm III treated cells but the signal was still dim compared to the cells fixed with 4% formaldehyde only (n = 1) (Figure 5.2.4). However, cells stained with anti-FcRL4 PE detected 9.19% FcRL4+ cells when fixed and permeabilised compared to 9.16% when fixed with 4% formaldehyde, suggesting that this was the most effective antibody for detecting FcRL4 when cells were permeabilised with BD Perm II (Figure 5.2.4).

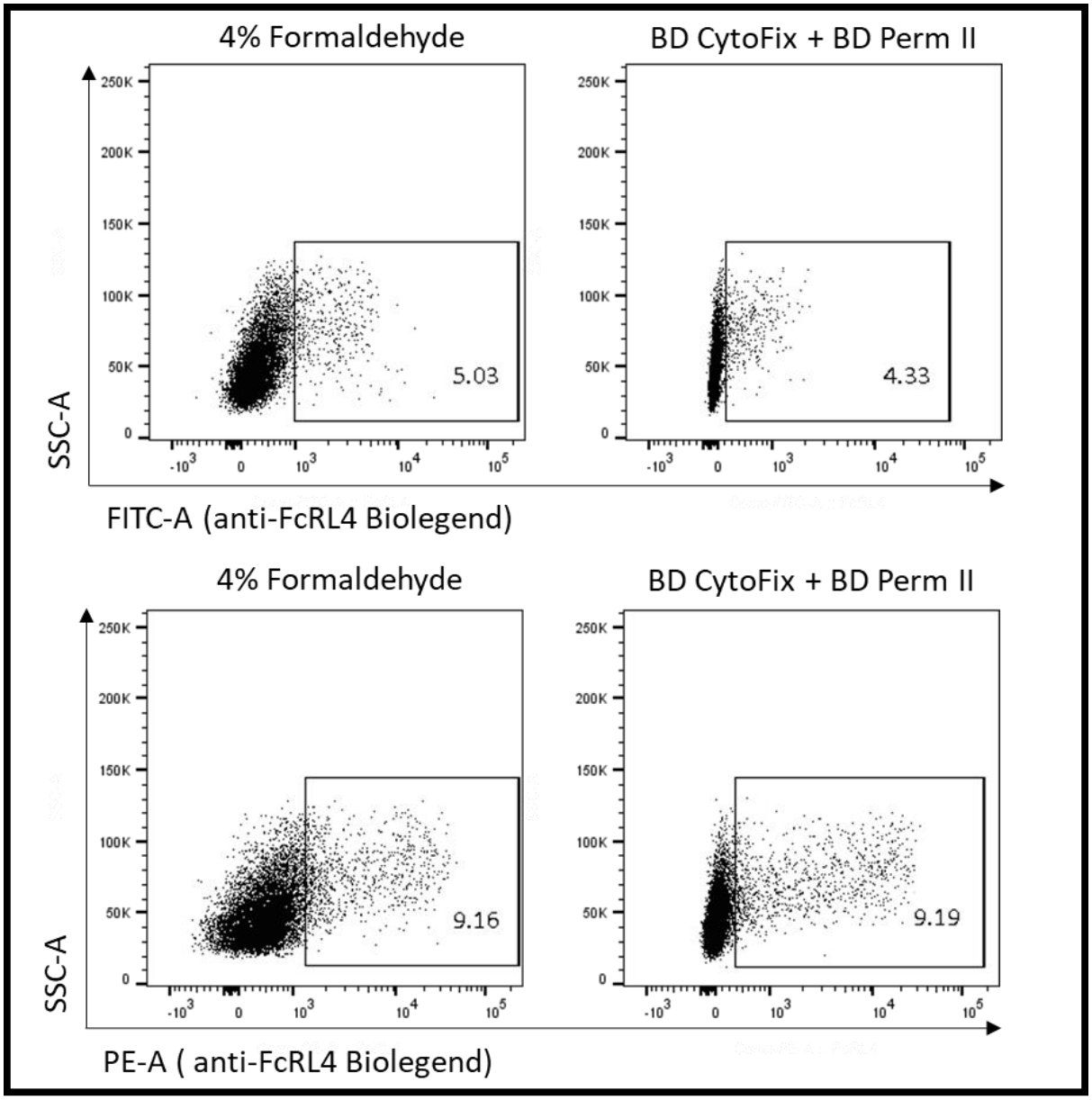

Figure 5.2.4., FcRL4 staining in cells fixed with BD CytoFix and permeabilised with BD Perm II. *(n = 1) representative FACS plots of the percentage of FcRL4+ ex-vivo tonsil cells detected in samples fixed with 4% formaldehyde or treated with BD CytoFix + BD Perm II. Ex-vivo tonsil cells were subsequently stained with either the Biolegend FITC lightning linked antibody* ***(Top)*** *or Biolegend PE-conjugated antibody* ***(Bottom).*** *These were gated on the lymphocyte, singlet, CD3- and CD19+ populations before gating on the FcRL4+ populations. Number in the gate represents the percentage of FcRL4+ cells.*

5.2.5 Intracellular Antibody Validation

5.2.5.1 10µg/ml anti-IgG + IgM f(ab')$_2$ fragment 0-60mins

To validate the antibodies staining phosphorylated proteins, PBMCs were stimulated with an anti-IgG + IgM f(ab')$_2$ fragment to activate signalling pathways through the BCR. Cells were fixed at 0, 5, 15, 30 and 60mins, stained for CD3 to remove T cells and stained for CD19 to define B cells. They were then permeabilised overnight and stained for phosphorylated proteins using company-recommended dilutions. The only exceptions were pFgr and pHck, as the recommended titrations were intended for western blots and would need to be used at higher concentrations for detection using flow cytometry. pERK1/2, pHck, pPLC-γ2, pSHP-2 and pSyk peaked at 5 minutes (Figure 5.2.5.1I, II & III), pFgr at 15mins (Figure 5.2.5.1I & III) and pBtk/Itk and pp65-NF-κB at 60mins (Figure 5.2.5.1I & III) (n =1). Although pSHP-1 appeared to peak at 5mins (Figure 5.2.5.1II & III), there was little change in phosphorylation across the time course. Additionally, pAkt had been investigated previously (data not shown) and demonstrated a similar staining pattern to pSHP-1. A possible explanation was that the timepoints the cells were fixed at were too far apart to detect a response to the anti-IgG + IgM f(ab')$_2$ fragment.

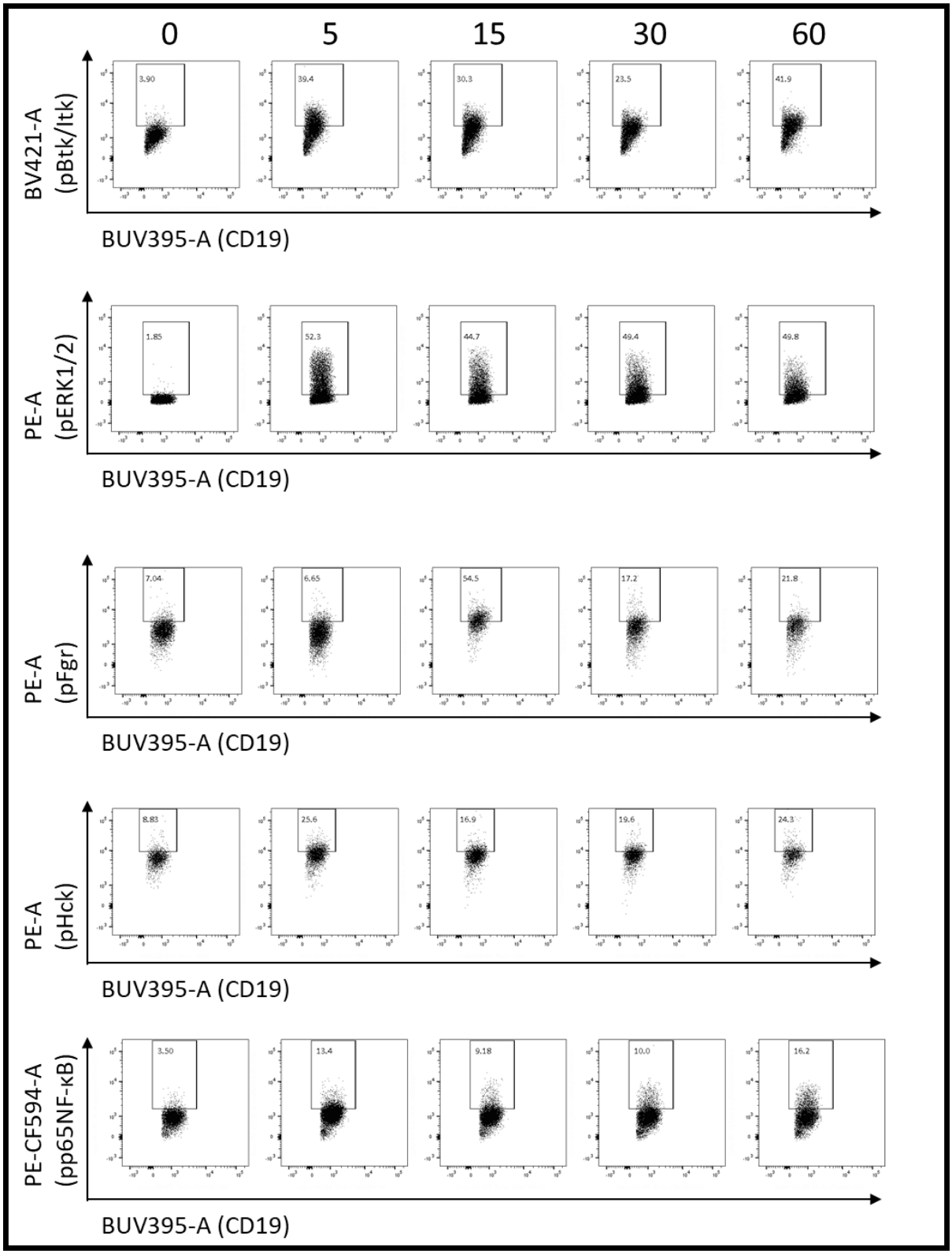

Figure 5.2.5.1I., Change in phosphorylation of pBtk/Itk, pERK1/2, pFgr, pHck and pp65NF-κB in CD19+ PBMC cells stimulated with 10µg/ml anti-IgG + IgM f(ab')$_2$ fragment 0-60mins*. (n = 1) Representative FACS plots demonstrating the changes in phosphorylation when CD19+ B cells from PBMCs were fixed with BD CytoFix at 0, 5, 15, 30 and 60mins after stimulation with 10µg/ml IgG + IgM f(ab')$_2$ fragment. Cells were stained with CD3 and CD19 to define a CD3-CD19+ population, permeabilised and stained for pPLCγ2, pSHP-1, pSHP-2 and pSyk. To determine the cells that were positive for phosphorylation events, an unstimulated sample was stained for pBtk/Itk, pERK1/2, pFgr, pHck and pp65NF-κB and a gate applied just above this population. The number in the gate represents the percentage of CD19+ cells where phosphorylation events could be detected in stimulated samples.*

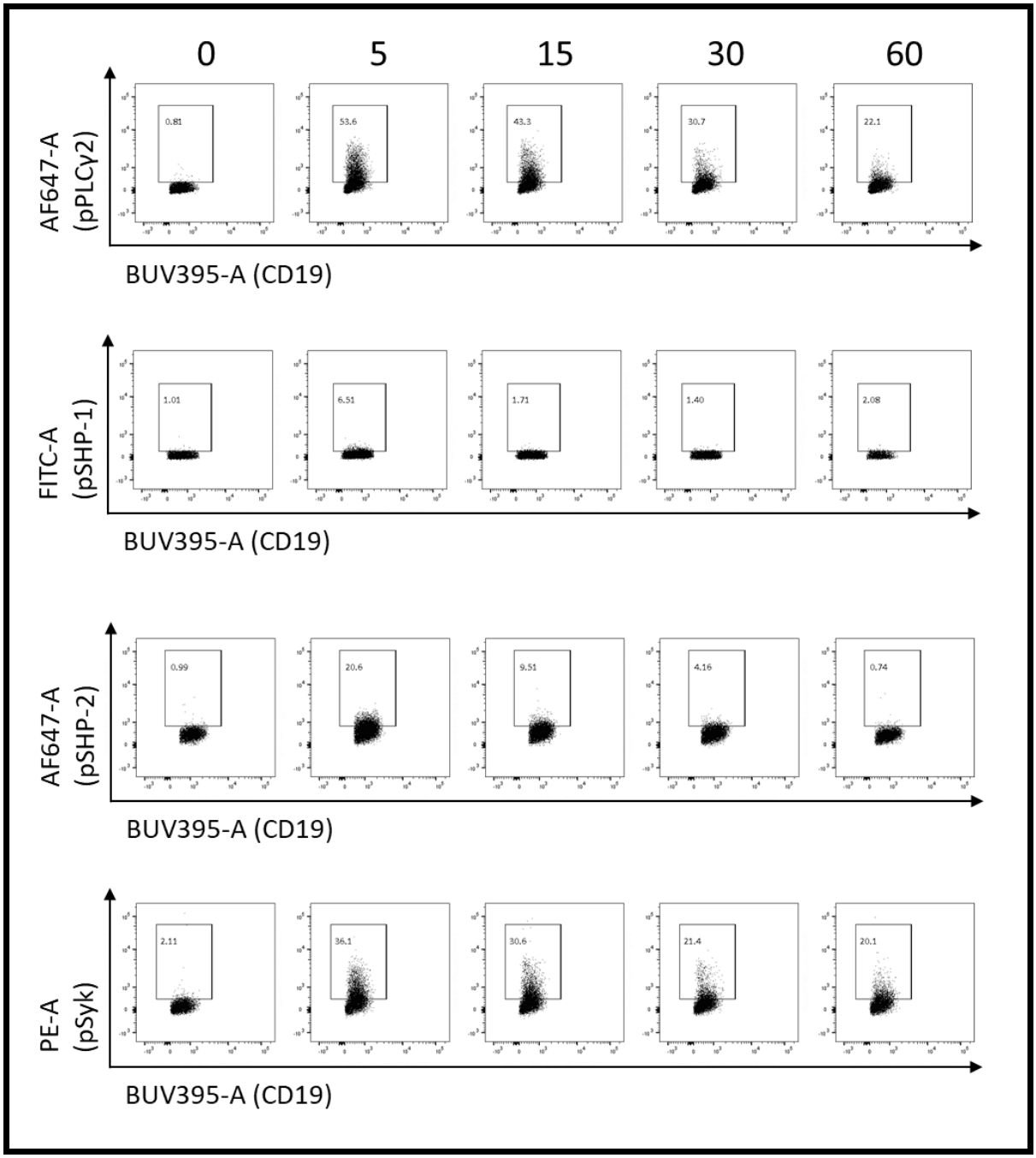

Figure 5.2.5.1II., Change in phosphorylation of pPLCγ2, ppSHP-1, pSHP-2 and pSyk in CD19+ PBMC cells stimulated with 10µg/ml IgG + IgM f(ab')$_2$ fragment 0-60mins*. (n = 1) Representative FACS plots demonstrating the changes in phosphorylation when CD19+ B cells from PBMCs were fixed with BD CytoFix at 0, 5, 15, 30 and 60mins after stimulation with 10µg/ml IgG + IgM f(ab')$_2$ fragment. Cells were stained with CD3 and CD19 to define a CD3-CD19+ population, permeabilised and stained for pPLCγ2, pSHP-1, pSHP-2 and pSyk. To determine the cells that were positive for phosphorylation events, an unstimulated sample was stained for pPLCγ2, pSHP-1, pSHP-2 and pSyk and a gate applied just above this population. The number in the gate represents the percentage of CD19+ cells where phosphorylation events could be detected in stimulated samples.*

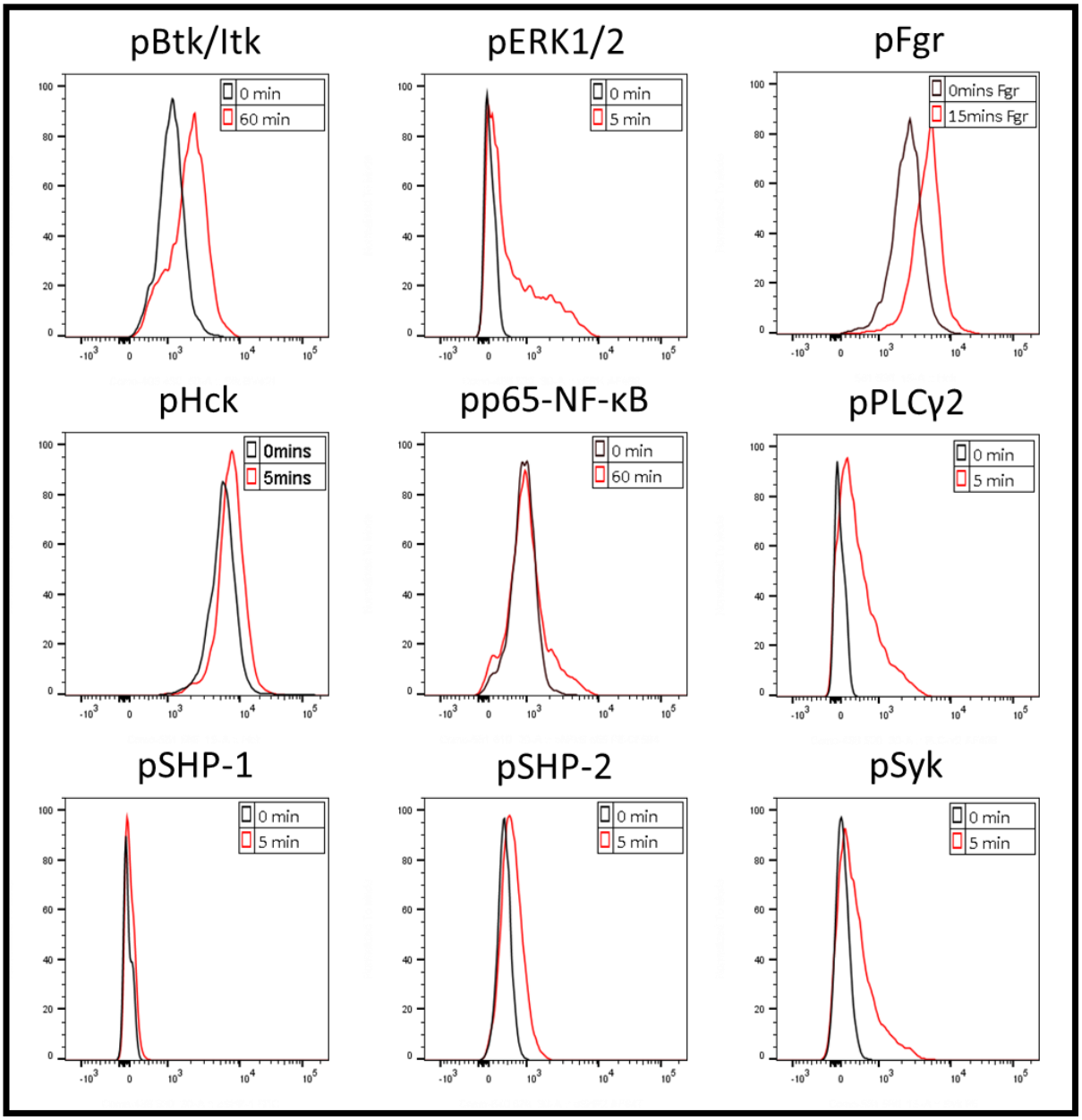

Figure 5.2.5.1III., Peak phosphorylation of pBtk/Itk, pERK1/2, pFgr, pHck, pp65NF-κB, pPLCγ2, pSHP-1, pSHP-2 and pSyk in CD19+ PBMC cells stimulated with 10µg/ml IgG + IgM f(ab')$_2$ fragment 0-60mins*. (n = 1) Representative histograms demonstrating the timepoint at which peak phosphorylation is reached. Cells were stained with CD3 and CD19 to define a CD3-CD19+ population. Peak phosphorylation was determined as the highest percentage in the gate that was set for each signalling molecule compared to the unstimulated (0mins). The black line represents the unstimulated sample and the red line represents the peak phosphorylation timepoint. The time at which peak phosphorylation was detected is detailed in the top right-hand corner of each histogram.*

5.2.5.2 10µg/ml anti-IgG + IgM f(ab')$_2$ fragment stimulation 0-20mins

CD19+ B cells from PBMCs were stimulated with 10µg/ml anti-IgG + IgM f(ab')$_2$ fragment for 20mins and fixed at more regular intervals to determine a more specific timepoint at which peak phosphorylation was reached and determine if anti-pAkt and anti-pSHP-1 were able to sufficiently detect their target. pFgr and pHck were not included in this set of experiments, as their peak phosphorylation was not detected early on in the original time course and they were being investigated as signalling molecules downstream of FcRL4 when the samples would be treated with HA colostrum IgA IC. The peak phosphorylation for each signalling molecule were as followed: pBtk/Itk – 5mins (Figure 5.2.5.2I &IV), pERK1/2 – 8mins (Figure 5.2.5.2I & IV), pp65-NF-κB – 20mins (Figure 5.2.5.2II & IV), pPLCγ2 – 4mins (Figure 5.2.5.2II & IV), pSHP-2 – 8mins (Figure 5.2.5.2III & IV), pSyk – 4mins (Figure 5.2.5.2III & IV). Additionally, pAkt peaked at 8mins (Figure 5.2.5.2I & IV) and pSHP-1 at 10mins (Figure 5.2.5.2III & IV), which confirmed the timepoints investigated in Figure 5.2.5.1 were too far apart to detect peak phosphorylation of these particular signalling proteins (n = 1). To stain for multiple phosphorylated proteins at one time, cells were grouped based on their similarity in peak phosphorylation. Therefore, pBtk/Itk, pPLC-γ2 and pSyk were grouped and stimulated for 4mins and pAkt, pERK1/2 and pp65-NF-κB for 10mins.

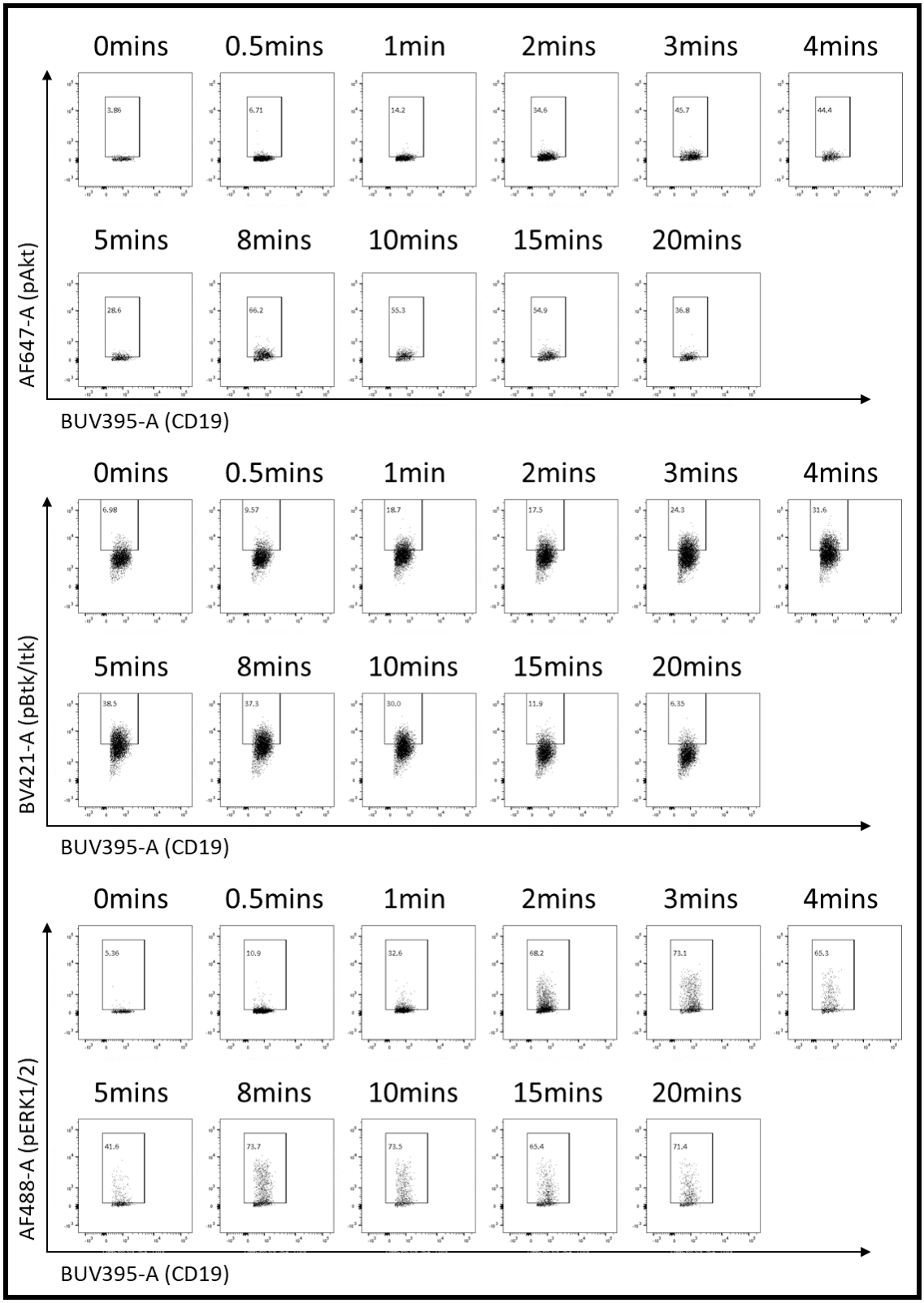

Figure 5.2.5.2I., Change in phosphorylation of pAkt, pBtk/Itk and pERK1/2 in CD19+ PBMC's stimulated with 10µg/ml IgG + IgM f(ab')$_2$ fragment 0-20mins*. (n = 1) Representative FACS plots demonstrating the changes in phosphorylation when CD19+ B cells from PBMCs were fixed with BD CytoFix at 0, 0.5, 1, 2, 3, 4, 5, 8, 10, 15 and 20mins after stimulation with 10µg/ml IgG + IgM f(ab')$_2$ fragment. Cells were stained with CD3 and CD19 to define a CD3-CD19+ population, permeabilised and stained for pAkt, pBtk/Itk and pERK1/2. To determine the cells that were positive for phosphorylation events, an unstimulated sample was stained for pAkt, pBtk/Itk and pERK1/2 and a gate applied just above this population. The number in the gate represents the percentage of CD19+ cells where phosphorylation events could be detected in stimulated samples.*

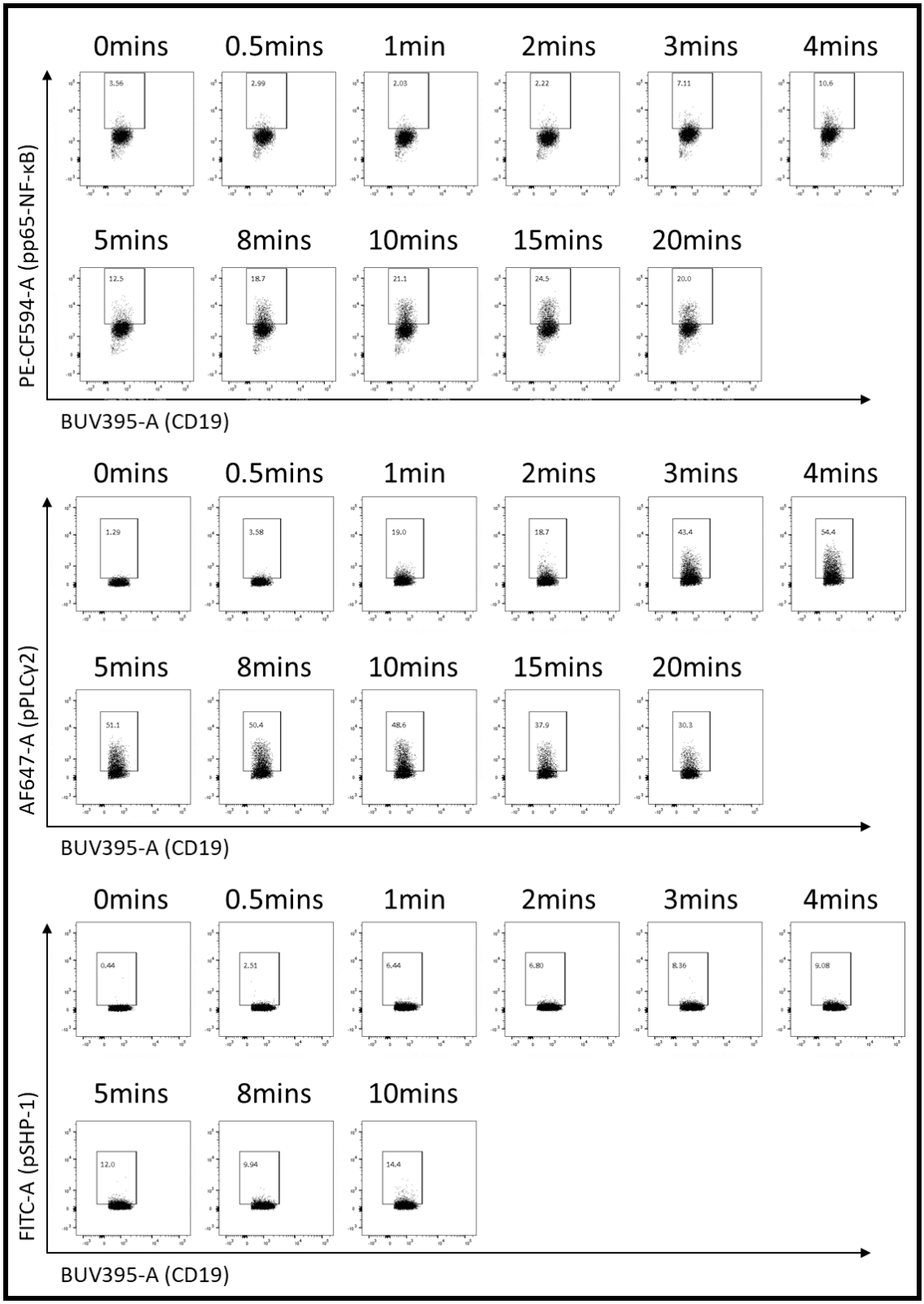

Figure 5.2.5.2II., Change in phosphorylation of pp65NF-κB, pPLCγ2 and pSHP-1 in CD19+ PBMC's stimulated with 10µg/ml IgG + IgM f(ab')$_2$ fragment 0-20mins. *(n = 1) Representative FACS plots demonstrating the changes in phosphorylation when CD19+ B cells from PBMCs were fixed with BD CytoFix at 0, 0.5, 1, 2, 3, 4, 5, 8, 10, 15 and 20mins after stimulation with 10µg/ml IgG + IgM f(ab')$_2$ fragment. Cells were stained with CD3 and CD19 to define a CD3-CD19+ population, permeabilised and stained for pp65NF-κB, pPLCγ2, pSHP-1. To determine the cells that were positive for phosphorylation events, an unstimulated sample was stained for pp65NF-κB, pPLCγ2, pSHP-1and a gate applied just above this population. The number in the gate represents the percentage of CD19+ cells where phosphorylation events could be detected in stimulated samples.*

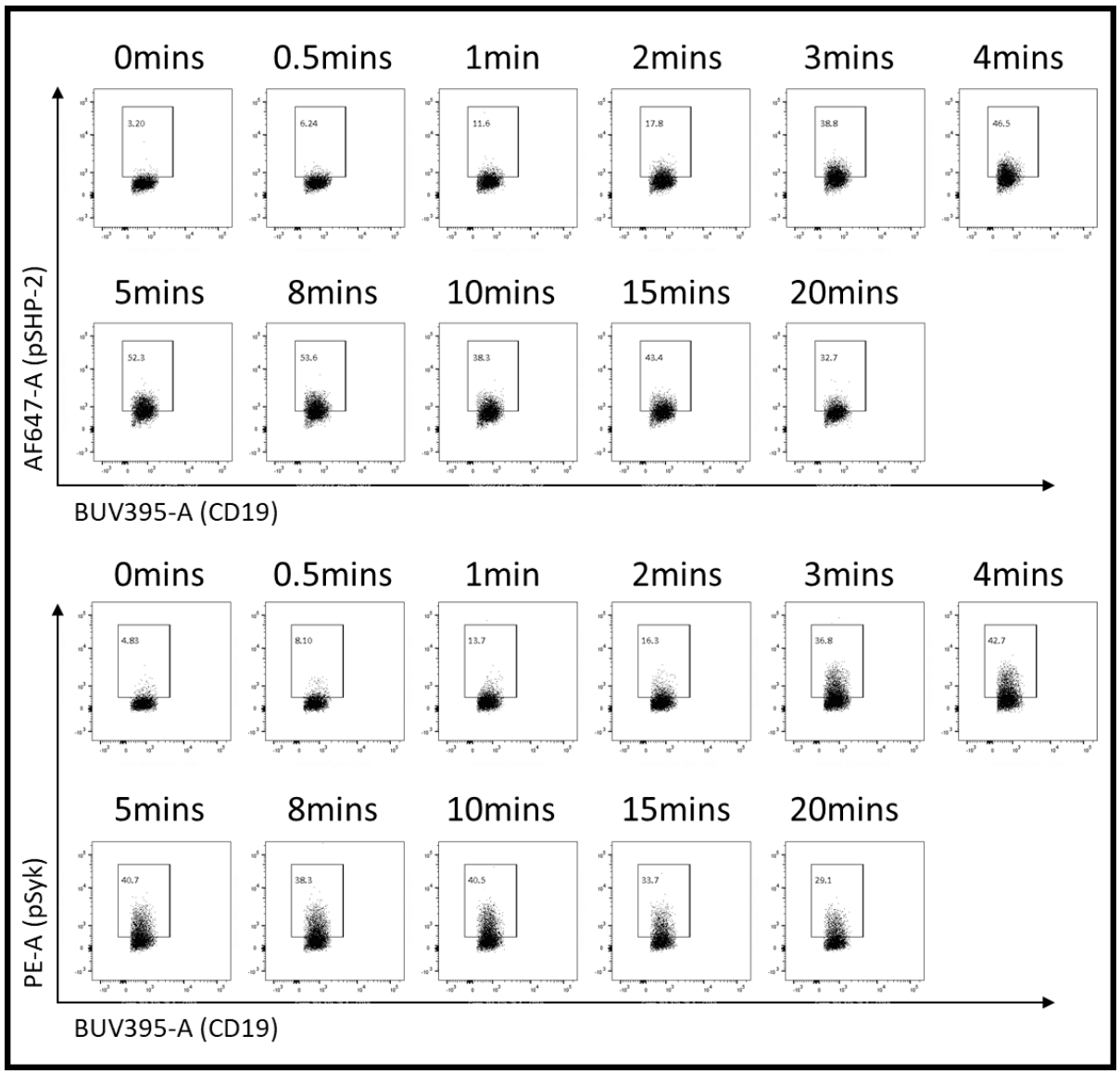

Figure 5.2.5.2III., Change in phosphorylation of pSHP-2 and pSyk in CD19+ PBMC's stimulated with 10µg/ml IgG + IgM f(ab')$_2$ fragment 0-20mins*. (n = 1) Representative FACS plots demonstrating the changes in phosphorylation when CD19+ B cells from PBMCs were fixed with BD CytoFix at 0, 0.5, 1, 2, 3, 4, 5, 8, 10, 15 and 20mins after stimulation with 10µg/ml IgG + IgM f(ab')$_2$ fragment. Cells were stained with CD3 and CD19 to define a CD3-CD19+ population, permeabilised and stained for pSHP-2 and pSyk. To determine the cells that were positive for phosphorylation events, an unstimulated sample was stained for p SHP-2 and pSyk and a gate applied just above this population. The number in the gate represents the percentage of CD19+ cells where phosphorylation events could be detected in stimulated samples.*

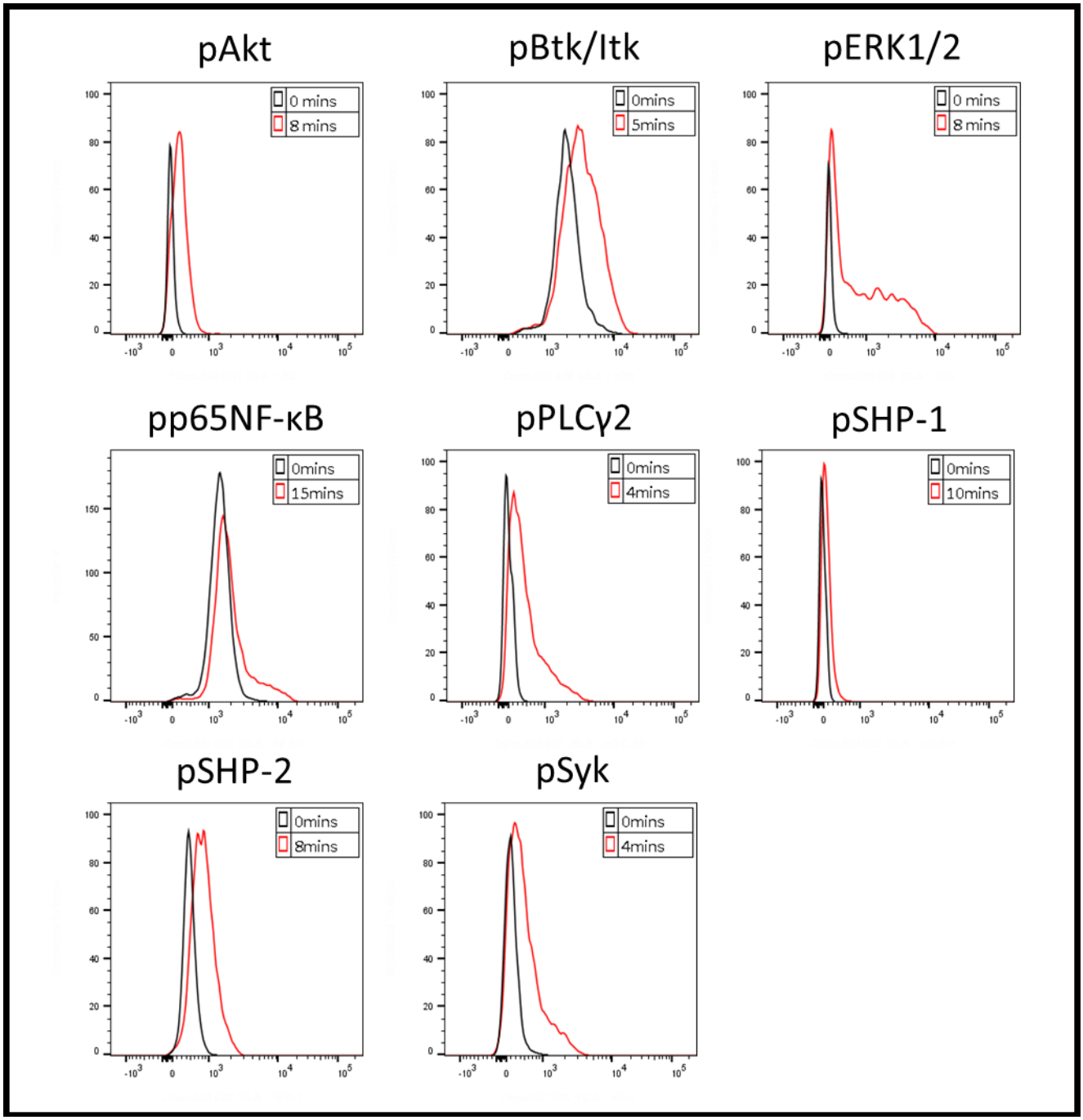

Figure 5.2.5.2IV., Peak phosphorylation of pAkt, pBtk/Itk, pERK1/2, pp65NF-κB, pPLCγ2, pSHP-1, pSHP-2 and pSyk in CD19+ PBMC cells stimulated with 10µg/ml IgG + IgM f(ab')$_2$ fragment 0-20mins. *(n = 1) Representative histograms demonstrating the timepoint at which peak phosphorylation is reached. Cells were stained with CD3 and CD19 to define a CD3-CD19+ population. Peak phosphorylation was determined as the highest percentage in the gate that was set for each signalling molecule compared to the unstimulated (0mins). The black line represents the unstimulated sample and the red line represents the peak phosphorylation timepoint. The time at which peak phosphorylation was detected is detailed in the top right-hand corner of each histogram.*

5.2.5.3 50µg/ml HA Colostrum IgA stimulation 0-20mins

Next, to identify the peak phosphorylation of pFgr, pHck, pSHP-1 and pSHP-2 when stimulated through FcRL4, PBMCs were stimulated with 50µg/ml HA colostrum IgA IC for the same length of time and intervals as those in Figures 8 & 9. PBMCs usually express low levels of FcRL4, so they were initially stimulated with 10µg/ml TLR-7L, 5µM TLR-9bL and 10ng/ml TGFβ to upregulate expression of FcRL4 on their surface. pFgr peaked at 3mins (Figure 5.2.5.3I & III), pHck at 2mins (Figure 5.2.5.3I & III), pSHP-1 at 5mins (Figure 5.2.5.3I & III) and pSHP-2 0.5mins (Figure 5.2.5.3II & III) (n = 1). Again, to stain for phosphorylated proteins at one time, pSHP-1 and pSHP-2 were grouped and stimulated for 5mins whilst pFgr and pHck were stimulated for 2mins.

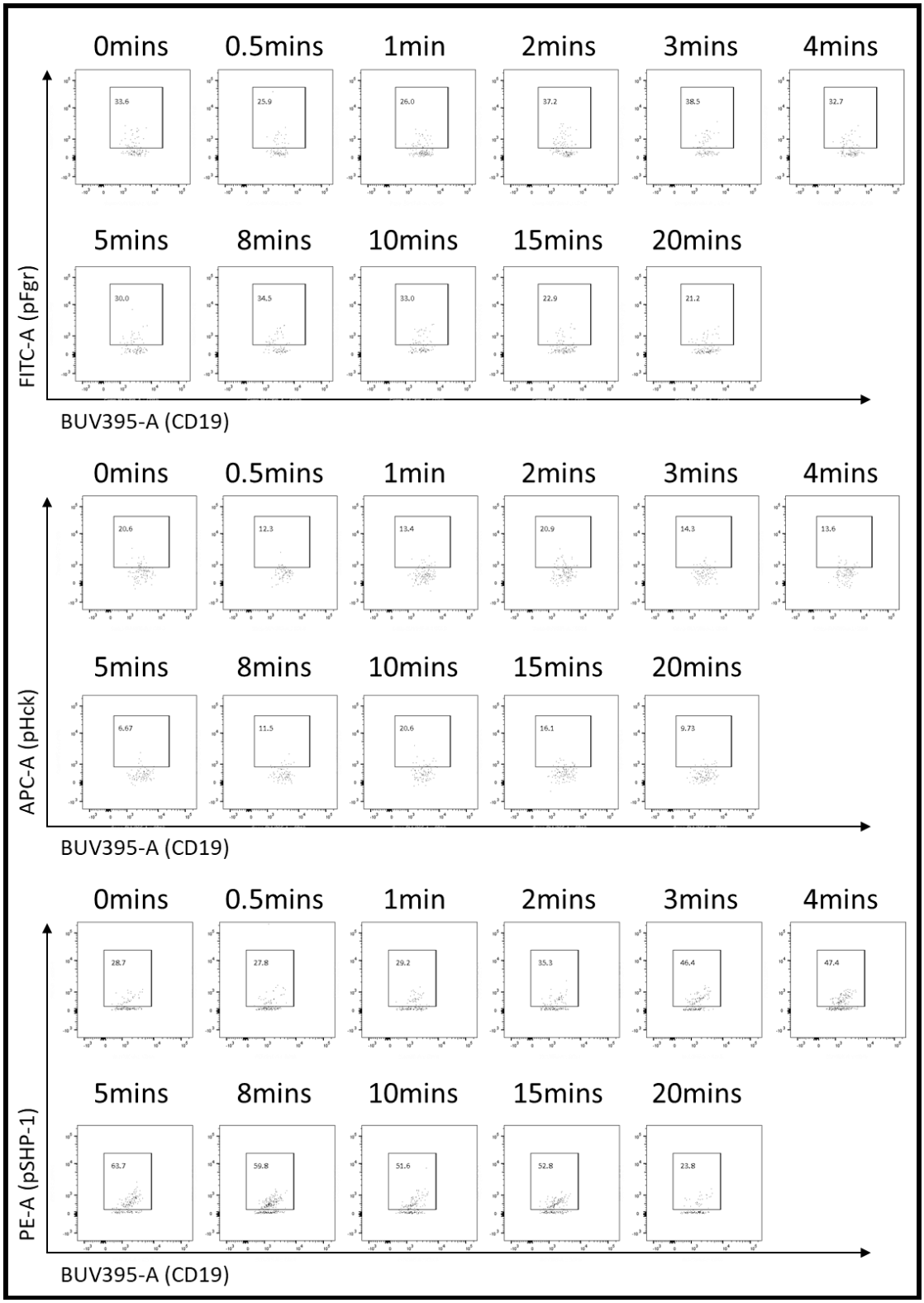

Figure 5.2.5.3I., Change in phosphorylation of pFgr pHck and pSHP-1 in stimulated FcRL4+ PBMCs in response to 50µg/ml HA colostrum IgA IC 0-20mins*. (n = 1) Representative FACS plots demonstrating the changes in phosphorylation when CD19+ B cells from PBMCs were fixed with BD CytoFix at 0, 0.5, 1, 2, 3, 4, 5, 8, 10, 15 and 20mins after stimulation with 50µg/ml HA colostrum IgA IC. Prior to stimulation, PBMCs were stimulated with 10µg/ml TLR-7L, 5µM TLR-9bL and 10ng/ml TGFβ for 24h, washed with PhosFlow buffer and rested for 2h at 37°C, 5% CO_2 before stimulating. Cells were stained with CD3, CD19 and FcRL4 to define a CD3-CD19+FcRL4+ population, permeabilised and stained for pFgr, pHck and pSHP-1. To determine the cells that were positive for phosphorylation events, an unstimulated sample was stained for pFgr, pHck and pSHP-1and a gate applied just above this population. The number in the gate represents the percentage of CD19+ cells where phosphorylation events could be detected in stimulated samples.*

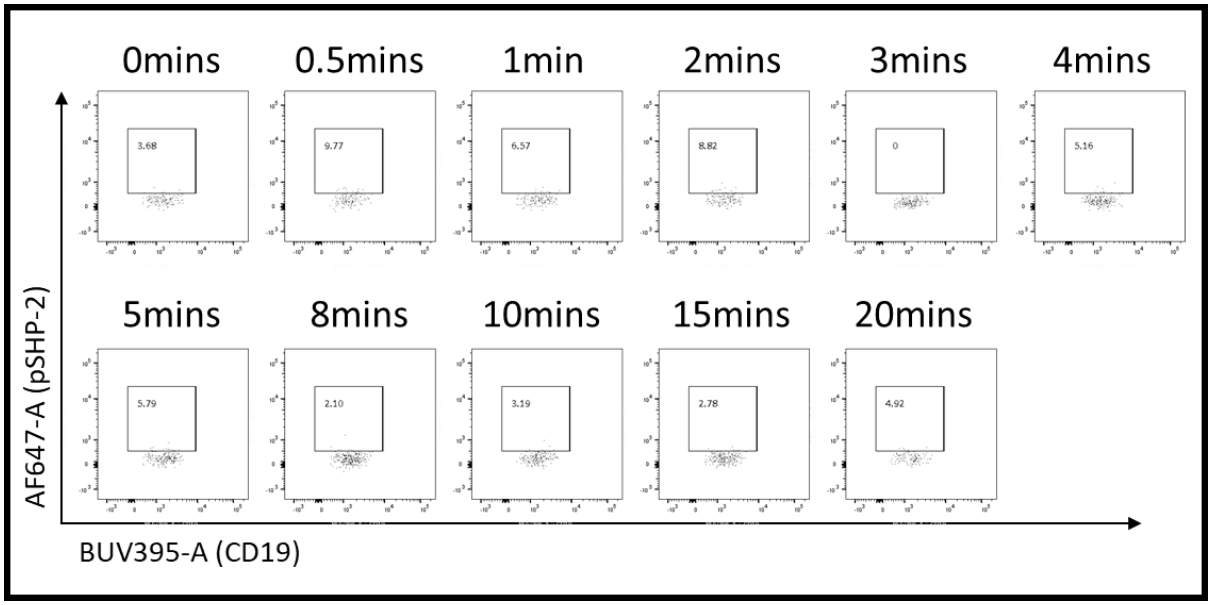

Figure 5.2.5.3II., Change in phosphorylation of pSHP-2 in stimulated FcRL4+ PBMCs in response to 50µg/ml HA colostrum IgA IC 0-20mins*. (n = 1) Representative FACS plots demonstrating the changes in phosphorylation when CD19+ B cells from PBMCs were fixed with BD CytoFix at 0, 0.5, 1, 2, 3, 4, 5, 8, 10, 15 and 20mins after stimulation with 50µg/ml HA colostrum IgA IC. Prior to stimulation, PBMCs were stimulated with 10µg/ml TLR-7L, 5µM TLR-9bL and 10ng/ml TGFβ for 24h, washed with PhosFlow buffer and rested for 2h at 37°C, 5% CO_2 before stimulating. Cells were stained with CD3, CD19 and FcRL4 to define a CD3-CD19+FcRL4+ population, permeabilised and stained for pSHP-2. To determine the cells that were positive for phosphorylation events, an unstimulated sample was stained for pSHP-2 and a gate applied just above this population. The number in the gate represents the percentage of CD19+ cells where phosphorylation events could be detected in stimulated samples.*

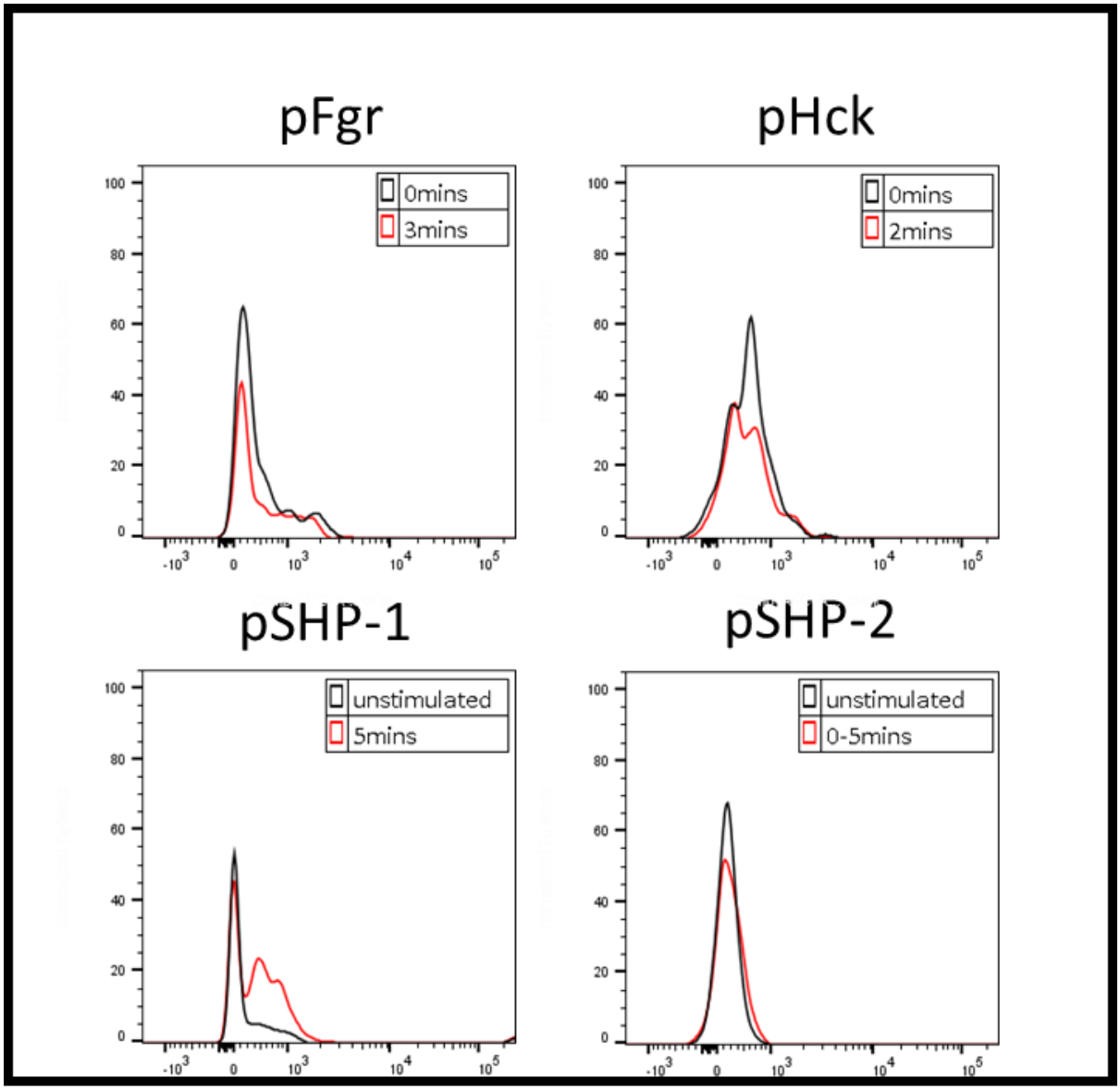

Figure 5.2.5.3III., Peak phosphorylation of pFgr, pHck, pSHP-1 and pSHP-2 in stimulated FcRL4+ PBMC stimulated with 50µg/ml HA colostrum IgA IC 0-20mins*. (n = 1) Representative histograms demonstrating the timepoint at which peak phosphorylation is reached. Cells were stained with CD3, CD19 and FcRL4 to define a CD3-CD19+FcRL4+ population. Peak phosphorylation was determined as the highest percentage in the gate that was set for each signalling molecule compared to the unstimulated (0mins). The black line represents the unstimulated sample and the red line represents the peak phosphorylation timepoint. The time at which peak phosphorylation was detected is detailed in the top right-hand corner of each histogram.*

5.2.5.4 Antibody Titration BD Perm III

Once peak phosphorylation had been determined, the antibodies were titrated to determine the optimum dilution (n = 1). The company recommended dilution and dilution that was used in subsequent experiments are detailed in Table 5.2.5.4.

Antibody	Company Dilution	Titrated Dilution
pAkt	1:5	1:20
pBtk/Itk	1:20	1:50
pERK1/2	1:20	1:50
pFgr	1:1000	1:100
pHck	1:1000	1:100
pp65-NF-κB	1:20	1:20
pPLCγ2	1:5	1:20
pSHP-1	1:20	1:20
pSHP-2	1:5	1:10
pSyk	1:5	1:10

Table 5.2.5.4., Antibody dilutions recommended by the company and those that were determined to be best for staining following titration

5.2.5.5 – Perm II Intracellular Antibody Staining

Initially, the antibodies staining for IC phosphorylated proteins were optimised in cells that were permeabilised in BD Perm III. However, as described in Figure 5.2.4, to obtain consistent and stable detection of FcRL4 BD Perm II was more compatible than BD Perm III. As the methanol concentration is lower in BD Perm II than Perm III, it does not permeabilise the cells as vigorously meaning that the antibodies directed at IC antibodies entry into the cell may be impeded. Therefore, the IC antibodies were validated in cells stimulated with anti-IgG + IgM $f(ab')_2$ fragment, fixed and permeabilised the BD Perm II and at the titration detailed in Table 5.2.5.4. The amount of phosphorylation detected was comparable between cells permeabilised with Perm II and Perm III, suggesting that Perm II is a compatible permeabilization buffer for staining with these particular antibodies (n = 1) (Figure 5.2.5.5I, II & III).

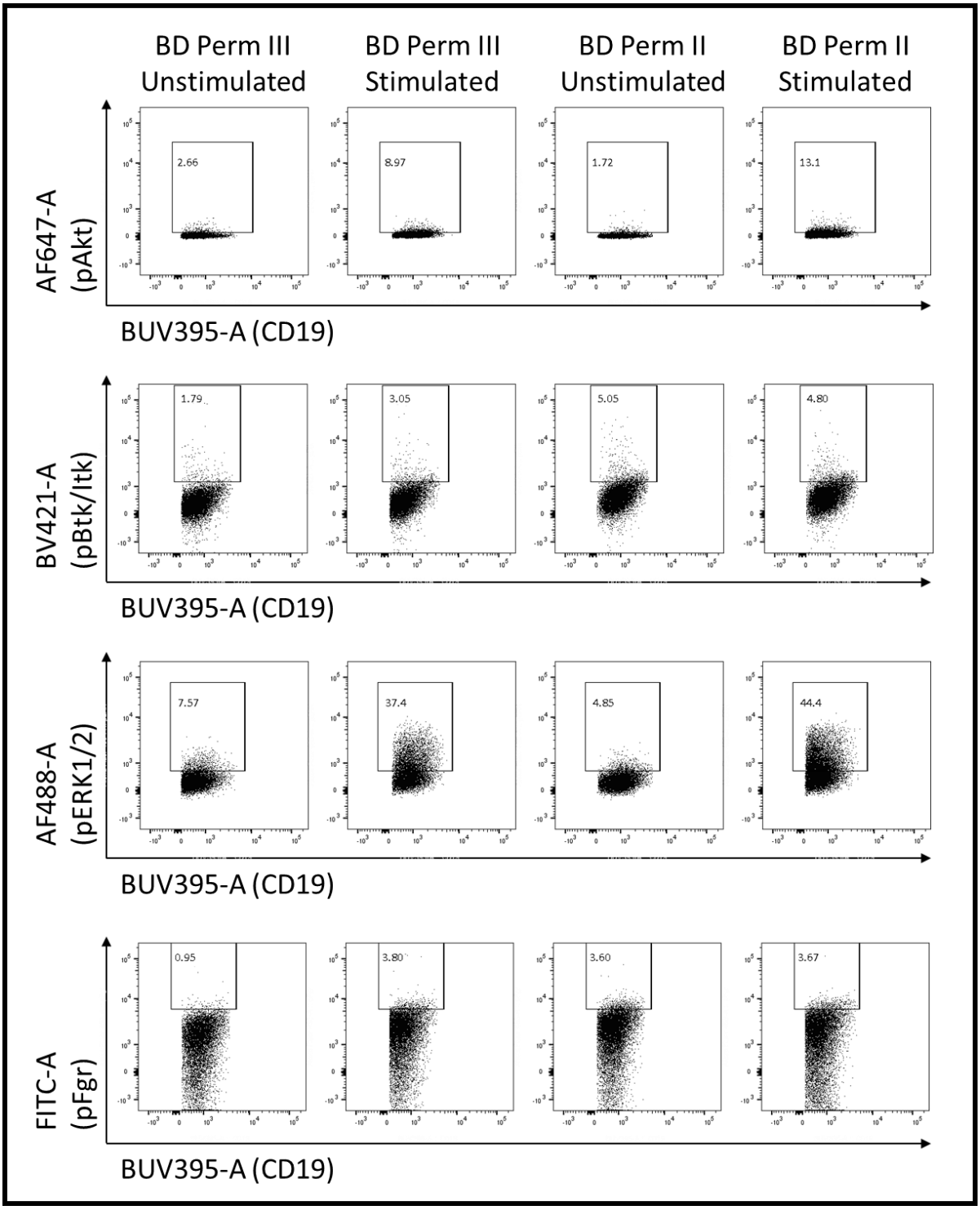

Figure 5.2.5.5I., Comparison of pAkt, pBtk/Itk, pERK1/2 and pFgr staining in ex-vivo CD19+ tonsil cells permeabilised with BD Perm III and Perm II*. (n = 1) Representative FACS plots demonstrating the changes in phosphorylation when ex-vivo tonsil cells were permeabilised with BD perm III and BD Perm II. Ex-vivo tonsil cells were stimulated with 10µg/ml IgG + IgM f(ab')$_2$ fragment and fixed with BD CytoFix at 2mins (pFgr), 4mins (pBtk/Itk) and 10mins (pAkt and pERK1/2). Cells were stained with CD3 and CD19 to define a CD3-CD19+ population, permeabilised and stained for pAkt, pBtk/Itk, pERK1/2 and pFgr. The number in the gate represents the percentage of CD19+ cells where phosphorylation events could be detected in stimulated samples.*

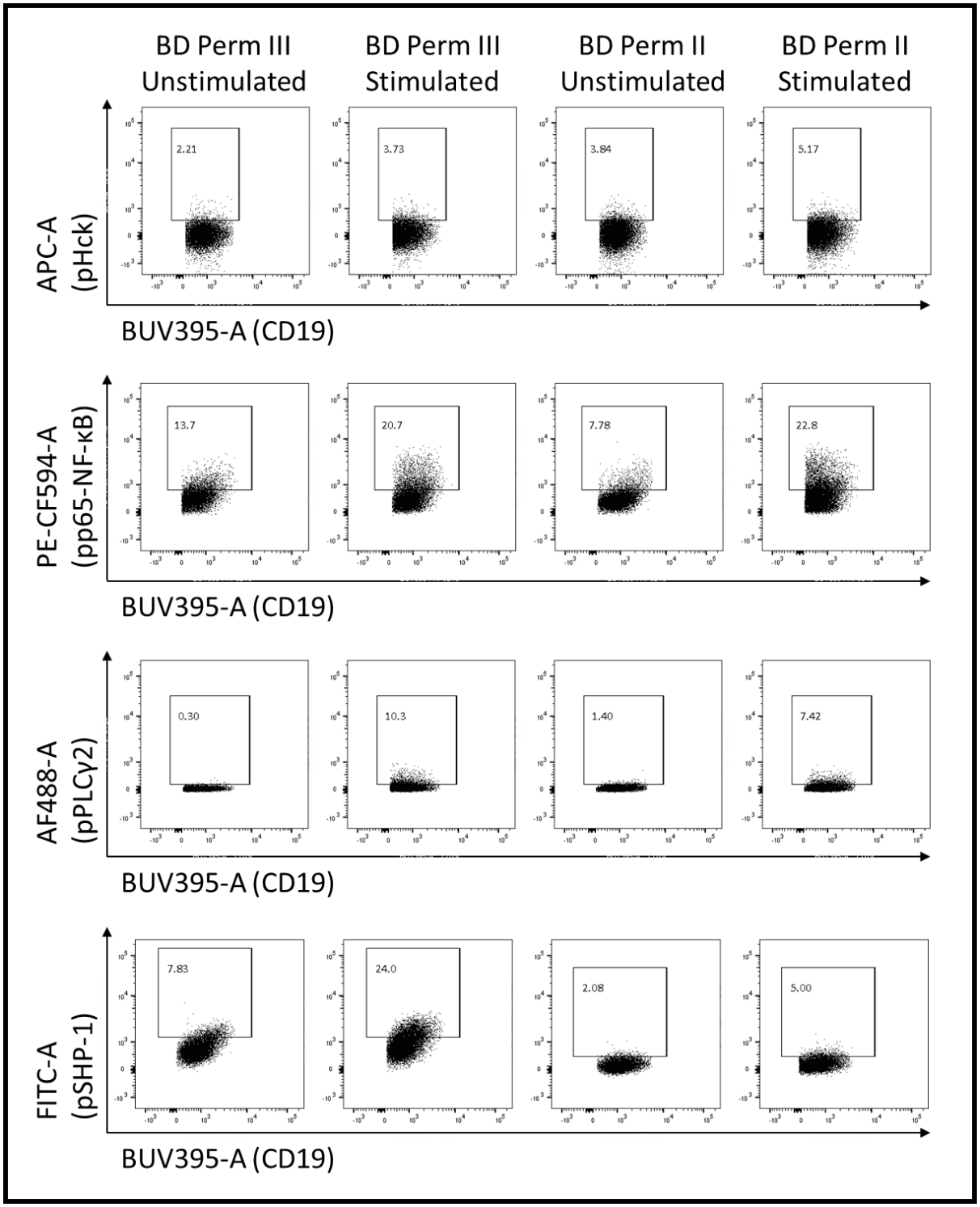

Figure 5.2.5.5II., Comparison of pHck, pp65NF-κB, PLCγ2 and pSHP-1 staining in ex-vivo CD19+ tonsil cells permeabilised with BD Perm III and Perm II*. (n = 1) Representative FACS plots demonstrating the changes in phosphorylation when ex-vivo tonsil cells were permeabilised with BD perm III and BD Perm II. Ex-vivo tonsil cells were stimulated with 10µg/ml IgG + IgM f(ab')$_2$ fragment and fixed with BD CytoFix at 2mins (pHck), 4mins (pPLCγ2), 5mins (pSHP-1) and 10mins (pp65NF-κB). Cells were stained with CD3 and CD19 to define a CD3-CD19+ population, permeabilised and stained for pHck, pp65NF-κB, pPLCγ2 and pSHP-1. The number in the gate represents the percentage of CD19+ cells where phosphorylation events could be detected in stimulated samples.*

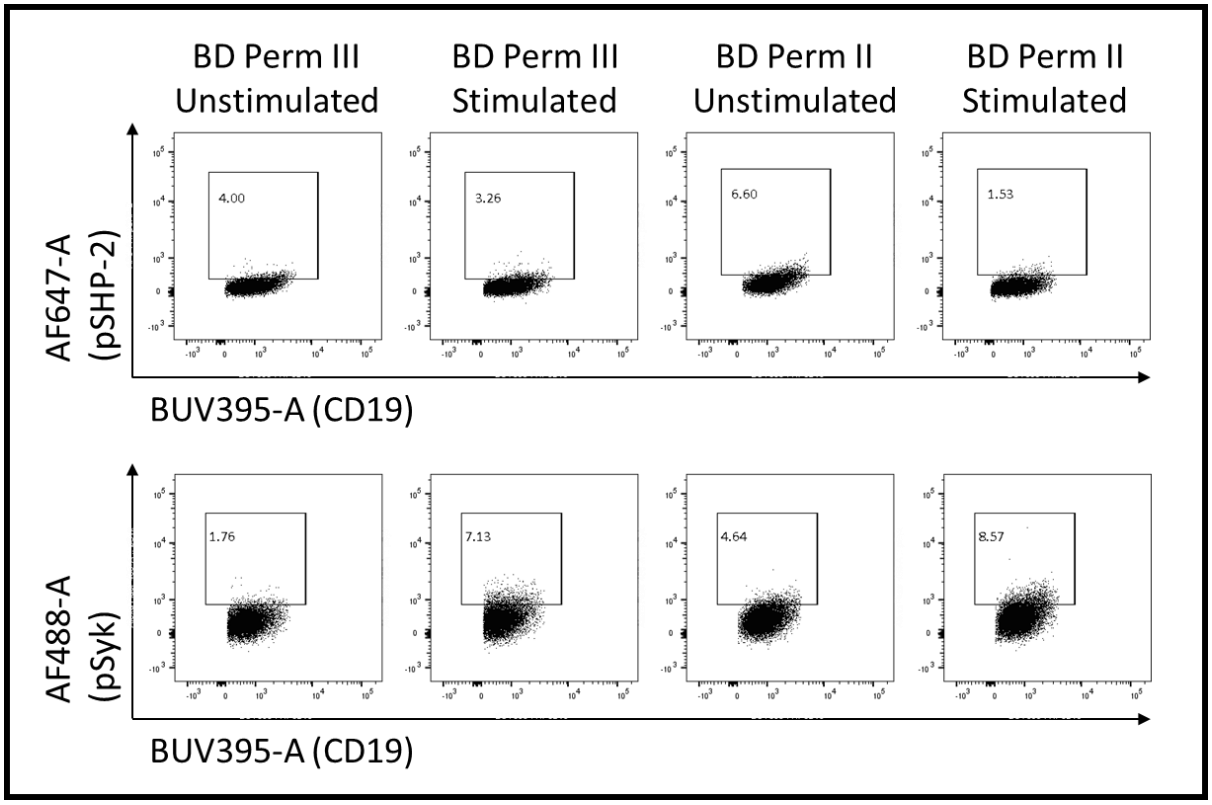

Figure 5.2.5.5III., Comparison of pSHP-2 and pSyk staining in ex-vivo CD19+ tonsil cells permeabilised with BD Perm III and Perm II*. (n = 1) Representative FACS plots demonstrating the changes in phosphorylation when ex-vivo tonsil cells were permeabilised with BD perm III and BD Perm II. Ex-vivo tonsil cells were stimulated with 10µg/ml IgG + IgM f(ab')$_2$ fragment and fixed with BD CytoFix at, 4mins (pSyk) and 5mins (pSHP-2). Cells were stained with CD3 and CD19 to define a CD3-CD19+ population, permeabilised and stained for pSHP-2 and pSyk. The number in the gate represents the percentage of CD19+ cells where phosphorylation events could be detected in stimulated samples.*

5.2.6 Signalling

For each signalling molecule, the differences between the FcRL4- and FcRL4+ cells were compared for each condition. For tonsils and SF, phosphorylation differences in CD3+ T cells were also used as a negative control (data not shown). The averages for each MFI were compared to each other but due to their being little to no significance for each signalling molecule these were not investigate further and can be found in the supplementary data. Next, to observe if there were changes in phosphorylation of signalling molecules, the baseline was determined on unstimulated cells and cells with a signal above baseline were quantified. This gating strategy was applied to each of the stimulation conditions to observe potential changes in the FcRL4- and FcRL4+ populations. Again, the gating strategy for FcRL4- and FcRL4+ B cells (defined as CD3-CD19+) in tonsils and RA SF can be seen in the supplementary data (Figure 8.6 & 7). Since the transduced priess cells are an immortalised EBV-transformed lymphoblastoid B cell line, there was no need to use a T cell exclusion marker or stain for B cells so the gating strategy used was gating on the FcRL4- and FcRL4+ cells only (Figure 8.5).

To determine the efficacy of stimulation with the IgG + IgM f(ab')$_2$ fragment and HA colostrum IgA IC, the changes in percentage of + cells for the BCR and IgA condition were compared to the unstimulated condition for both the FcRL4- and FcRL4+. To see if there was any difference in the magnitude of phosphorylation between the two groups, the unstimulated, BCR and IgA conditions were statistically interrogated against each other. To determine the effect of IgA stimulation on BCR signalling, the BCR IgA together (BCRIgA$_t$), BCR IgA separate (BCRIgA$_s$) and BCR IgA crosslinked (BCRIgA$_c$) were compared to the BCR

condition individually in the FcRL4- and FcRL4+ cells as well as the conditions being compared to one another between the FcRL4- and FcRL4+ cells.

Upon completion of analysis, pAkt, pBtk/Itk, pp65-NF-κB and pSHP-2 were not included in the final results due to either lack of responsiveness to stimulation or there being too much variation in the data between sample types making it difficult to determine the effect of IgA stimulation of FcRL4 on these signalling molecules.

5.2.6.1 pFgr

The percentage of pFgr+ cells were compared in the unstimulated, BCR and IgA between the FcRL4- and FcRL4+ transduced priess (n = 5), *ex-vivo* tonsil (n = 5) and *ex-vivo* RA SF (n = 4) cells. The percentage of pFgr+ cells was generally higher in FcRL4+ transduced priess and RA SF cells compared to the FcRL4- population but this did not reach significance (Figure 5.2.6.1I). In tonsils, the percentage of pFgr + was significantly higher in FcRL4+ cells compared to FcRL4- cells in the unstimulated and BCR conditions (unstimulated p = 0.0213, BCR p = 0.0052) (Figure 5.2.6.1I). In FcRL4- cells, was little change in the percentage of pFgr+ cells in the BCR condition when compared to the unstimulated and IgA conditions for the transduced priess, tonsil and RA SF samples (Figure 5.2.6.1II). A similar trend was seen in the FcRL4+ population of the transduced priess cells but in the tonsil and RA SF samples there was an increase in the percentage pFgr+ cells in the BCR condition compared to the unstimulated, although this didn't reach significance (Figure 5.2.6.1II).

The percentage of pFgr+ cells were compared in the BCRIgA$_t$, BCRIgA$_s$ and BCRIgA$_c$ conditions within the FcRL4- and FcRL4+ populations. There was no significant difference between the FcRL4- or FcRL4+ cells for the BCRIgA$_t$, BCRIgA$_s$ and BCRIgA$_c$ conditions in transduced priess cells and RA SF samples (Figure 5.2.6.1III). Comparatively in tonsil cells, the percentage of pFgr+ cells were generally higher in FcRL4+ cells across all conditions compared to FcRL4- cells and the difference in the BCRIgA$_s$ condition was significant (BCRIgA$_s$ p = 0.0299) (Figure 5.2.6.1III). When compared to the BCR, there was an increase in percentage of pFgr+ cells in the FcRL4- and FcRL4+ cells for the BCRIgA$_t$, BCRIgA$_s$ and BCRIgA$_c$ conditions in the transduced priess cells and RA SF sample (Figure 5.2.6.1IV). However, these differences were not significant. In tonsil there wasn't an increase in the percentage of pFgr+ for the FcRL4-

and FcRL4+ cells for the BCRIgA$_t$, BCRIgA$_s$ and BCRIgA$_c$ compared to the BCR (Figure 5.2.6.1IV).

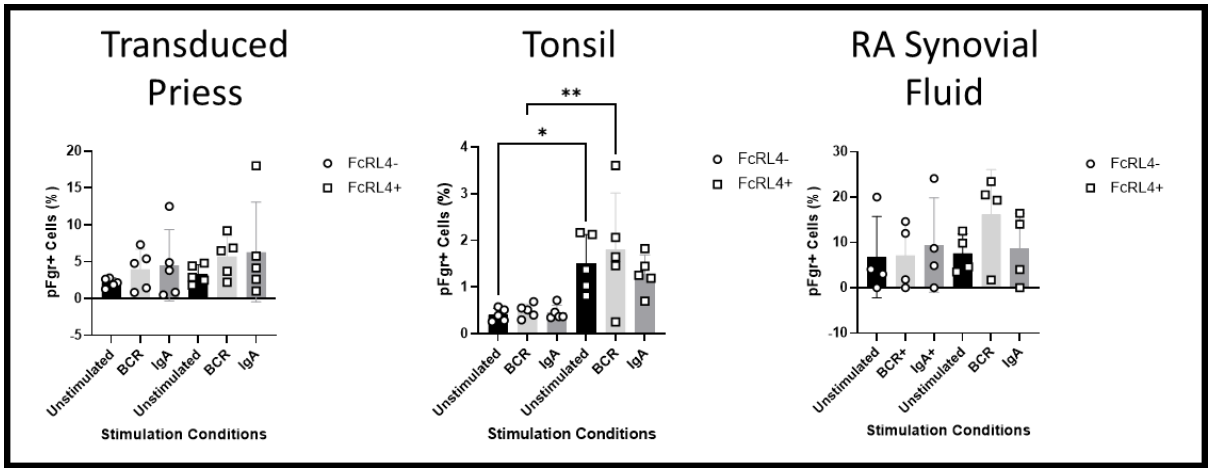

Figure 5.2.6.1I., pFgr is higher in FcRL4+ transduced priess, ex-vivo tonsil and RA SF cells compared to FcRL4-. *Transduced priess cells (n = 5), ex-vivo tonsil cells (n = 5), ex-vivo RA SF cells (n = 4) were either unstimulated, stimulated with 10µg/ml IgG + IgM f(ab')$_2$ fragment or with 50µg/ml HA colostrum IgA IC for 2mins. Cells were gated on the lymphocyte, singlet, CD3-, CD19+ and FcRL4+ population. FcRL4- cells were also gated to compare the difference of pFgr in FcRL4+ cells in response to stimulation with either 10µg/ml IgG + IgM f(ab')2 fragment and 50µg/ml HA colostrum IgA IC. The unstimulated sample was used to set the pFgr+ gate to determine the change in the percentage of pFgr+ cells between each stimulation condition. The means of unstimulated, BCR and IgA condition were compared to each other between the FcRL4- & FcRL4 populations in transduced priess, ex-vivo tonsil cells and ex-vivo RA SF cells. Statistical Test - –Šidák's multiple comparison corrected one-way ANOVA.*

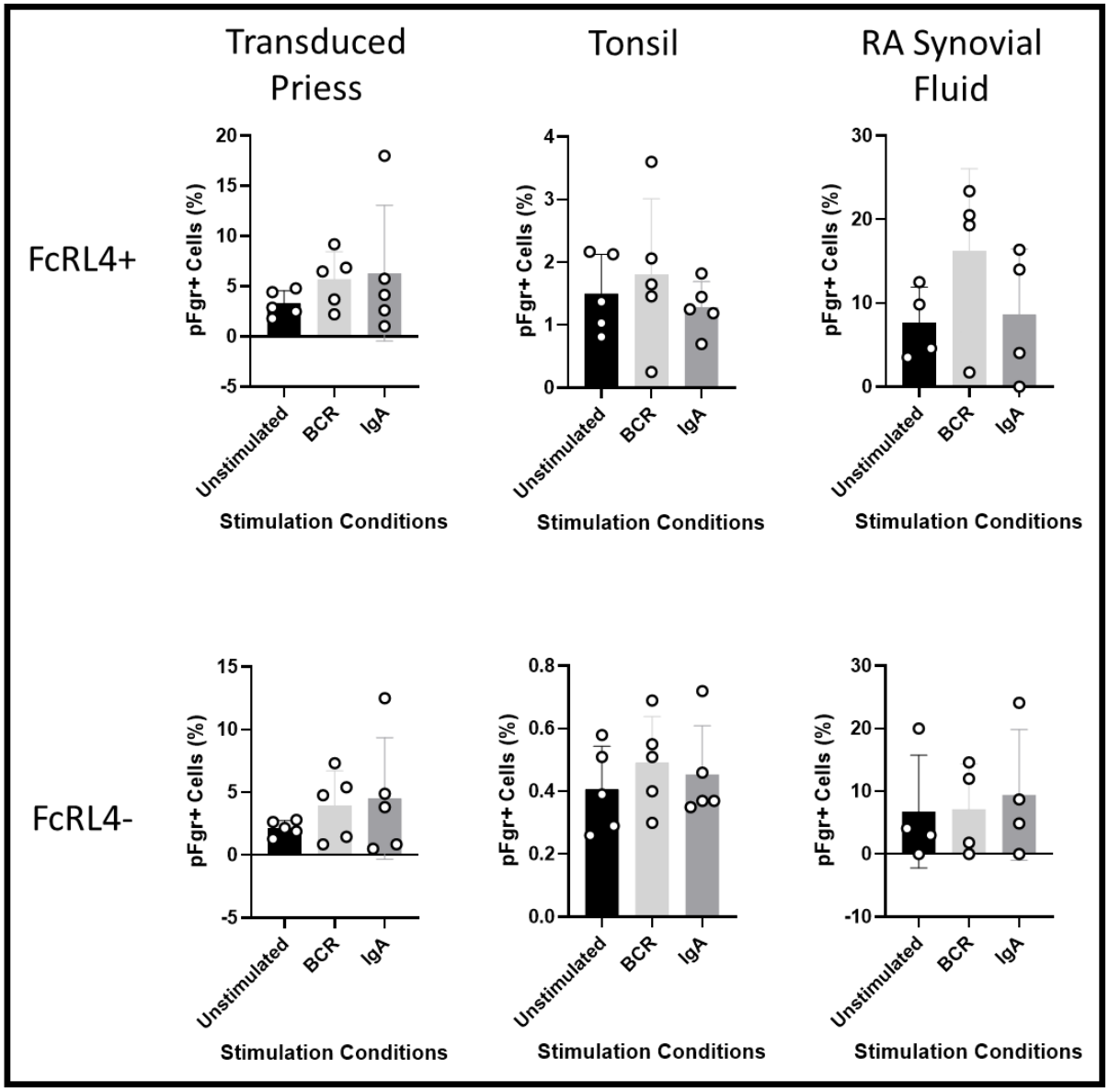

Figure 5.2.6.2II., pFgr does not change in response to BCR stimulation alone and IgA stimulation alone compared to the unstimulated condition*. Transduced priess cells (n = 5), Tonsil B cells (n = 5), RA SF B cells (n = 4) were either unstimulated, stimulated with 10µg/ml IgG + IgM f(ab')$_2$ fragment or with 50µg/ml HA colostrum IgA IC for 2mins. Cells were gated on the lymphocyte, singlet, CD3-, CD19+ and FcRL4+ population. FcRL4- cells were also gated to compare the difference of pFgr in FcRL4+ cells in response to stimulation with either 10µg/ml IgG + IgM f(ab')$_2$ fragment and 50µg/ml HA colostrum IgA IC. The unstimulated sample was used to set the pFgr+ gate to determine the change in the percentage of pFgr+ cells between each stimulation condition. This is the same data as Figure 5,2,6,1I but the means of the BCR and IgA condition were compared to the mean of the unstimulated condition within the FcRL4- and FcRL4+ population. The mean of the BCR and IgA condition were also compared to each other within the FcRL4- and FcRL4+ populations. Statistical test – Tukey's multiple comparison corrected RM one-way ANOVA.*

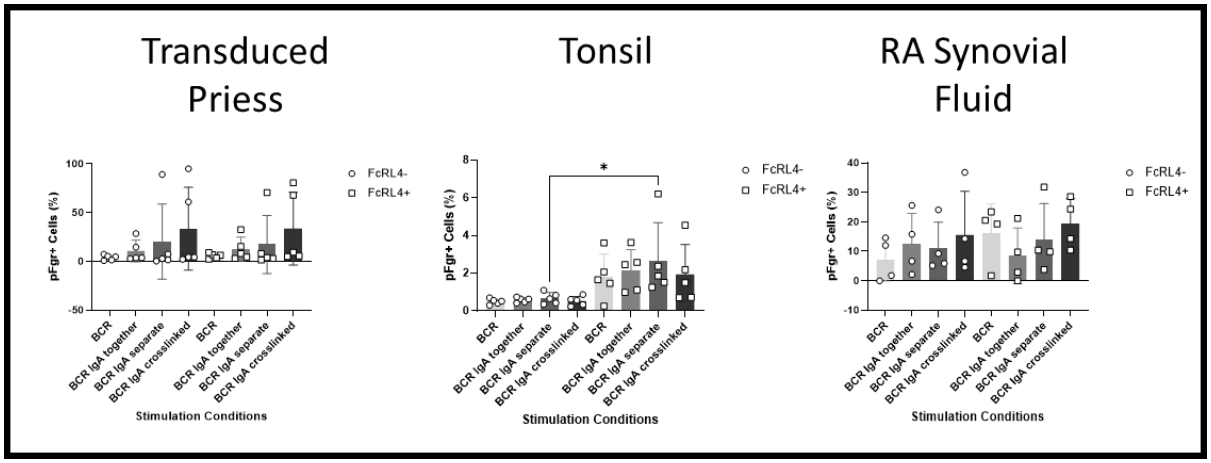

Figure 5.2.6.1III., pFgr is higher in FcRL4+ ex-vivo tonsil cells compared to FcRL4-. *Transduced priess cells (n = 5), ex-vivo tonsil cells (n = 5), ex-vivo RA SF cells (n = 4) were:* ***BCR stimulated*** *with 10µg/ml anti-IgG + IgM f(ab')$_2$ fragment for 2mins,* ***stimulated together (BCRIgA$_t$)*** *with 10µg/ml anti-IgG + IgM f(ab')$_2$ fragment and 50µg/ml HA colostrum IgA IC for 2mins,* ***stimulated separately (BCRIgA$_s$)*** *where cells were stimulated with 50µg/ml HA colostrum IgA IC for 30mins and 10µg/ml anti-IgG + IgM f(ab')$_2$ fragment for 2mins or* ***crosslinked (BCRIgA$_c$)*** *where 10µg/ml biotinylated anti-IgG + IgM f(ab')$_2$ fragment and 50µg/ml biotinylated HA colostrum IgA IC were crosslinked with 1µg/ml streptavidin for 30mins and then added to cells to stimulate for 2mins. Cells were gated on the lymphocyte, singlet, CD3-, CD19+ and FcRL4+ population. FcRL4- cells were also gated to compare the difference of pFgr in FcRL4+ cells in response to stimulation. The unstimulated sample was used to set the pFgr+ gate to determine the change in the percentage of pFgr+ cells between each stimulation condition. The means of the BCR, BCRIgA$_t$, BCRIgA$_s$ and BCRIgA$_c$ conditions were compared to each other between the FcRL4- & FcRL4 populations in transduced priess, ex-vivo tonsil cells and ex-vivo RA SF cells. Statistical Test - –Šidák's multiple comparison corrected one-way ANOVA.*

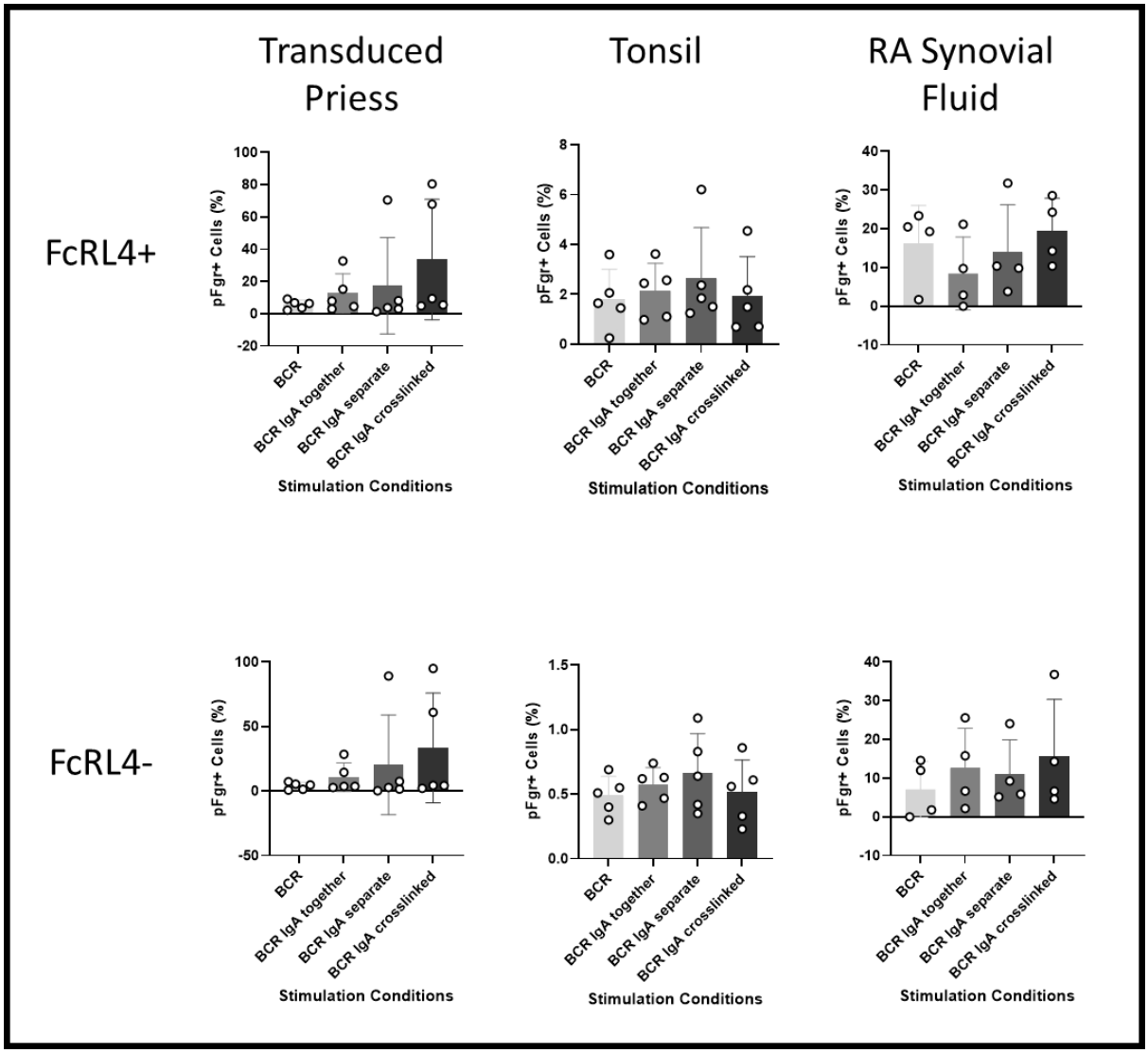

Figure 5.2.6.2IV., pFgr increases in response to BCR and IgA crosslinking compared to BCR stimulation alone in transduced priess cells and ex-vivo RA SF. *Transduced priess cells (n = 5), Tonsil B cells (n = 5), RA SF B cells (n = 4) were* ***stimulated with*** *10µg/ml anti-IgG + IgM f(ab')$_2$ fragment for 2mins****,*** ***stimulated together (BCRIgA$_t$)*** *with 10µg/ml anti-IgG + IgM f(ab')$_2$ fragment and 50µg/ml HA colostrum IgA IC for 2mins,* ***stimulated separately (BCRIgA$_s$)*** *where cells were stimulated with 50µg/ml HA colostrum IgA IC for 30mins and 10µg/ml anti-IgG + IgM f(ab')$_2$ fragment for 2mins or* ***crosslinked (BCRIgA$_c$)*** *where 10µg/ml biotinylated anti-IgG + IgM f(ab')$_2$ fragment and 50µg/ml biotinylated HA colostrum IgA IC were crosslinked with 1µg/ml streptavidin for 30mins and then added to cells to stimulate for 2mins. Cells were gated on the lymphocyte, singlet, CD3-, CD19+ and FcRL4+ population. FcRL4- cells were also gated to compare the difference of pFgr in FcRL4+ cells in response to stimulation. The unstimulated sample was used to set the pFgr+ gate to determine the change in the percentage of pFgr+ cells between each stimulation condition. This is the same data as Figure 5.2.6.1III but the means of each condition were compared to BCR condition within the FcRL4- and FcRL4+ populations. Statistical test – Dunnett's multiple comparison corrected RM one-way ANOVA.*

5.2.6.2 pHck

The percentage of pHck+ cells were compared in the unstimulated, BCR and IgA between the FcRL4- and FcRL4+ transduced priess (n = 5), *ex-vivo* tonsil (n = 5) and *ex-vivo* RA SF (n = 4) cells. The percentage of pHck+ cells were higher in the FcRL4+ transduced priess, tonsil and RA SF samples (Figure 5.2.6.2I). The difference between the IgA conditions for FcRL4- and FcRL4+ tonsil cells was significant (IgA p = 0.0027) (Figure 5.2.6.2I). In the FcRL4- population, the percentage of pHck+ cells increased in the BCR conditions compared to the unstimulated and IgA condition in the transduced priess cells, tonsil and RA SF samples (Figure 5.2.6.2II). Conversely, in the FcRL4+ population, the percentage of pHck+ increased in the BCR and IgA conditions compared to the unstimulated in the transduced priess cells, tonsil and RA SF samples (Figure 5.2.6.2II). However, this did not reach significance.

The percentage of pHck+ cells were compared in the $BCRIgA_t$, $BCRIgA_s$ and $BCRIgA_c$ conditions between the FcRL4- and FcRL4+ cells. The percentage of pHck+ cells were comparable between the $BCRIgA_t$, $BCRIgA_s$ and $BCRIgA_c$ conditions in the transduced priess cells and RA SF samples (Figure 5.2.6.4III). In tonsil samples, the percentage of pHck+ cells were

higher in the FcRL4+ cells compared to the FcRL4- cells in the $BCRIgA_t$, $BCRIgA_s$ and $BCRIgA_c$ condition. The difference between the $BCRIgA_c$ conditions reached significance ($BCRIgA_c$ p = 0.0303) (Figure 5.2.6.2III). When compared to the BCR, there was an increase in percentage of pHck+ in $BCRIgA_t$, $BCRIgA_s$ and $BCRIgA_c$ conditions for FcRL4+ and FcRL4- populations in the transduced priess cells, tonsil and RA SF samples (Figure 5.2.6.2IV). However, this did not reach significance.

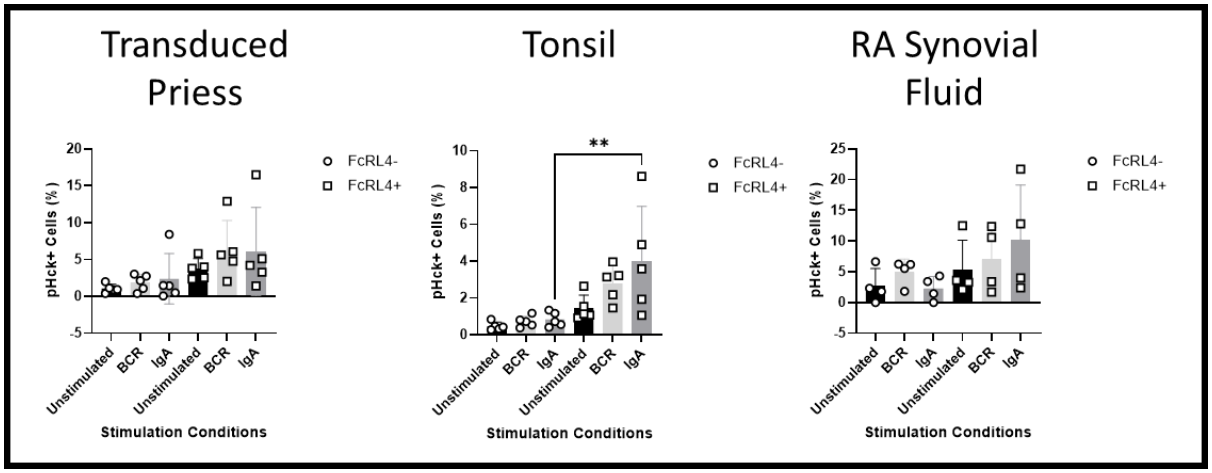

Figure 5.2.6.2I., pHck significantly increases in response to IgA stimulation alone compared to the unstimulated condition in FcRL4+ ex-vivo tonsil cells. *Transduced priess cells (n = 5), ex-vivo tonsil cells (n = 5), ex-vivo RA SF cells (n = 4) were either unstimulated, stimulated with 10µg/ml IgG + IgM f(ab')$_2$ fragment or with 50µg/ml HA colostrum IgA IC for 2mins. Cells were gated on the lymphocyte, singlet, CD3-, CD19+ and FcRL4+ population. FcRL4- cells were also gated to compare the difference of pHck in FcRL4+ cells in response to stimulation with either 10µg/ml IgG + IgM f(ab')$_2$ fragment and 50µg/ml HA colostrum IgA IC. The unstimulated sample was used to set the pHck+ gate to determine the change in the percentage of pHck+ cells between each stimulation condition. The means of unstimulated, BCR and IgA condition were compared to each other between the FcRL4- & FcRL4 populations in transduced priess, ex-vivo tonsil cells and ex-vivo RA SF cells. Statistical Test - –Šidák's multiple comparison corrected one-way ANOVA.*

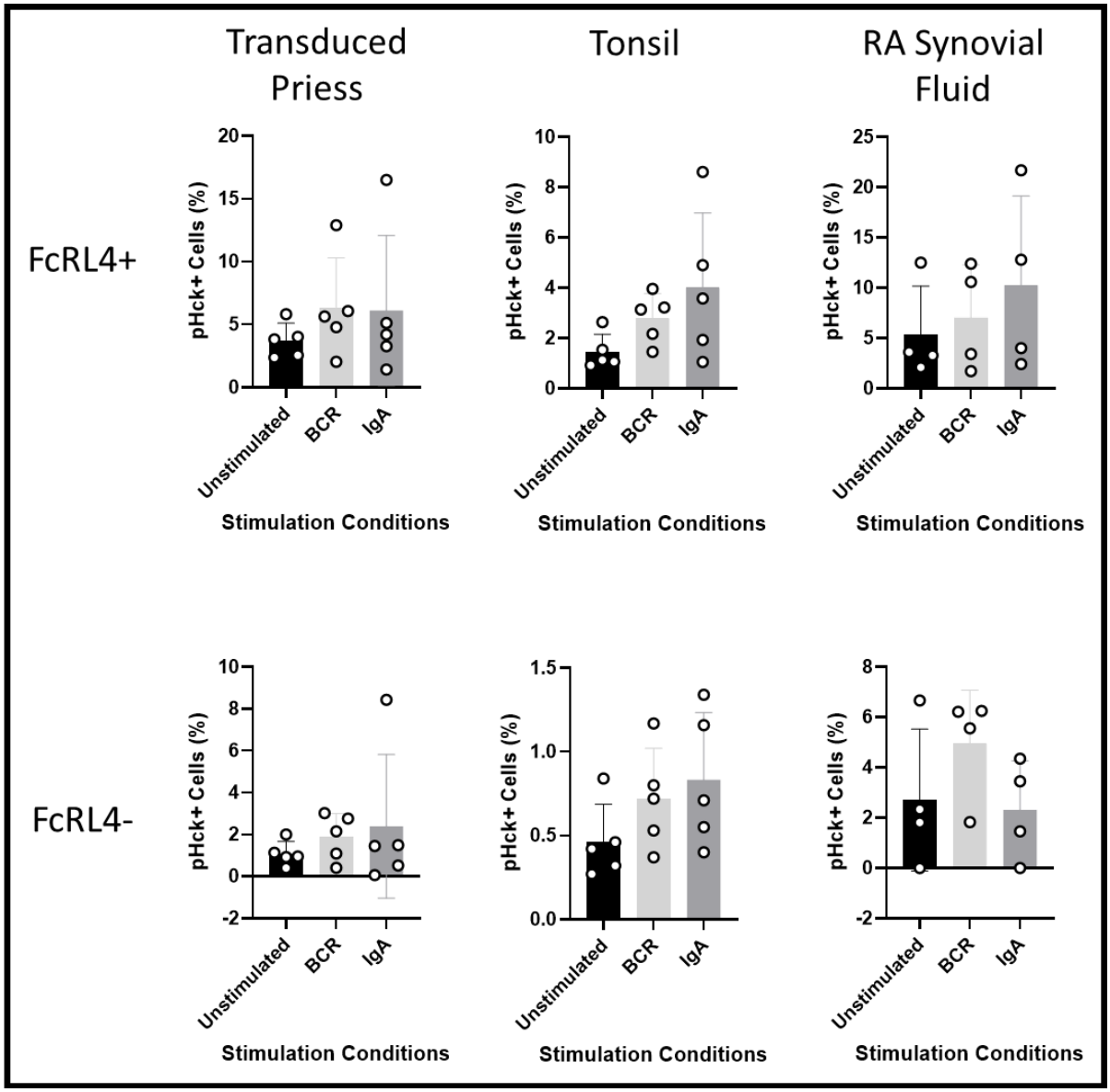

Figure 5.2.6.2II., pHck increases in response to stimulation with HA colostrum IgA alone in FcRL4+ ex-vivo tonsil and RA SF cells. *Transduced priess cells (n = 5), Tonsil B cells (n = 5), RA SF B cells (n = 4) were either unstimulated, stimulated with 10µg/ml IgG + IgM f(ab')$_2$ fragment or with 50µg/ml HA colostrum IgA IC for 2mins. Cells were gated on the lymphocyte, singlet, CD3-, CD19+ and FcRL4+ population. FcRL4- cells were also gated to compare the difference of pHck in FcRL4+ cells in response to stimulation with either 10µg/ml IgG + IgM f(ab')$_2$ fragment and 50µg/ml HA colostrum IgA IC. The unstimulated sample was used to set the pHck+ gate to determine the change in the percentage of pHck+ cells between each stimulation condition. This is the same data as Figure 5.2.6.2I but the means of the BCR and IgA condition were compared to the mean of the unstimulated condition within the FcRL4- and FcRL4+ population. The mean of the BCR and IgA condition were also compared to each other within the FcRL4- and FcRL4+ populations. Statistical test – Tukey's multiple comparison corrected RM one-way ANOVA.*

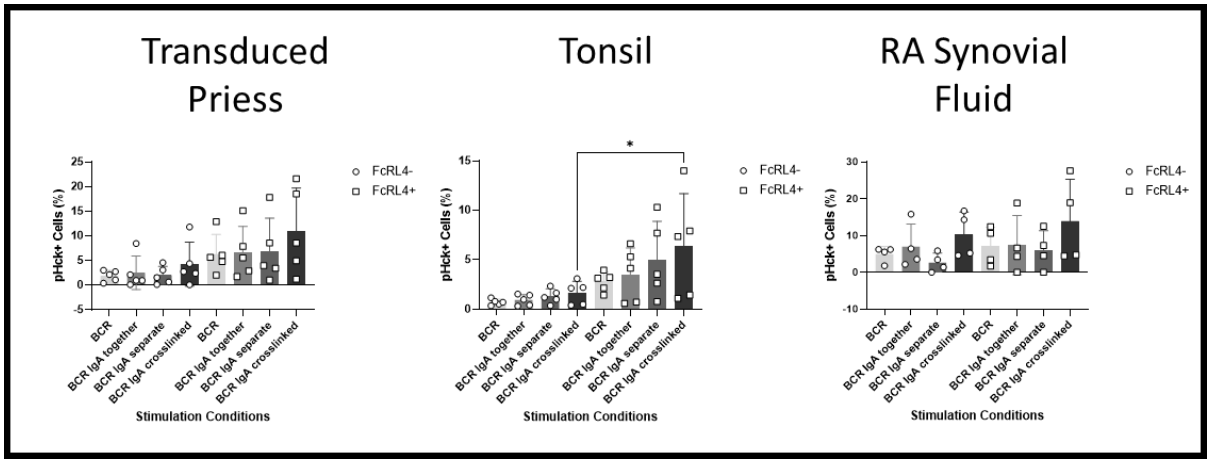

Figure 5.2.6.2III., pHck is higher in FcRL4+ transduced priess, ex-vivo tonsil and RA SF cells when in the BCRIgA$_c$ condition compared to FcRL4-. *Transduced priess cells (n = 5), ex-vivo tonsil cells (n = 5), ex-vivo RA SF cells (n = 4) were:* ***stimulated together (BCRIgA$_t$)*** *with 10µg/ml anti-IgG + IgM f(ab')$_2$ fragment and 50µg/ml HA colostrum IgA IC for 2mins,* ***stimulated separately (BCRIgA$_s$)*** *where cells were stimulated with 50µg/ml HA colostrum IgA IC for 30mins and 10µg/ml anti-IgG + IgM f(ab')$_2$ fragment for 2mins or* ***crosslinked (BCRIgA$_c$)*** *where 10µg/ml biotinylated anti-IgG + IgM f(ab')$_2$ fragment and 50µg/ml biotinylated HA colostrum IgA IC were crosslinked with 1µg/ml streptavidin for 30mins and then added to cells to stimulate for 2mins. Cells were gated on the lymphocyte, singlet, CD3-, CD19+ and FcRL4+ population. FcRL4- cells were also gated to compare the difference of pHck in FcRL4+ cells in response to stimulation. The unstimulated sample was used to set the pHck+ gate to determine the change in the percentage of pHck+ cells between each stimulation condition. The means of the BCR, BCRIgA$_t$, BCRIgA$_s$ and BCRIgA$_c$ conditions were compared to each other between the FcRL4- & FcRL4 populations in transduced priess, ex-vivo tonsil cells and ex-vivo RA SF cells. Statistical Test - –Šidák's multiple comparison corrected one-way ANOVA.*

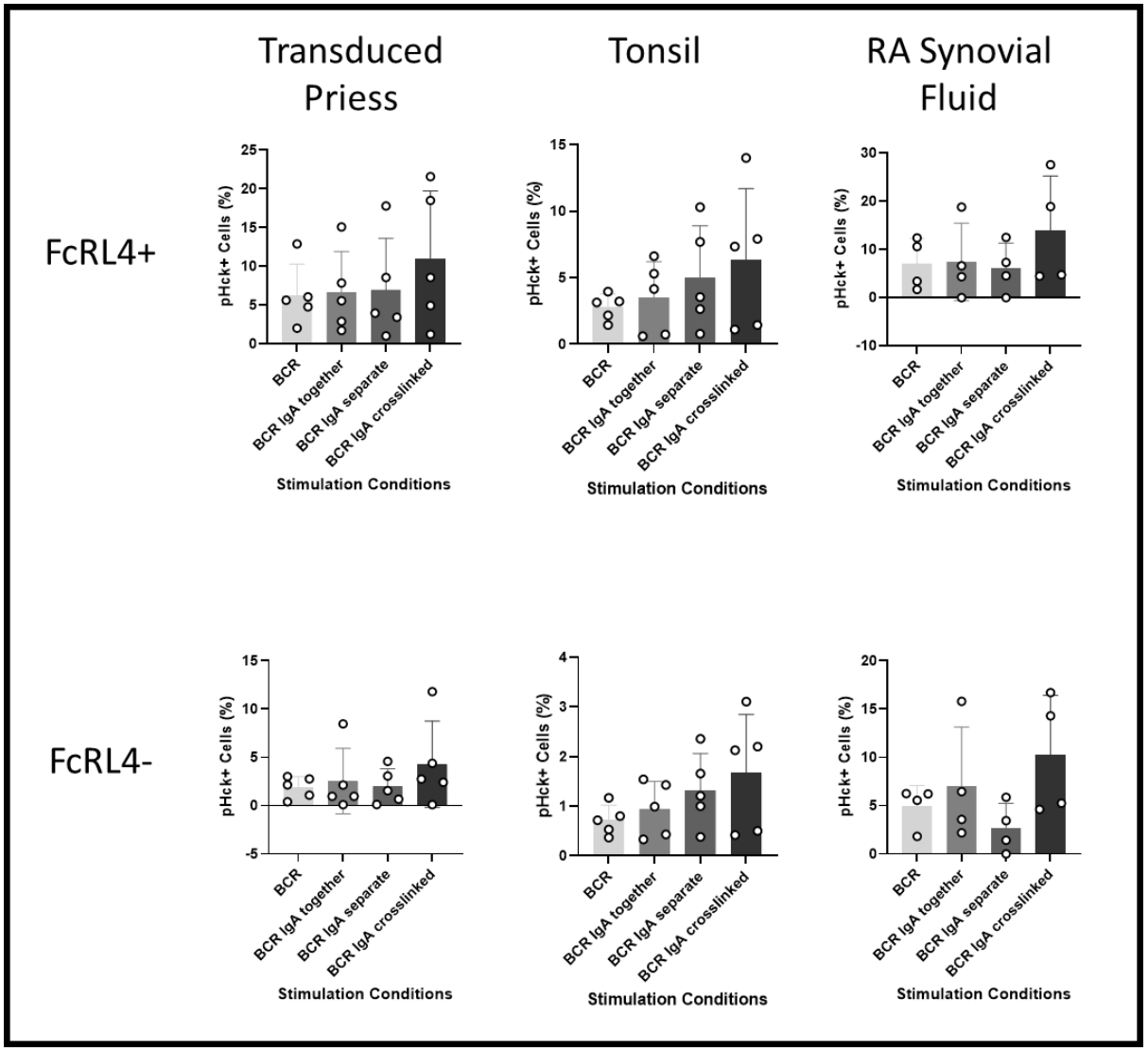

Figure 5.2.6.2IV., pHck increases in response to BCR and IgA crosslinking compared to BCR stimulation alone in FcRL4+ and FcRL4- transduced priess, ex-vivo tonsil and RA SF cells. *Transduced priess cells (n = 5), Tonsil B cells (n = 5), RA SF B cells (n = 4) were* ***stimulated with*** *10µg/ml anti-IgG + IgM f(ab')$_2$ fragment for 2mins****, stimulated together (BCRIgA$_t$)*** *with 10µg/ml anti-IgG + IgM f(ab')$_2$ fragment and 50µg/ml HA colostrum IgA IC for 2mins,* ***stimulated separately (BCRIgA$_s$)*** *where cells were stimulated with 50µg/ml HA colostrum IgA IC for 30mins and 10µg/ml anti-IgG + IgM f(ab')$_2$ fragment for 2mins or* ***crosslinked (BCRIgA$_c$)*** *where 10µg/ml biotinylated anti-IgG + IgM f(ab')$_2$ fragment and 50µg/ml biotinylated HA colostrum IgA IC were crosslinked with 1µg/ml streptavidin for 30mins and then added to cells to stimulate for 2mins. Cells were gated on the lymphocyte, singlet, CD3-, CD19+ and FcRL4+ population. FcRL4- cells were also gated to compare the difference of pHck in FcRL4+ cells in response to stimulation. The unstimulated sample was used to set the pHck+ gate to determine the change in the percentage of pHck+ cells between each stimulation condition. This is the same data as Figure 5.2.6.2III but the means of each condition were compared to BCR condition within the FcRL4- and FcRL4+ populations. Statistical test – Dunnett's multiple comparison corrected RM one-way ANOVA.*

5.2.6.3 pSHP-1

The percentage of pSHP-1+ cells were compared in the unstimulated, BCR and IgA between the FcRL4- and FcRL4+ transduced priess (n = 5), *ex-vivo* tonsil (n = 5) and *ex-vivo* RA SF cells (n = 4). There was a significantly higher percentage of pSHP-1+ cells in the FcRL4+ population compared to FCRL4- population in the transduced priess cell sample (unstimulated, BCR and IgA conditions p = <0.0001) (Figure 5.2.6.3I). Similarly in the tonsil and RA SF samples, there was a greater percentage of pSHP-1+ cells in the unstimulated, BCR and IgA conditions of the FcRL4+ cells compared to the FcRL4- but these did not reach significance (Figure 5.2.6.3I). The percentage of pSHP-1+ cells increased in the BCR condition compared to the unstimulated condition for both the FcRL4- and FcRL4+ population in the transduced priess cells, tonsil and RA SF samples (Figure 5.2.6.3II). In the transduced priess cells and RA SF samples, the percentage of pSHP-1+ was similar between the BCR and IgA conditions for both FcRL4+ cells and FcRL4- populations whilst there was a decrease in percentage of pSHP-1+ in the IgA condition in the tonsil samples (Figure 5.2.6.3II).

The percentage of pSHP-1+ cells in the BCRIgA$_t$, BCRIgA$_s$ and BCRIgA$_c$ conditions were compared between the FcRL4- and FcRL4+ cells. There was a significant difference between the FcRL4- and FcRL4+ cells for the BCRIgA$_t$, BCRIgA$_s$ and BCRIgA$_c$ conditions in the transduced priess cell samples (all p = <0.0001) (Figure 5.2.6.3III). Generally, the percentage of SHP-1+ was higher in FcRL4+ cells compared to FcRL4- cells in the tonsil and RA SF samples but this did not reached significance (Figure 5.2.6.3III). In the FcRL4- and FcRL4+ populations, there was little change in percentage of pSHP-1+ cells in the BCRIgA$_t$, BCRIgA$_s$ and BCRIgA$_c$ conditions compared to the BCR condition in the transduced priess, tonsil and RA SF samples (Figure 5.2.6.3IV).

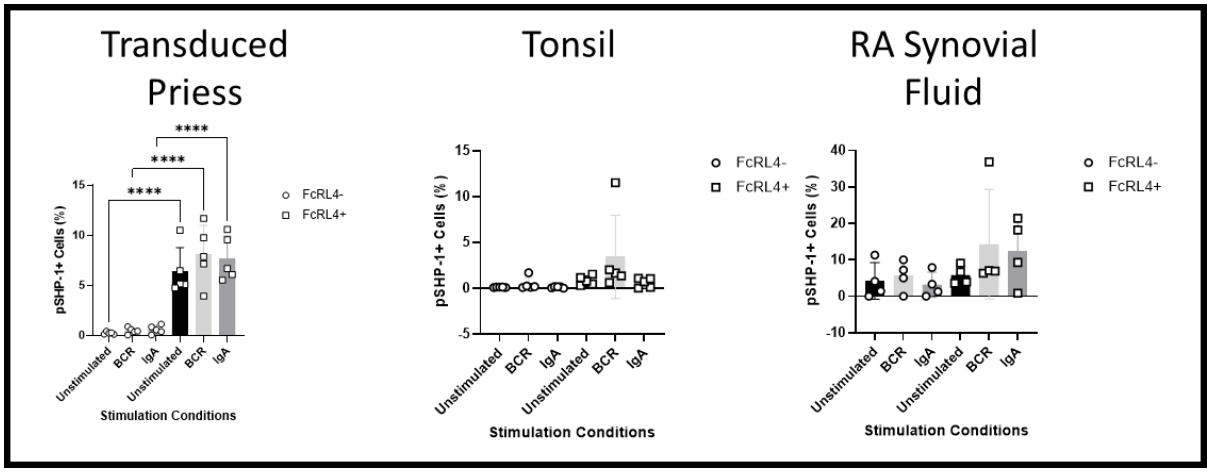

Figure 5.2.6.3I., pSHP-1 significantly higher in the unstimulated, BCR and IgA conditions in FcRL4+ transduced priess compared to the FcRL4- transduced priess. *Transduced priess cells (n = 5), ex-vivo tonsil cells (n = 5), ex-vivo RA SF cells (n = 4) were either unstimulated, stimulated with 10µg/ml IgG + IgM f(ab')$_2$ fragment or with 50µg/ml HA colostrum IgA IC for 5mins. Cells were gated on the lymphocyte, singlet, CD3-, CD19+ and FcRL4+ population. FcRL4- cells were also gated to compare the difference of pSHP-1 in FcRL4+ cells in response to stimulation with either 10µg/ml IgG + IgM f(ab')$_2$ fragment and 50µg/ml HA colostrum IgA IC. The unstimulated sample was used to set the pSHP-1+ gate to determine the change in the percentage of pSHP-1+ cells between each stimulation condition. The means of unstimulated, BCR and IgA condition were compared to each other between the FcRL4- & FcRL4 populations in transduced priess, ex-vivo tonsil cells and ex-vivo RA SF cells. Statistical Test - –Šidák's multiple comparison corrected one-way ANOVA.*

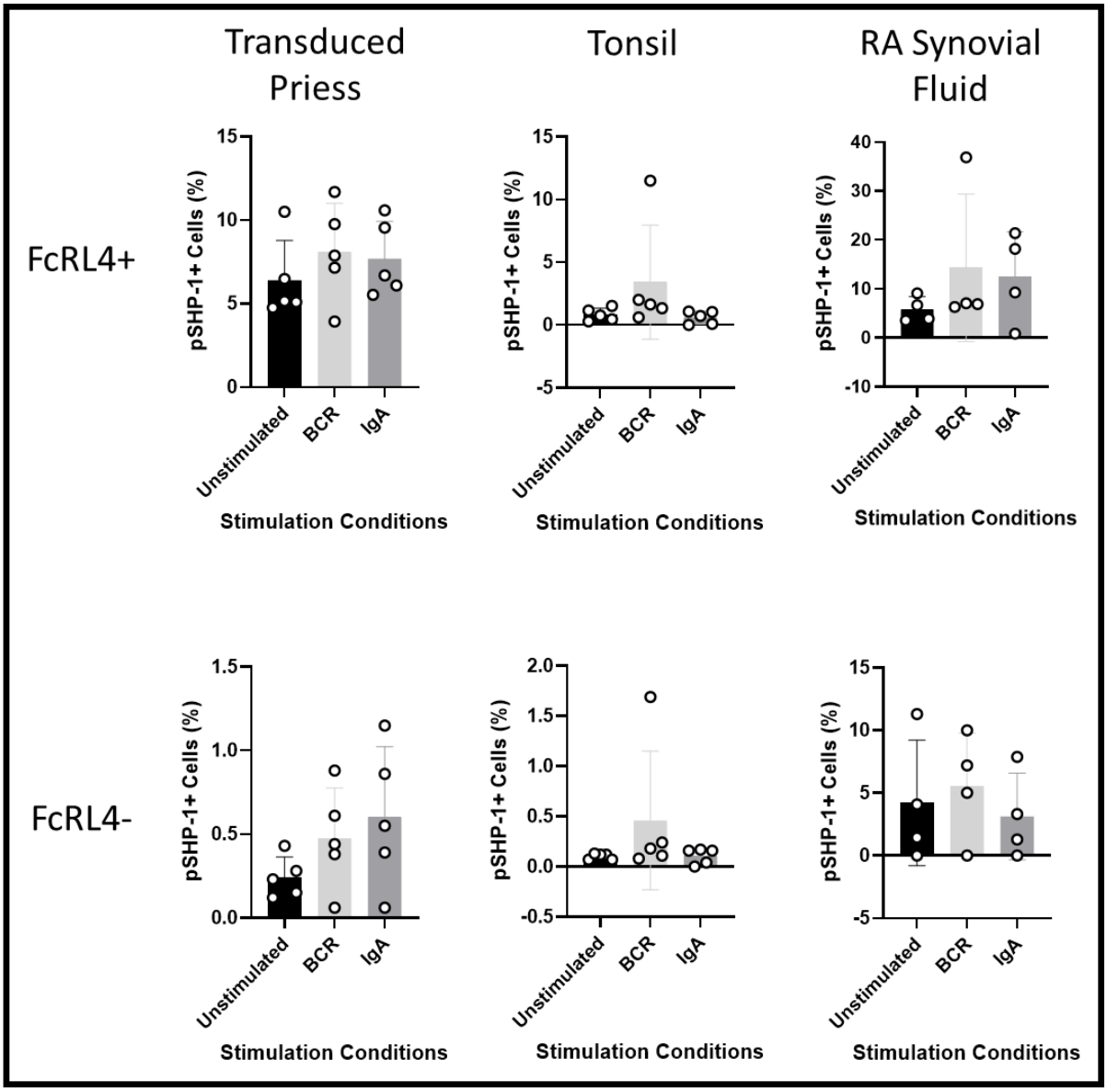

Figure 5.2.6.3II., pSHP-1 increases upon stimulation of the BCR in FcRL4+ and FcRL4- transduced priess, ex-vivo tonsil and RA SF cells. *Transduced priess cells (n = 5), Tonsil B cells (n = 5), RA SF B cells (n = 4) were either unstimulated, stimulated with 10µg/ml IgG + IgM f(ab')$_2$ fragment or with 50µg/ml HA colostrum IgA IC for 5mins. Cells were gated on the lymphocyte, singlet, CD3-, CD19+ and FcRL4+ population. FcRL4- cells were also gated to compare the difference of pSHP-1 in FcRL4+ cells in response to stimulation with either 10µg/ml IgG + IgM f(ab')$_2$ fragment and 50µg/ml HA colostrum IgA IC. The unstimulated sample was used to set the pSHP-1+ gate to determine the change in the percentage of pSHP-1+ cells between each stimulation condition. This is the same data as Figure 5.2.6.3I but the means of the BCR and IgA condition were compared to the mean of the unstimulated condition within the FcRL4- and FcRL4+ population. The mean of the BCR and IgA condition were also compared to each other within the FcRL4- and FcRL4+ populations. Statistical test – Tukey's multiple comparison corrected RM one-way ANOVA.*

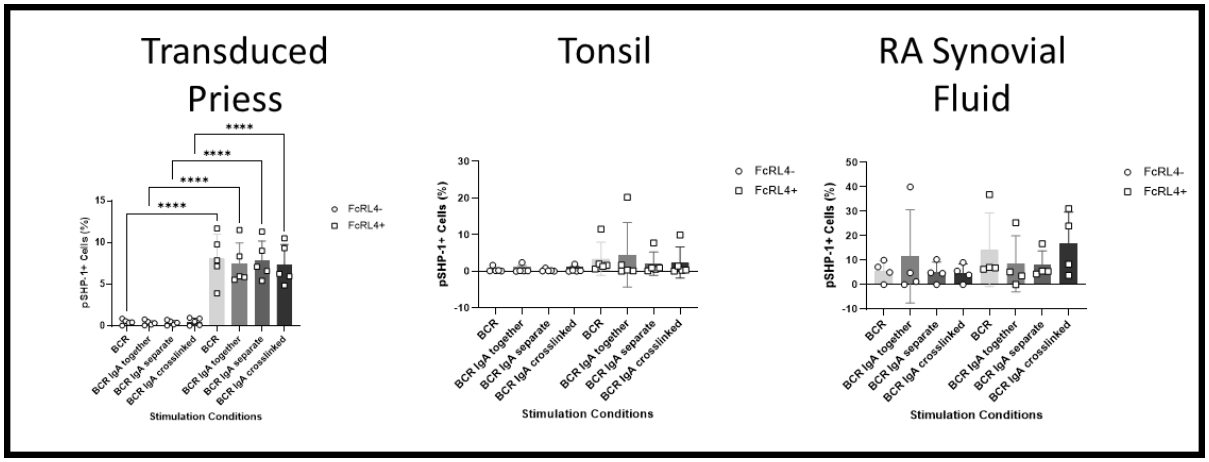

Figure 5.2.6.3III., pSHP-1 significantly higher in the BCR, BCRIgA$_t$, BCRIgA$_s$ and BCRIgA$_c$ and IgA in FcRL4+ transduced priess compared to the FcRL4- transduced priess. *Transduced priess cells (n = 5), ex-vivo tonsil cells (n = 5), ex-vivo RA SF cells (n = 4) were:* ***BCR stimulated*** *with 10µg/ml anti-IgG + IgM f(ab')$_2$ fragment for 5mins* ***stimulated together (BCRIgA$_t$)*** *with 10µg/ml anti-IgG + IgM f(ab')$_2$ fragment and 50µg/ml HA colostrum IgA IC for 5mins,* ***stimulated separately (BCRIgA$_s$)*** *where cells were stimulated with 50µg/ml HA colostrum IgA IC for 30mins and 10µg/ml anti-IgG + IgM f(ab')$_2$ fragment for 5mins or* ***crosslinked (BCRIgA$_c$)*** *where 10µg/ml biotinylated anti-IgG + IgM f(ab')$_2$ fragment and 50µg/ml biotinylated HA colostrum IgA IC were crosslinked with 1µg/ml streptavidin for 30mins and then added to cells to stimulate for 5mins. Cells were gated on the lymphocyte, singlet, CD3-, CD19+ and FcRL4+ population. FcRL4- cells were also gated to compare the difference of pSHP-1 in FcRL4+ cells in response to stimulation. The unstimulated sample was used to set the pSHP-1+ gate to determine the change in the percentage of pSHP-1+ cells between each stimulation condition. The means of the BCR, BCRIgA$_t$, BCRIgA$_s$ and BCRIgA$_c$ conditions were compared to each other between the FcRL4- & FcRL4 populations in transduced priess, ex-vivo tonsil cells and ex-vivo RA SF cells. Statistical Test - –Šidák's multiple comparison corrected one-way ANOVA.*

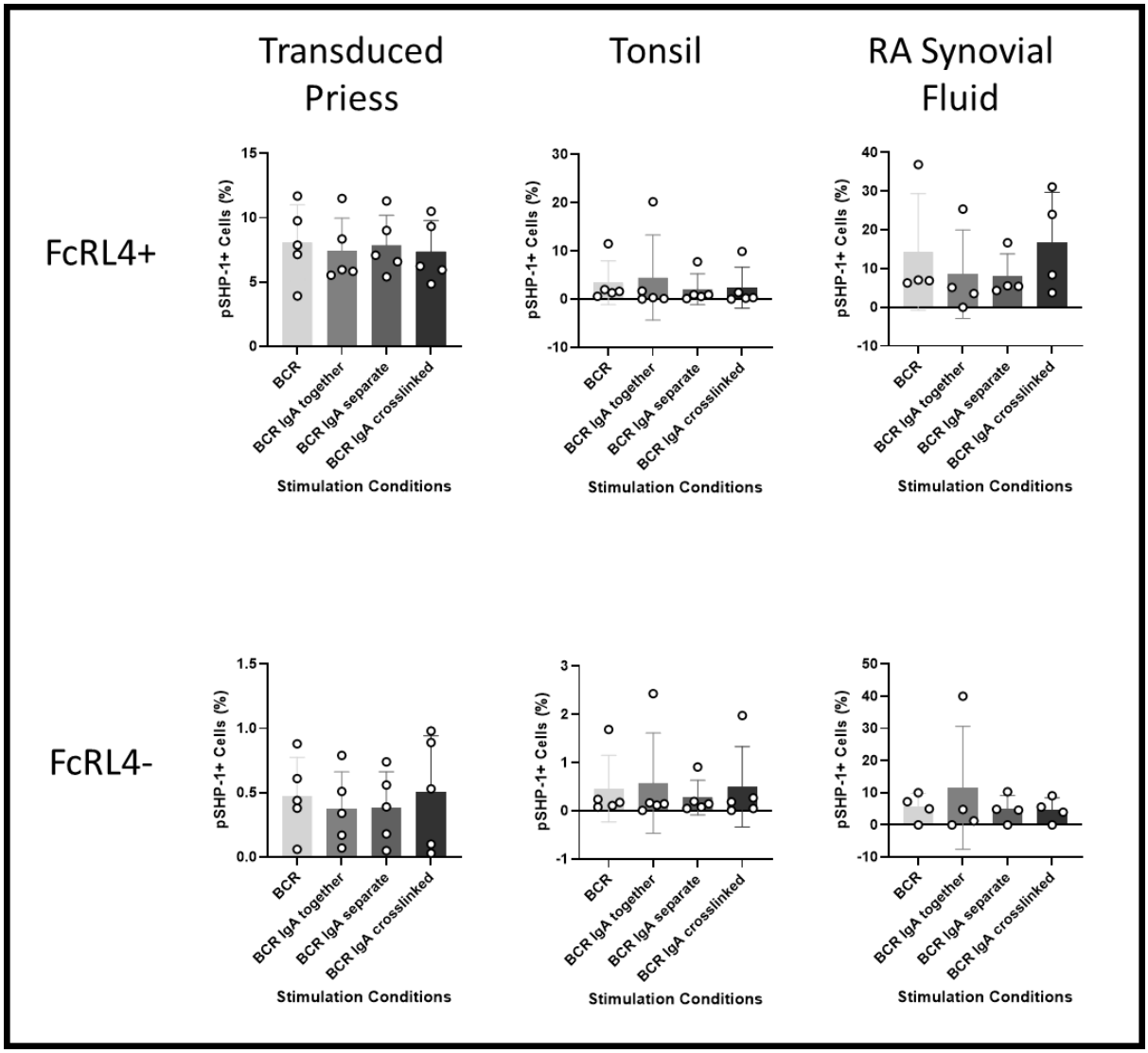

Figure 5.2.6.3IV., pSHP-1 doesn't change in the BCRIgA$_t$, BCRIgA$_s$ and BCRIgA$_c$ compared to the BCR condition in FcRl4+ and FcRL4- transduced priess, ex-vivo tonsil and RA SF cells. *Transduced priess cells (n = 5), Tonsil B cells (n = 5), RA SF B cells (n = 4) were **stimulated with** 10µg/ml anti-IgG + IgM f(ab')$_2$ fragment for 5mins**, stimulated together (BCRIgA$_t$)** with 10µg/ml anti-IgG + IgM f(ab')$_2$ fragment and 50µg/ml HA colostrum IgA IC for 5mins, **stimulated separately (BCRIgA$_s$)** where cells were stimulated with 50µg/ml HA colostrum IgA IC for 30mins and 10µg/ml anti-IgG + IgM f(ab')$_2$ fragment for 5mins or **crosslinked (BCRIgA$_c$)** where 10µg/ml biotinylated anti-IgG + IgM f(ab')$_2$ fragment and 50µg/ml biotinylated HA colostrum IgA IC were crosslinked with 1µg/ml streptavidin for 30mins and then added to cells to stimulate for 5mins. Cells were gated on the lymphocyte, singlet, CD3-, CD19+ and FcRL4+ population. FcRL4- cells were also gated to compare the difference of pSHP-1 in FcRL4+ cells in response to stimulation. The unstimulated sample was used to set the pSHP-1+ gate to determine the change in the percentage of pSHP-1+ cells between each stimulation condition. This is the same data as Figure 5.2.6.3III but the means of each condition were compared to BCR condition within the FcRL4- and FcRL4+ populations. Statistical test – Dunnett's multiple comparison corrected RM one-way ANOVA.*

5.2.6.4 pSyk

The percentage of pSyk+ cells were compared in the unstimulated, BCR and IgA between the FcRL4- and FcRL4+ transduced priess (n = 5), *ex-vivo* tonsil (n = 5) and *ex-vivo* RA SF (n = 4) cells. There was no significant difference in the percentage of pSyk+ cells in transduced priess cells or RA SF samples (Figure 5.2.6.4I). In the tonsil samples, the percentage of pSyk+ in the BCR condition was significantly higher in FcRL4+ cells compared to FCRL4- population (BCR p = 0.0055) (Figure 5.2.6.4I). The percentage of pSyk+ did not change in the BCR condition compared to the unstimulated and IgA conditions in transduced priess cell samples (Figure 5.2.6.4II). Comparatively in the tonsil and RA SF samples, there was an increase in the percentage of pSyk+ cells in the BCR condition compared to the unstimulated and IgA conditions for both FcRL4- and FcRL4+ population. The difference was significant in the FcRL4- and FcRL4+ populations of the tonsil sample (compared to unstimulated: FcRL4- p = 0.0231, FcRL4+ p = 0.0466), (compared to IgA FcRL4- p = 0.0165, FcRL4+ p = 0.0180) (Figure 5.2.6.4II).

The percentage of pSyk+ cells in BCRIgA$_t$, BCRIgA$_s$ and BCRIgA$_c$ conditions were compared between the FcRL4- and FcRL4+ population. There was no significant difference in the BCRIgA$_t$, BCRIgA$_s$ and BCRIgA$_c$ between the FcRL4- and FcRL4+ cells for the transduced priess cell, tonsil and RA SF samples (Figure 5.2.6.4III). There was no change in the percentage of pSyk+ in the BCRIgA$_t$, BCRIgA$_s$ and BCRIgA$_c$ conditions when compared to the BCR condition in FcRL4- and FcRL4+ populations in the transduced priess cell samples (Figure 5.2.6.4IV). In the tonsil and RA SF samples, the percentage of pSyk+ cells decreased in both the FcRL4- and FcRL4+ populations in the BCRIgA$_t$, BCRIgA$_s$ and BCRIgA$_c$ conditions when compared to the BCR condition (Figure 5.2.6.4IV). These differences were significantly different in the FcRL4-

and FcRL4+ populations in the tonsil sample (FcRL4- BCRIgA$_t$ p = 0.0168, BCRIgA$_s$ p = 0.0184, BCRIgA$_c$ p = 0.0203) (FcRL4+ BCRIgA$_t$ p = 0.0310, BCRIgA$_s$ p = 0.0012, BCRIgA$_c$ p = 0.0314) (Figure 5.2.6.4IV).

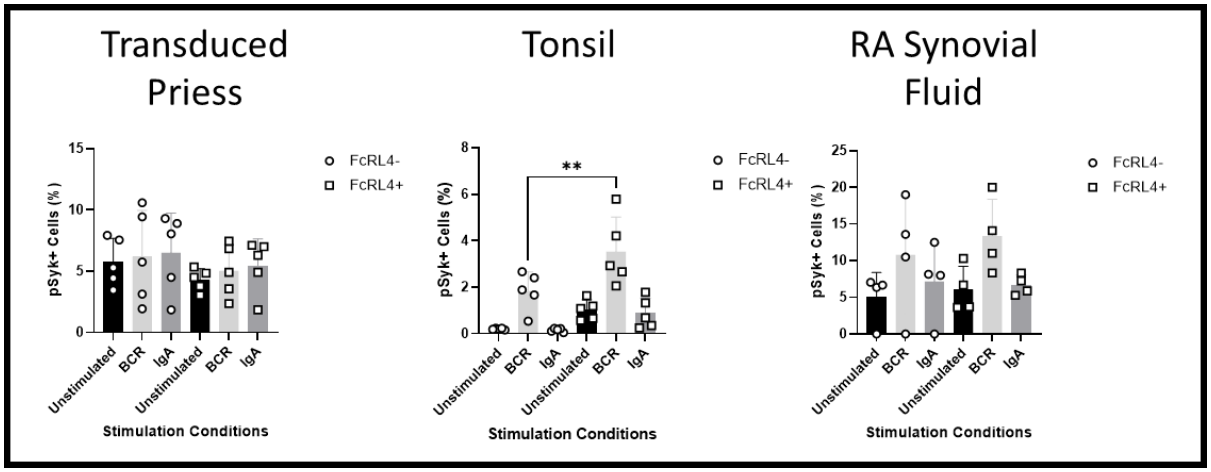

Figure 5.2.6.4I., pSyk is significantly higher in the BCR condition in FcRL4+ ex-vivo tonsil cells compared to the FcRL4-. *Transduced priess cells (n = 5), ex-vivo tonsil cells (n = 5), ex-vivo RA SF cells (n = 4) were either unstimulated, stimulated with 10µg/ml IgG + IgM f(ab')$_2$ fragment or with 50µg/ml HA colostrum IgA IC for 4mins. Cells were gated on the lymphocyte, singlet, CD3-, CD19+ and FcRL4+ population. FcRL4- cells were also gated to compare the difference of pSyk in FcRL4+ cells in response to stimulation with either 10µg/ml IgG + IgM f(ab')$_2$fragment and 50µg/ml HA colostrum IgA IC. The unstimulated sample was used to set the pSyk+ gate to determine the change in the percentage of pSyk+ cells between each stimulation condition. The means of unstimulated, BCR and IgA condition were compared to each other between the FcRL4- & FcRL4 populations in transduced priess, ex-vivo tonsil cells and ex-vivo RA SF cells. Statistical Test - –Šidák's multiple comparison corrected one-way ANOVA.*

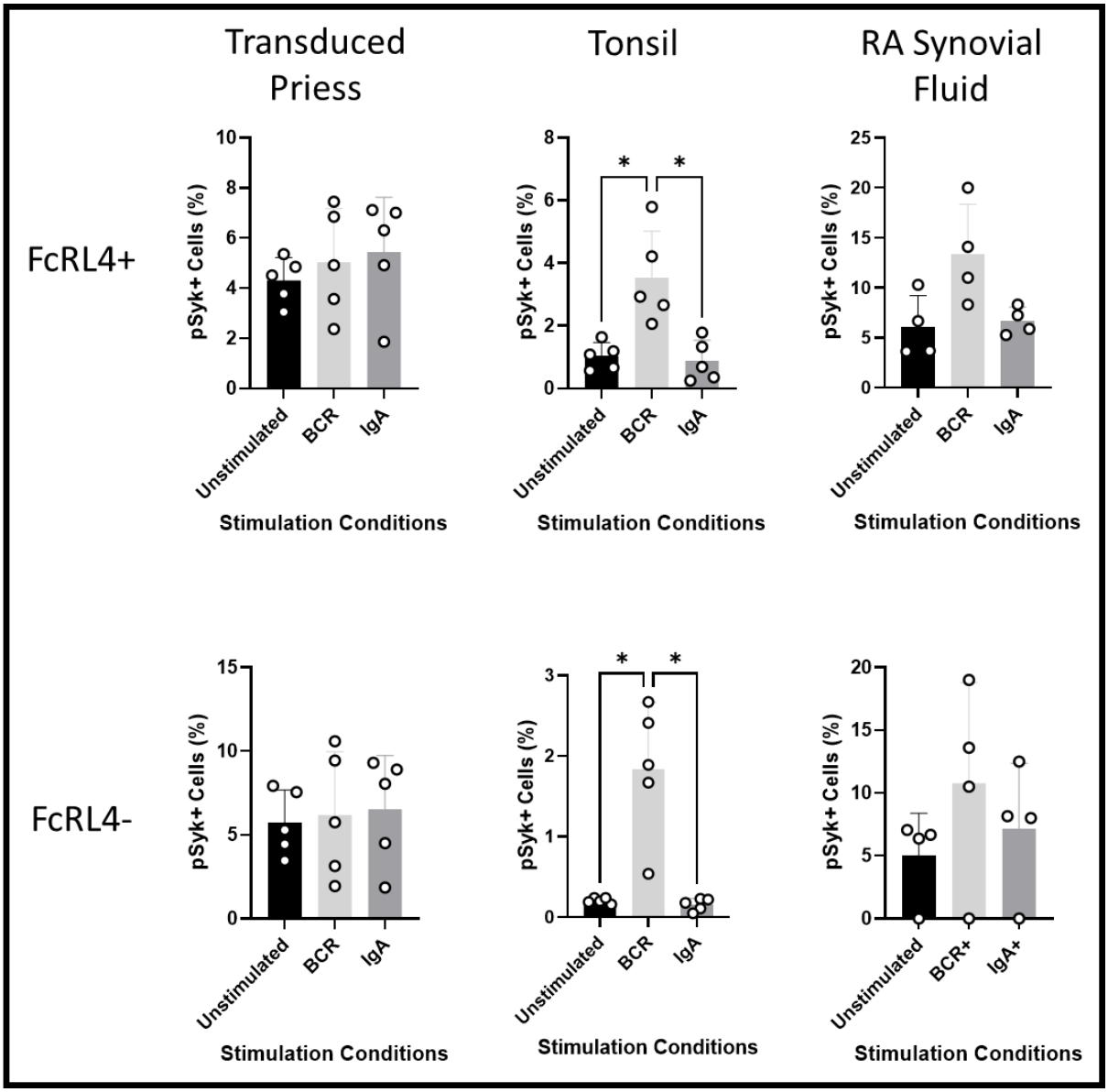

Figure 5.2.6.4II., pSyk increases in response to BCR stimulation alone and does not change in response to IgA stimulation alone compared to the unstimulated condition in ex-vivo tonsil and RA SF samples. *Transduced priess cells (n = 5), Tonsil B cells (n = 5), RA SF B cells (n = 4) were either unstimulated, stimulated with 10µg/ml IgG + IgM f(ab')$_2$ fragment or with 50µg/ml HA colostrum IgA IC for 4mins. Cells were gated on the lymphocyte, singlet, CD3-, CD19+ and FcRL4+ population. FcRL4- cells were also gated to compare the difference of pSyk in FcRL4+ cells in response to stimulation with either 10µg/ml IgG + IgM f(ab')$_2$ fragment and 50µg/ml HA colostrum IgA IC. The unstimulated sample was used to set the pSyk+ gate to determine the change in the percentage of pSyk+ cells between each stimulation condition. This is the same data as Figure 5.2.6.4I but the means of the BCR and IgA condition were compared to the mean of the unstimulated condition within the FcRL4- and FcRL4+ population. The mean of the BCR and IgA condition were also compared to each other within the FcRL4- and FcRL4+ populations. Statistical test – Tukey's multiple comparison corrected RM one-way ANOVA.*

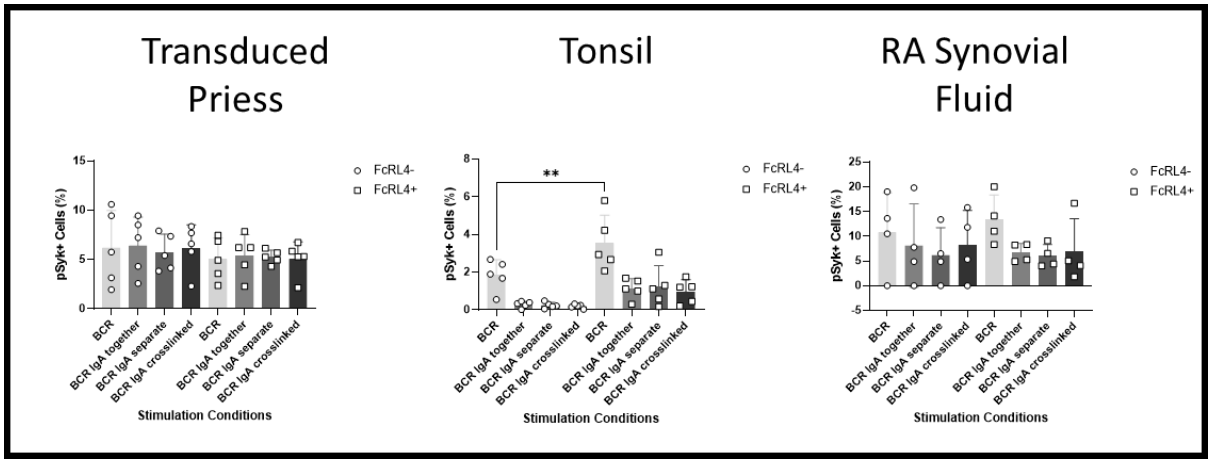

Figure 5.2.6.4III., there is no difference in pSyk in the BCR, BCRIgA$_t$, BCRIgA$_s$ and BCRIgA$_c$ conditions in FcRL4+ and FcRL4- transduced priess, ex-vivo tonsil and RA SF cells. *Transduced priess cells (n = 5), ex-vivo tonsil cells (n = 5), ex-vivo RA SF cells (n = 4) were:* ***BCR stimulated*** *with 10µg/ml anti-IgG + IgM f(ab')$_2$ fragment for 4mins****, stimulated together (BCRIgA$_t$)*** *with 10µg/ml anti-IgG + IgM f(ab')$_2$ fragment and 50µg/ml HA colostrum IgA IC for 4mins,* ***stimulated separately (BCRIgA$_s$)*** *where cells were stimulated with 50µg/ml HA colostrum IgA IC for 30mins and 10µg/ml anti-IgG + IgM f(ab')$_2$ fragment for 4mins or* ***crosslinked (BCRIgA$_c$)*** *where 10µg/ml biotinylated anti-IgG + IgM f(ab')$_2$ fragment and 50µg/ml biotinylated HA colostrum IgA IC were crosslinked with 1µg/ml streptavidin for 30mins and then added to cells to stimulate for 4mins. Cells were gated on the lymphocyte, singlet, CD3-, CD19+ and FcRL4+ population. FcRL4- cells were also gated to compare the difference of pSyk in FcRL4+ cells in response to stimulation. The unstimulated sample was used to set the pSyk+ gate to determine the change in the percentage of pSyk+ cells between each stimulation condition. The means of the BCR, BCRIgA$_t$, BCRIgA$_s$ and BCRIgA$_c$ conditions were compared to each other between the FcRL4- & FcRL4 populations in transduced priess, ex-vivo tonsil cells and ex-vivo RA SF cells. Statistical Test - –Šidák's multiple comparison corrected one-way ANOVA.*

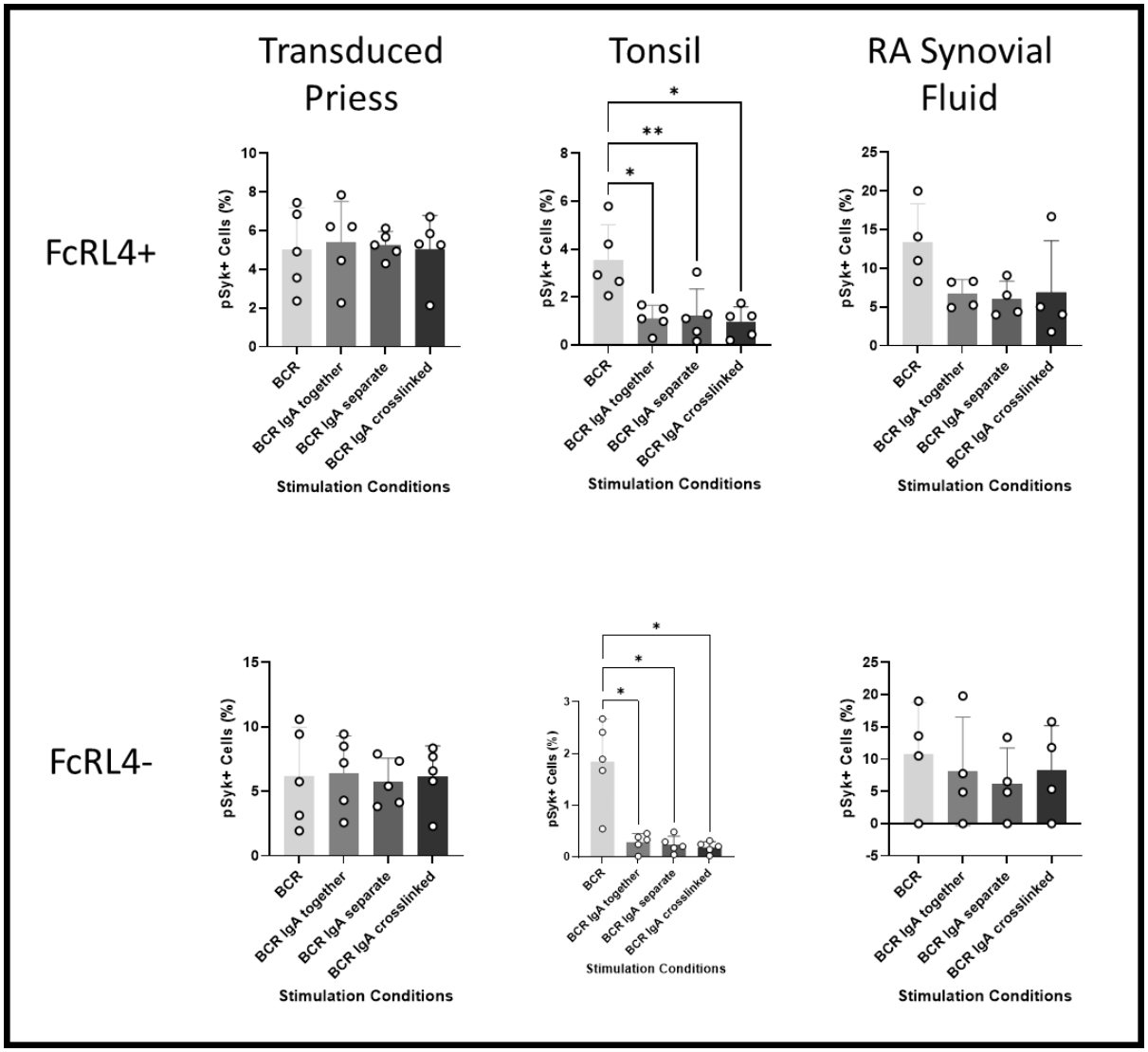

Figure 5.2.6.4IV., pSyk decreases in response to BCR and IgA crosslinking compared to BCR stimulation alone in ex-vivo tonsil and RA SF samples*. Transduced priess cells (n = 5), Tonsil B cells (n = 5), RA SF B cells (n = 4) were* ***stimulated with*** *10µg/ml anti-IgG + IgM f(ab')$_2$ fragment for 4mins****, stimulated together (BCRIgA$_t$)*** *with 10µg/ml anti-IgG + IgM f(ab')$_2$ fragment and 50µg/ml HA colostrum IgA IC for 4mins,* ***stimulated separately (BCRIgA$_s$)*** *where cells were stimulated with 50µg/ml HA colostrum IgA IC for 30mins and 10µg/ml anti-IgG + IgM f(ab')$_2$ fragment for 4mins or* ***crosslinked (BCRIgA$_c$)*** *where 10µg/ml biotinylated anti-IgG + IgM f(ab')$_2$ fragment and 50µg/ml biotinylated HA colostrum IgA IC were crosslinked with 1µg/ml streptavidin for 30mins and then added to cells to stimulate for 4mins. Cells were gated on the lymphocyte, singlet, CD3-, CD19+ and FcRL4+ population. FcRL4- cells were also gated to compare the difference of pSyk in FcRL4+ cells in response to stimulation. The unstimulated sample was used to set the pSyk+ gate to determine the change in the percentage of pSyk+ cells between each stimulation condition. This is the same data as Figure 5.2.6.4III but the means of each condition were compared to BCR condition within the FcRL4- and FcRL4+ populations. Statistical test – Dunnett's multiple comparison corrected RM one-way ANOVA.*

5.2.6.5 pPLCγ2

The percentage of pPLCγ2+ cells were compared in the unstimulated, BCR and IgA between the FcRL4- and FcRL4+ transduced priess (n = 5), *ex-vivo* tonsil (n = 5) and *ex-vivo* RA SF (n = 4) cells. The percentage of PLCγ2+ cells was similar between the unstimulated, BCR and IgA conditions in the transduced priess cells and RA SF samples (Figure 5.2.6.5I). Comparatively in the tonsil, the percentage of pPLCγ2+ cells in the BCR conditions were significantly greater in the FcRL4- cells compared to the FcRL4+ cells (BCR p = 0.0013) (Figure 5.2.6.5I). The percentage of pPLCγ2+ FcRL4- cells increased in the BCR condition compared to the unstimulated condition but there was no change in pPLCγ2+ FcRL4+ cells in the transduced priess cell sample (Figure 5.2.6.5II). In the tonsil and RA SF sample, there was an increase of pPLCγ2+ cells in the BCR condition compared to the unstimulated condition, which reached significance in the FcRL4- and FcRL4+ cells of the tonsil sample (FcRL4- p = 0.0271, FcRL4+ p = 0.0204) (Figure 5.2.6.5II). There was also a significant increase in percentage of pPLCγ2+ the BCR condition compared to the IgA condition for both the FcRL4- or FcRL4+ cells in the tonsil sample (FcRL4- p = 0.0274, FcRL4+ p = 0.0041) (Figure 5.2.6.5II).

The percentage of pPLCγ2+ cells in the BCRIgA$_t$, BCRIgA$_s$ and BCRIgA$_c$ conditions were compared between the FcRL4- and FcRL4+ populations. There was no difference in the percentage of pPLCγ2+ cells in the FcRL4- and FcRL4+ populations in the transduced priess cell sample (Figure 5.2.6.5III). In the tonsil and SF, there was a decrease in the percentage of pPLCγ2+ in BCRIgA$_t$, BCRIgA$_s$ and BCRIgA$_c$ conditions in the FcRL4- and FcRL4+ populations, although this was not significant (Figure 5.2.6.5III). There was no change in the percentage of pPLCγ2+ cells in the BCRIgA$_t$, BCRIgA$_s$ and BCRIgA$_c$ conditions for either the FcRL4- and FcRL4+ populations in untransduced priess cell samples (Figure 5.2.6.5IV). Comparatively,

there was a decrease in percentage of pPLCγ2+ cells in the BCRIgA$_t$, BCRIgA$_s$ and BCRIgA$_c$ conditions when compared to the BCR in the tonsil and RA SF samples (Figure 5.2.6.5IV). In the tonsil samples, the difference was significant in the FcRL4- populations (BCRIgA$_t$ p = 0.0483, BCRIgA$_s$ p = 0.0223, BCRIgA$_c$ p = 0.0271) and the FcRL4+ population (BCRIgA$_s$ p = 0.0351, BCRIgA$_c$ = 0.0179) (Figure 5.2.6.5IV).

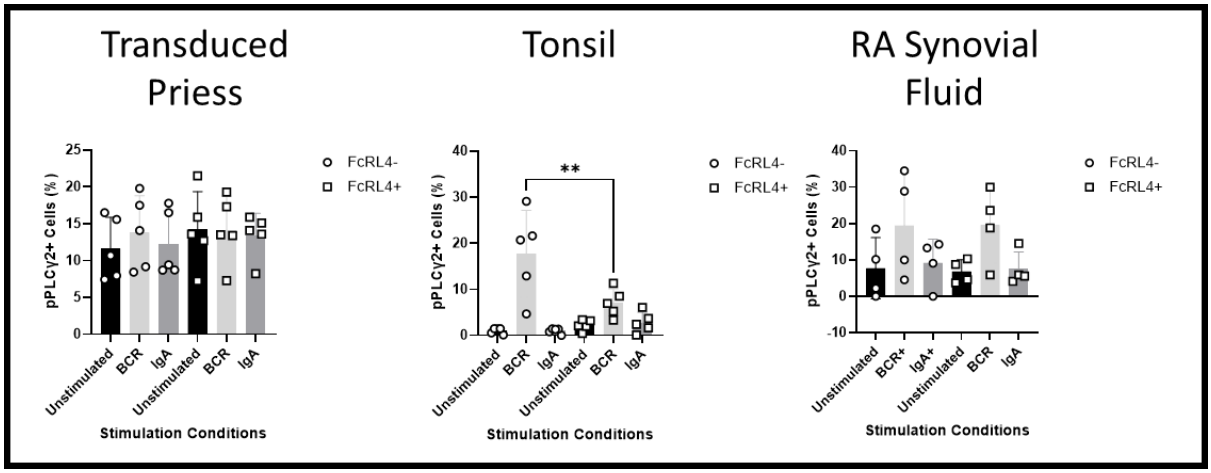

Figure 5.2.6.5I., pPLCγ2 is significantly higher in the BCR condition in FcRL4- ex-vivo tonsil cells compared to the FcRL4+. *Transduced priess cells (n = 5), ex-vivo tonsil cells (n = 5), ex-vivo RA SF cells (n = 4) were either unstimulated, stimulated with 10µg/ml IgG + IgM f(ab')$_2$ fragment or with 50µg/ml HA colostrum IgA IC for 4mins. Cells were gated on the lymphocyte, singlet, CD3-, CD19+ and FcRL4+ population. FcRL4- cells were also gated to compare the difference of pPLCγ2 in FcRL4+ cells in response to stimulation with either 10µg/ml IgG + IgM f(ab')$_2$ fragment and 50µg/ml HA colostrum IgA IC. The unstimulated sample was used to set the pPLCγ2+ gate to determine the change in the percentage of pPLCγ2+ cells between each stimulation condition. The means of unstimulated, BCR and IgA condition were compared to each other between the FcRL4- & FcRL4 populations in transduced priess, ex-vivo tonsil cells and ex-vivo RA SF cells. Statistical Test - –Šidák's multiple comparison corrected one-way ANOVA.*

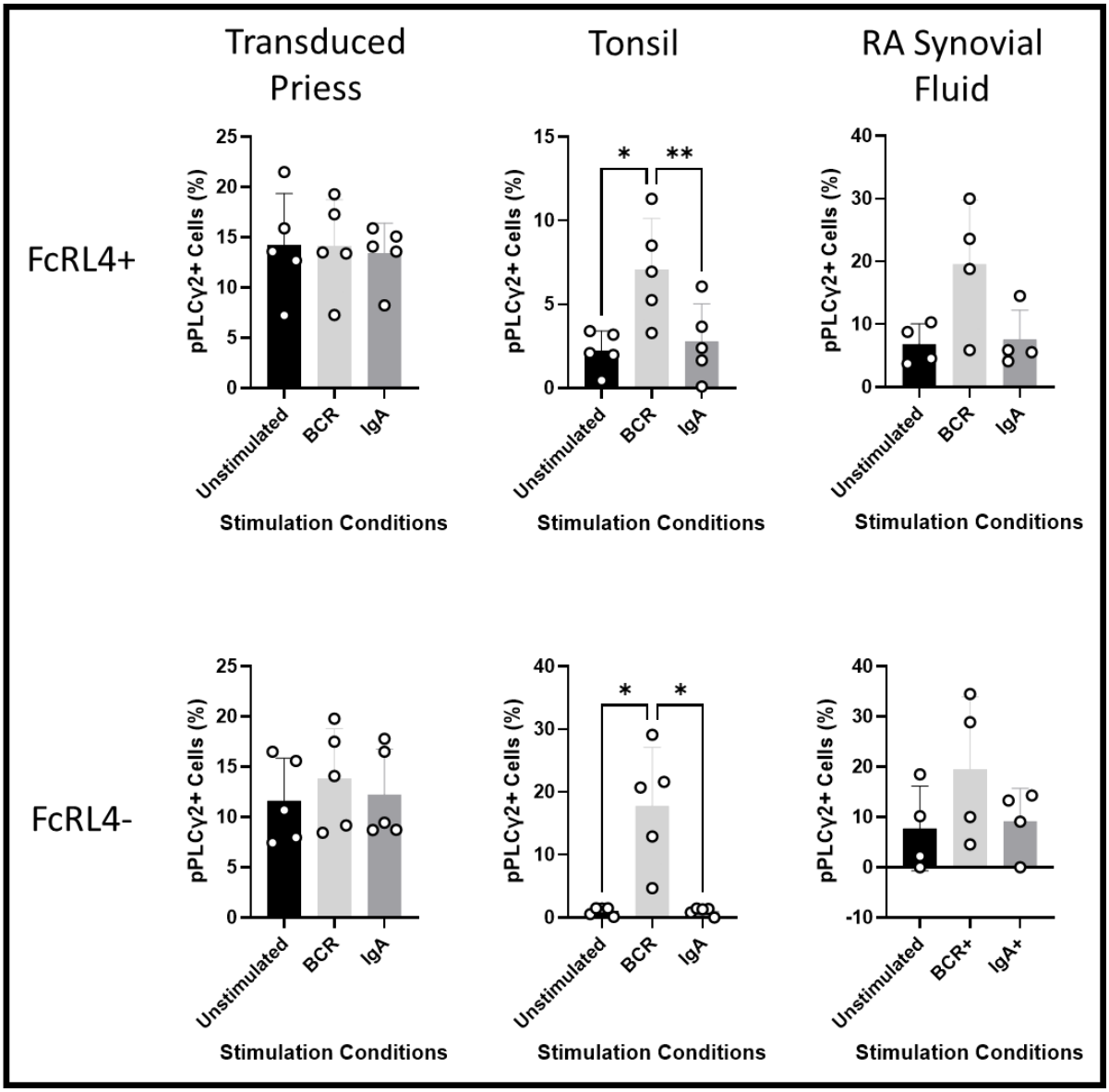

Figure 5.2.6.5II., pPLCγ2 increase in response to BCR stimulation alone and does not change in response to IgA stimulation alone compared to the unstimulated condition in ex-vivo tonsil and RA SF samples. *Transduced priess cells (n = 5), Tonsil B cells (n = 5), RA SF B cells (n = 4) were either unstimulated, stimulated with 10µg/ml IgG + IgM f(ab')$_2$ fragment or with 50µg/ml HA colostrum IgA IC for 4mins. Cells were gated on the lymphocyte, singlet, CD3-, CD19+ and FcRL4+ population. FcRL4- cells were also gated to compare the difference of pPLCγ2 in FcRL4+ cells in response to stimulation with either 10µg/ml IgG + IgM f(ab')$_2$ fragment and 50µg/ml HA colostrum IgA IC. The unstimulated sample was used to set the pPLCγ2+ gate to determine the change in the percentage of pPLCγ2+ cells between each stimulation condition. This is the same data as Figure 5.2.6.5I but the means of the BCR and IgA condition were compared to the mean of the unstimulated condition within the FcRL4- and FcRL4+ population. The mean of the BCR and IgA condition were also compared to each other within the FcRL4- and FcRL4+ populations. Statistical test – Tukey's multiple comparison corrected RM one-way ANOVA.*

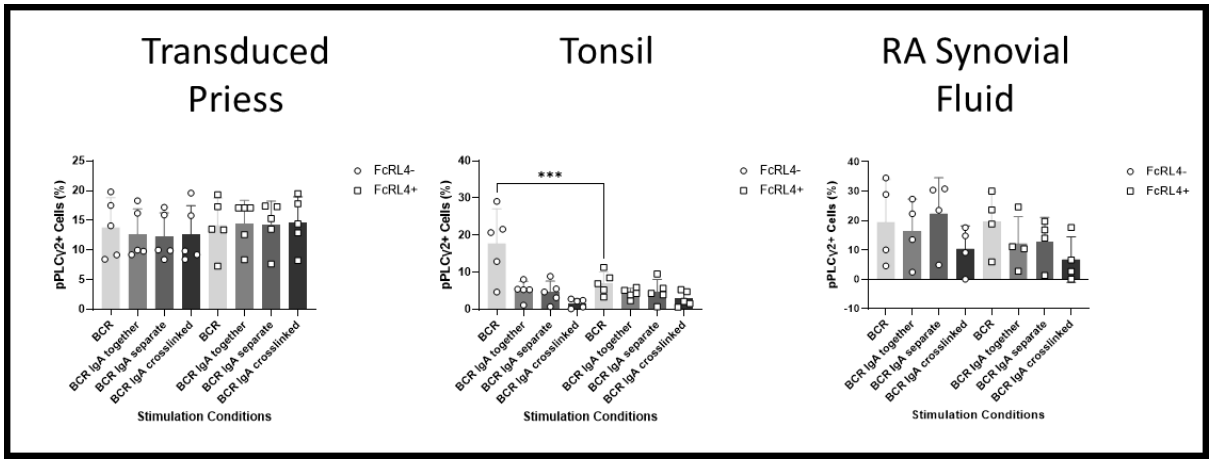

Figure 5.2.6.5III., there is no difference in pPLCγ2 in the BCR, BCRIgA$_t$, BCRIgA$_s$ and BCRIgA$_c$ conditions in FcRL4+ and FcRL4- transduced priess, ex-vivo tonsil and RA SF cells. *Transduced priess cells (n = 5), ex-vivo tonsil cells (n = 5), ex-vivo RA SF cells (n = 4) were:* ***BCR stimulated*** *with 10µg/ml anti-IgG + IgM f(ab')$_2$ fragment for 4mins,* ***stimulated together (BCRIgA$_t$)*** *with 10µg/ml anti-IgG + IgM f(ab')$_2$ fragment and 50µg/ml HA colostrum IgA IC for 4mins,* ***stimulated separately (BCRIgA$_s$)*** *where cells were stimulated with 50µg/ml HA colostrum IgA IC for 30mins and 10µg/ml anti-IgG + IgM f(ab')$_2$ fragment for 4mins or* ***crosslinked (BCRIgA$_c$)*** *where 10µg/ml biotinylated anti-IgG + IgM f(ab')$_2$ fragment and 50µg/ml biotinylated HA colostrum IgA IC were crosslinked with 1µg/ml streptavidin for 30mins and then added to cells to stimulate for 4mins. Cells were gated on the lymphocyte, singlet, CD3-, CD19+ and FcRL4+ population. FcRL4- cells were also gated to compare the difference of pPLCγ2 in FcRL4+ cells in response to stimulation. The unstimulated sample was used to set the pPLCγ2+ gate to determine the change in the percentage of pPLCγ2+ cells between each stimulation condition. The means of the BCR, BCRIgA$_t$, BCRIgA$_s$ and BCRIgA$_c$ conditions were compared to each other between the FcRL4- & FcRL4 populations in transduced priess, ex-vivo tonsil cells and ex-vivo RA SF cells. Statistical Test - –Šidák's multiple comparison corrected one-way ANOVA.*

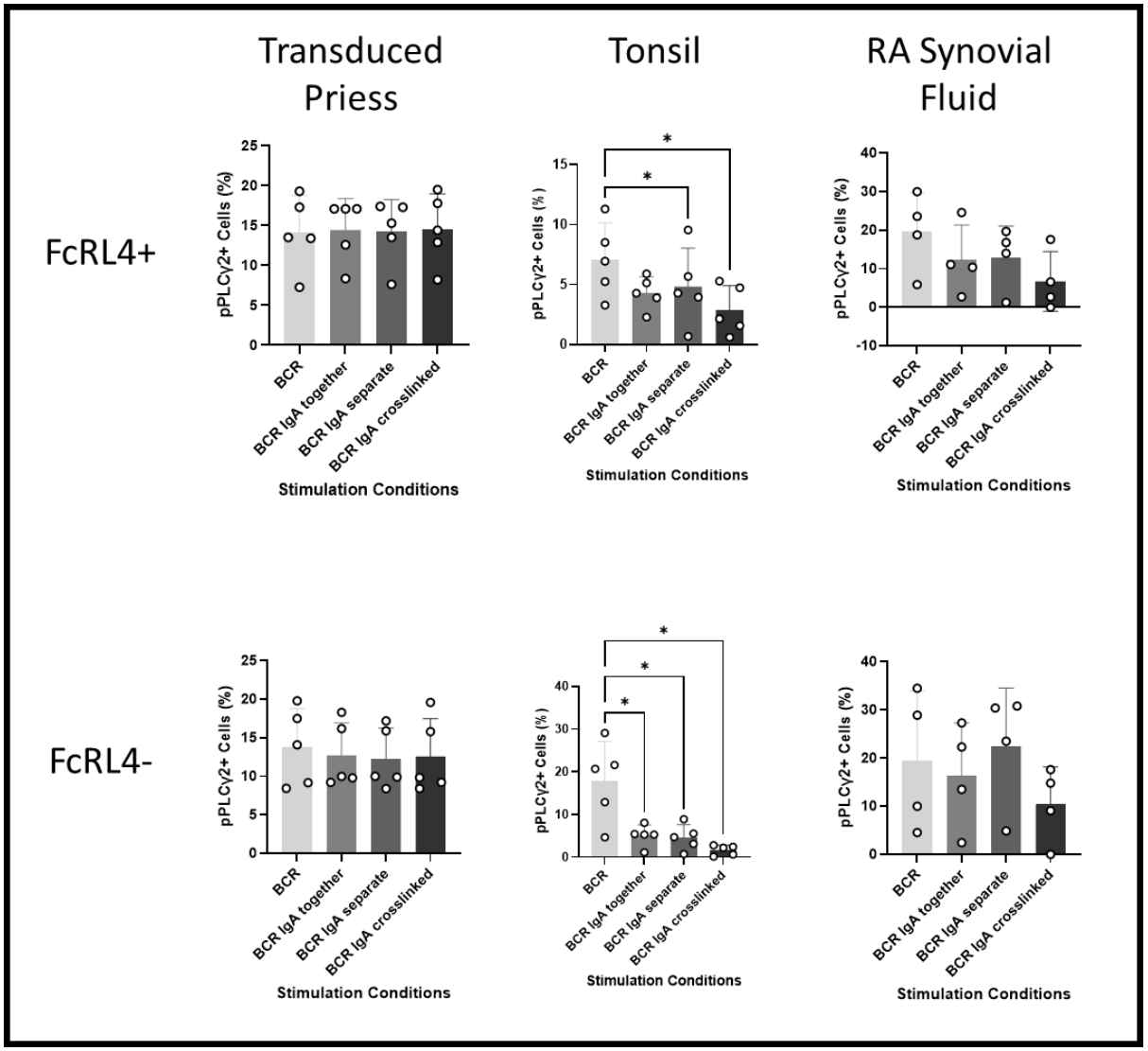

Figure 5.2.6.5IV., pPLCγ2 decrease in response to BCR and IgA crosslinking compared to BCR stimulation alone in ex-vivo tonsil and RA SF samples. *Transduced priess cells (n = 5), Tonsil B cells (n = 5), RA SF B cells (n = 4) were* ***stimulated with*** *10µg/ml anti-IgG + IgM f(ab')$_2$ fragment for 4mins****, stimulated together (BCRIgA$_t$)*** *with 10µg/ml anti-IgG + IgM f(ab')$_2$ fragment and 50µg/ml HA colostrum IgA IC for 4mins,* ***stimulated separately (BCRIgA$_s$)*** *where cells were stimulated with 50µg/ml HA colostrum IgA IC for 30mins and 10µg/ml anti-IgG + IgM f(ab')$_2$ fragment for 4mins or* ***crosslinked (BCRIgA$_c$)*** *where 10µg/ml biotinylated anti-IgG + IgM f(ab')$_2$ fragment and 50µg/ml biotinylated HA colostrum IgA IC were crosslinked with 1µg/ml streptavidin for 30mins and then added to cells to stimulate for 4mins. Cells were gated on the lymphocyte, singlet, CD3-, CD19+ and FcRL4+ population. FcRL4- cells were also gated to compare the difference of pPLCγ2 in FcRL4+ cells in response to stimulation. The unstimulated sample was used to set the pPLCγ2+ gate to determine the change in the percentage of pPLCγ2+ cells between each stimulation condition. This is the same data as Figure 5.2.6.5III but the means of each condition were compared to BCR condition within the FcRL4- and FcRL4+ populations. Statistical test – Dunnett's multiple comparison corrected RM one-way ANOVA.*

5.2.6.6 pERK1/2

The percentage of pERK1/2+ cells were compared in the unstimulated, BCR and IgA conditions between the FcRL4- and FcRL4+ transduced priess (n = 5), *ex-vivo* tonsil (n = 5) and *ex-vivo* RA SF (n = 4) cells. There was no significant difference between the FcRL4- and FcRL4+ cells in transduced priess cells and RA SF samples (Figure 5.2.6.6I) but there was a significant difference between the BCR conditions in tonsil samples (BCR p = 0.0082) (Figure 5.2.6.6I)., There was an increase in the percentage of pERK1/2+ FcRL4- and FcRL4+ transduced priess cells and RA SF cells when the BCR condition was compared to the unstimulated and IgA conditions (Figure 5.2.6.6II). However, this did not reach significance. In comparison, there was a significant increase in the percentage of pERK1/2+ FcRL4- and FcRL4+ tonsil cells in the BCR condition compared to the unstimulated condition (FcRL4- BCR p = 0.0251, FcRL4+ BCR p = 0.0134) (Figure 5.2.6.6II). There was no significant difference between the BCR and IgA conditions for either FcRL4- or FcRL4+ tonsil cells (Figure 5.2.6.6II).

The percentage of pERK1/2+ cells were compared in the BCRIgA$_t$, BCRIgA$_s$ and BCRIgA$_c$ conditions between the FcRL4- and FcRL4+. There was no significant difference between the BCRIgA$_t$, BCRIgA$_s$ and BCRIgA$_c$ conditions for transduced priess cells, tonsil B cells and RA SF B cells (Figure 5.2.6.6III). When the BCRIgA$_t$, BCRIgA$_s$ and BCRIgA$_c$ conditions were compared to the BCR condition in FcRL4+, the percentage of pERK1/2+ cells decreased in the BCRIgAc condition for transduced priess, tonsil and RA SF samples but this did not reach significance (Figure 5.2.6.6IV). There was a similar decrease in the percentage of pERK1/2+ cells in FcRL4- transduced priess and RA SF cells (Figure 5.2.6.6IV). However, in the FcRL4- tonsil cells, there was a significant decrease in the percentage of pERK1/2+ cells for the for the BCRIgA$_t$,

BCRIgA$_s$ and BCRIgA$_c$ conditions compared to the BCR condition (BCRIgA$_t$ p= 0.0237, BCRIgA$_s$ p = 0.0396, BCRIgA$_c$ p = 0.0162) (Figure 5.2.6.6IV).

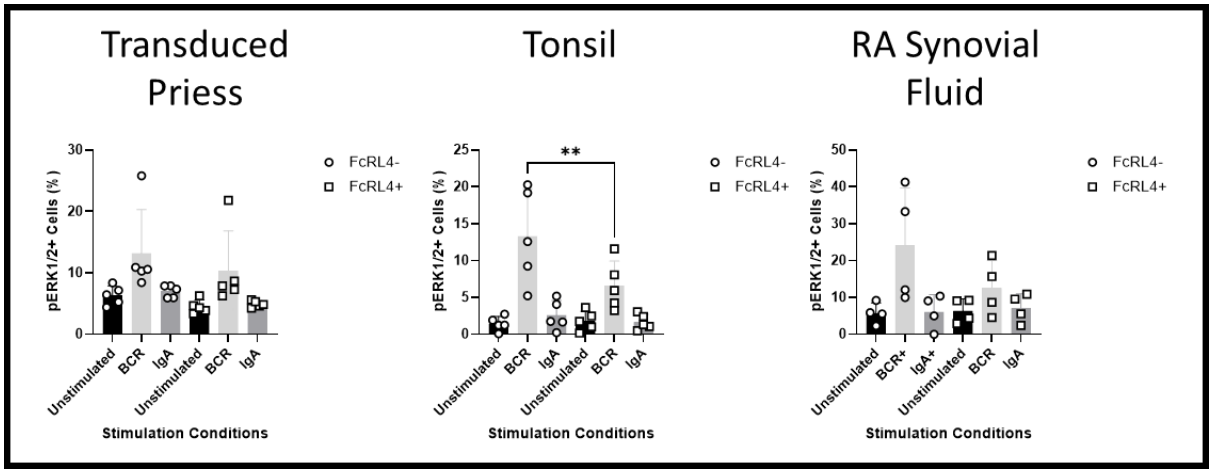

Figure 5.2.6.6I., pERK1/2 is higher in the BCR condition in FcRL4- transduced priess, ex-vivo tonsil and RA SF cells compared to the FcRL4+. *Transduced priess cells (n = 5), ex-vivo tonsil cells (n = 5), ex-vivo RA SF cells (n = 4) were either unstimulated, stimulated with 10µg/ml IgG + IgM f(ab')$_2$ fragment or with 50µg/ml HA colostrum IgA IC for 10mins. Cells were gated on the lymphocyte, singlet, CD3-, CD19+ and FcRL4+ population. FcRL4- cells were also gated to compare the difference of pERk1/2 in FcRL4+ cells in response to stimulation with either 10µg/ml IgG + IgM f(ab')$_2$ fragment and 50µg/ml HA colostrum IgA IC. The unstimulated sample was used to set the pERK1/2+ gate to determine the change in the percentage of pERK1/2+ cells between each stimulation condition. The means of unstimulated, BCR and IgA condition were compared to each other between the FcRL4- & FcRL4 populations in transduced priess, ex-vivo tonsil cells and ex-vivo RA SF cells. Statistical Test - –Šidák's multiple comparison corrected one-way ANOVA.*

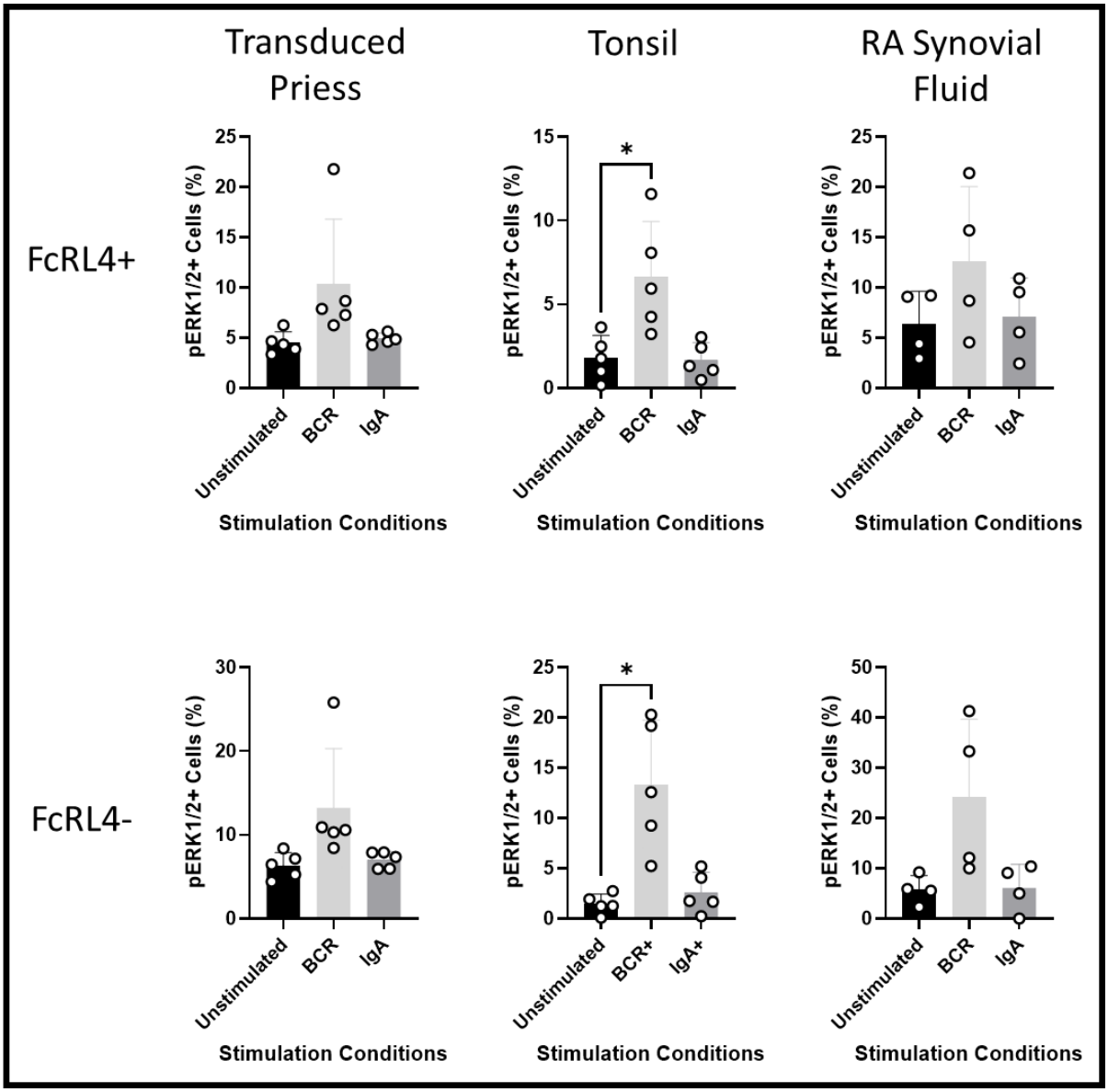

Figure 5.2.6.6II., pERK1/2 significantly increases in response to BCR stimulation alone and does not change in response IgA stimulation alone compared to the unstimulated condition in FcRL4+ and FcRL4- ex-vivo tonsil cells. *Transduced priess cells (n = 5), Tonsil B cells (n = 5), RA SF B cells (n = 4) were either unstimulated, stimulated with 10µg/ml IgG + IgM f(ab')$_2$ fragment or with 50µg/ml HA colostrum IgA IC for 10mins. Cells were gated on the lymphocyte, singlet, CD3-, CD19+ and FcRL4+ population. FcRL4- cells were also gated to compare the difference of pERK1/2 in FcRL4+ cells in response to stimulation with either 10µg/ml IgG + IgM f(ab')$_2$ fragment and 50µg/ml HA colostrum IgA IC. The unstimulated sample was used to set the pERK1/2+ gate to determine the change in the percentage of pERK1/2+ cells between each stimulation condition. This is the same data as Figure 5.2.6.6I but the means of the BCR and IgA condition were compared to the mean of the unstimulated condition within the FcRL4- and FcRL4+ population. The mean of the BCR and IgA condition were also compared to each other within the FcRL4- and FcRL4+ populations. Statistical test – Tukey's multiple comparison corrected RM one-way ANOVA.*

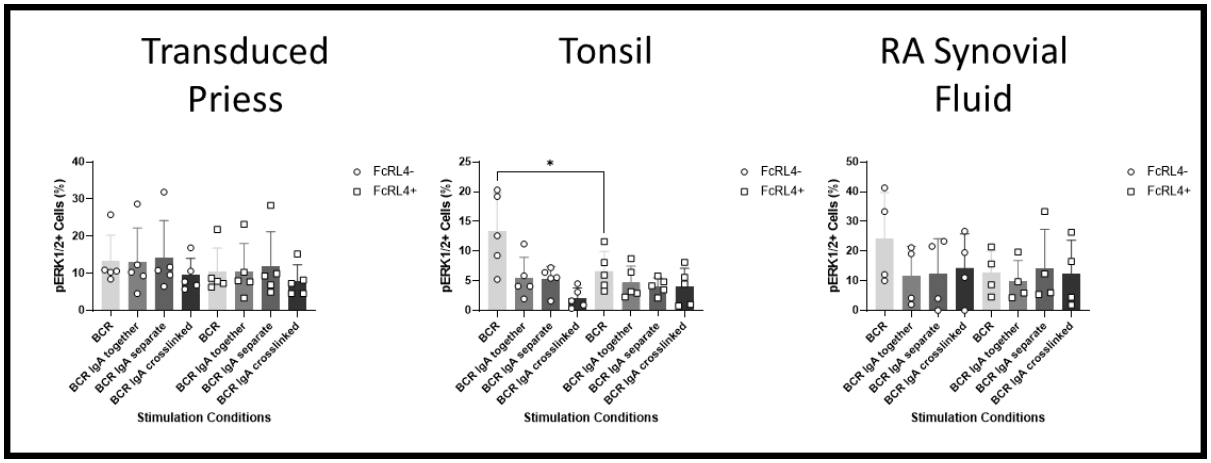

Figure 5.2.6.6III., there is no difference in pERK1/2 in the BCR, BCRIgA$_t$, BCRIgA$_s$ and BCRIgA$_c$ conditions in FcRL4+ and FcRL4- transduced priess, ex-vivo tonsil and RA SF cells. *Transduced priess cells (n = 5), ex-vivo tonsil cells (n = 5), ex-vivo RA SF cells (n = 4) were:* ***BCR stimulated*** *with 10µg/ml anti-IgG + IgM f(ab')$_2$ fragment for 10mins****, stimulated together (BCRIgA$_t$)*** *with 10µg/ml anti-IgG + IgM f(ab')$_2$ fragment and 50µg/ml HA colostrum IgA IC for 10mins,* ***stimulated separately (BCRIgA$_s$)*** *where cells were stimulated with 50µg/ml HA colostrum IgA IC for 30mins and 10µg/ml anti-IgG + IgM f(ab')$_2$ fragment for 10mins or* ***crosslinked (BCRIgA$_c$)*** *where 10µg/ml biotinylated anti-IgG + IgM f(ab')$_2$ fragment and 50µg/ml biotinylated HA colostrum IgA IC were crosslinked with 1µg/ml streptavidin for 30mins and then added to cells to stimulate for 10mins. Cells were gated on the lymphocyte, singlet, CD3-, CD19+ and FcRL4+ population. FcRL4- cells were also gated to compare the difference of pERK1/2 in FcRL4+ cells in response to stimulation. The unstimulated sample was used to set the pERK1/2+ gate to determine the change in the percentage of pERK1/2+ cells between each stimulation condition. The means of the BCR, BCRIgA$_t$, BCRIgA$_s$ and BCRIgA$_c$ conditions were compared to each other between the FcRL4- & FcRL4 populations in transduced priess, ex-vivo tonsil cells and ex-vivo RA SF cells. Statistical Test - –Šidák's multiple comparison corrected one-way ANOVA.*

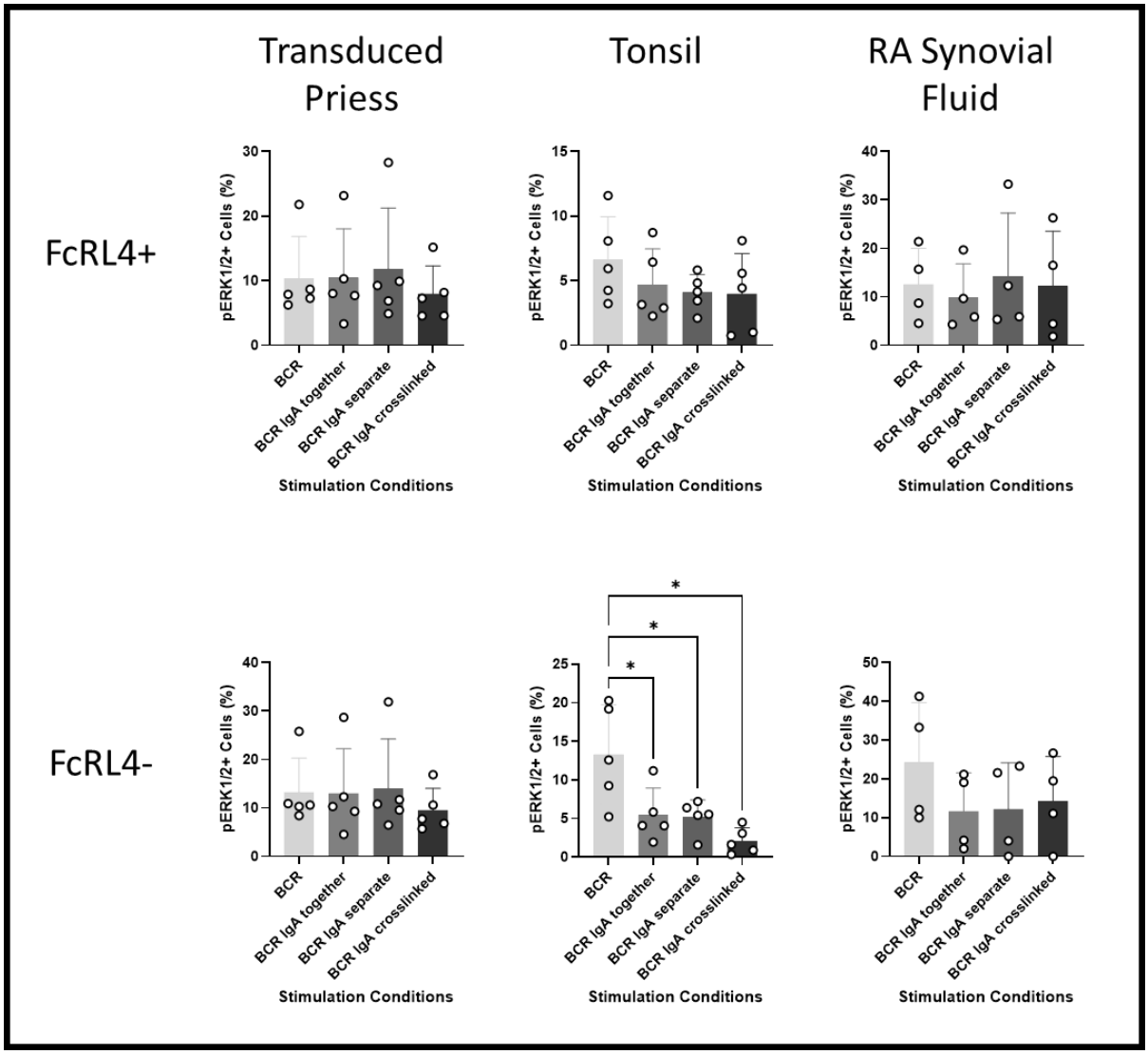

Figure 5.2.6.6IV., pERK1/2 decreases in response to BCR and IgA crosslinking compared to BCR stimulation alone. *Transduced priess cells (n = 5), Tonsil B cells (n = 5), RA SF B cells (n = 4) were* ***stimulated with*** *10µg/ml anti-IgG + IgM f(ab')$_2$ fragment for 10mins,* ***stimulated together (BCRIgA$_t$)*** *with 10µg/ml anti-IgG + IgM f(ab')$_2$ fragment and 50µg/ml HA colostrum IgA IC for 10mins,* ***stimulated separately (BCRIgA$_s$)*** *where cells were stimulated with 50µg/ml HA colostrum IgA IC for 30mins and 10µg/ml anti-IgG + IgM f(ab')$_2$ fragment for 10mins or* ***crosslinked (BCRIgA$_c$)*** *where 10µg/ml biotinylated anti-IgG + IgM f(ab')$_2$ fragment and 50µg/ml biotinylated HA colostrum IgA IC were crosslinked with 1µg/ml streptavidin for 30mins and then added to cells to stimulate for 10mins. Cells were gated on the lymphocyte, singlet, CD3-, CD19+ and FcRL4+ population. FcRL4- cells were also gated to compare the difference of pERK1/2 in FcRL4+ cells in response to stimulation. The unstimulated sample was used to set the pERK1/2+ gate to determine the change in the percentage of pERK1/2+ cells between each stimulation condition. This is the same data as Figure 5.2.6.6III but the means of each condition were compared to BCR condition within the FcRL4- and FcRL4+ populations. Statistical test – Dunnett's multiple comparison corrected RM one-way ANOVA.*

5.3 Discussion

We addressed the second part of the hypothesis that binding of IgA ICs to FcRL4 regulated signalling downstream of the BCR in primary cells. FcRL4 expresses three ITIMs on its cytoplasmic domain suggesting that it has the capacity to inhibit signalling downstream of the BCR. As previously tested, Ehrhardt's group identified through immunoprecipitation of FcRL4 chimeras found that the Src kinases Fgr and Hck associated with phosphorylated ITIMs of FcRL4, which resulted in the recruitment and activation of SHP-1 and SHP-2 [128,139]. Here, no change in phosphorylation of SHP-2 was observed upon crosslinking of FcRL4 with the BCR, we also observed increased phosphorylation of Fgr and Hck in the FcRL4+ transduced priess cells, tonsil B cells and RA SF B cells compared to FcRL4+ cells stimulated with anti-IgG + IgM $f(ab')_2$ fragment only. There was also increased phosphorylation of SHP-1 upon FcRL4 and BCR crosslinking in FcRL4+ RA SF B cells and general higher levels of phosphorylation in FcRL4+ in FcRL4+ transduced priess cells when compared to FcRL4- cells. The phosphorylation of SHP-1 is important for the negative regulation of the BCR through co-receptors CD11b and FcγRIIβ, as their activation results in the docking of SHP-1 to CD22 and CD19 respectively, via phosphorylation of docking sites created by Lyn, which results in the phosphorylation SHP-1 [144,145]. Together, these results support the idea that crosslinking of IgA IC-stimulated FcRL4 with the BCR increases the recruitment of inhibitory signalling molecules.

Their inhibitory capacity was reflected in the decreased phosphorylation of Syk, PLCγ2 and ERK upon receptor crosslinking (Figure 5.2.6.1II, 5.2.6.4II & 5.2.6.6II). Syk is important for B cell survival, as it regulates autophagy through Nrf2. The potential consequence of FcRL4 downregulating signalling through Syk is increased cell death [54,71]. ERK1/2 is also important

for B cell survival, as it promotes the expression of anti-apoptotic genes, Bcl-2 and Bcl-Xl [146]. However, when ERK1/2 is inhibited in a Raf-1 dependent manner, B cells fail to proliferate [146]. The implications of dysregulated cell proliferation has been demonstrated by the absence of FcγRIIβ and CD11b. Functional FcγRIIβ has been shown to inhibit antibody dependent enhancement of dengue fever [121]. However, a hypofunctional polymorphism in the FcγRIIβ gene, identified in malaria and RA patients, is associated with excessive B cell activation and survival [121,132]. Similarly CD11b reduces the production of snRNP autoantibodies in SLE but CD11b KO mice model found that B cells expressed more CD138 and there was greater production of snRNP autoantibodies compared to the WT, suggesting a switch in B cell function [144]. This suggests that FcRL4 capacity to negatively regular BCR signalling could be to act as a switch to dampen B cell activation and prevent excessive proliferation. This may be true in patients with chronic hepatitis B, as CD19+ PB B cells stimulated with anti-f(ab')$_2$ and CD40L upregulated FcRL4, suggesting that BCR activation initiates the expression of negatively regulating co-receptors to prevent persistent activation of B cells [132].

In some cases, regardless of the stimulatory signals the cell received there was very little change in phosphorylation between conditions. In the transduced priess cells, the amount of pSyk and pPLCγ2 hardly changed when the receptors were crosslinked compared to stimulation of the BCR alone in FcRL4+ transduced priess cells. However, this was most likely due to the chronically elevated levels of pSHP-1, as this would inhibit pPLCγ2 and pSyk so the addition of extra inhibitory stimuli is unlikely to induce further dephosphorylation. This suggests that FcRL4 may reduce responsiveness to the BCR by maintaining a higher basal level of inhibitory signals and increase the threshold required for BCR activation.

For most signalling molecules analysed, there was a high amount of variability between samples, represented by the SD error bars. One possible explanation for this was cell viability. Cell viability could not be determined in these experiments, as viability dyes that are usually employed to identify dead cells, work by entering cells whose membranes are more permeable due to apoptosis. However, the PhosFlow protocol requires cells to be permeabilised to allow entry of staining antibodies and therefore would be more accessible to viability dyes. This would cause exclusion of the majority of live cells. To reduce the number of dead cells, samples were filtered prior to stimulation in culture and FSC-A/SSC-A on FlowJo10.7.1 was able to exclude debris and dying cells, which exhibits as a population on the far left of the FACS plot. This doesn't guarantee complete exclusion and therefore a lack of responsiveness in cells could be attributed to their being a higher population of inviable cells.

To ascertain differences in phosphorylation of signalling molecules, FcRL4+ B cells they were compared to their FcRL4- counterpart. For some signalling molecules a similar pattern of phosphorylation was observed between the FcRL4- & FcRL4+ B cells. For the transduced priess cell, a possible explanation is that GFP staining was used to define the FcRL4+ population. In Figure 3.2.3.2C, the percentage of GFP+ (FcRL4) cells was significantly less than the percentage of PE+ (FcRL4) cells. Therefore, cells that are FcRL4+ could have been included in the FcRL4- population.

Another possibility for the similarities seen between FcRL4- and FcRL4+ B cells could be because another IgA receptor is expressed by the FcRL4- B cells. FcRL3 is another member of the FcRL family that is expressed on B cells as well as T and NK cells. Additionally, sc-RNAseq of RA synovial tissue sample found that FcRL3 is expressed on multiple B cell subsets [28]. Its IC

domain, expresses an ITAM and an ITIM and a recent study identified that FcRL3 is capable of binding sIgA on both B cells and Tregs [122,147,148]. The IgA IC used was heat aggregated from colostrum, which is enriched with sIgA, which could bind to FcRL3 [149]. If FcRL3 was present, it could act as an inhibitory co-receptor for the BCR and downregulate pErk1/2, pPLCγ2 and pSyk in a similar manner to FcRL4. An experiment that crosslinked the BCR with a FcRL3 chimera resulted in reduced Ca^{2+} mobilisation and reduced cell death, similar to other experiments done investigating FcRL4 [134,142,148]. Therefore, expression of FcRL3 on FcRL4- B cells may be able to explain why there were similarities in signalling between FcRL4- and FcRL4+ B cells but this needs to be investigated further. However, the AMP2 scRNAseq dataset of RA synovial tissue shows that FcRL4 expression is limited to a small population with an autoimmunity-related B cell gene expression pattern, whilst FcRL3 is broadly expressed across B cell subsets[28]. As we have observed IgA binding in FcRL4+ B cells, it is unlikely that FcRL3 plays a major role in IgA IC capture in these cells.

In summary, IgA IC binding to FcRL4+ cells increase phosphorylation of the inhibitory Src kinases Fgr and Hck and phosphatase SHP-1 in response to crosslinking with the BCR. This resulted in the reduced phosphorylation of the BCR signalling molecules Syk, PLCγ2 and ERK1/2, suggesting that crosslinking of FcRL4 and the BCR downregulated signalling through the BCR. Although similar patterns of inhibition were observed in FcRL4-, the influence of other IgA receptors on signalling need to be investigated to understand the specificity of signalling to FcRL4.

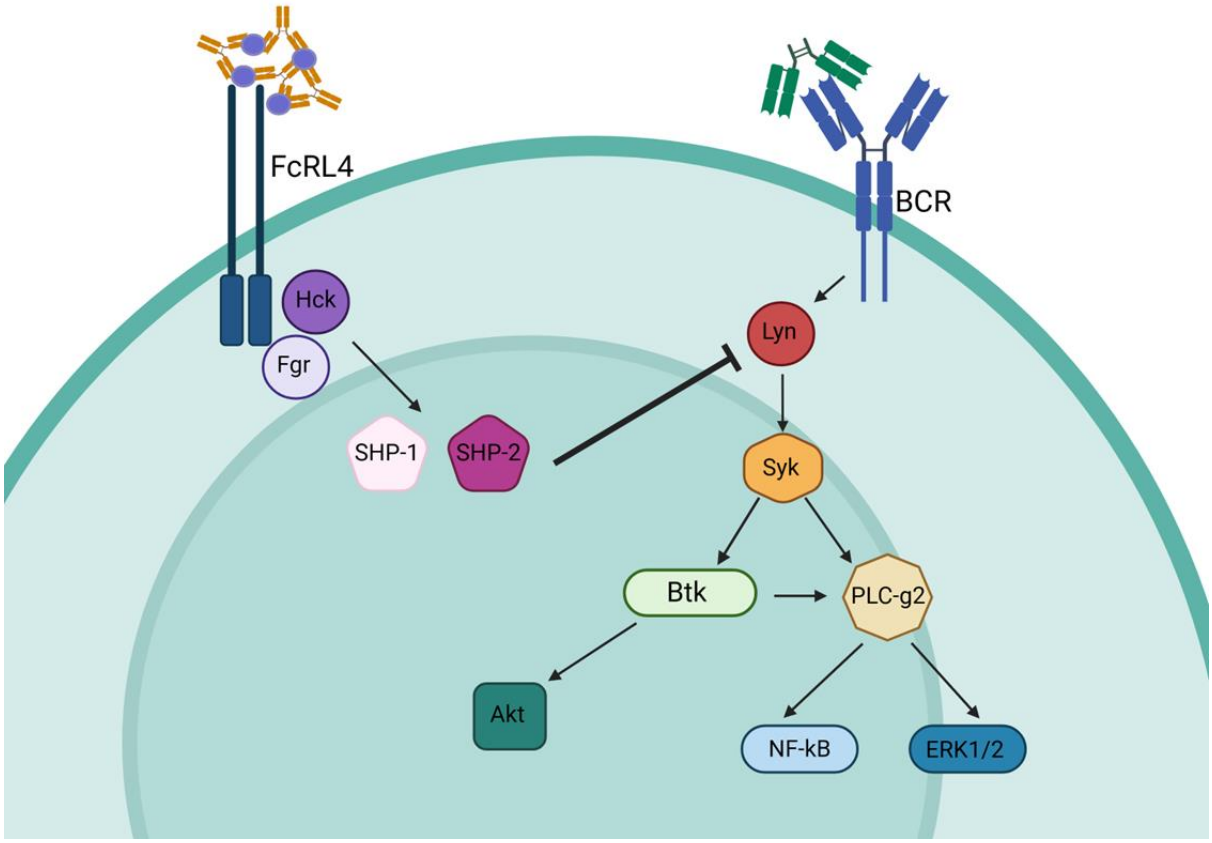

***Figure 5.3., Schematic of the signalling molecules investigated downstream of FcRL4 and the BCR**. Engagement of FcRL4 by HA colostrum IgA IC recruits and phosphorylates Hck and Fgr. These activate and phosphorylate SHP-1 and SHP-2, which inhibit Lyn by dephosphorylating it. Inactivation of Lyn reduces phosphorylation of Syk, which reduces phosphorylation of Btk and PLCγ2. Reduced phosphorylation of Btk and PLCγ2 reduces phosphorylation of Akt, ERK1/2 and p65-NF-κB.*

6 Discussion

6.1 Summary

FcRL4 expressed on transduced priess cells, tonsil B cells and RA SF B cells can capture IgA IC's. IgA IC bound FcRL4 was internalised to acidic intracellular compartments by *in vitro* and *ex vivo* FcRL4+ B cells. Expression of co-stimulatory molecules CD80, CD86 and HLA-DR had been previously identified in FcRL4+ tonsil B cells and RA SF B cells. Their expression was also confirmed in the FcRL4 transduced priess cells, suggesting that these cells could be antigen presenting cells. FcRL4 transduced priess cells could T cells specific for citrullinated enolase-derived peptides by presenting a citrullinated enolase derived peptide on their surface. Further work needs to be done to link IgA IC internalisation with presentation of citrullinated enolase to fully understand the antigen presenting capabilities of FcRL4+ B cells. Finally, crosslinking of IgA IC bound FcRL4 to the BCR increase phosphorylation of inhibitory signalling molecules Hck, Fgr and SHP-1 whilst downregulating phosphorylation of signalling molecules ERK1/2, PLCγ2 and Syk, indicating that FcRL4 is able to regulate BCR activation.

6.2 Functional Consequences

FcRL4+ B cells are enriched in the RA synovium, the parotid glands of individuals with SjS and the PB of individuals infected with HIV and CVID. The FcRL4+ B cell phenotype overlaps with a subset of B cells known as ABCs. When discovered in 2011, the subset was described as being age associated due to their presence in middle age individual. However, recent studies suggest there is no link between age and the frequency of ABCs and are now more commonly termed autoimmunity associated B cells [60]. ABCs are expanded in individuals

diagnosed with RA, SLE, malaria and MS and the expansion of the ABCs is often associated with a more severe diseases phenotype [59,61,126]. In a murine model of lupus, ABCs were either CD80+PD-L2+ or CD73+CD80+, which are phenotypes associated with secondary PC differentiation. Additionally, FcRL5, a plasmablast marker, is also expressed on ABCs [120]. Together, these results suggest that ABCs may be poised to rapidly differentiate into PCs. However, as RA SF FcRL4+ B cells do not express high levels of PC-related genes, such as BLIMP-1, IRF4 and high levels of Ig, suggesting they may have the potential to preferentially differentiate into PCs they are not yet in the process [128]. Although FcRL4 expression is associated with ABCs it appears to only define those that have infiltrated inflammatory tissues whilst those in the PB express very low levels of FcRL4. Additionally, functional experiments investigating ABCs are often done in cells isolated from murine mice models or the PB, where FcRL4 expression is at low levels in the PB and is not expressed in mice [119].

It hasn't been possible to target ABCs therapeutically, as targeting CD11c or T-Bet with depleting antibodies would deplete DCs, macrophages and Th1 cells respectively. The restriction of FcRL4 expression to tissue resident memory B cells means that a smaller population of immune cells will be removed upon treatment with anti-FcRL4 depleting antibody. The overlap of FcRL4+ and ABCs may in future be used to target ABCS with an anti-FcRL4 antibody-based drug.

In RA, RANKL-producing B cells were characterised by their expression of FcRL4 [110]. However, our experiments investigating the effects of IgA IC bound FcRL4 on BCR signalling suggest that FcRL4 may have an immunoregulatory role by inhibiting signalling pathways that induce a proinflammatory phenotype. Additionally, the relationship between cytokine expression, FcRL4 signalling and IgA IC binding is yet to be explored. Therefore, RANKL production has

not been investigated as a consequence of IgA binding and it is not known if IgA binding to FcRL4 induces RANKL production or if RANKL production precedes FcRL4 expression, which when bound to IgA IC's downregulates RANKL production by inhibiting proinflammatory signalling pathways.

In our experiments we weren't able to confirm if citrullinated antigens are captured in IgA ICs and be presented as an antigen by FcRL4+ B cells. These experiments are still planned, it took too long for us to source a recombinant high affinity IgA with specificity for citrullinated enolase. It has now arrived and will be tested as soon as possible. If IgA ICs could not be processed and presented on the surface of FcRL4+ B cells then it would suggest that the IC is degraded following internalisation. If this was the case it would suggest that the expression of FcRL4 could be to assist in removing ICs. One antigen it could potentially be removing is BEVs. These are nanosize vesicles derived from gram-negative bacteria and express high levels of LPS on their surface. FcRL4+ B cells overexpress IgA as a BCR, suggesting a link to mucosal immunity [19]. It may be beneficial to clear certain proinflammatory BEVs, for example BEVs from *P.Gingivalis* induce macrophage and monocyte unresponsiveness by cleaving the CD14 and reducing TLR-4 signalling [20]. This could be relevant to RA, as some individuals diagnosed with RA had also been diagnosed with periodontitis prior to disease onset as well as having higher titres of bacteria in their blood with active periodontitis disease [14,18]. This breach in mucosal tolerance may be rescued if BEVs are removed from the environment and prevented from inducing a proinflammatory phenotype.

6.3 Future Work & Limitations

Initial functional experiments investigating internalisation appear to confirm that IgA IC binding to FcRL4 results in its internalisation. However, the consequence of its internalisation was not entirely explored during this project. Fluorescent microscopy could be used to determine which intracellular compartments that IgA IC-FcRL4 localise to by co-staining for markers such as, EEA1 for early endosomes and LAMP1 for lysosomes [150]. It was also not possible to determine the fate of the IgA IC once it has been internalised. As mentioned previously, autophagy is a process by which the cell breaks down intracellular components to either use as fuel or to present on their surface. To explore the potential role of autophagy on internalised IgA IC, quantitative RT-PCR can be used to identify changes in autophagic markers such as Beclin-1, ATG5, LC3II at the RNA level between FcRL4+ cells cultured with IgA IC's or not. Additionally, internalisation and trafficking of a receptor is tightly regulated by signalling pathways that localise themselves to specific subcellular compartments [69]. As Hck and SHP-1 have been linked to initially internalisation and autophagy respectively in separate experiments, there could be similar patterns of signalling molecule localisation upon IgA IC binding to FcRL4.

The functional role of FcRL4+ B cells as APCs could not be entirely explored using the current set of experiments. The most likely limitation was the antigen, as the FcRL4+ transduced priess cells could present citrullinated enolase derived peptide on surface-expressed MHC-II to activate citrullinated enolase-recognising T cell hybridoma. Additionally, FcRL4+ transduced priess cells could internalise IgA IC's, which would allow them to be processed and presented. To overcome this, we have been in collaboration with Prof Toes' team in Leiden, working on production of a human citrullinated protein-specific recombinant IgA to

build fully characterised ICs. The antibodies are now in our lab, but it was too late to include them into the thesis. This work will be continued in Prof Scheel-Toellner's laboratory.

The impact of IgA IC binding to FcRL4 on BCR signalling has been demonstrated using PhosFlow experiments and suggests that FcRL4 inhibits signalling downstream of the BCR. Transcriptomic analysis and subsequent quantitative RT-PCR of FcRL4+ B cells identified that they were proliferative [60,110,128]. Downregulation of signalling molecules Syk, PLCγ2 and ERK1/2 induce a non-proliferative and even an apoptotic phenotype in cells. This phenotype has been described as 'exhausted' in FcRL4+ B cells isolated from the PB of HIV patients with a high viraemic load [131,133]. In accordance with our results, this suggests that stimulation of FcRL4 with IgA IC might induce a non-proliferative phenotype. However, what is not known about previous experiments that characterised FcRL4+ B cells is whether FcRL4 had bound to IgA ICs recently. In our experiments, inhibition of signalling molecules was observed in cells stimulated 2-10mins, meaning that there is a possibility over time that IgA inhibition decreases either by the IgA IC being degraded once internalised and therefore ceasing inhibition or IgA IC dissociates from FcRL4 so an inhibitory signal is no longer induced. Therefore, use of proliferation assays would be able to determine whether FcRL4+ B cells become less proliferative when bound to IgA IC's.

Finally, in some of the FcRL4- samples, the changes in phosphorylation of signalling molecules were similar to those observed in FcRL4+ B cells. When IgA binding was investigated in induced transduced priess cells a small population of FcRL4- cells were IgA+ suggesting that priess cells may express another IgA receptor that can also bind IgA IC and impact signalling downstream of the BCR. Besides FcRL4, other known IgA receptors include FcαRI, TFR1, ASPGR, FcRL3 and SIGNR1 [108]. Out of these, only FcRL3 is known to be express

on B cells and expresses an ITIM on its IC domain, which makes it a candidate as an alternative receptor that can downregulate phosphorylation of signalling molecules downstream of the BCR [148]. To further clarify this, transduced priess cells, tonsil B cells and RA SF B cells need to be co-stained for FcRL3 and FcRL4 to determine if there is a population of FcRL3+ B cells.

For functional experiments and for exploration of the functional consequences of depletion of FcRL4+ B cells it would be interesting to have an animal model. This is difficult as FcRL4 is only expressed in higher primates. For preclinical models of targeted depletion of FcRL4+ B cells this would still be necessary.

6.4 Concluding Remarks

Overall, expression of FcRL4 on B cells appears to act as a molecular switch to downregulate BCR signalling and prioritise internalisation of IgA immune complexes. Fully understanding the function of FcRL4+ B cells could solidify the argument to target FcRL4 therapeutically as it is expressed on ABCs, which are pathogenic B cells associated with autoimmune diseases. ABCs are also defined by their expression of CD11c and T-Bet but these are also expressed by DCs, macrophages and Th1 cells respectively so therapies directed at either CD11c or T-Bet would cause severe immunosuppression by depleting entire immune cell populations. However, if FcRL4 was targeted as a therapy to deplete ABCs, only a subset of memory B cells would be depleted and would have less of an immunosuppressive effect in patients.

7 References

1. Rosenblum, M. D., Remedios, K. A. & Abbas, A. K. Mechanisms of human autoimmunity. *J. Clin. Invest.* **125**, 2228–2233 (2015).
2. Wang, L., Wang, F.-S. & Gershwin, M. E. Human autoimmune diseases: a comprehensive update. *J Intern Med* **278**, 369–395 (2015).
3. Desai, M. K. & Brinton, R. D. Autoimmune Disease in Women: Endocrine Transition and Risk Across the Lifespan. *Front. Endocrinol.* **10**, 265 (2019).
4. Fairweather, D., Beetler, D. J., McCabe, E. J. & Lieberman, S. M. Mechanisms underlying sex differences in autoimmunity. *J Clin Invest* **134**, e180076 (2024).
5. Ray, D. & Yung, R. Immune senescence, epigenetics and autoimmunity. *Clinical Immunology* **196**, 59–63 (2018).
6. Theofilopoulos, A. N., Kono, D. H. & Baccala, R. The multiple pathways to autoimmunity. *Nat Immunol* **18**, 716–724 (2017).
7. Van Kempen, T. S., Wenink, M. H., Leijten, E. F. A., Radstake, T. R. D. J. & Boes, M. Perception of self: distinguishing autoimmunity from autoinflammation. *Nat Rev Rheumatol* **11**, 483–492 (2015).
8. Raychaudhuri, S. *et al.* Five amino acids in three HLA proteins explain most of the association between MHC and seropositive rheumatoid arthritis. *Nat Genet* **44**, 291–296 (2012).
9. Dunn, S. E. *et al.* Peroxisome proliferator-activated receptor (PPAR)alpha expression in T cells mediates gender differences in development of T cell-mediated autoimmunity. *J Exp Med* **204**, 321–330 (2007).
10. Johnson, D. & Jiang, W. Infectious diseases, autoantibodies, and autoimmunity. *Journal of Autoimmunity* **137**, 102962 (2023).
11. Rosser, E. C. *et al.* Microbiota-Derived Metabolites Suppress Arthritis by Amplifying Aryl-Hydrocarbon Receptor Activation in Regulatory B Cells. *Cell Metab* **31**, 837-851.e10 (2020).

12. Firestein, G. S. & McInnes, I. B. Immunopathogenesis of Rheumatoid Arthritis. *Immunity* **46**, 183–196 (2017).

13. Kronzer, V. L. & Davis, J. M. Etiologies of Rheumatoid Arthritis: Update on Mucosal, Genetic, and Cellular Pathogenesis. *Curr Rheumatol Rep* **23**, 21 (2021).

14. Deane, K. D. *et al.* Genetic and environmental risk factors for rheumatoid arthritis. *Best Practice & Research Clinical Rheumatology* **31**, 3–18 (2017).

15. Figus, F. A., Piga, M., Azzolin, I., McConnell, R. & Iagnocco, A. Rheumatoid arthritis: Extra-articular manifestations and comorbidities. *Autoimmunity Reviews* **20**, 102776 (2021).

16. Van Der Woude, D. & Van Der Helm-van Mil, A. H. M. Update on the epidemiology, risk factors, and disease outcomes of rheumatoid arthritis. *Best Practice & Research Clinical Rheumatology* **32**, 174–187 (2018).

17. Wang, Y. *et al.* Rheumatoid arthritis patients display B-cell dysregulation already in the naïve repertoire consistent with defects in B-cell tolerance. *Sci Rep* **9**, 19995 (2019).

18. Brewer, R. C. *et al.* Oral mucosal breaks trigger anti-citrullinated bacterial and human protein antibody responses in rheumatoid arthritis. *Sci. Transl. Med.* **15**, eabq8476 (2023).

19. Amara, K. *et al.* B cells expressing the IgA receptor FcRL4 participate in the autoimmune response in patients with rheumatoid arthritis. *Journal of Autoimmunity* **81**, 34–43 (2017).

20. Juodeikis, R. & Carding, S. R. Outer Membrane Vesicles: Biogenesis, Functions, and Issues. *Microbiol Mol Biol Rev* **86**, e00032-22 (2022).

21. Sharif, K., Sharif, A., Jumah, F., Oskouian, R. & Tubbs, R. S. Rheumatoid arthritis in review: Clinical, anatomical, cellular and molecular points of view: RA in review. *Clin. Anat.* **31**, 216–223 (2018).

22. McInnes, I. B. & Schett, G. The Pathogenesis of Rheumatoid Arthritis. *N Engl J Med* **365**, 2205–2219 (2011).

23. Bollow, M. Rheumatoide Arthritis der Hand: Teil 1: Klinische Aspekte. *Radiologe* **61**, 351–361 (2021).

24. Sudoł-Szopińska, I. *et al.* The pathogenesis of rheumatoid arthritis in radiological studies. Part I: Formation of inflammatory infiltrates within the synovial membrane. *J Ultrason* **12**, 202–213 (2012).

25. Salmon, M. *et al.* Inhibition of T cell apoptosis in the rheumatoid synovium. *J. Clin. Invest.* **99**, 439–446 (1997).

26. Hardt, U. *et al.* Integrated single cell and spatial transcriptomics reveal autoreactive differentiated B cells in joints of early rheumatoid arthritis. *Sci Rep* **12**, 11876 (2022).

27. Ge, Y. *et al.* Identification of differentially expressed genes, signaling pathways and immune infiltration in rheumatoid arthritis by integrated bioinformatics analysis. *Hereditas* **158**, 5 (2021).

28. Zhang, F. *et al.* Deconstruction of rheumatoid arthritis synovium defines inflammatory subtypes. *Nature* **623**, 616–624 (2023).

29. Meednu, N. *et al.* Production of RANKL by Memory B Cells: A Link Between B Cells and Bone Erosion in Rheumatoid Arthritis: B CELL PRODUCTION OF RANKL IN RA. *Arthritis & Rheumatology* **68**, 805–816 (2016).

30. Thomas, M. D., Srivastava, B. & Allman, D. Regulation of peripheral B cell maturation. *Cellular Immunology* **239**, 92–102 (2006).

31. Tiegs, S. L., Russell, D. M. & Nemazee, D. Receptor editing in self-reactive bone marrow B cells. *Journal of Experimental Medicine* **177**, 1009–1020 (1993).

32. Pillai, S., Mattoo, H. & Cariappa, A. B cells and autoimmunity. *Current Opinion in Immunology* **23**, 721–731 (2011).

33. Reijm, S., Kissel, T. & Toes, R. E. M. Checkpoints controlling the induction of B cell mediated autoimmunity in human autoimmune diseases. *Eur. J. Immunol.* **50**, 1885–1894 (2020).

34. Rodríguez-Pinto, D. B cells as antigen presenting cells. *Cellular Immunology* **238**, 67–75 (2005).

35. Akkaya, M., Kwak, K. & Pierce, S. K. B cell memory: building two walls of protection against pathogens. *Nat Rev Immunol* **20**, 229–238 (2020).

36. Kerfoot, S. M. *et al.* Germinal Center B Cell and T Follicular Helper Cell Development Initiates in the Interfollicular Zone. *Immunity* **34**, 947–960 (2011).

37. Rao, D. A. T Cells That Help B Cells in Chronically Inflamed Tissues. *Front. Immunol.* **9**, 1924 (2018).

38. Hervé, M. *et al.* CD40 ligand and MHC class II expression are essential for human peripheral B cell tolerance. *The Journal of Experimental Medicine* **204**, 1583–1593 (2007).

39. Kurosaki, T., Kometani, K. & Ise, W. Memory B cells. *Nat Rev Immunol* **15**, 149–159 (2015).

40. Weill, J.-C., Weller, S. & Reynaud, C.-A. Human Marginal Zone B Cells. *Annu. Rev. Immunol.* **27**, 267–285 (2009).

41. Glaros, V. *et al.* Limited access to antigen drives generation of early B cell memory while restraining the plasmablast response. *Immunity* **54**, 2005-2023.e10 (2021).

42. De Silva, N. S. & Klein, U. Dynamics of B cells in germinal centres. *Nat Rev Immunol* **15**, 137–148 (2015).

43. Pipi, E. *et al.* Tertiary Lymphoid Structures: Autoimmunity Goes Local. *Front. Immunol.* **9**, 1952 (2018).

44. Berek, C., Berger, A. & Apel, M. Maturation of the immune response in germinal centers. *Cell* **67**, 1121–1129 (1991).

45. Shlomchik, M. J. & Weisel, F. Germinal center selection and the development of memory B and plasma cells. *Immunological Reviews* **247**, 52–63 (2012).

46. Storb, U. & Stavnezer, J. Immunoglobulin Genes: Generating Diversity with AID and UNG. *Current Biology* **12**, R725–R727 (2002).

47. Xu, Z., Zan, H., Pone, E. J., Mai, T. & Casali, P. Immunoglobulin class-switch DNA recombination: induction, targeting and beyond. *Nat Rev Immunol* **12**, 517–531 (2012).

48. Zan, H. & Casali, P. Regulation of *Aicda* expression and AID activity. *Autoimmunity* **46**, 83–101 (2013).

49. Johnsen, H. E. *et al.* Cell of origin associated classification of B-cell malignancies by gene signatures of the normal B-cell hierarchy. *Leukemia & Lymphoma* **55**, 1251–1260 (2014).

50. Wang, L. D. & Clark, M. R. B-cell antigen-receptor signalling in lymphocyte development. *Immunology* **110**, 411–420 (2003).

51. Yoshida, T. *et al.* Memory B and memory plasma cells. *Immunological Reviews* **237**, 117–139 (2010).

52. McHeyzer-Williams, L. J., Milpied, P. J., Okitsu, S. L. & McHeyzer-Williams, M. G. Class-switched memory B cells remodel BCRs within secondary germinal centers. *Nat Immunol* **16**, 296–305 (2015).

53. Basso, K. & Dalla-Favera, R. Germinal centres and B cell lymphomagenesis. *Nat Rev Immunol* **15**, 172–184 (2015).

54. Taher, T. E. *et al.* Intracellular B Lymphocyte Signalling and the Regulation of Humoral Immunity and Autoimmunity. *Clinic Rev Allerg Immunol* **53**, 237–264 (2017).

55. Taylor, J. J., Pape, K. A. & Jenkins, M. K. A germinal center–independent pathway generates unswitched memory B cells early in the primary response. *Journal of Experimental Medicine* **209**, 597–606 (2012).

56. Lee, D. S. W., Rojas, O. L. & Gommerman, J. L. B cell depletion therapies in autoimmune disease: advances and mechanistic insights. *Nat Rev Drug Discov* **20**, 179–199 (2021).

57. Wienands, J. & Engels, N. Control of memory B cell responses by extrinsic and intrinsic mechanisms. *Immunology Letters* **178**, 27–30 (2016).

58. Ota, Y. *et al.* Generation mechanism of RANKL+ effector memory B cells: relevance to the pathogenesis of rheumatoid arthritis. *Arthritis Res Ther* **18**, 67 (2016).

59. Portugal, S., Obeng-Adjei, N., Moir, S., Crompton, P. D. & Pierce, S. K. Atypical memory B cells in human chronic infectious diseases: An interim report. *Cellular Immunology* **321**, 18–25 (2017).

60. Vidal-Pedrola, G. *et al.* Characterization of age-associated B cells in early drug-naïve rheumatoid arthritis patients. *Immunology* **168**, 640–653 (2023).

61. Kugler-Umana, O., Devarajan, P. & Swain, S. L. Understanding the Heterogeneous Population of Age-Associated B Cells and Their Contributions to Autoimmunity and Immune Response to Pathogens. *Crit Rev Immunol* **40**, 297–309 (2020).

62. Du, S. W. *et al.* Functional Characterization of CD11c+ Age-Associated B Cells as Memory B Cells. *J Immunol* **203**, 2817–2826 (2019).

63. Pupovac, A. & Good-Jacobson, K. L. An antigen to remember: regulation of B cell memory in health and disease. *Current Opinion in Immunology* **45**, 89–96 (2017).

64. Rincón-Arévalo, H. *et al.* Atypical phenotype and response of B cells in patients with seropositive rheumatoid arthritis. *Clinical and Experimental Immunology* **204**, 221–238 (2021).

65. Holla, P. *et al.* Shared transcriptional profiles of atypical B cells suggest common drivers of expansion and function in malaria, HIV, and autoimmunity. *Sci. Adv.* **7**, eabg8384 (2021).

66. Moens, L., Kane, A. & Tangye, S. G. Naïve and memory B cells exhibit distinct biochemical responses following BCR engagement. *Immunol Cell Biol* **94**, 774–786 (2016).

67. Rip, J., De Bruijn, M. J. W., Kaptein, A., Hendriks, R. W. & Corneth, O. B. J. Phosphoflow Protocol for Signaling Studies in Human and Murine B Cell Subpopulations. *The Journal of Immunology* **204**, 2852–2863 (2020).

68. Gauld, S. B. & Cambier, J. C. Src-family kinases in B-cell development and signaling. *Oncogene* **23**, 8001–8006 (2004).

69. Chaturvedi, A., Martz, R., Dorward, D., Waisberg, M. & Pierce, S. K. Endocytosed BCRs sequentially regulate MAPK and Akt signaling pathways from intracellular compartments. *Nat Immunol* **12**, 1119–1126 (2011).

70. Corneth, O. B. J., Neys, S. F. H. & Hendriks, R. W. Aberrant B Cell Signaling in Autoimmune Diseases. *Cells* **11**, 3391 (2022).

71. Park, S.-J., Jang, J.-W. & Moon, E.-Y. Bisphenol A-induced autophagy ameliorates human B cell death through Nrf2-mediated regulation of Atg7 and Beclin1 expression by Syk activation. *Ecotoxicology and Environmental Safety* **260**, 115061 (2023).

72. Bournazos, S., Gupta, A. & Ravetch, J. V. The role of IgG Fc receptors in antibody-dependent enhancement. *Nat Rev Immunol* **20**, 633–643 (2020).

73. Avalos, A. M. & Ploegh, H. L. Early BCR Events and Antigen Capture, Processing, and Loading on MHC Class II on B Cells. *Front. Immunol.* **5**, (2014).

74. Clarke, A. J. & Simon, A. K. Autophagy in the renewal, differentiation and homeostasis of immune cells. *Nat Rev Immunol* **19**, 170–183 (2019).

75. Wang, Y. & Gao, W. Effects of TNF-α on autophagy of rheumatoid arthritis fibroblast-like synoviocytes and regulation of the NF-κB signaling pathway. *Immunobiology* **226**, 152059 (2021).

76. Yao, Y. *et al.* Resveratrol induces autophagy impeding BAFF-stimulated B-cell proliferation and survival by inhibiting the Akt/mTOR pathway. *Biochemical Pharmacology* **202**, 115139 (2022).

77. Su, J.-C. *et al.* RFX1-dependent activation of SHP-1 induces autophagy by a novel obatoclax derivative in hepatocellular carcinoma cells. *Oncotarget* **5**, 4909–4919 (2014).

78. Spillane, K. M. & Tolar, P. Mechanics of antigen extraction in the B cell synapse. *Molecular Immunology* **101**, 319–328 (2018).

79. Barroso, M., Tucker, H., Drake, L., Nichol, K. & Drake, J. R. Antigen-B Cell Receptor Complexes Associate with Intracellular major histocompatibility complex (MHC) Class II Molecules. *Journal of Biological Chemistry* **290**, 27101–27112 (2015).

80. Chen, X. & Jensen, P. E. The role of B lymphocytes as antigen-presenting cells. *Arch. Immunol. Ther. Exp.* **56**, 77–83 (2008).

81. Hua, Z. & Hou, B. The role of B cell antigen presentation in the initiation of CD4+ T cell response. *Immunol Rev* **296**, 24–35 (2020).

82. O'Neill, S. K. *et al.* Antigen-Specific B Cells Are Required as APCs and Autoantibody-Producing Cells for Induction of Severe Autoimmune Arthritis. *The Journal of Immunology* **174**, 3781–3788 (2005).

83. Jöhrens, K. *et al.* T-bet-positive and IRTA1-positive monocytoid B cells differ from marginal zone B cells and epithelial-associated B cells in their antigen profile and topographical distribution. *Haematologica* **90**, 1070–1077 (2005).

84. Cyster, J. G. Chemokines and Cell Migration in Secondary Lymphoid Organs. *Science* **286**, 2098–2102 (1999).

85. Roth, R., Gee, R. J. & Mamula, M. J. B Lymphocytes as Autoantigen-presenting Cells in the Amplification of Autoimmunity. *Ann NY Acad Sci* **815**, 88–100 (1997).

86. Shimabukuro-Vornhagen, A. *et al.* Antigen-presenting human B cells are expanded in inflammatory conditions. *Journal of Leukocyte Biology* **101**, 577–587 (2017).

87. Rivera, A., Chen, C.-C., Ron, N., Dougherty, J. P. & Ron, Y. Role of B cells as antigen-presenting cells in vivo revisited: antigen-specific B cells are essential for T cell expansion in lymph nodes and for systemic T cell responses to low antigen concentrations. *International Immunology* **13**, 1583–1593 (2001).

88. Marston, B., Palanichamy, A. & Anolik, J. H. B cells in the pathogenesis and treatment of rheumatoid arthritis. *Curr Opin Rheumatol* **22**, 307–315 (2010).

89. Yeo, L. *et al.* Cytokine mRNA profiling identifies B cells as a major source of RANKL in rheumatoid arthritis. *Annals of the Rheumatic Diseases* **70**, 2022–2028 (2011).

90. LeBien, T. W. & Tedder, T. F. B lymphocytes: how they develop and function. *Blood* **112**, 1570–1580 (2008).

91. Barr, T. A. *et al.* B cell depletion therapy ameliorates autoimmune disease through ablation of IL-6–producing B cells. *Journal of Experimental Medicine* **209**, 1001–1010 (2012).

92. Zhang, L. *et al.* BAFF, involved in B cell activation through the NF-κB pathway, is related to disease activity and bone destruction in rheumatoid arthritis. *Acta Pharmacol Sin* **42**, 1665–1675 (2021).

93. Zikherman, J., Parameswaran, R. & Weiss, A. Endogenous antigen tunes the responsiveness of naive B cells but not T cells. *Nature* **489**, 160–164 (2012).

94. Meffre, E. & O'Connor, K. C. Impaired B-cell tolerance checkpoints promote the development of autoimmune diseases and pathogenic autoantibodies. *Immunol Rev* **292**, 90–101 (2019).

95. Weyand, C. M. & Goronzy, J. J. The immunology of rheumatoid arthritis. *Nat Immunol* **22**, 10–18 (2021).

96. O'Neill, S. K. *et al.* Endocytic sequestration of the B cell antigen receptor and toll-like receptor 9 in anergic cells. *Proc. Natl. Acad. Sci. U.S.A.* **106**, 6262–6267 (2009).

97. Albani, S., Koffeman, E. C. & Prakken, B. Induction of immune tolerance in the treatment of rheumatoid arthritis. *Nat Rev Rheumatol* **7**, 272–281 (2011).

98. Floudas, A. *et al.* ACPA Status Correlates with Differential Immune Profile in Patients with Rheumatoid Arthritis. *Cells* **10**, 647 (2021).

99. Magalhães, R., Stiehl, P., Morawietz, L., Berek, C. & Krenn, V. Morphological and molecular pathology of the B cell response in synovitis of rheumatoid arthritis. *Virchows Archiv* **441**, 415–427 (2002).

100. Sun, W. *et al.* B cells inhibit bone formation in rheumatoid arthritis by suppressing osteoblast differentiation. *Nat Commun* **9**, 5127 (2018).

101. Barnas, J. L., Looney, R. J. & Anolik, J. H. B cell targeted therapies in autoimmune disease. *Current Opinion in Immunology* **61**, 92–99 (2019).

102. Song, Y. W. & Kang, E. H. The pathogenic role of rheumatoid factor in rheumatoid arthritis. *International Journal of Clinical Rheumatology* **5**, 651–658 (2010).

103. Malmström, V., Catrina, A. I. & Klareskog, L. The immunopathogenesis of seropositive rheumatoid arthritis: from triggering to targeting. *Nat Rev Immunol* **17**, 60–75 (2017).

104. Klareskog, L., Amara, K. & Malmström, V. Adaptive immunity in rheumatoid arthritis: anticitrulline and other antibodies in the pathogenesis of rheumatoid arthritis. *Current Opinion in Rheumatology* **26**, 72–79 (2014).

105. Gerstner, C. *et al.* Functional and Structural Characterization of a Novel HLA-DRB1*04:01-Restricted α-Enolase T Cell Epitope in Rheumatoid Arthritis. *Front. Immunol.* **7**, 494 (2016).

106. Harre, U. *et al.* Induction of osteoclastogenesis and bone loss by human autoantibodies against citrullinated vimentin. *J. Clin. Invest.* **122**, 1791–1802 (2012).

107. Ben Mkaddem, S., Rossato, E., Heming, N. & Monteiro, R. C. Anti-inflammatory role of the IgA Fc receptor (CD89): From autoimmunity to therapeutic perspectives. *Autoimmunity Reviews* **12**, 666–669 (2013).

108. Mkaddem, S. B. *et al.* IgA, IgA Receptors, and Their Anti-inflammatory Properties. in *Fc Receptors* (eds. Daeron, M. & Nimmerjahn, F.) vol. 382 221–235 (Springer International Publishing, Cham, 2014).

109. Tolnay, M. Lymphocytes sense antibodies through human FCRL proteins: Emerging roles in mucosal immunity. *Journal of Leukocyte Biology* **111**, 477–487 (2022).

110. Yeo, L. *et al.* Expression of FcRL4 defines a pro-inflammatory, RANKL-producing B cell subset in rheumatoid arthritis. *Ann Rheum Dis* **74**, 928–935 (2015).

111. Edwards, J. C. W., Leigh, R. D. & Cambridge, G. Expression of molecules involved in B lymphocyte survival and differentiation by synovial fibroblasts. *Clinical and Experimental Immunology* **108**, 407–414 (2003).

112. Takemura, S., Klimiuk, P. A., Braun, A., Goronzy, J. J. & Weyand, C. M. T Cell Activation in Rheumatoid Synovium Is B Cell Dependent. *The Journal of Immunology* **167**, 4710–4718 (2001).

113. Boumans, M. J. H. *et al.* Rituximab abrogates joint destruction in rheumatoid arthritis by inhibiting osteoclastogenesis. *Ann Rheum Dis* **71**, 108–113 (2012).

114. Edwards, J. C. W. *et al.* Efficacy of B-Cell–Targeted Therapy with Rituximab in Patients with Rheumatoid Arthritis. *N Engl J Med* **350**, 2572–2581 (2004).

115. Anolik, J. H., Looney, R. J., Lund, F. E., Randall, T. D. & Sanz, I. Insights into the heterogeneity of human B cells: diverse functions, roles in autoimmunity, and use as therapeutic targets. *Immunol Res* **45**, 144–158 (2009).

116. Lim, S. H. *et al.* Fc gamma receptor IIb on target B cells promotes rituximab internalization and reduces clinical efficacy. *Blood* **118**, 2530–2540 (2011).

117. Alenazy, M. F. *et al.* Abatacept enhances blood regulatory B cells of rheumatoid arthritis patients to a level that associates with disease remittance. *Sci Rep* **11**, 5629 (2021).

118. Khanzadeh, A., Habibagahi, Z., Hosseini, A. & Amirghofran, Z. Investigation of the human FCRL1, 2, and 4 gene expressions in patients with rheumatoid arthritis. *Rheumatol Int* **36**, 1149–1156 (2016).

119. Li, F. J. *et al.* Emerging Roles for the FCRL Family Members in Lymphocyte Biology and Disease. in *Fc Receptors* (eds. Daeron, M. & Nimmerjahn, F.) vol. 382 29–50 (Springer International Publishing, Cham, 2014).

120. Capone, M. & Matthew, J. Fc Receptor-Like Proteins in Pathophysiology of B-cell Disorder. *J Clin Cell Immunol* **7**, (2016).

121. Anania, J. C., Chenoweth, A. M., Wines, B. D. & Hogarth, P. M. The Human FcγRII (CD32) Family of Leukocyte FcR in Health and Disease. *Front. Immunol.* **10**, 464 (2019).

122. Agarwal, S. *et al.* Human Fc Receptor-like 3 Inhibits Regulatory T Cell Function and Binds Secretory IgA. *Cell Reports* **30**, 1292-1299.e3 (2020).

123. Wilson, T. J., Fuchs, A. & Colonna, M. Cutting Edge: Human FcRL4 and FcRL5 Are Receptors for IgA and IgG. *The Journal of Immunology* **188**, 4741–4745 (2012).

124. Falini, B. *et al.* Expression of the IRTA1 receptor identifies intraepithelial and subepithelial marginal zone B cells of the mucosa-associated lymphoid tissue (MALT). *Blood* **102**, 3684–3692 (2003).

125. Jourdan, M. *et al.* Characterization of human FCRL4-positive B cells. *PLoS ONE* **12**, e0179793 (2017).

126. Sanz, I., Wei, C., Lee, F. E.-H. & Anolik, J. Phenotypic and functional heterogeneity of human memory B cells. *Seminars in Immunology* **20**, 67–82 (2008).

127. Du, W. *et al.* The Multiple Roles of B Cells in the Pathogenesis of Sjögren's Syndrome. *Front. Immunol.* **12**, 684999 (2021).

128. Ehrhardt, G. R. A. *et al.* Discriminating gene expression profiles of memory B cell subpopulations. *Journal of Experimental Medicine* **205**, 1807–1817 (2008).

129. Gjertsson, I. *et al.* A close-up on the expanding landscape of CD21–/low B cells in humans. *Clinical and Experimental Immunology* **210**, 217–229 (2022).

130. Haacke, E. A. *et al.* FcRL4+ B-cells in salivary glands of primary Sjögren's syndrome patients. *Journal of Autoimmunity* **81**, 90–98 (2017).

131. Siewe, B., Nipper, A. J., Sohn, H., Stapleton, J. T. & Landay, A. FcRL4 Expression Identifies a Pro-inflammatory B Cell Subset in Viremic HIV-Infected Subjects. *Front. Immunol.* **8**, 1339 (2017).

132. Poonia, B., Ayithan, N., Nandi, M., Masur, H. & Kottilil, S. HBV induces inhibitory FcRL receptor on B cells and dysregulates B cell-T follicular helper cell axis. *Sci Rep* **8**, 15296 (2018).

133. Jelicic, K. *et al.* The HIV-1 envelope protein gp120 impairs B cell proliferation by inducing TGF-β1 production and FcRL4 expression. *Nat Immunol* **14**, 1256–1265 (2013).

134. Sohn, H. W., Krueger, P. D., Davis, R. S. & Pierce, S. K. FcRL4 acts as an adaptive to innate molecular switch dampening BCR signaling and enhancing TLR signaling. *Blood* **118**, 6332–6341 (2011).

135. Hatzivassiliou, G. *et al.* IRTA1 and IRTA2, Novel Immunoglobulin Superfamily Receptors Expressed in B Cells and Involved in Chromosome 1q21 Abnormalities in B Cell Malignancy. *Immunity* **14**, 277–289 (2001).

136. Liu, Y. *et al.* FCRL4 Is an Fc Receptor for Systemic IgA, but Not Mucosal Secretory IgA. *The Journal of Immunology* **205**, 533–538 (2020).

137. Häusler, D. *et al.* Glatiramer acetate immune modulates B-cell antigen presentation in treatment of MS. *Neurol Neuroimmunol Neuroinflamm* **7**, e698 (2020).

138. Lei, S. *et al.* Abnormal HCK /glutamine/autophagy axis promotes endometriosis development by impairing macrophage phagocytosis. *Cell Proliferation* e13702 (2024) doi:10.1111/cpr.13702.

139. Liu, Y. *et al.* Involvement of the HCK and FGR src-Family Kinases in FCRL4-Mediated Immune Regulation. *The Journal of Immunology* **194**, 5851–5860 (2015).

140. Kim, N. Y., Sethi, G., Um, J.-Y. & Ahn, K. S. Euphorbiasteroid Induces Apoptosis as Well as Autophagy through Modulating SHP-1/STAT3 Pathway in Hepatocellular Carcinoma Cells. *IJMS* **24**, 13713 (2023).

141. Tsui, C. *et al.* Dynamic reorganisation of intermediate filaments coordinates early B-cell activation. *Life Sci. Alliance* **1**, e201800060 (2018).

142. Ehrhardt, G. R. A. *et al.* The inhibitory potential of Fc receptor homolog 4 on memory B cells. *Proc. Natl. Acad. Sci. U.S.A.* **100**, 13489–13494 (2003).

143. Kardava, L. *et al.* Attenuation of HIV-associated human B cell exhaustion by siRNA downregulation of inhibitory receptors. *J. Clin. Invest.* **121**, 2614–2624 (2011).

144. Ding, C. *et al.* Integrin CD11b negatively regulates BCR signalling to maintain autoreactive B cell tolerance. *Nat Commun* **4**, 2813 (2013).

145. Hu, C. *et al.* Yishen-tongbi decoction inhibits excessive activation of B cells by activating the FcγRIIb/Lyn/SHP-1 pathway and attenuates the inflammatory response in CIA rats. *Biomedicine & Pharmacotherapy* **134**, 111166 (2021).

146. Jazirehi, A. R., Vega, M. I., Chatterjee, D., Goodglick, L. & Bonavida, B. Inhibition of the Raf–MEK1/2–ERK1/2 Signaling Pathway, Bcl-xL Down-Regulation, and Chemosensitization of Non-Hodgkin's Lymphoma B Cells by Rituximab. *Cancer Research* **64**, 7117–7126 (2004).

147. Davis, R. S., Wang, Y.-H., Kubagawa, H. & Cooper, M. D. Identification of a family of Fc receptor homologs with preferential B cell expression. *Proc. Natl. Acad. Sci. U.S.A.* **98**, 9772–9777 (2001).

148. Kochi, Y. *et al.* FCRL3, an Autoimmune Susceptibility Gene, Has Inhibitory Potential on B-Cell Receptor-Mediated Signaling. *The Journal of Immunology* **183**, 5502–5510 (2009).

149. Puerta, A. *et al.* Capillary gel electrophoresis of very high molecular weight glycoproteins. Commercial and tailor-made gels for analysis of human monomeric and secretory immunoglobulin A. *Journal of Chromatography A* **1688**, 463689 (2023).

150. Hernández-Pérez, S. *et al.* B cells rapidly target antigen and surface-derived MHCII into peripheral degradative compartments. *Journal of Cell Science* **133**, jcs235192 (2020).

8 Appendix

Sample ID	HLA Type
1	DRB1*01:01:01:01,DRB1*11:01
2	**DRB1*04:01:01:01,DRB1*15:01:01:01**
3	DRB1*13:01:01:01,DRB1*15:01:01:01
4	DRB1*07:01:01:01,DRB1*11:04
5	DRB1*01:03:01:01,DRB1*14:01:01/14:54:01:01
6	DRB1*13:01:01:01,DRB1*14:04:01:01
7	DRB1*07:01:01:01,DRB1*13:02:01:01
8	DRB1*07:01:01:01,-
9	**DRB1*04:01:01:01,DRB1*15:01:01:01**

***Table 8.1., HLADRB1-typing data from tonsil samples**. HLA-typing focussed on the HLADRB1 locus and the alleles expressed on detailed in the right-hand column*

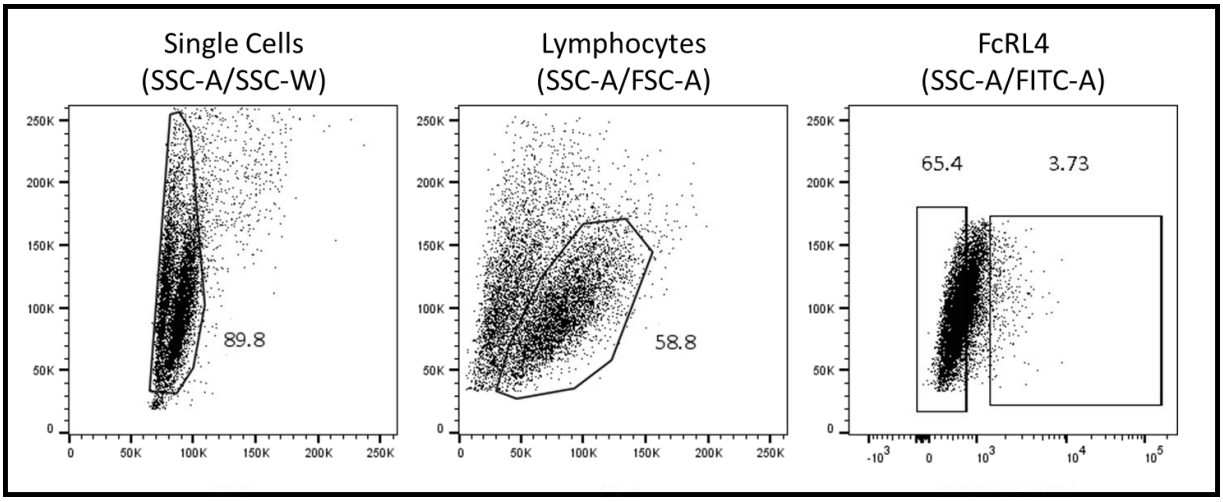

Figure 8.2., Gating strategy used for the induced transduced priess cells used in the HA colostrum IgA IC/pHrodo internalisation experiments*. (n = 1) Representative FACS plots of induced transduced priess cells to demonstrate how FcRL4+ and FcRL4- cells were gated. Induced transduced priess cells were initially gated on the singlet population and then the lymphocyte population before gating on the FcRL4+ (FITC-A+) and FcRL4- (FITC-A-) populations. The number next to the gate represents the percentage of cells in each population.*

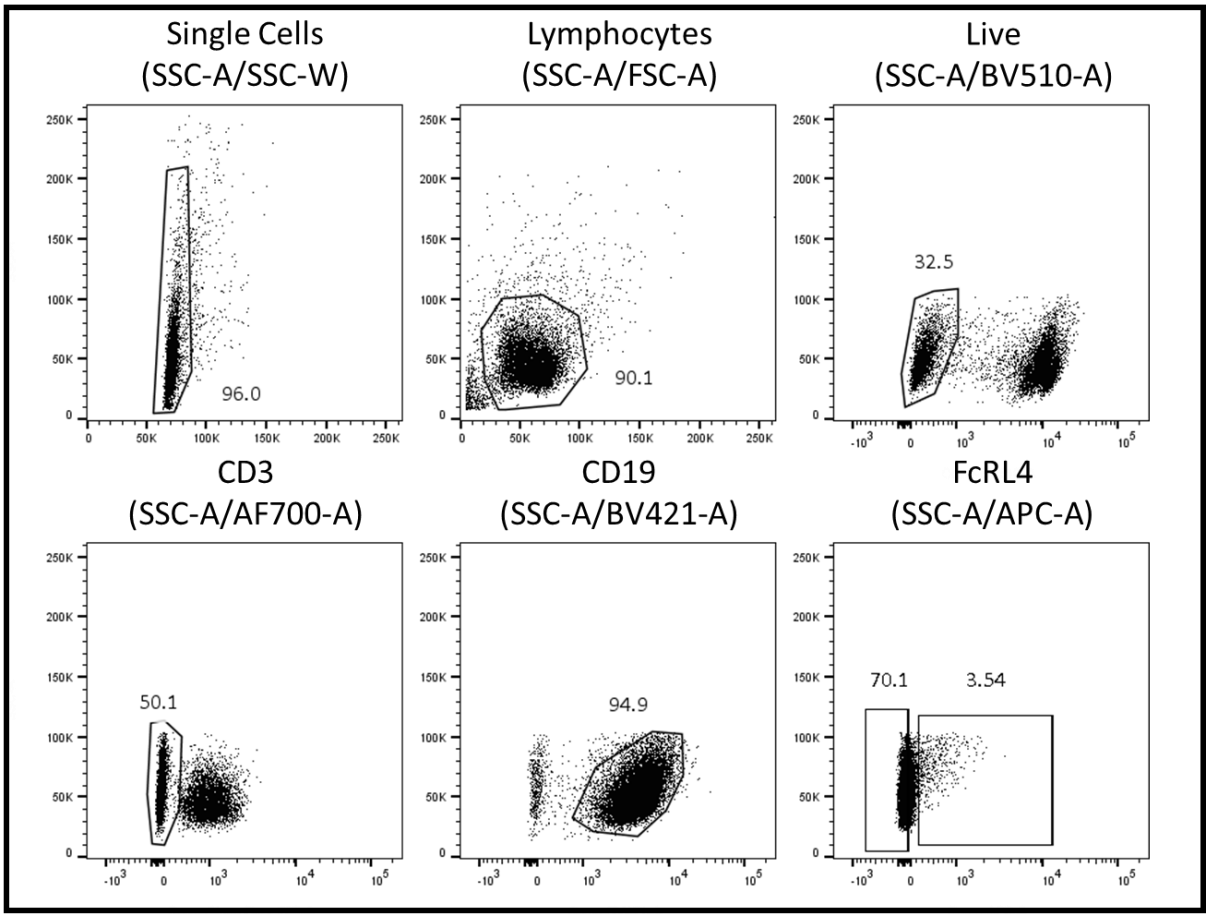

Figure 8.3., Gating strategy used for the ex-vivo tonsil cells used in the HA colostrum IgA IC/pHrodo internalisation experiments*. (n = 1) Representative FACS plots of ex-vivo tonsil cells to demonstrate how FcRL4+ and FcRL4- cells were gated. Ex-vivo tonsil cells were initially gated on the singlet population, the lymphocyte population and then the live population, defined as BV510-. The FcRL4+ (APC-A+) and FcRL4- (APC-A-) populations were then defined as CD3- (AF700-) and CD19+ (BV421+). The number next to the gate represents the percentage of cells in each population.*

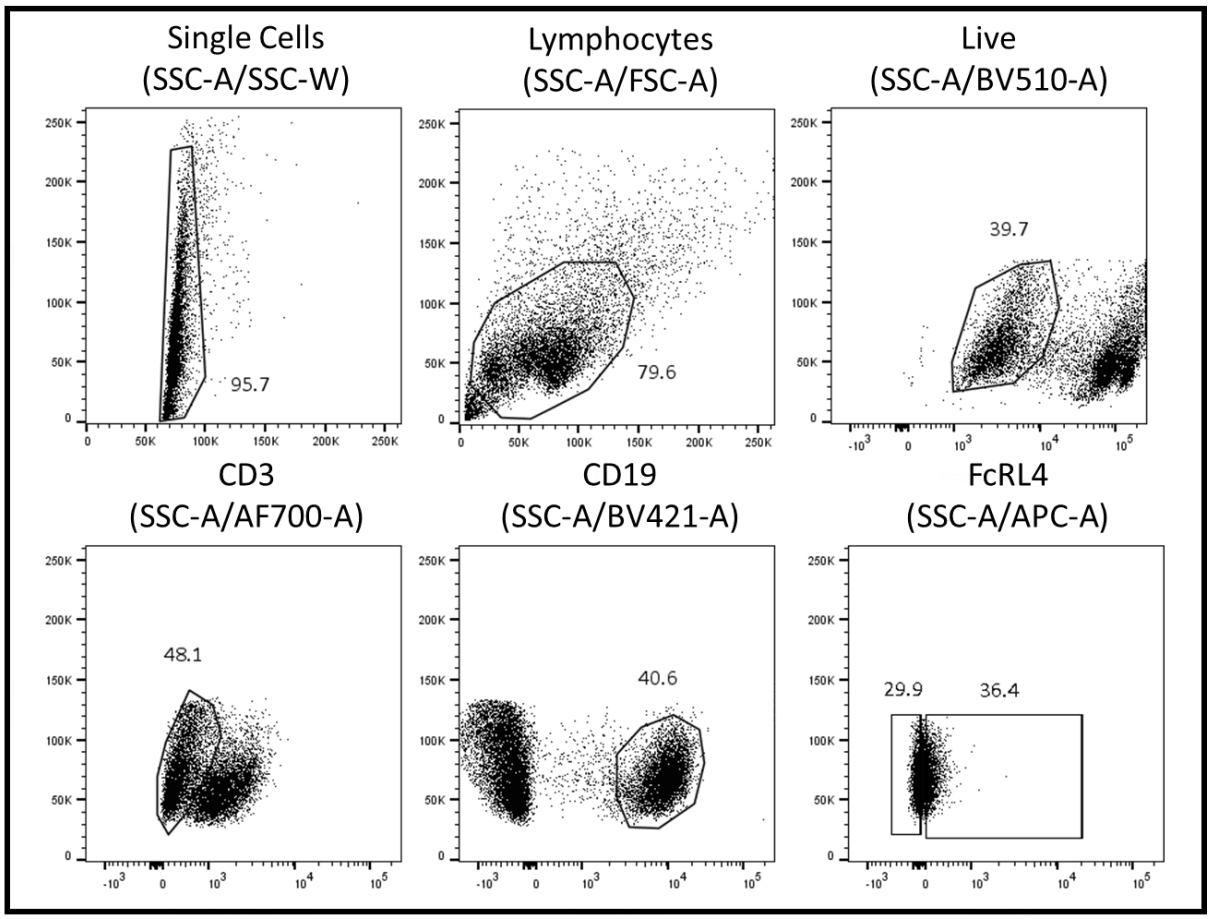

Figure 8.4., Gating strategy used for the ex-vivo RA SF cells used in the HA colostrum IgA IC/pHrodo internalisation experiments*. (n = 1) Representative FACS plots of ex-vivo RA SF cells to demonstrate how FcRL4+ and FcRL4- cells were gated. Ex-vivo tonsil cells were initially gated on the singlet population, the lymphocyte population and then the live population, defined as BV510-. The FcRL4+ (APC-A+) and FcRL4- (APC-A-) populations were then defined as CD3- (AF700-) and CD19+ (BV421+). The number next to the gate represents the percentage of cells in each population.*

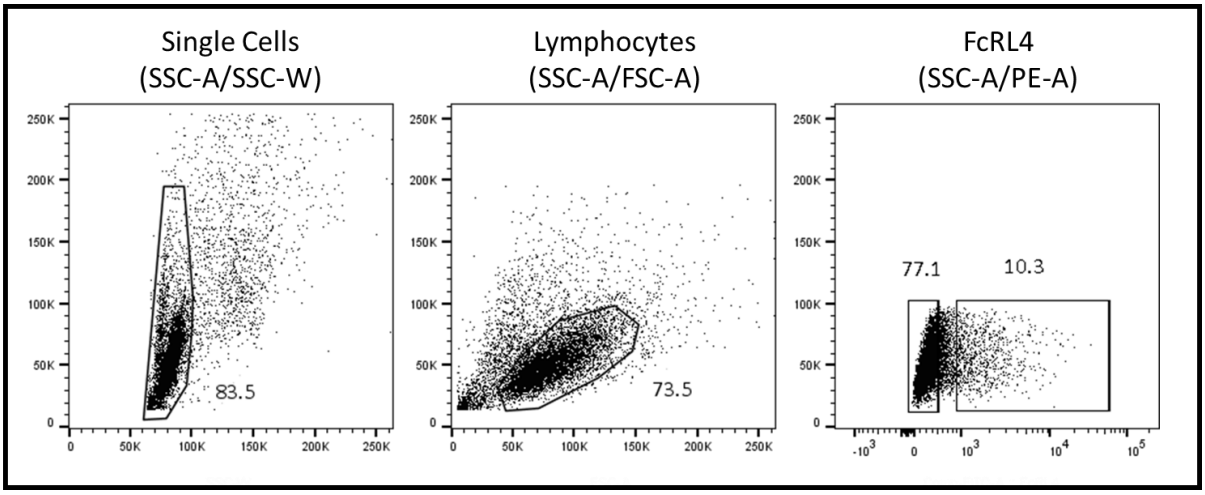

Figure 8.5., Gating strategy used for the induced transduced priess cells used in the PhosFlow experiments*. (n = 1) Representative FACS plots of induced transduced priess cells to demonstrate how FcRL4+ and FcRL4- cells were gated. Induced transduced priess cells were initially gated on the singlet population and then the lymphocyte population before gating on the FcRL4+ (FITC-A+) and FcRL4- (FITC-A-) populations. The number next to the gate represents the percentage of cells in each population.*

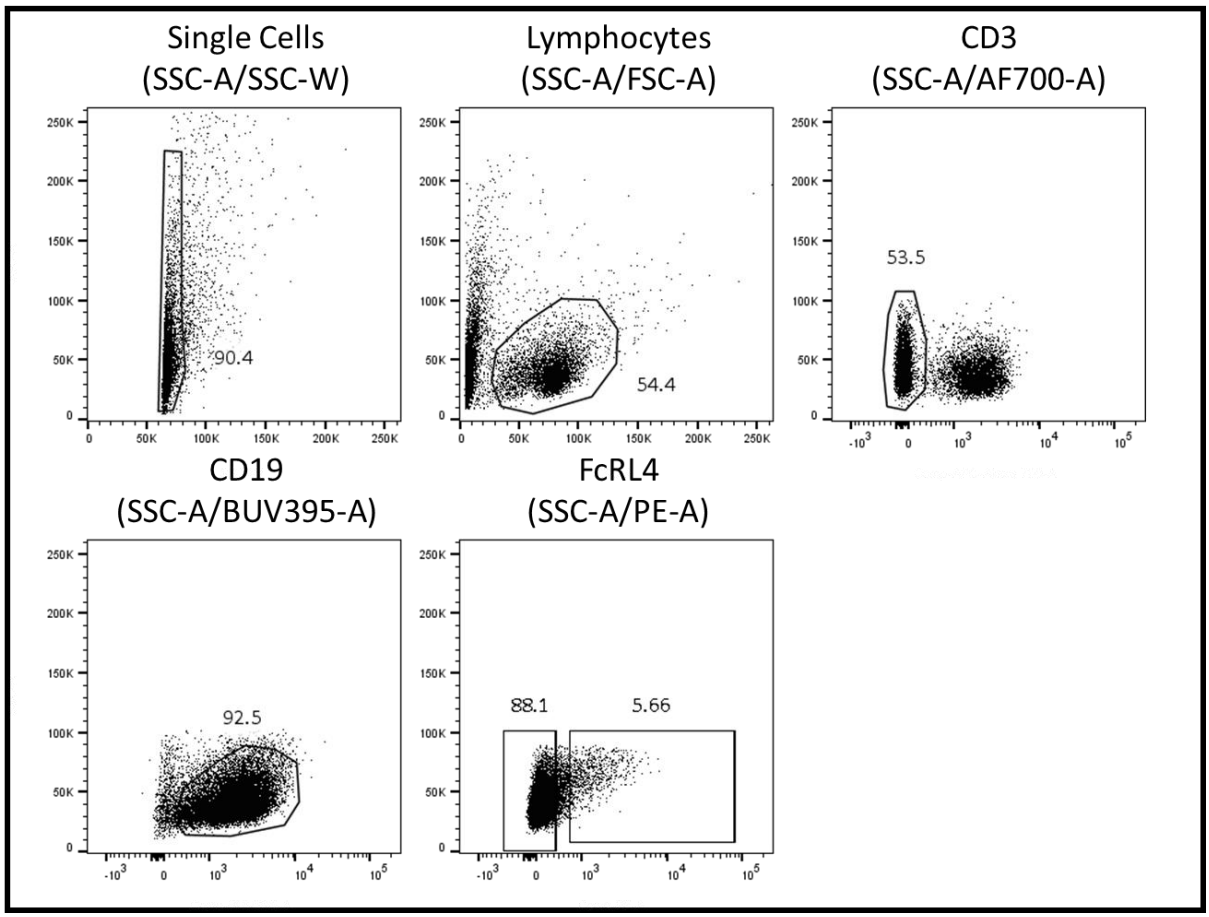

Figure 8.6., Gating strategy used for the ex-vivo tonsil cells used in the PhosFlow experiments*. (n = 1) Representative FACS plots of ex-vivo tonsil cells to demonstrate how FcRL4+ and FcRL4- cells were gated. Ex-vivo tonsil cells were initially gated on the singlet population, the lymphocyte population and then the live population, defined as BV510-. The FcRL4+ (PE-A+) and FcRL4- (PE-A-) populations were then defined as CD3- (AF700-) and CD19+ (BUV395+). The number next to the gate represents the percentage of cells in each population.*

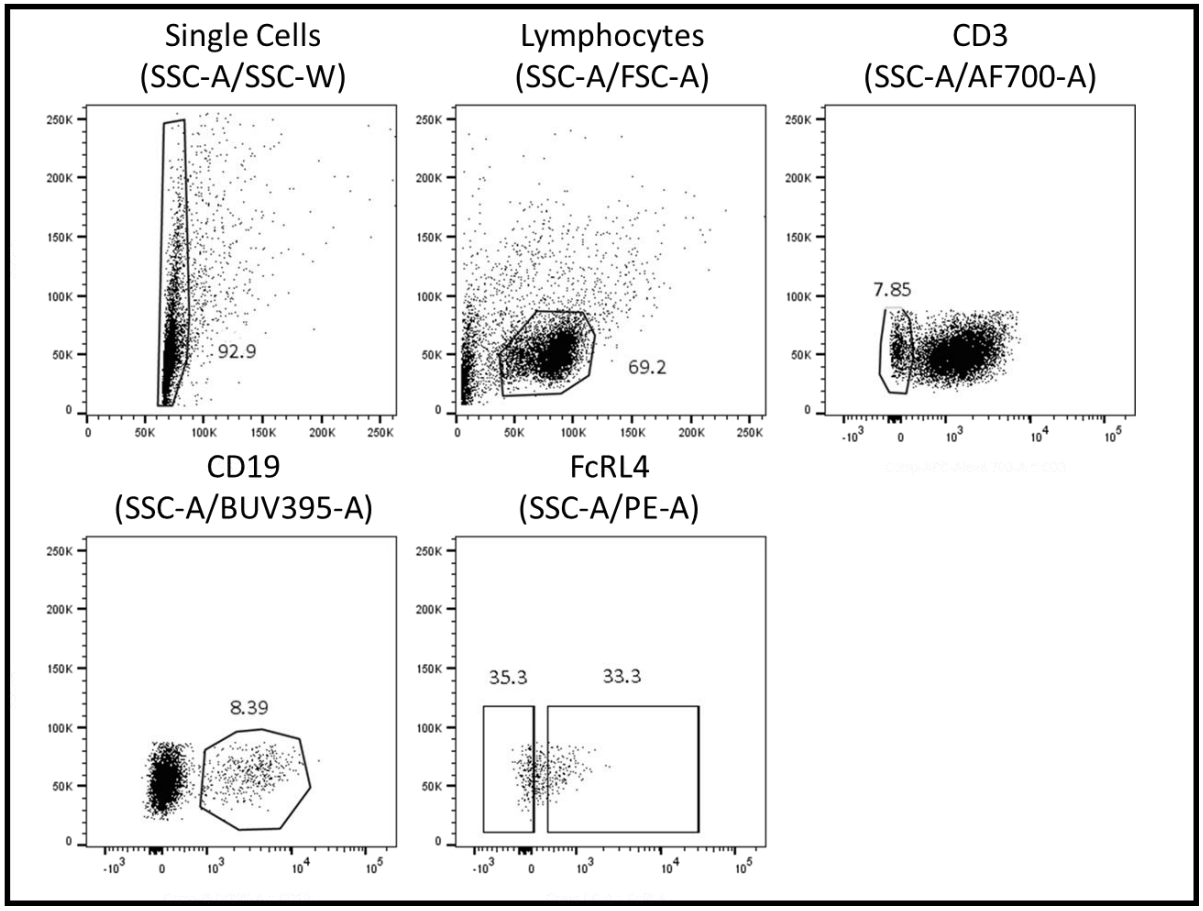

Figure 8.7., Gating strategy used for the ex-vivo RA SF cells used in the PhosFlow experiments*. (n = 1) Representative FACS plots of ex-vivo RA SF cells to demonstrate how FcRL4+ and FcRL4- cells were gated. Ex-vivo tonsil cells were initially gated on the singlet population, the lymphocyte population and then the live population, defined as BV510-. The FcRL4+ (PE-A+) and FcRL4- (PE-A-) populations were then defined as CD3- (AF700-) and CD19+ (BUV395+). The number next to the gate represents the percentage of cells in each population.*